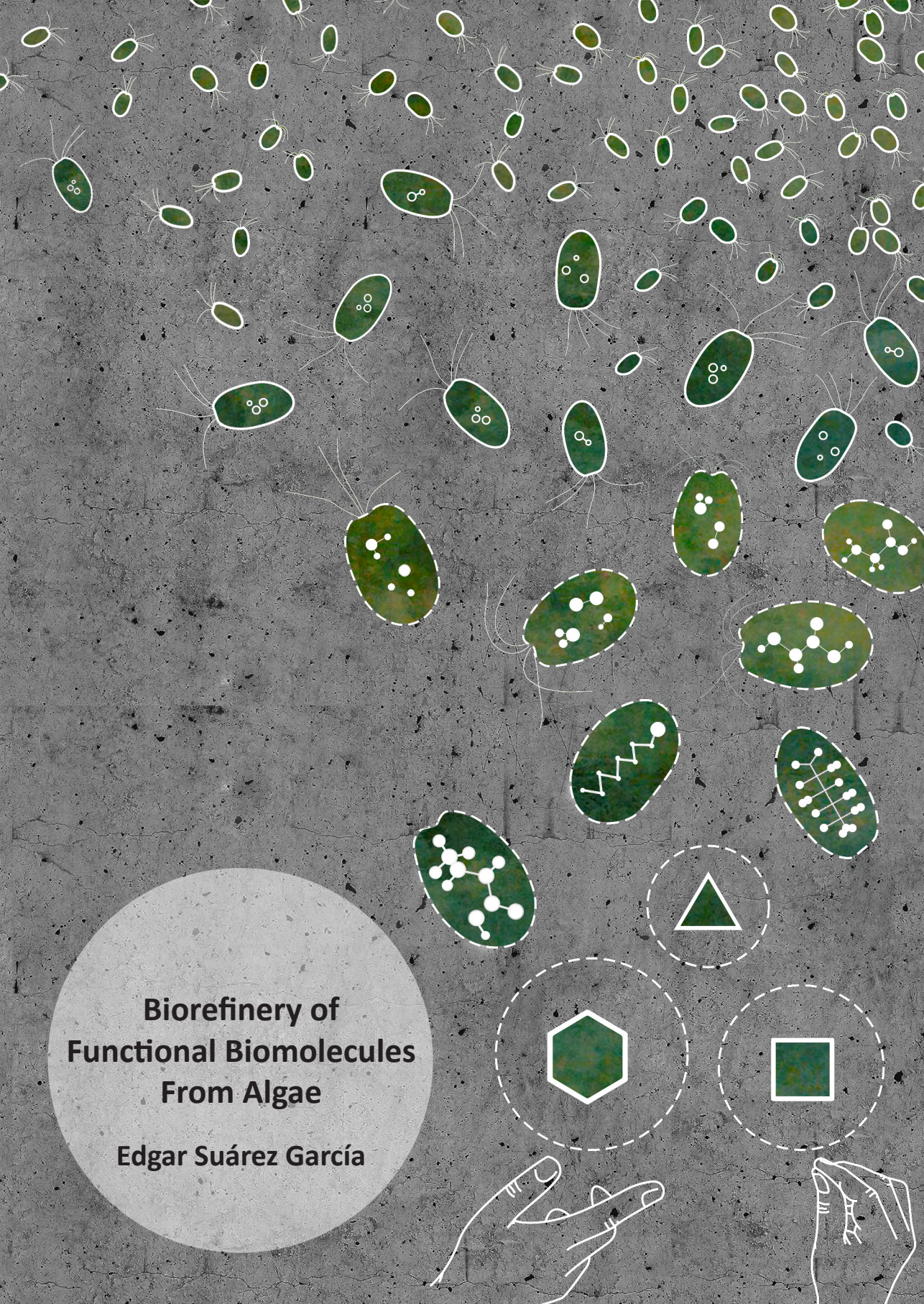

Biorefinery of Functional Biomolecules From Algae

Edgar Suárez García

Biorefinery of Functional Biomolecules From Algae

Edgar Suarez Garcia

Thesis committee

Promotors
Prof. Dr R.H. Wijffels
Professor of Bioprocess Engineering
Wageningen University & Research

Prof. Dr M.H.M. Eppink
Special professor Biorefinery with Focus on Mild Separation Technologies of Complex Biomolecules
Wageningen University & Research

Co-promotor
Dr C. van den Berg
Assistant professor, Bioprocess Engineering
Wageningen University & Research

Other members
Prof. Dr A.J. van der Goot, Wageningen University & Research
Dr M. Ottens, Delft University of Technology
Dr T. Jongsma, ISPT-Institute for Sustainable Process Technology, Amersfoort
Dr J. Arfsten, Nestlé Research Konolfingen, Switzerland

This research was conducted under the auspices of the Graduate School VLAG (Advanced studies in Food Technology, Agrobiotechnology, Nutrition and Health Sciences)

Biorefinery of Functional Biomolecules From Algae

Edgar Suarez Garcia

Thesis

submitted in fulfilment of the requirements for the degree of doctor
at Wageningen University
by the authority of the Rector Magnificus,
Prof. Dr A.P.J. Mol,
in the presence of the
Thesis Committee appointed by the Academic Board
to be defended in public
on Friday 15 March 2019
at 4 p.m. in the Aula.

E. Suarez Garcia
Biorefinery of functional biomolecules from algae,
255 pages.

PhD thesis, Wageningen University, Wageningen, the Netherlands, (2019)
With references, with summary in English

ISBN: 978-94-6343-595-6
DOI: 10.18174/470566

I now understand what it means to stand on the shoulders of giants.

Gracias a mis padres, hermanos y hermanas.

Table of Contents

Chapter 1	General introduction and thesis outline	9
Chapter 2	Energy efficient bead milling of microalgae: Effect of bead size on disintegration and release of proteins and carbohydrates	21
Chapter 3	Understanding mild cell disintegration of microalgae in bead mills for the selective release of biomolecules	51
Chapter 4	Techno-functional properties of crude extracts from the green microalga *Tetraselmis suecica*	79
Chapter 5	Selective and energy efficient extraction of functional proteins from microalgae for food applications	105
Chapter 6	Fractionation of proteins and carbohydrates from crude microalgae extracts using an Ionic liquid based-Aqueous Two Phase System	125
Chapter 7	Ionic liquid-assisted selective extraction and partitioning of biomolecules from macroalgae	153
Chapter 8	Mild permeabilization of microalgae cells for the selective release of biomolecules using ionic liquids	173
Chapter 9	General Discussion: Integrated biorefineries for algal biomolecules	195
References		215
Summary		235
Resumen		242
Acknowledgements		248
About the author		251

Chapter 1

General introduction and thesis outline.

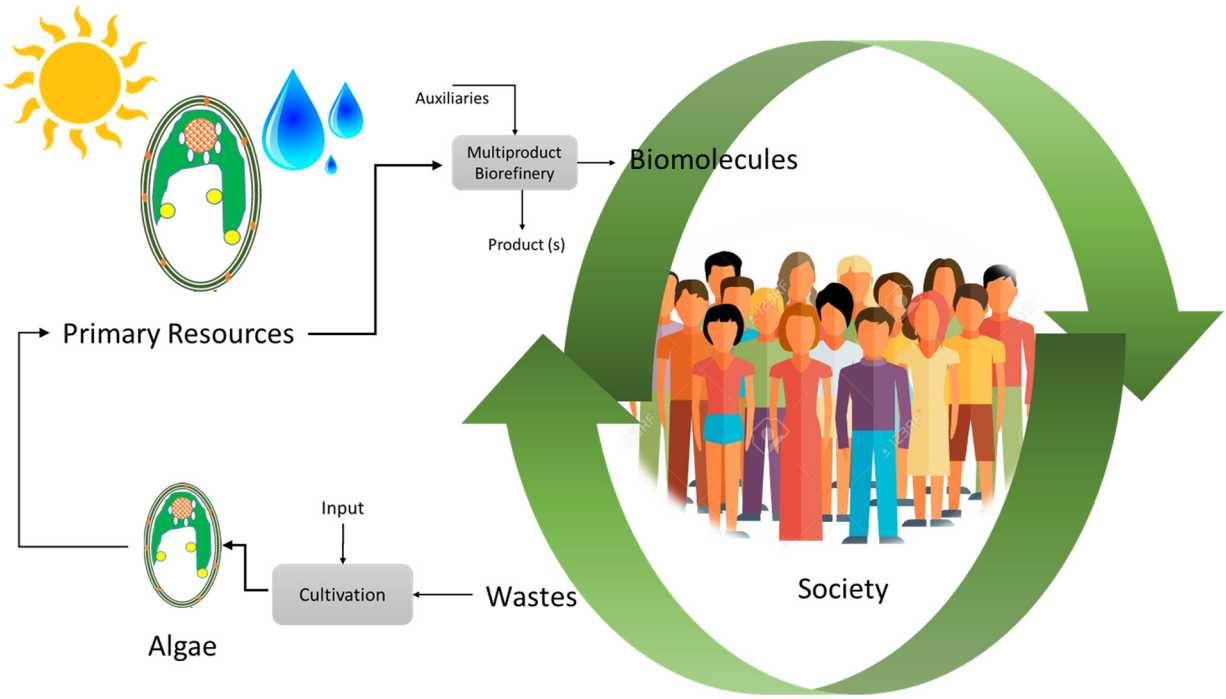

1.1. Supplying the needs of a growing population

With an increasing world population, expected to reach 9.5 billion by 2050, the demand for energy, consumer goods, feed and food will increase substantially. According the Food and Agriculture Organization of the United Nations (FAO), food production must increase 70 % by 2050 in order to supply the growing population, an expansion that will see major contributions from four main food groups: cereals, oil crops, sugar cane/beet and meat (Alexandratos and Bruinsma, 2012). The expansion in the production of these groups most likely will have a detrimental impact on the forests, fresh water reserves and on the availability of arable land (Zhang, 2013)

Although all food categories are crucial to a healthy diet, in this work we focus on proteins. The demand of proteins for human consumption in the year 2050 will depend on the consumer and production habits. Estimations based on maximum eating levels foresee an increment of 78 % from the current total consumption (Henchion et al., 2017). The current estimate of global protein consumption is 202 million tons year, from which plant proteins account for 57 %, meat 17% , dairy 10 % , fish 6% and others (animal-based) 10 % (Henchion et al., 2017).

Regarding Europe, a citizen consumes on average 22 kg (DW)/year of animal based proteins and 16 kg/year plant based proteins (FAO, 2001), figures that remained practically unchanged by 2013 (FAO, 2013). Europe demands 26 6 million ton of crude plant-based proteins, 35% of which is produced in Europe and the rest imported, mainly from USA and Brazil (EC, 2018). These imports, particularly from Brazil, represent a serious threat to the natural resources in the rain forest. In addition, it poses food security risks to Europe. In order to meet the future protein demand, without threatening natural resources and with minimum dependency on imports, novel renewable sources of proteins are needed.

1.2. Algae diversity and sustainability

Algae are photosynthetic organisms which occur in nearly all ecosystems around the planet. Two main groups are commonly recognized: microalgae (unicellular) and macroalgae or seaweed (multicellular) They make use of carbon dioxide, nutrients and solar energy to produce the building blocks necessary for their cell-structure and physiological processes, but also some strains are capable of heterotrophic metabolism (Gladue and Maxey, 1994).

In general, algae contain proteins, carbohydrates, lipids, pigments and ash (Trivedi et al., 2015). Although the composition varies greatly depending on the strain and cultivation conditions, averaged values for the two model organisms investigated in this thesis, *Tetraselmis suecica* (Michels et al., 2014a; Schwenzfeier et al., 2011) and *Ulva lactuca* (De Pádua et al., 2004; Postma et al., 2018), are shown in Table 1.

Table 1. Overall composition (DW) for the model organisms *T. suecica* (microalgae) and *U. lactuca* (macroalgae). Data from (Michels et al., 2014a; Schwenzfeier et al., 2011) and (De Pádua et al., 2004; Postma et al., 2018).

Composition	***T. suecica***	***U. lactuca***
Protein	40 %	15 %
Carbohydrates	35 %	55 %
Lipids	15 %	5 %
Ash	10 %	25 %

Certain microalgae strains, e.g., *Nannochloropsis granulata*, can accumulate up to 60 % (DW) lipids (Ma et al., 2014), while other strains, such as *Tetraselmis suecica* can accumulate up to 45 % starch (Kermanshahi-pour et al., 2014). Cyanobacteria are well known to produce large quantities of poly-peptides and pigmented proteins (Olguín et al., 1994; Trautmann et al., 2016), whereas microalgae can reach up to 60 % protein content depending on the culture conditions (Becker, 2007). Macroalgae are, in

general, rich in carbohydrates (Bikker et al., 2016), contain low amounts of lipids and the protein content is moderate. Red and green algae can reach up to 35 % (DW) of protein (Øverland et al., 2018).

1.3. Algae Structure

In broad terms, algae contain an outer cell-wall which encloses the cytoplasm and several organelles (Fig. 1). The cell-wall is usually composed of polysaccharides, with small content of proteins and ash (Baudelet et al., 2017; Domozych et al., 2012; Lahaye and Robic, 2007) The rigidity of the cell-wall depends on the nature of the polysaccharides present and on their interactions with proteins and other molecules (Alhattab et al., 2018). Some strains contain a pseudo cell-wall rich in exopolysaccharide mucilage (Safi et al., 2014a), which can break easily at high shear forces. Other strains are rich in more recalcitrant polymers such as sporopollenin (Desai et al., 2016a), cellulose (Baudelet et al., 2017) and pectin-like (Kermanshahi-pour et al., 2014)

The chloroplast contains all the machinery necessary for photosynthesis, including the light harvesting system and the pyrenoid, which is densely packed with the enzyme Rubisco (Ribulose-1,5-bisphosphate Carboxylase Oxygenase), and surrounded by starch granules (in green algae). Macroalgae (Fig. 1) are often subdivided in categories depending on their main pigments: red, green and brown (Ghadiryanfar et al., 2016), but also strains of microalgae (Fig. 1) can produce special photosynthetic pigments such as beta carotenes (Bharathiraja et al., 2015), astaxanthin (Desai et al., 2016a) and chlorophyll (green algae). Similarly, cyanobacteria are known to produce protein-pigment complexes (Cuellar-Bermudez et al., 2015; Olguín et al., 1994)

The diversity in composition of algae offers a great potential for industrial applications. This is because the physicochemical properties of the biomolecules are different depending on the algae strain (Draaisma et al., 2013), implying that their functional properties are also different (Guil-Guerrero et al., 2004). This diversity also constitutes

a challenge for the development efficient biorefinery strategies, which can be applied to multiple feed streams.

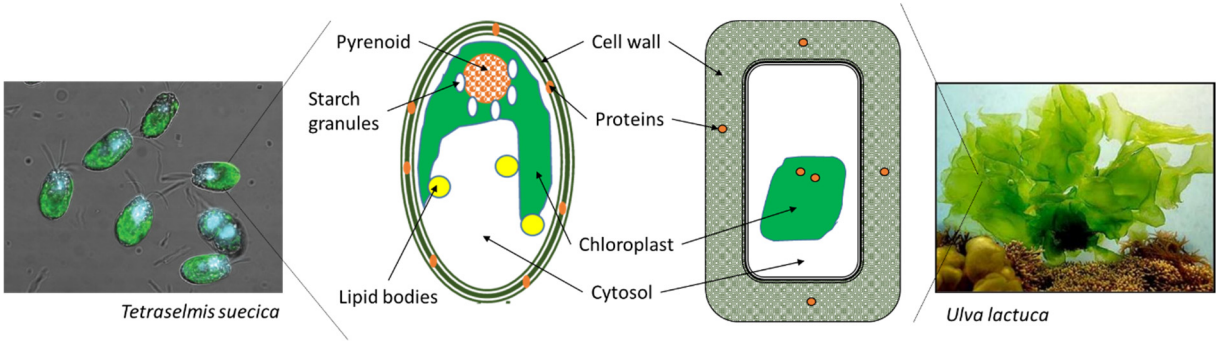

Figure 1. Schematic representation of *Tetraselmis suecica* (left) and *Ulva lactuca* (right), and corresponding microscope (Greenwell et al., 2010) and photography (Ginneken and Vries, 2018) images. Some important organelles and cell-structures are indicated.

1.4. From composition to functionality

The scope of algae goes beyond a mere source of biomolecules (Behera et al., 2015). In recent years, the interest of the scientific community and governments have shifted towards algae as source of nutraceuticals and bioactive molecules for food and feed (Bleakley and Hayes, 2017; Cuellar-Bermudez et al., 2015; Draaisma et al., 2013). The amino acid profile of algal proteins compares favourably to several reference protein sources, such as soy, milk and egg, indicating that a balanced diet can be derived from algal biomass (Becker, 2007; Fleurence, 1999; Galland-Irmouli et al., 1999; Vanthoor-koopmans et al., 2012). Besides the nutritional aspect, algae have also been explored as source of taste enhancers (Becker, 2007) and bioactive peptides with numerous medical and health benefits (Bleakley and Hayes, 2017).

Furthermore, the functional activity of algal biomolecules, in particular proteins, have been highlighted in several publications. Water and oil absorption capacities, emulsification, foaming and gelation behaviour (Gifuni et al., 2018; Guil-Guerrero et al., 2004; Samarakoon and Jeon, 2012; Schwenzfeier et al., 2014) of algal proteins are comparable to commercial isolates, indicating their remarkable market potential.

In addition to the nutritional and health benefits of algae proteins, several key aspects favour the utilization of algal biomass as renewable feedstock, since their cultivation is independent of fresh water and arable land, and their productivities are superior in comparison to traditional crops (Vanthoor-koopmans et al., 2012). However, in order to obtain algal biomolecules, efficient and mild extraction and fractionation processes are needed. These processes are commonly known as biorefinery.

1.5. Algae Biorefinery

Biorefinery is defined as "the sustainable processing of biomass into a spectrum of marketable products and energy" (Trivedi et al., 2015). Eppink et al., (2017) proposed that an algal biorefinery is similar to a modern dairy plant in which a mixture of proteins, carbohydrates and fat are processed and fractionated. However, due to the complex cell structure, the biorefinery of algae requires additional unit operations for harvesting and cell disintegration. Thus, the typical algae biorefinery involves a sequence of extraction and fractionation steps, requiring energy and auxiliaries (chemicals, solvents, membranes) and resulting in a main product and several side streams or by-products (Fig. 2).

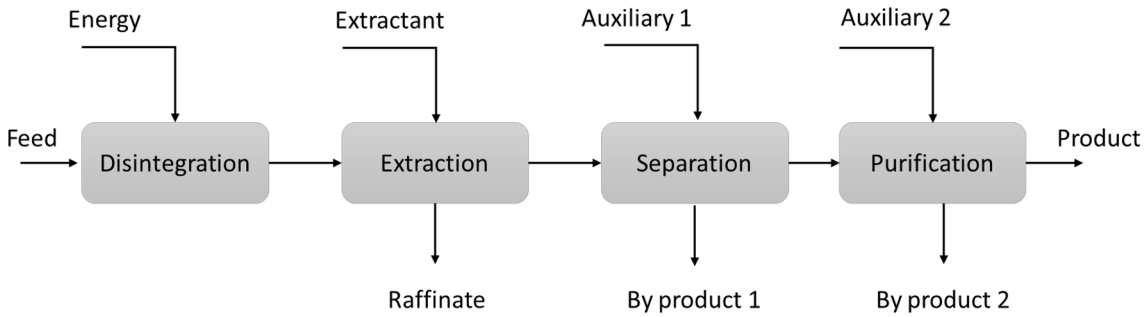

Figure 2. Typical sequence of unit operations in a generic biorefinery.

In general, the first step in the biorefinery of algae is cell disintegration. Upon disruption, intracellular organelles and molecules in the cytoplasm are accessible for extraction. Disintegration has been conducted using thermal, physical and chemical methods (Günerken et al., 2015; Phong et al., 2018b). Examples of physical methods

are mechanical disintegration (Postma et al., 2017), ultrasound (Parniakov et al., 2015) and pulse electric fields (’t Lam et al., 2017). These usually have high energy demands and/or lead to poor disruption performances. Enzymatic and chemical hydrolysis can result in high efficiencies (Sari et al., 2013), but have as main disadvantage the high costs and product degradation which impact negatively the process economics. Furthermore, if harsh conditions are used (e.g., high temperatures, extreme pHs), labile biomolecules can be damaged, which implies a loss of their potential commercial value.

The next step after/during cell disintegration is extraction, for which several technologies have been investigated (Eppink et al., 2017)(Vanthoor-koopmans et al., 2012). Most reported investigations make use of an aqueous buffer in which water-soluble molecules are extracted (Safi et al., 2014a). This implies that a substantial fraction of the molecules in the initial biomass remain in the insoluble phase, and thus, are regarded as a side product. Under alkaline (Ursu et al., 2014) or acid conditions (Ba et al., 2016), the extraction performance can be enhanced, however, if extreme pHs are used, the functional activity of proteins and other biomolecules can be compromised.

Similarly, ionic liquids have been implemented in algae biorefinery as green extractants. However, most reported processes use temperatures above 80^{o}C , high concentrations and long processing times in order to achieve significant biomolecule solubilisation (Malihan et al., 2017; Orr and Rehmann, 2016; Pezoa-Conte et al., 2015; Teixeira, 2012). Besides, most ionic liquids are expensive (Brandt et al., 2013), can be toxic and are difficult to recover due to their viscosity and negligible vapour pressure (Mai et al., 2014).

The separation and purification of algal biomolecules have only been reported in few investigations. This can be explained by the elevated cost of the purification processes, which makes it attractive only to high value products for the food, cosmetic and pharmaceutical sector (Eppink et al., 2017). The typical processes reported for algae

are ultrafiltration (Safi et al., 2014b; Ursu et al., 2014), pH-shift (Cavonius et al., 2015), aqueous two-phase partitioning (Jordan and Vilter, 1991), chromatography, dialysis (Schwenzfeier et al., 2011), three phase partitioning (Waghmare et al., 2016) and precipitation (Wong and Cheung, 2001).

Although the performance of a biorefinery process depends on the algal strain, the application of a sequence of unit operations like illustrated in Fig. 2, often leads to low yields or low purities (Tamayo et al., 2018). Therefore, there is a clear need to develop novel biorefinery concepts, which are mild, energy efficient and economically competitive.

1.6. From concept to reality

Currently, the production of bulk commodities from aquatic biomass is not feasible due to the high costs associated with production and biorefinery. Techno-economic estimations conducted by Ruiz Gonzalez et al., (2016) presented a production cost forecast of 3.4 € kg^{-1} biomass, under optimal cultivation conditions with regards to scale, location and market. Nevertheless, the production costs in practice can be as high as 69 € kg^{-1} (Acién et al., 2012), with realistic estimates at 8-11 € kg^{-1} after process optimization (Enzing et al., 2014), clearly indicating that only premium markets are feasible.

Globally, more than 24 million tonnes of algae are farmed globally, of which the vast majority corresponds to seaweed for traditional food products (Draaisma et al., 2013). From this, several processes have been developed successfully at commercial scale, typically combining simple cultivation strategies and products for high end markets. According to Bharathiraja et al., (2015), more than 1500 ton (DW) per year of algae are cultivated to produce carotenes and astaxanthin, which can be marketed at a price of 215-7150 € kg^{-1}. On the contrary, protein extracts, with a market price of 11-50 € kg^{-1}, are produced from 5000 ton/year algal biomass (Bharathiraja et al., 2015).

In terms of food products, whole algae are commercialized as blends in so called healthy foods, bread/pasta, candies and meat replacers (Becker, 2007). However, further commercial developments are hampered not only by high cultivation costs, but by the unpleasant taste and colour characteristic of algae biomass (Henchion et al., 2017). In this regard, biorefinery is crucial, in order to purify the biomolecules which are directly contributing to the functional properties, while leaving behind the compounds which are contributing to the off-taste.

The economic potential of algal-based products continues to increase at approximately 10 % per year (Enzing et al., 2014). Global marine biotechnology market in 2011 was estimated at € 2.4 billion, an increase of 240 % compared to the year 1999 (Enzing et al., 2014). Several companies have successfully launched protein-based products from algal biomass. An example of this is Corbion®, a company based in the Netherlands, through its subsidiary Terravia® commercializes AlgaVia®, a whole algal product with 65% protein for sale as a food additive (http://algavia.com/ingredients/proteins/).

There is an evident need to develop novel biorefinery approaches which allow the extraction of functional molecules under mild conditions and at high yields. Cost reductions can be achieved by integration of unit operations, efficient processing, decrease in energy/chemical consumption and multiproduct valorisation.

1.7. Aim of this thesis

The overall aim of this thesis is to understand algal cell disintegration, extraction and fractionation of biomolecules, and their potential applications in food products.

1.8. Thesis outline

This thesis covers three main aspects of algae biorefinery: Disintegration, extraction and fractionation. As illustrated in Fig. 3, the general content can be subdivided into

two main sections: mechanical disintegration by means of bead milling and extraction/fractionation mediated by ionic liquids.

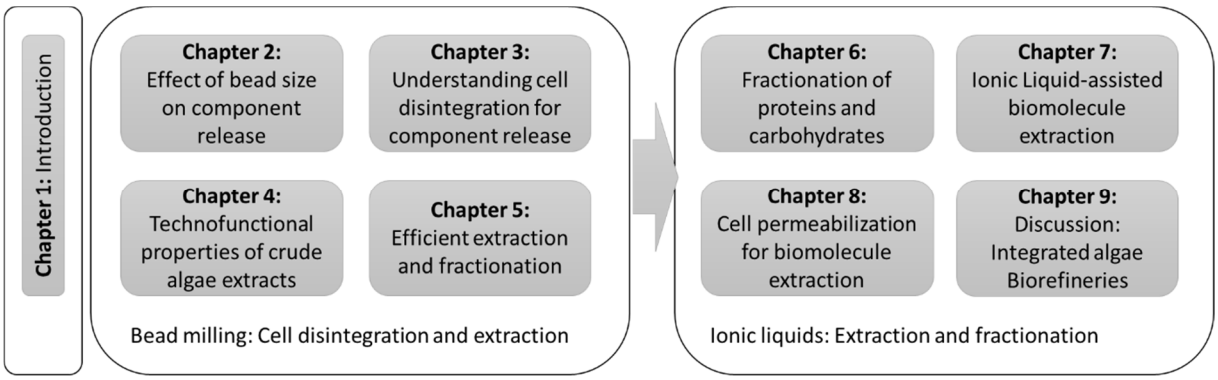

Figure 3. Thesis outline.

Chapter 2 investigates bead milling as an efficient disintegration technology for microalgae. The effect of bead size on the kinetics of cell disintegration, protein and carbohydrate release, yields and energy consumption, is studied for three industrially relevant microalgae strains. The lack of fundamental understanding on the disintegration mechanism in bead mills motivated the research performed in **chapter 3**. A model is proposed in order to predict the cell disintegration rates, having as input process and cell-related parameters

In **chapter 4**, bead milling and ultrafiltration are implemented in order to extract and fractionate biomolecules from microalgae and to evaluate the technical functionality of the resulting extracts. Similarly, **chapter 5** explores an efficient disintegration-extraction strategy to produce functional biomolecules with potential application as food ingredients.

In chapters 6-8, ionic liquids are investigated as promising extractants. **Chapter 6** examines the partitioning of biomolecules in crude extracts from microalgae in an aqueous two-phase system based using ionic liquids. An activity coefficient model is used to correlate the experimental data and the partition coefficients. **Chapter 7** and **chapter 8** investigate ionic liquids for the selective dissolution of biomolecules from macro and microalgae, under mild conditions. In both studies a single extraction step

is coupled to an ultrafiltration unit to allow biomolecule fractionation and to recover the spent ionic liquid.

An overview on the typical biorefinery approaches and several novel concepts which are recommended for future research are presented in the general discussion (**chapter 9**). We propose that new biorefineries must be based on the knowledge of cell structure and market application and must prioritize mild, selective and integrated approaches.

Chapter 2

Energy efficient bead milling of microalgae: Effect of bead size on disintegration and release of proteins and carbohydrates

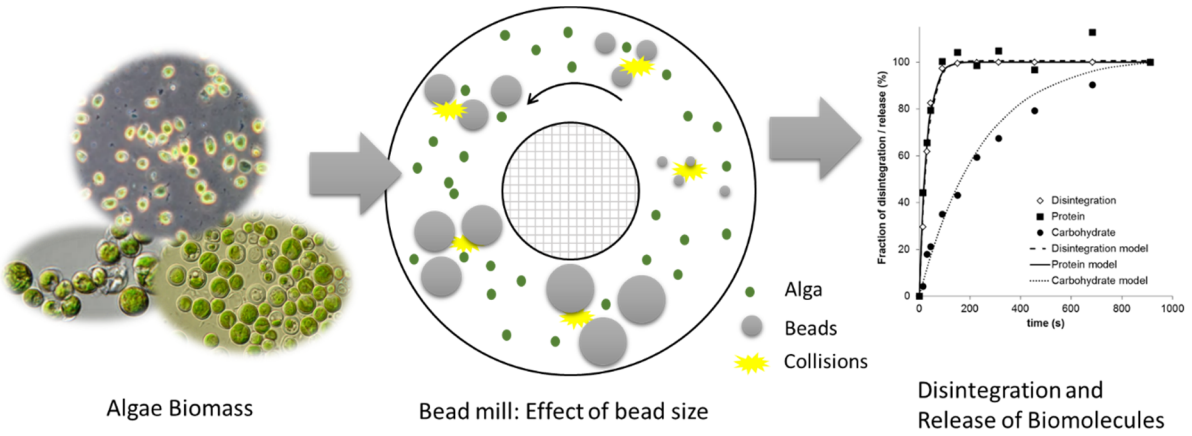

Published as:

P.R.Postma*, E.Suarez Garcia*, C.Safi, K.Yonathan, G.Olivieri, M.J.Barbosa., R.H.Wijffels, M.H.M.Eppink (2017). Energy efficient bead milling of microalgae: Effect of bead size on disintegration and release of proteins and carbohydrates. Bioresource Technology 224, 670-679.

* Equal contributions.

Abstract

The disintegration of three industry relevant algae (*Chlorella vulgaris, Neochloris oleoabundans* and *Tetraselmis suecica*) was studied in a lab scale bead mill at different bead sizes (0.3 mm-1 mm). Cell disintegration, proteins and carbohydrates released into the water phase followed a first order kinetics. The process is selective towards proteins over carbohydrates during early stages of milling. In general, smaller beads led to higher kinetic rates, with a minimum specific energy consumption of ≤ 0.47 kWh kgDW-1 for 0.3 mm beads. After analysis of the stress parameters (stress number and stress intensity), it appears that optimal disintegration and energy usage for all strains occurs in the 0.3-0.4 mm range. During the course of bead milling, the native structure of the marker protein Rubisco was retained, confirming the mildness of the disruption process.

1. Introduction

There is a growing demand for sustainable protein sources and bio-based products as an alternative for traditional agricultural crops. Microalgae are a potential source of renewable high value proteins, carbohydrates, lipids and pigments for food, feed and chemical industries (Vanthoor-Koopmans et al., 2013). Such products are typically located intracellular, either in the cytoplasm, in internal organelles or bound to cell membranes, and in most cases, the cells need to be disintegrated before extraction. This step can be done by chemical hydrolysis (Safi et al., 2014a), high pressure homogenization (Safi et al., 2014a), ultrasonication (Grimi et al., 2014), pulsed electric fields (Goettel et al., 2013; Grimi et al., 2014; Postma et al., 2016) or bead milling (Doucha and Lívanský, 2008; Günerken et al., 2015; Montalescot et al., 2015; Postma et al., 2015).

Bead mills are commonly applied in the chemical industry for the manufacture of paints/lacquers and grinding of minerals (Kula and Schütte, 1987) and have been successfully applied for the disintegration of yeast (Bunge et al., 1992), cyanobacteria (Balasundaram et al., 2012) and microalgae (Emre et al., 2016; Postma et al., 2015) for the release of intracellular products, under low energy inputs and mild conditions. The efficiency of cell disintegration in bead mills depends on several parameters such as chamber and agitator geometry, biomass concentration, agitator speed (i.e., tip speed of agitator), suspension flow rate, bead filling ratio, bead type and bead diameter. A high bead filling ratio (> 55 % v/v) was found to be optimal for disruption according to Montalescot et al., (2015). In addition, Doucha and Lívanský, (2008) found that zirconium oxide (ZrO_2) beads are more efficient than glass beads because of their higher specific density. Postma et al., (2015) investigated the disintegration of *C. vulgaris* by bead milling at lab scale using ZrO_2 beads with a diameter of 1 mm (65% v/v bead filling) and found that an agitator speed u_s of 6 m s^{-1} provides a lower specific energy consumption; though with a biomass concentration of 145 g kg_{DW}^{-1} a lower specific energy input could be obtained, a concentration of 87.5 g kg_{DW}^{-1} showed to have a better biomass suspension handling and higher protein yields.

Furthermore, for the disintegration of the microalga *Chlorella sp.* it was found that similar specific energy consumptions were achieved for the same flow rate, biomass concentration and agitator speed for beads of 0.3-0.4 and 0.6-0.8 mm (Doucha and Lívanský, 2008). On the other hand, the disintegration of the microalga *Scenedesmus sp.* and *Nannochloropsis oculata* was improved when smaller beads (0.35 – 0.6 mm) were applied (Hedenskog et al., 1969; Montalescot et al., 2015).

Bunge et al., (1992) studied the release of enzymes from *Arthrobacter* by means of bead milling. It was found that small glass beads (Ø 0.205-0.460mm) at moderate to high biomass concentrations and low to moderate agitator speeds result in optimal energy utilization. Schütte et al. (1983) found that smaller beads (0.55-0.85 mm) are more beneficial to release intracellular products from the cytoplasm of yeast over larger beads (1 mm). On the other hand, the larger beads are better at releasing products from the periplasm.

To describe the comminution of cells in bead mills as a function of different process parameters, Kwade and Schwedes, (2002) and Bunge et al., (1992) presented a very clear description of the so-called Stress Model (SM). The SM assumes that the disruption process in stirred media mills (e.g., bead mill) is governed by the number of stress events (i.e., bead to bead collisions) and by the intensity of such events. Quantitatively, this is expressed by the Stress Number (*SN*) (Eq. 1-2) and the Stress Intensity (*SI*) (Eq. 4) (Bunge et al., 1992; Kwade and Schwedes, 2002); two types of behaviors are also recognized: 1) disintegration/deagglomeration of cells, characterized by the fact that a cell is either intact or disrupted; and 2) grinding of crystalline materials, applicable for materials in which the particle size decreases during the milling process.

Accordingly, the *SN* (-) can be calculated for Disintegration (SN_D) and for Grinding (SN_G) as:

$$SN \propto \frac{\varphi_b(1-\varepsilon)}{\{1-\varphi_b(1-\varepsilon)\}c_V}\frac{nt}{d_b} \propto C \cdot SN_D \quad (1)$$

$$SN \propto \frac{\varphi_b(1-\varepsilon)}{\{1-\varphi_b(1-\varepsilon)\}c_V}\frac{nt}{d_b^2} \propto C \cdot SN_G \quad (2)$$

with

$$C = \frac{\varphi_b(1-\varepsilon)}{\{1-\varphi_b(1-\varepsilon)\}c_V} \quad (3)$$

where φ_b is the bead filling ratio (-), ε is the bead bulk porosity (-), c_V the volume cell concentration (-), n the agitator revolutions (s^{-1}), t the milling time (s) and d_b the bead diameter (m).

Furthermore, the *SI* (Nm) can be regarded as the magnitude of the kinetic energy of a single bead and can be calculated as:

$$SI \propto d_b^3 \rho_b u_s^2 \quad (4)$$

in which ρ_b is the specific density of the beads (kg m^{-3}) and u_s is the agitator tip speed (m s^{-1}). A cell can only be intact or disintegrated upon the release of the intracellular products. Therefore, an optimal stress intensity SI_{opt} can be considered. At or above SI_{opt} cells break with a single stress event; below SI_{opt}, multiple stress events are required to break the cell.

Consequently, the theoretical specific energy input is proportional to the product of the number of stress events times the energy of such events:

$$\tilde{E}_M \propto \frac{SN \cdot SI}{M} \quad (5)$$

where M is the mass of biomass (kg_{DW}) in the system and $\tilde{E}_M$ is the theoretical specific energy input (kWh kg_{DW}^{-1}).

The SM was first applied to microalgae by Montalescot et al., (2015). However, to our knowledge, it has not been applied in combination with the release of water soluble microalgae components. In large scale disruption trials for yeasts and bacteria, Schütte

et al., (1983) observed that cytoplasmic enzymes were better solubilized by smaller beads, and that periplasmic enzymes were more easily released by larger beads. We therefore hypothesize that smaller beads could interact more effectively with internal organelles over larger beads and thus are better able to release proteins (e.g., Rubisco) from the pyrenoids and carbohydrates from the cell wall or starch granules. If the process is operated above SI_{opt}, smaller beads would also lead to higher kinetics, higher yields and lower energy consumption.

The aim of this work is to investigate the effect of the bead size on the disintegration, release of water soluble components and energy consumption during the bead milling of *C. vulgaris*, *N. oleoabundans* and *T. suecica*.

2. Methods

2.1. Microalgae, cultivation and harvesting

Chlorella vulgaris (SAG 211-11b, EPSAG Göttingen, Germany) was cultivated according to Postma et al. (Postma et al., 2016).

Neochloris oleoabundans (UTEX 1185, University of Texas Culture Collection of Algae, USA) was cultivated using a fully automated 1400L vertical stacked tubular photo-bioreactor (PBR) located in a greenhouse (AlgaePARC, The Netherlands). The algae were cultivated in Bold's Basal medium (CCAP, 2015) at a pH value of 8.0 and the temperature was controlled at 30°C. The light intensity was set at an average of 400 µmol m^{-2} s^{-1}.

Tetraselmis suecica (UTEX LB2286, University of Texas Culture Collection of Algae, USA) was cultivated in repeated batches in a 25L flat panel PBR (AlgaePARC, The Netherlands) at 20°C. Ten fluorescent lamps (Philips 58W/840) provided a continuous incident light intensity of 373 µmol m^{-2} s^{-1}. The PBR was located in a greenhouse and thus, it was also exposed to natural light during the period October 2015 -January 2016 (Wageningen, The Netherlands). Mixing and pH control (pH 7.5) were provided by

sparging gas (0.254 vvm) composed of a mix of air and 5 % v/v CO_2. Walne medium was supplied at a ratio of 8.8 mL L^{-1} medium (Michels et al., 2014b).

To obtain a biomass paste, *C. vulgaris* was centrifuged (4000x g, 15 min) using a swing bucket centrifuge (Allegra X-30R, Beckman Coulter, USA) while *N. oleoabundans* and *T. suecica* were centrifuged (80Hz, ~3000x g, 0.75 m^3 h^{-1}) using a spiral plate centrifuge (Evodos 10, Evodos, The Netherlands). After centrifugation, the biomass paste of all three algae was stored at 4°C in the dark and used within two days. Prior to disintegration experiments, the biomass paste was resuspended in phosphate-buffered saline (PBS) (1.54 mM KH_2PO_4, 2.71 mM $Na_2HPO_4.2\ H_2O$, 155.2 mM NaCl at pH 7.0) to obtain a biomass concentration (C_x) of about 90 g kg^{-1}. C_x is expressed as g dried biomass per kg algae suspension.

2.2. Bead mill experimental procedure

The bead mill experiments were performed in a horizontal stirred bead mill (Dyno-Mill Research Lab, Willy A. Bachofen AF Maschinenfabrik, Switzerland) operated in batch recirculation mode. The operation procedure was previously described by Postma et al., (2015). In brief, the mill consists of a milling chamber ($V_{chamber}$ 79.6 mL) in which the beads are accelerated by a single DYNO®-accelerator (Ø 56.2 mm). To maintain the feed temperature at 25°C, a cooling water bath connected to a cooling jacket integrated in the milling chamber and a cooling coil in the feed funnel were used. Yttrium stabilized ZrO_2 beads (Tosoh YTZ®) with four diameters (0.3, 0.4, 0.65 and 1 mm, specific density ρ_b of 6 g cm^{-3}, bulk density ε of 3.8 g cm^{-3}) were applied. The beads were loaded at a constant filling volume of 65% v/v.

First order release kinetics was used to calculate the kinetic constant k_i for the disintegration percentage (k_{dis}), protein release (k_{prot}) or carbohydrate release (k_{carb}) as:

$$\frac{X_i(t)}{X_{i,max}} = 1 - e^{-k_i \cdot t} \qquad (6)$$

where $X_i\ (t)$ represents the degree of disintegration (Dis), the protein concentration or the carbohydrate concentration at time t, and $X_{i,max}$ represents the maximal degree of

disintegration, protein concentration or carbohydrate concentration in the liquid phase.

Upon reviewing our previous work (Postma et al., 2015), an error in the calculation of the residence time was noticed. The bead bulk density ε was not correctly incorporated, leading to an underestimation of the free volume in the milling chamber. The residence time t_r should be recalculated as:

$$t_r = t \cdot \frac{V_{Chamber,free}}{V_{total}} \quad (7)$$

$$\text{with } V_{Chamber,free} = V_{Chamber} \cdot \frac{\varepsilon}{\rho_b} \cdot \varphi_b \quad (8)$$

in which t is the batch disintegration time, $V_{Chambe,free}$ represents the volume inside the chamber filled with algae suspension (46.8 mL) and V_{total} (~185 mL) is the total batch volume. $V_{Chamber}$ is the milling chamber volume (79.6 mL), ε is the bead bulk density (3.8 kg m^{-3}) and φ_b is the bead filling ratio (0.65). For a correct comparison of the kinetic data in this work with the previous publication (Postma et al., 2015), the kinetic data and doubling times of the previous work (Postma et al., 2015) have to be multiplied and divided by a factor 0.595, respectively.

2.3. Analytical methods

Sample collection. Samples were taken at different time intervals directly from the feeding funnel, which was maintained under gentle stirring. The maximum sampled volume was always < 2.5 % of the feed volume. For all cases, bead milling experiments were conducted for 1 h (batch processing time).

Biomass quantification. The dry weight concentration was determined as described by Lamers et al. (2010). The DW/OD_{750} ratio for *C. vulgaris*, *N. oleoabundans* and *T. suecica* were determined experimentally to be 0.312, 0.350 and 0.537, respectively. These ratios were used to calculate the initial biomass concentration. The cell size and cell number were measured with a cell counter (Beckman Coulter Multisizer 3, USA). The

samples were diluted using Coulter® Isoton® II dilution buffer. The cell size and cell number were used to calculate the total cell volume.

Disintegration, protein and carbohydrate analysis. The disintegration percentage was analyzed as described by Postma et al., (2015), protein analysis on dry weight (DW) and the water soluble protein after bead milling were analyzed as described by Postma et al., (2015) according to the method developed by Lowry (Lowry et al., 1951). The carbohydrate content on DW and the water soluble carbohydrates after bead milling were determined as described by Postma et al., (2016) according to the method developed by Dubois (Dubois et al., 1956).
The protein and carbohydrate yield after bead milling are expressed as:

$$Y_i = \frac{C_i(t) - C_i(0)}{C_{i,Biomass}} \qquad (9)$$

where $C_i(t)$ and $C_i(0)$ are the concentrations of component *i* in the supernatant at time *t* and 0, respectively. $C_{i,Biomass}$ is the total content of component *i* within the total biomass (DW), where *i* can be protein or carbohydrates.

Starch analysis. To determine the total starch content on biomass DW, lyophilized algae were dissolved in 1 mL 80% ethanol and bead beated at 6000 RPM for 3 cycles with 120 s breaks in between cycles, after which the total starch content was determined using a commercial kit (Total Starch, Megazyme International, Ireland). The absorbance was measured at a wavelength of 510 nm with a spectrophotometer (DR6000, Hach Lang, USA).

Scanning Electron Microscopy. 150 µL microalgae suspension was applied on poly-L-lysine coated cover slips (Ø 8 mm) and incubated for 1h. Subsequently the samples were rinsed in fresh PBS and fixed for 1h in 3% glutaraldehyde in PBS. After washing twice in PBS, the samples were post-fixed in 1% OsO_4 for one hour, rinsed with demineralized water and dehydrated in a graded (30-50-70-90-100-100%) ethanol

series. Subsequently, the samples were critical point dried with CO_2 (EM CPD 300, Leica, Wetzlar, Germany). The cover slips were attached to sample holders using carbon adhesive tabs (EMS, Washington, USA) and sputter coated with 10 nm Wolfram (EM SCD 500, Leica, Wetzlar, Germany). The samples were analyzed in a high resolution scanning electron microscope at 2 KV at room temperature (Magellan 400, FEI, Eindhoven, The Netherlands). Images were contrast enhanced with Photoshop CS5.

Native PAGE analysis. Native PAGE analysis was performed as described by Postma et al., (2016). In addition, scanned gels were analyzed by ImageJ (IJ 1.46r) to convert the Rubisco band intensity in a density chromatogram. Subsequently, the chromatogram was integrated. From the peak areas, the relative density was determined over the course of bead milling:

$$Relative\ density\ (-) = \frac{A_{Peak,final}}{A_{Peak,t}} \qquad (10)$$

where $A_{Peak,final}$ is the peak area of Rubisco in the final sample and $A_{Peak,t}$ the peak area of Rubisco at time t.

2.4. Statistical analysis

Statistical analysis was performed by analysis of variance (ANOVA). When groups were significantly different at an α level of 0.05, Tukey's honest significance test was performed to find which groups differed.

3. Results and discussion

The overall effect of bead size is studied first in terms of kinetic rates and product yields. The mechanism of disintegration is then analyzed using the stress model and subsequently the specific energy consumption and selective protein release are presented.

3.1. Disintegration and product release kinetics

As a follow up of the work of Postma et al., (2015), in which a benchmark for the disintegration of *C. vulgaris* using 1 mm ZrO_2 beads was proposed, one goal of this study was to evaluate the effect of decreasing the bead size during bead milling of microalgae. Fig. 1 shows the fraction of cell disintegration, protein and carbohydrate release for *T. suecica* for 0.3 mm beads. It can be observed that a disintegration percentage and protein release of over 99 % can be reached in a total processing time of 400 s. Nevertheless, the maximal amount of carbohydrate was only found at the end of the experiment without reaching a plateau. For the other bead sizes and algae species, disintegration percentages >99 % were obtained. By means of Least Square Error Regression (LSER) the first order model (Eq. 6) was fitted to the experimental disintegration percentage, protein and carbohydrate release data. In all cases, the coefficient of correlation ranged between 0.8856 and 0.9997.

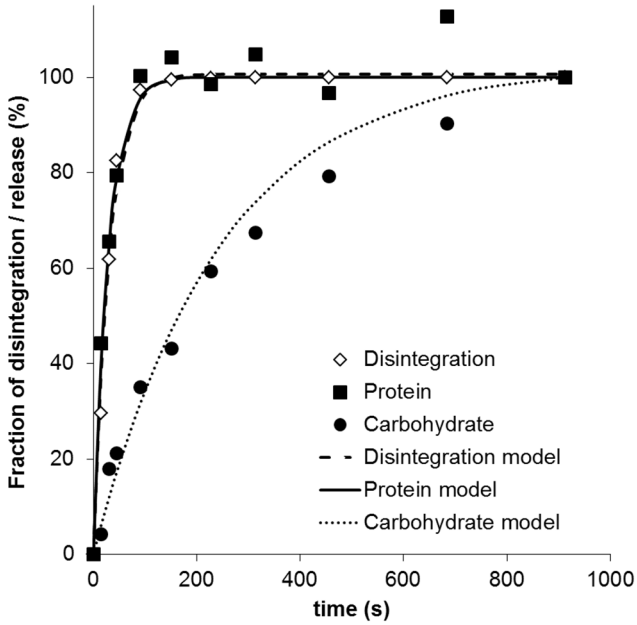

Figure 1. Relative disintegration and release of protein and carbohydrate for *T. suecica* using 0.3 mm beads.

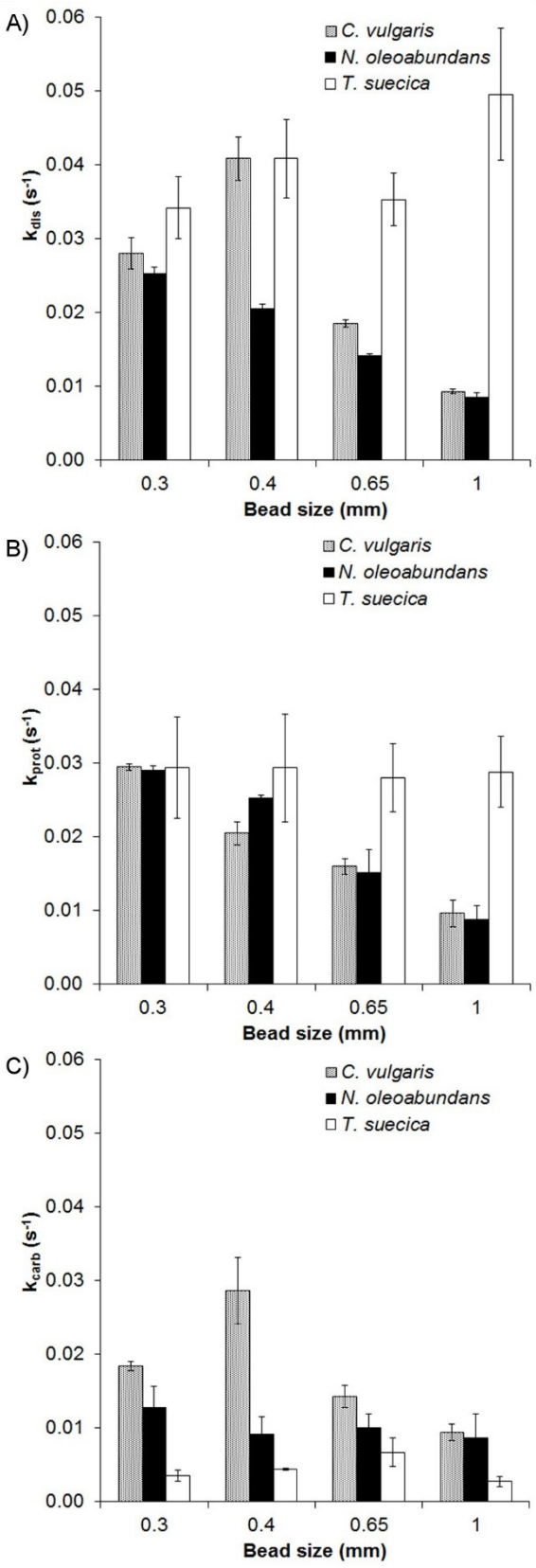

Figure 2. Kinetic constants for disintegration k_{dis} (A), protein (B) and carbohydrate (C) release as a function of the bead size (mm) for *C. vulgaris*, *N. oleoabundans* and *T. suecica.*

Fig. 2A-C presents an overview of kinetics constants for disintegration, proteins and carbohydrates release, respectively, for all algae strains and bead sizes. *Chlorella vulgaris* showed a clear optimum bead size of 0.4 mm for disintegration and release of carbohydrates. The k_{dis} of 0.041 ± 0.003 $s^{-1}$from this study represents a significant four-fold increase ($p < 0.05$) with respect to the benchmark of 1 mm beads (k_{dis} = 0.009 ± 0.001 s^{-1}). The protein release constant (Fig. 2B) using the 1 mm beads was similar to the previously determined benchmark (Postma et al., 2015). It can be observed that *C. vulgaris* shows an increasing trend in the protein release rate for a decreasing bead size.

For *N. oleoabundans* a clear upward trend in the k_{dis} and k_{prot} was observed when decreasing the bead size, but no evident optimum bead size appeared. The best disintegration results obtained with a k_{dis} of 0.025 ± 0.001 s^{-1} was 3 fold faster using 0.3 mm beads than the 1 mm beads. The carbohydrate release for *N. oleoabundans* did not show significant differences (p = 0.44). *Neochloris oleoabundans* and *C. vulgaris* exhibit several structural similarities, including cell size (average 3.3 µm and 3.2 µm, respectively) and morphology. Yet, we observed different kinetic constants, in particular, for carbohydrates. This is most likely caused by differences in the cell composition and cell wall structure of both algae, which contain cellulose-like polymer structures. The genus *Chlorella* is known to have amino sugars as constituents in the rigid cell wall, and it is suspected that chitin-like glycans are present (Kapaun and Reisser, 1995). To our knowledge, no literature exists on the polymeric links present in *N. oleoabundans*.

Among the strains tested, the disintegration rates of *T. suecica* were higher, and statistically independent of bead size. This clearly suggests a weaker cell structure (Kermanshahi-pour et al., 2014). A maximum k_{dis} of 0.050 ± 0.009 s^{-1} was determined, which is almost five-fold higher than the rates for *C. vulgaris* and *N. oleoabundans* (1 mm beads), but only 60% of the rate obtained by Halim et al. (2013) when disrupting *T. suecica* using ultrasound for similar batch volume and processing time. No significant trend was observed in the protein or carbohydrate release rate with respect to the

bead size. The similar trends and magnitudes of k_{dis} and k_{prot} for all strains suggest that most of the proteins that were measured in the soluble phase are released to the bulk directly upon cell bursting. Differences in k_{dis} and k_{prot} are probably due to diffusion limiting transport. The absolute carbohydrate release rate was lower for *T. suecica* compared to *C. vulgaris* and *N. oleoabundans*. From the literature it is known that *T. suecica* can accumulate significant amounts of carbohydrates in the form of starch granules (Kermanshahi-pour et al., 2014), which are hardly soluble. For *T. suecica* the measured starch-carbohydrate ratio was always between 0.5 and 0.9, while for *C. vulgaris* and *N. oleoabundans* it was below 0.3 and 0.1, respectively.

Montalescot et al., (2015) observed no difference in the kinetic constant for bead diameters of 0.325 and 0.625 mm for the disintegration of the microalgae *N. oculata* (algae diameter 3 µm). Their reported value (k_{dis} of ~0. 006 s^{-1}), however, is on average a factor 5-6 lower than the k_{dis} values obtained in the current study for similar bead sizes (0.3 – 0.65 mm).

3.2. *Protein and carbohydrate yield*

Different algae batches were used per bead size, and the composition (total protein, total carbohydrate and starch on biomass DW) of each batch was measured to calculate the product yield using Eq. 9; an overview is shown in Table 1.

According to Postma et al., (2015), 2.5 – 8 times more energy is required for continuing the bead milling process beyond 85-90% protein release in order to reach the maximum release. Therefore the yields in Fig. 3 are presented at 87.5% of the maximal release, which corresponds to 3τ (i.e., characteristic time of the protein/carbohydrate release kinetic). τ can be described as:

$$\tau = k_i^{-1} \cdot \ln(2) \qquad (11)$$

Considering the difference in protein and carbohydrate release kinetics, it is important to note that the time at which 87.5% release of each component is achieved is different for each species and bead size. For *C. vulgaris*, the highest water soluble protein yield

(Fig. 3A) of 36.3% was obtained using 0.4 mm beads. For both *T. suecica* and *N. oleoabundans*, no significant differences ($p > 0.05$) between the protein yields were found at different bead sizes. The protein yields obtained for *C. vulgaris* using the 1 mm beads were similar to the yields found in previous work (Postma et al., 2015) under the same operating conditions.

Table 1. Overview of biomass composition of *T. suecica*, *C. vulgaris* and *N. oleoabundans* for each bead milling experiment.

Experimental conditions		**Biomass composition**		
Algae	**d_b (mm)**	**Protein $\%_{DW}$ ± SD**	**Carbohydrate $\%_{DW}$ ± SD**	**Starch $\%_{DW}$ ± SD**
T. suecica	0.3	43.3 ± 2.7	21.2 ± 2.1	18.7 ± 0.1
	0.4	29.0 ± 0.0	33.7 ± 2.3	28.1 ± 0.9
	0.65	36.9 ± 0.3	16.0 ± 1.7	8.6 ± 0.1
	1	40.7 ± 3.5	23.6 ± 2.2	12.4 ± 0.2
C. vulgaris	0.3	53.1 ± 1.7	17.9 ± 0.6	4.6 ± 0.0
	0.4	57.0 ± 1.4	14.0 ± 0.7	2.8 ± 0.3
	0.65	53.4 ± 1.1	15.7 ± 0.3	5.3 ± 0.4
	1	51.6 ± 3.2	15.7 ± 0.4	3.4 ± 0.4
N. oleoabundans	0.3	47.3 ± 5.8	11.5 ± 2.1	1.3 ± 0.2
	0.4	50.8 ± 6.3	12.2 ± 1.3	1.0 ± 0.0
	0.65	51.2 ± 1.9	17.1 ± 2.5	1.5 ± 0.2
	1	55.6 ± 0.6	11.4 ± 1.7	0.9 ± 0.1

Schwenzfeier et al., (2011) found a water-soluble protein yield of 21% using *Tetraselmis sp.*, which is similar to the average yields found for *T. suecica* in this work. For *N. oleoabundans* under nitrogen replete cultivation conditions, up to 35% of water-soluble protein was released after bead milling (Emre et al., 2016). In addition, ’t Lam et al., (2017) found protein yields up to 50% after bead milling of *N. oleoabundans*. These studies, however, aimed at completed disintegration rather than optimizing energy consumption.

On average, a carbohydrate yield (Fig. 3B) of 62.7 ± 4.5% and 46.6 ± 17.2% was observed for *C. vulgaris* and *T. suecica*, respectively, independent of the bead size (based on Tukey’s test). For *N. oleoabundans*, the carbohydrate yield improved ($p < 0.05$) from 22.4% to 40.3% from 1 mm to 0.3 mm, respectively. However, a clear trend

could not be observed with decreasing bead sizes (Fig. 3B). Large variations in the carbohydrate yields were observed for *T. suecica*, which might be explained by natural variation or stress factors that altered the biomass composition. Analysis of the total starch content (Table 1) on biomass DW revealed that *T. suecica* contained considerably more starch with the same fluctuation as the yield, compared to *C. vulgaris* and *N. oleoabundans*. As was observed in the previous section, the carbohydrate release kinetics behaved independent of the bead size and were not influenced by the biomass composition.

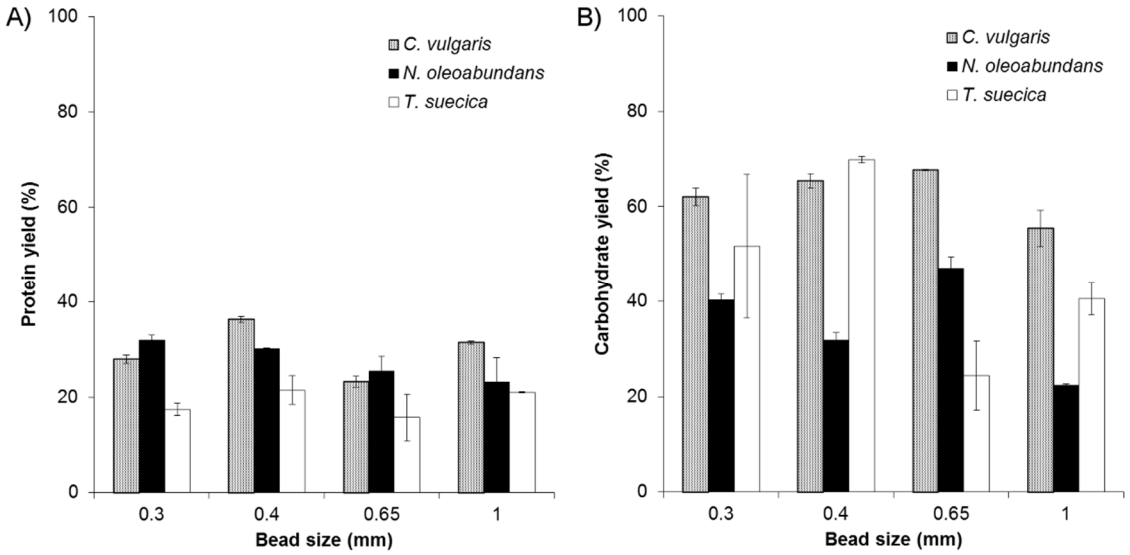

Figure 3. Protein (A) and carbohydrate (B) yield as function of the bead size (mm). The shown protein and carbohydrate yield correspond to 87.5% of the maximal release (i.e. 3τ).

3.3. Disintegration mechanism

The disintegration of microalgae cells and the breakage of organelles and internal structures to release water-soluble biomolecules are the result of the shear generated by collisions of beads in the mill chamber. Using Eq. 4, the *SI* was calculated to be $5.8 \cdot 10^{-6}$, $1.4 \cdot 10^{-5}$, $5.9 \cdot 10^{-5}$ and $2.2 \cdot 10^{-4}$ Nm per bead for 0.3, 0.4, 0.65 and 1 mm beads, respectively. Since the same agitator tip speed and volumetric bead filling was used for each bead size, the total kinetic energy for each bead size should be equal, under the assumption that all beads acquire the agitator's tip speed. This explains the statistically

similar rates observed for *T. suecica*, but cannot clarify why higher kinetic constants were measured at lower bead sizes for *C. vulgaris* and *N. oleoabundans.*

In this study, the *SN* (Eq. 1-2)), which quantifies the amount of stress events during bead milling, is a function solely of bead size. The corresponding *SN* for the case of disintegrations (Eq. 1) for all strains is presented in Fig. 4A-C. For *C. vulgaris* and *N. oleoabundans*, the disintegration percentage can be described by a single curve, independent of the bead size. This clearly indicates that the theoretical amount of shear (*SI*) and corresponding energy delivered by all beads sizes go beyond an optimal disruption barrier (SI_{opt}). A similar behavior was found for the disintegration of yeast cells by Bunge et al., (1992), where the stress frequency (similar to stress number) was found to describe the disintegration percentage by a single curve. On the contrary, for *T. suecica*, a dependence on the bead size with respect to the stress number can be observed (Fig. 4A). For a constant stress number (e.g. $1x10^7$), an increase in the bead size (i.e., increase in stress intensity) caused a larger disintegration percentage. This confirms the apparent trend (i.e., increased rate with increased bead size) in the disintegration kinetics (Fig. 2A). Furthermore, it shows that *SI* was below SI_{opt} because under the investigated bead diameters, bead sizes below 1 mm only gave the same level of disintegration when the stress number was increased.

When plotting the disintegration percentage as a function of the measured specific energy consumption E_M (Fig. 4D-F), the data for *T. suecica* are described by a single curve. Regardless of the bead size, the same energy is used to reach equal levels of disintegration. This is explained by the fact the specific energy consumption is proportional to the product of *SI* and *SN* (Eq. 5). For *C. vulgaris* and *N. oleoabundans*, on the contrary, in order to achieve similar disintegration percentages with different beads, a higher energy consumption is required; for both algae, the small range of beads (0.3-0.4 mm) leads to the lowest energy consumptions (i.e., optimal energy utilization was achieved). Fig. 4 supports the idea that the cellular structure of *N. oleoabundans* (i.e., cell wall/membrane) presents higher resistance to shear damage,

followed by *C.vulgaris* and *T. suecica*. Furthermore, Günther et al., (2016) reported the bursting energy for *C. vulgaris* in the range of $6.88 \cdot 10^{-3}$ – $2.52 \cdot 10^{-4}$ kWh kg_{DW}^{-1} dry biomass and attributed this variation to differences in cell turgor and cell elasticity. The corresponding disintegration energy for *T. suecica* was $1.87 \cdot 10^{-4}$ kWh kg_{DW}^{-1} (one order of magnitude smaller) as estimated by Lee et al., (2013).

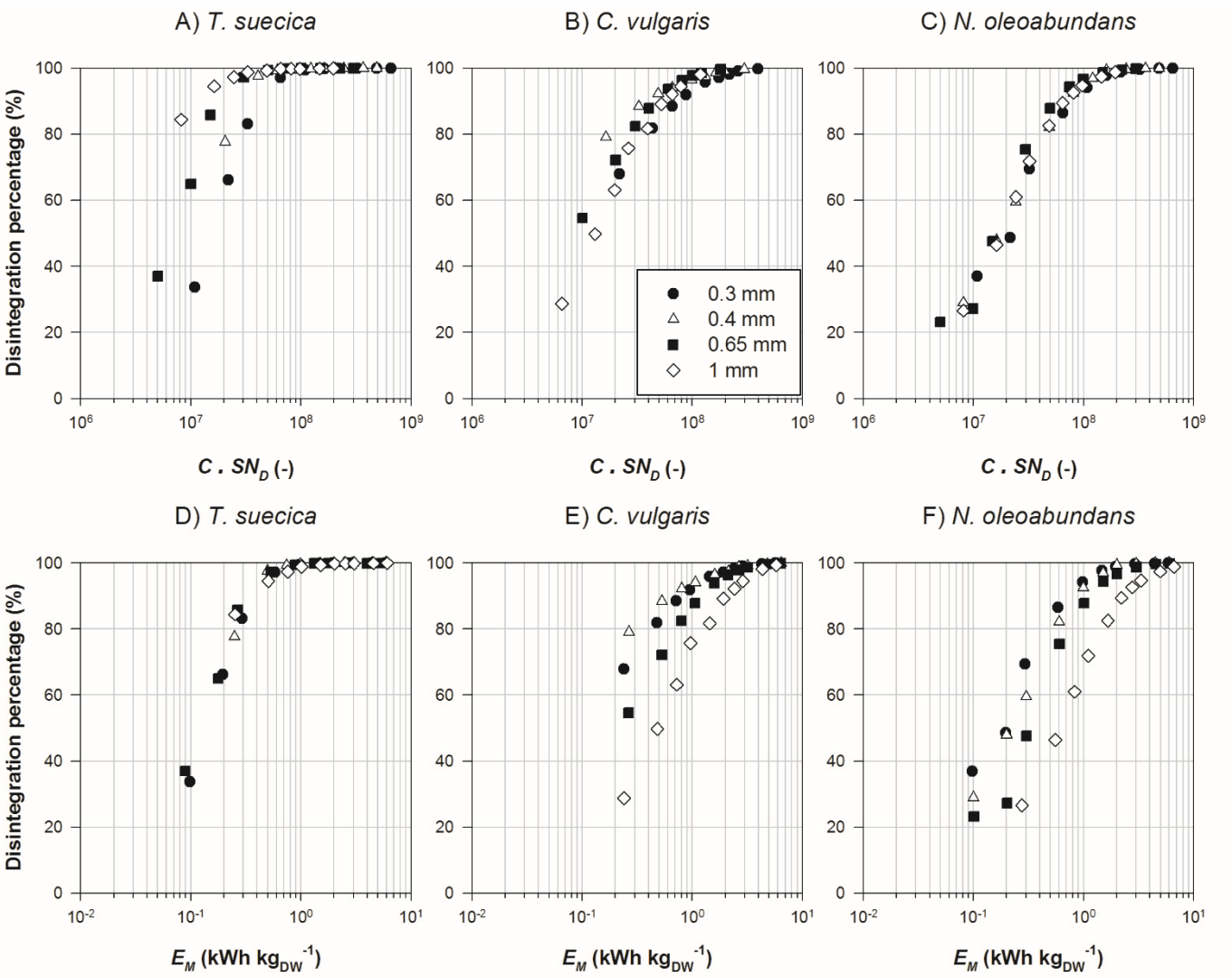

Figure 1 Semi-log plot of disintegration percentage (%) as a function of stress number $C \cdot SN_D$ (-) for *T. suecica* (A), *C. vulgaris* (B) and *N. oleoabundans* (C). Semi-log plot of disintegration percentage as a function of the specific energy consumption E_M (kWh kg_{DW}^{-1}) for *T. suecica* (D), *C. vulgaris* (E) and *N. oleoabundans* (F).

Scanning electron microscopy (SEM) micrographs of *C. vulgaris* were made prior to bead milling and after 50% and 87.5% disintegration using both 1 mm and 0.3 mm beads (Appendix Fig. A.1). Before disintegration, the cells have uniform spherical

shape, but appeared to be cracked upon bead impact after which the cell content was released, leaving an empty cell wall envelope. During disintegration, no visual differences could be observed in the breakage mechanism between bead sizes at the same disintegration rate of 87.5%.

For the release of proteins, a similar behavior was obtained with respect to the disintegration when plotting the fraction of release (normalized with respect to $Y_{Prot,max}$ of individual experiment) versus the *SN* or E_M (Appendix Fig. A.2). This suggests that most of the soluble proteins are present in the cytoplasm or inside weak organelles. Upon disintegration, all proteins quickly migrate to the bulk medium. Conceptually, the process of protein release is similar to disintegration.

On the other hand, the release of carbohydrates revealed a different tendency (Appendix Fig. A.3). For all three algae species, the release of carbohydrates was found to depend on both *SN* and *SI* when plotting the release fraction versus $C{\cdot}SN_G$ (Appendix Fig. A.3 A-C). Furthermore, it was observed that the release of carbohydrates can be described using the specific energy consumption at a first glance by a single curve (Appendix Fig. A.3 D-F). Similar behavior was also observed for weak/medium-hard crystalline materials like limestone (Kwade and Schwedes, 2002), from which we hypothesize that carbohydrates from the cell wall and starch granules behave like crystalline material. During the course of the disintegration process the cell wall debris and starch granules are stressed multiple times, breaking off polymers, oligomers and monomers, thereby solubilizing simple sugars.

3.4. *Specific energy consumption*

The specific energy consumption for the release of 87.5% (3τ) of the maximal protein release ($E_{M,3\tau}$) for the benchmark set with *C. vulgaris* was 1.71 kWh kg_{DW}^{-1} (Postma et al., 2015). This was confirmed in the current work for *C. vulgaris* and *N. oleoabundans* (which behave similarly) with a specific energy consumption of 1.42 kWh kg_{DW}^{-1} and 1.78 kWh kg_{DW}^{-1}, respectively. An overview of τ and $E_{M,3\tau}$ is given in Table 2, in which it can be observed that *T. suecica* can give the same protein release regardless of the

bead size using the same specific energy consumption on average 0.47 kWh kg_{DW}^{-1} (p = 0.65). In this regard, Lee et al., (2013) measured that the minimum specific energy $E_{M,min}$ required to break up one kg *T. suecica* is $1.87 \cdot 10^{-4}$ kWh kg_{DW}^{-1}, and compared it with an energy efficient disruption process (hydrodynamic cavitation) with an E_M of 9.2 kWh kg_{DW}^{-1} for a 1% w/w yeast suspension. In contrast, our findings (E_M: 0.47 kWh kg_{DW}^{-1}) show a twenty-fold improvement of E_M compared to that process. Nonetheless, it is clear that mechanical disintegration methods are highly energy inefficient since a large fraction of the total energy is used to displace beads and fluid and another fraction is lost due to mechanical dissipation. According to Eq. 5, the specific energy consumption of the system is proportional to the *SI* and *SN*. The theoretical specific energy input of the beads $\tilde{E}_{M,3\tau}$ at 87.5% release of the protein content was calculated for each experiment. The ratio of $\tilde{E}_{M,3\tau}/E_{M,3\tau}$ gives an indication of how much energy was utilized to give the beads momentum and which part of the energy was dissipated. For 0.3, 0.4, 0.65 and 1 mm beads (for all algae), this ratio was below 1%, 2%, 5% and 11%, respectively, showing that the total required bead energy decreases with bead size. This might be caused by the increased probability of impact at lower bead sizes due to a high *SN (*i.e., more beads colliding in the mill) while maintaining an *SI* above SI_{opt}. Moreover, this shows that running a bead milling process close to SI_{opt} provides extra potential energy savings.

Fig. 4E-F show that the energy utilization of the bead mill can be improved when smaller beads are applied during bead milling for *C. vulgaris* and *N. oleoabundans*. Decreasing the bead size from 1 to 0.3 mm can improve the energy utilization by a factor 3.3 and 3.9 ($p < 0.05$) for *C. vulgaris* and *N. oleoabundans*, respectively (Table 2). The lowest specific energy input found in this study was 0.45 kWh kg_{DW}^{-1} for *C. vulgaris* using a bead diameter of 0.3 mm resulting in a Y_{Prot} of 28% and a Y_{Carb} of 52%. Doucha and Lívanský, (2008) reported energy consumptions between 2.8 and 10.0 kWh kg_{DW}^{-1} at 77.7% or 90.6% disintegration of *Chlorella sp.*, though no product release was reported. Furthermore, $>55 \cdot 10^3$ kWh kg_{DW}^{-1} was required for 90% disintegration of *N.*

oculata by Montalescot et al., (2015). Safi et al., (2014a) reported a Y_{prot} 49.6% for an E_M of 7.5 kWh kg_{DW}^{-1} for *C. vulgaris* using high pressure homogenization. In addition, Postma et al., (2016) reported an E_M of only 0.55 kWh kg_{DW}^{-1} for disintegration of *C. vulgaris* using pulsed electric field, though Y_p was below 5%.

Table 2. Overview of characteristic process time τ, specific energy consumption $E_{M,3\tau}$, protein concentration C_{Prot}, carbohydrate concentration C_{Carb} and selectivity S at 87.5% protein release.

Experimental conditions		**Energy consumption**		**Product release**		
Algae	**d_b (mm)**	**τ ± SD (s)**	**$E_{M,3\tau}$ ± SD (kWh kg_{DW}^{-1})**	**C_{Prot} ± SD (g L^{-1})**	**C_{Carb} ± SD (g L^{-1})**	**S (C_{Prot}/C_{Carb})**
T. suecica	0.3	24.3 ± 5.7	0.47 ± 0.11	6.7 ± 0.5	2.4 ± 0.7	2.8 ± 0.4
	0.4	24.4 ± 6.1	0.48 ± 0.12	5.7 ± 0.8	6.7 ± 1.5	0.9 ± 0.8
	0.65	25.1 ± 4.1	0.45 ± 0.07	5.3 ± 1.7	1.5 ± 0.3	3.4 ± 0.8
	1	24.4 ± 4.1	0.49 ± 0.06	7.7 ± 0.0	1.8 ± 0.0	4.4 ± 0.0
C. vulgaris	0.3	23.6 ± 0.3	0.45 ± 0.01	13.3 ± 0.4	8.3 ± 0.1	1.6 ± 0.2
	0.4	34.0 ± 2.6	0.72 ± 0.05	19.3 ± 0.3	9.2 ± 0.1	2.1 ± 0.2
	0.65	43.5 ± 2.9	0.92 ± 0.06	11.0 ± 0.6	9.1 ± 0.1	1.2 ± 0.3
	1	73.7 ± 13.7	1.42 ± 0.26	14.7 ± 0.2	7.8 ± 0.7	1.9 ± 0.4
N. oleoabundans	0.3	23.9 ± 0.5	0.47 ± 0.01	13.5 ± 0.5	2.8 ± 0.3	4.8 ± 0.3
	0.4	27.4 ± 0.4	0.55 ± 0.01	13.8 ± 0.0	2.1 ± 0.2	6.7 ± 0.1
	0.65	46.7 ± 9.4	0.94 ± 0.19	11.9 ± 1.4	6.3 ± 0.4	1.9 ± 0.7
	1	80.8 ± 17.3	1.78 ± 0.38	11.3 ± 2.5	2.2 ± 0.4	5.2 ± 1.3

With respect to the estimated energy content of a microalgae being 6.82 kWh kg_{DW}^{-1}, and the assumption that no more than 10% of the energy content of the algae should be used for extraction/disintegration (National Algal Biofuels Technology Roadmap target, (US DOE, 2010)), the total energy for extraction should not exceed 0.682 kWh kg_{DW}^{-1} (Coons et al., 2014). The $E_{M,3\tau}$ values presented in this work show that the specific energy consumption for bead milling can drop below this target, especially with the smaller 0.3 mm beads. To our knowledge, this is the first study to present such figures using fresh biomass.

As described above, it is known that mechanical disintegration techniques are energy inefficient processes in which a large part of the energy is not utilized for the effective

breakage of cells. In a first assumption, the total energy is used to move parts (agitator), to displace beads and fluid, and dissipated into heat, which needs to be removed from the system by means of cooling. For the energy-efficient hydrodynamic cavitation process proposed by Lee et al., (2013), this means that only 0.002% of the required energy is utilized. Therefore, almost all energy needs to be removed as heat and thereby inevitably doubles the effective utilized energy. This would be true for all processes in which only an algae suspension is "moved" (e.g., high pressure homogenization, hydrodynamic cavitation, and ultrasound). However, in a bead milling process, not only is an algae suspension moved, but also the beads require energy to be displaced. The actual energy required for cooling of an algae suspension was also measured for *T. suecica*, using 0.4 mm beads and the conditions described in section 2.2. During the course of one experiment (1h) a ΔT of 18.2 °C was measured, which in terms of power, only corresponds to 4.2% of the E_M. Although the energy needed to cool down the engine is not yet included, it is evident that the cooling requirements could be ignored by running the bead milling shorter times (i.e., at 3τ) and by considering that after bead milling for 3τ (5 min) the suspension has heated up from 21.6 °C up to 24.3 °C, at which mild processing is still assured.

3.5. *Selective protein release*

An overview of the protein and carbohydrate concentration at 3τ protein release in the water-soluble phase is given in Table 2. *C. vulgaris* gives on average the highest absolute protein and carbohydrate concentration in the supernatant. High product concentrations are desirable if further fraction/purification is required, which reduces the amount of water that needs to be removed. Table 2 also provides an overview of the selectivity *S* (i.e., concentration ratio of released protein and released carbohydrate). In general, the process is selective towards proteins, in particular, at early stages of disruption (S > 1 for all times). The protein selectivity was highest for *N. oleoabundans*, followed by *T. suecica* and *C. vulgaris*. *S* can be regarded as a quality parameter for the bead milling process, i.e., a higher selectivity for the desired product

makes further processing easier (e.g. less impurities). Therefore, S could be used to tune the desired properties of the end product. Schwenzfeier et al., (2011) found that "algae juice" (i.e., supernatant after bead milling), "crude protein isolate" and "purified protein isolate" from *Tetraselmis sp.* have good solubility at pH values (5.5 - 6.5), a range where seed protein isolates show low solubility. These extracts exhibit a selectivity factor of around 2. In addition, it was shown that the carbohydrate fraction contributes considerably to the high emulsion and foam stability over a large pH range (Schwenzfeier et al., 2014). This suggests that the protein-carbohydrate concentrates found in the current work might possess similar functionality.

The proteins released by bead milling were analyzed by means of Native PAGE to provide insight about the size of the released proteins and whether they were negatively affected (i.e., degradation or aggregation) (Fig. 5A-C). Overall, it can be observed that the microalgal proteins have a large size distribution. To investigate the hypothesis that smaller beads are favorable over larger beads to specifically release products from intracellular organelles, Rubisco (Ribulose-1,5-biphosphate carboxylase oxygenase) was chosen as a biomarker. Moreover, it is mainly located in an intracellular organelle called the pyrenoid (Meyer et al., 2012), which is present in the investigated strains. Rubisco consists of 8 large subunits (~56 kDa) and 8 small subunits (~14 kDa) making a native size of ~540 kDa. As can be observed from Fig. 5A-C, Rubisco is released over time during the bead milling process. The release of native and active Rubisco was also observed in a previous study (Postma et al., 2016).

The band intensities of Rubisco were graphically processed to a density chromatogram allowing peak identification and integration. With respect to the maximal amount of Rubisco obtained, a relative density plot was created (Fig. 5D-F). The most distinct difference was observed between the 1 mm and the 0.3 mm beads. With respect to the different microalgae used in this study, *T. suecica* (Fig. 5D) did not reveal any difference in the specific release of Rubisco. This could be due to the starch sheaths which *T. suecica* synthesizes around the pyrenoid structure, which make the pyrenoid not easily accessible (van den Hoek et al., 1995). Both *C. vulgaris* (Fig. 5E) and *N.*

oleoabundans (Fig. 5F) showed that with a smaller bead size of 0.3 mm the release of Rubisco can be enhanced which further supports our hypothesis.

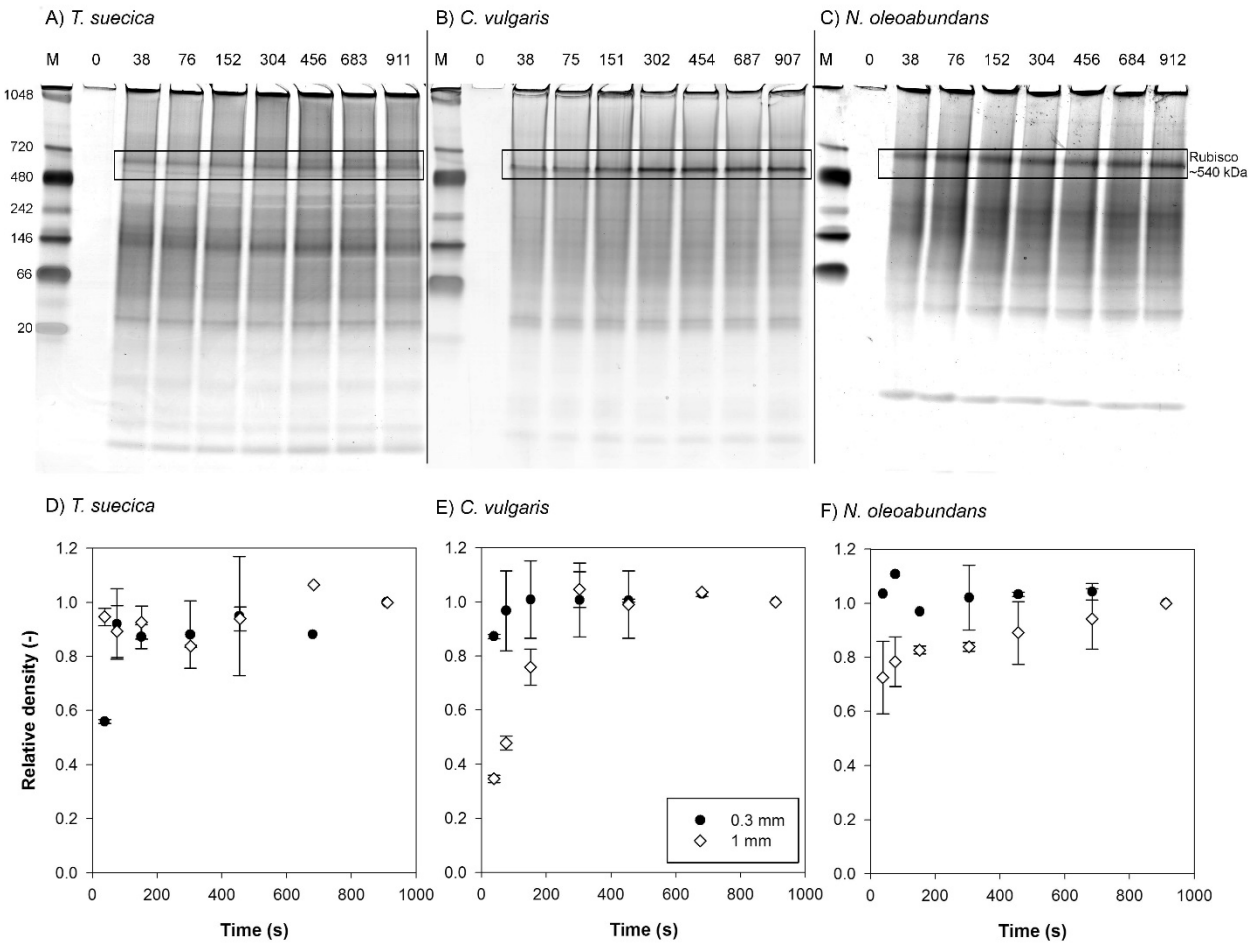

Figure 5. Native PAGE gel after bead milling using 1 mm beads for *T. suecica* (A), *C. vulgaris* (B) and *N. oleoabundans* (C). Values on left in kDa, M: marker. Lanes are indicated by the time in s after start of bead milling. The black box marks the Rubisco band (~540 kDa). Relative density (-) versus time of bead milling (s) for *T. suecica* (D), *C. vulgaris* (E) and *N. oleoabundans* (F).

4. Conclusions

The kinetics of disintegration and component release was improved for *C. vulgaris* and *N. oleoabundans* at lower bead sizes, but remained unaffected for *T. suecica*, which appeared to be significantly weaker. For all strains, energy consumption was reduced to ≤ 0.47 kWh kg_{DW}^{-1} and the native structure of the released

proteins was retained. Analysis of the stress parameters revealed that the bead mill was operated close to an optimum for *C. vulgaris* and *N. oleoabundans* at 0.3-0.4 mm beads. Finally, selective protein release was achieved in early stages of disintegration, for *C. vulgaris* and *N. oleoabundans*, using smaller beads.

Acknowledgements

We would like to thank Tiny Franssen-Verheijen of Wageningen University Electron Microscopy Centre for her help with the SEM, and prof. dr. Shirley Pomponi for proofreading of this manuscript. This project is conducted under the framework and financed by the IPOP Biorefinery from Wageningen University and Research Centre (The Netherlands) and the STW AlgaePro4U (nr. 12635). Part of this work was in cooperation with TKI AlgaePARC Biorefinery (nr. TKIBE01009)

Abbreviations

Symbol	Definition	units
A	Peak area	[AU]
C	Constant	[-]
C_i	Concentration of component *i* in supernatant	[g L^{-1}]
$C_{i,Biomass}$	Total concentration of component *i* in biomass	[g L^{-1}]
C_V	Volume cell concentration	[-]
d_b	Bead diameter	[m]
E_M	Specific energy consumption	[kWh kg_{DW}^{-1}]
$\tilde{E}_M$	Theoretical specific energy consumption	[kWh kg_{DW}^{-1}]
$E_{M,3\tau}$	Specific energy consumption at 3τ	[kWh kg_{DW}^{-1}]
$E_{M,min}$	Minimal specific energy consumption	[kWh kg_{DW}^{-1}]
k_{carb}	Carbohydrate release first order kinetic constant	[s^{-1}]
k_{dis}	Disintegration first order kinetic constant	[s^{-1}]
k_{prot}	Protein release first order kinetic constant	[s^{-1}]
M	Mass of biomass on dry weight	[Kg]
n	Agitator speed (revolutions)	[s^{-1}]
SN	Stress Number	[-]
SN_D	Reduced Stress Number for disintegration	[-]
SN_G	Reduced Stress Number for grinding	[-]
SI	Stress Intensity	[J] / [Nm]
SI_{opt}	Optimal Stress Intensity	[J] / [Nm]
t	Disruption/milling time	[s]
u_s	Agitator tip speed	[m s^{-1}]

V	Volume	[mL]
X_i	Degree of disintegration (Dis), protein concentration or carbohydrate concentration	[-]
$X_{i,max}$	Maximal degree of disintegration (Dis), protein concentration or carbohydrate concentration	[-]
Y_{carb}	Carbohydrate yield	[%]
Y_{prot}	Protein yield	[%]
ε	Bead bulk density	[kg m^{-3}]
φ_b	Bead filling ratio	[-]
ρ_b	Specific density beads	[kg m^{-3}]
τ	Characteristic time of process kinetic	[s]

Appendix

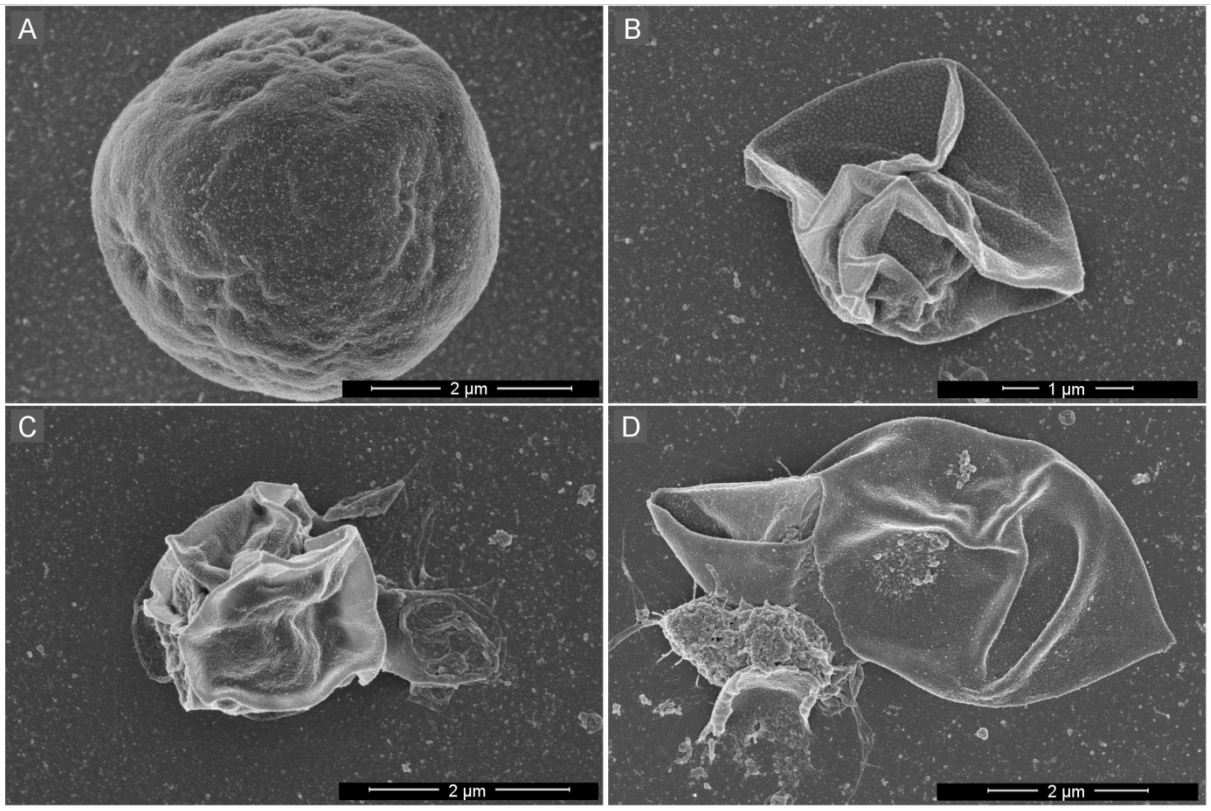

Figure A1. SEM micrographs of *C. vulgaris* before disintegration (A), after 50% disintegration using 1 mm beads (B), 87.5% disintegration using 1 mm beads (C) and 87.5% disintegration using 0.3 mm beads (D).

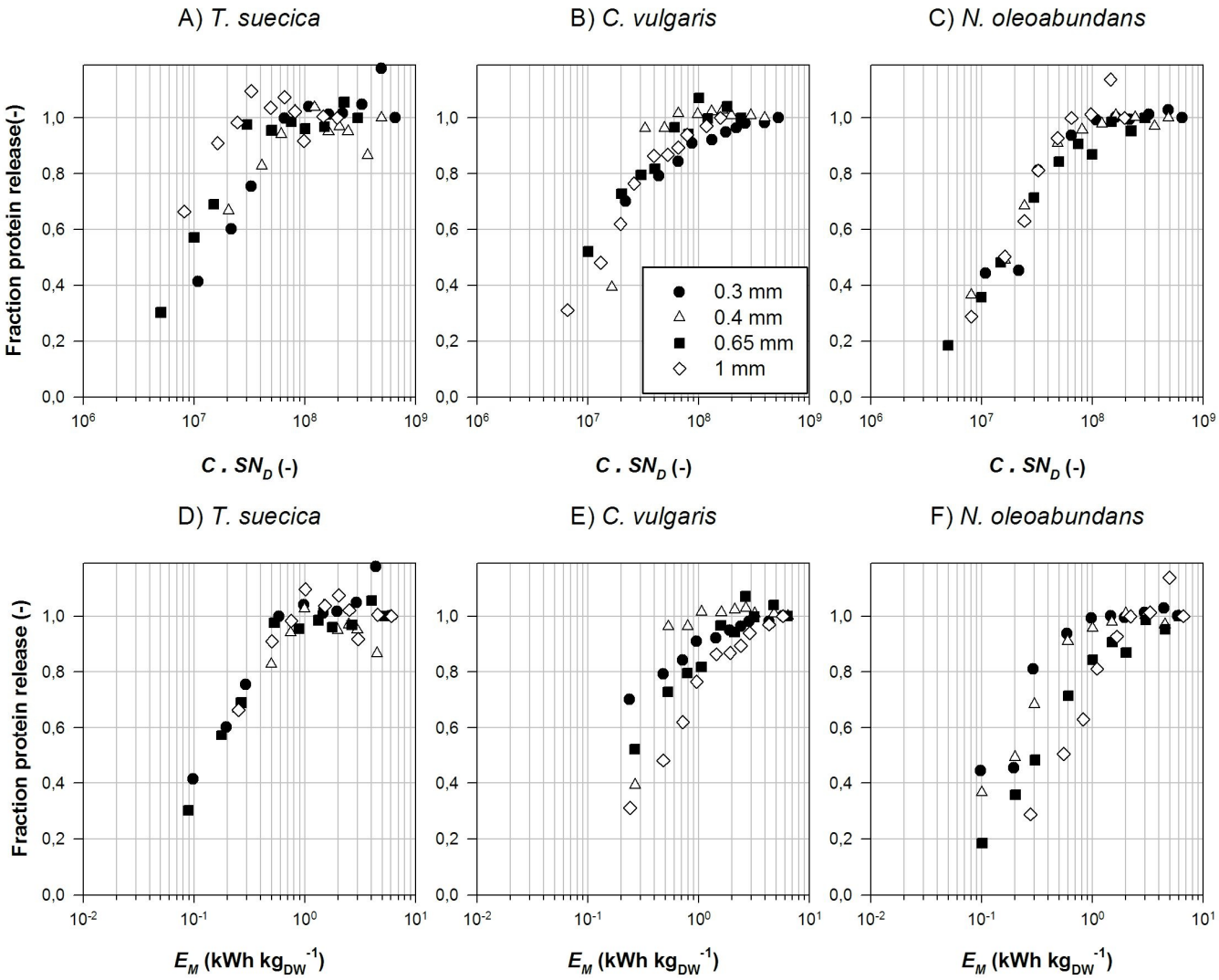

Figure A2. Semi-log plot of fraction protein release as a function of stress number $C{\cdot}SN_D$ (-) for *T. suecica* (A), *C. vulgaris* (B) and *N. oleoabundans* (C). Semi-log plot of fraction protein release as a function of the specific energy consumption E_M (kWh kg_{DW}^{-1}) for *T. suecica* (D), *C. vulgaris* (E) and *N. oleoabundans* (F)

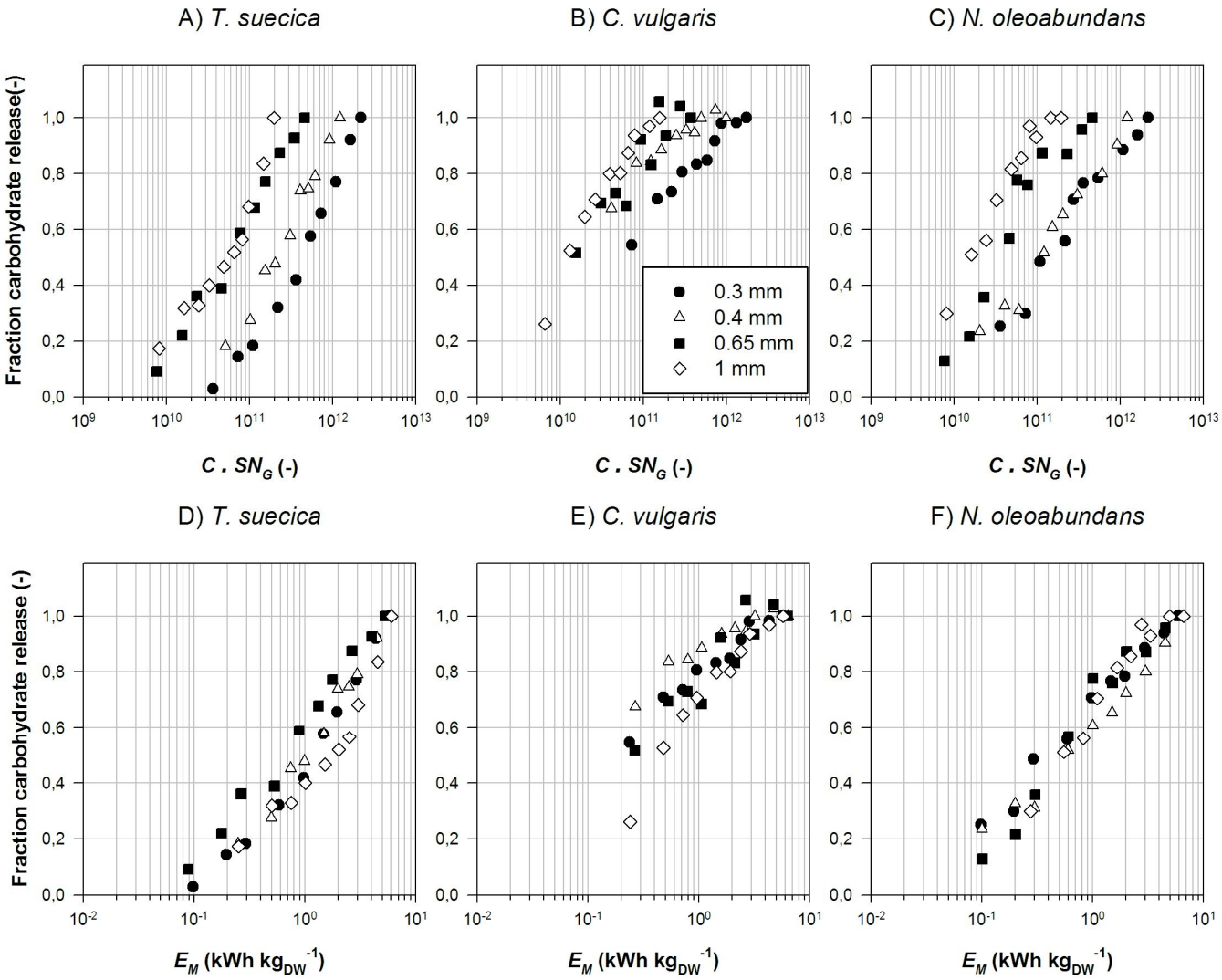

Figure A3. Semi-log plot of fraction carbohydrate release as a function of stress number $C{\cdot}SN_D$ (-) for *T. suecica* (A), *C. vulgaris* (B) and *N. oleoabundans* (C). Semi-log plot of fraction carbohydrate release as a function of the specific energy consumption E_M (kWh kg_{DW}^{-1}) for *T. suecica* (D), *C. vulgaris* (E) and *N. oleoabundans* (F).

Chapter 3

Understanding mild cell disintegration of microalgae in bead mills for the selective release of biomolecules

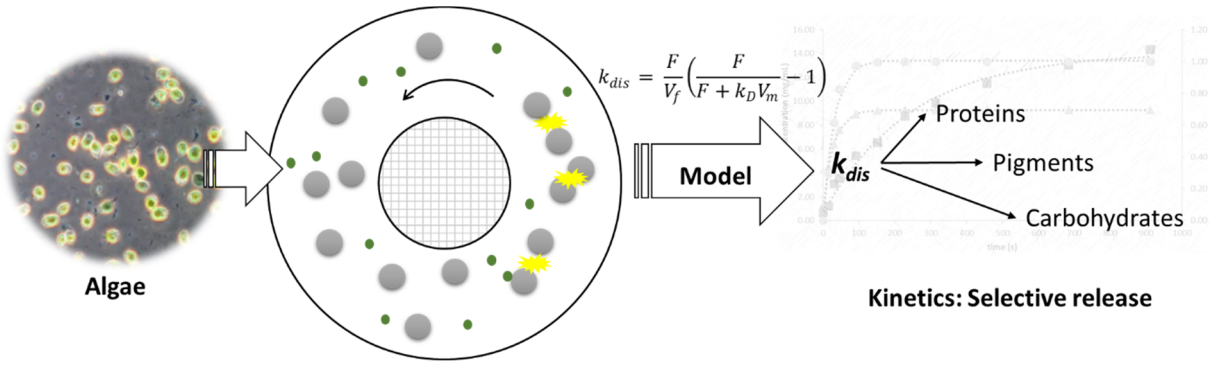

Bead Mill: Energy efficient Cell Disintegration

Submitted as:

E. Suarez Garcia, C. Lo, M.H.M. Eppink, R.H. Wijffels, C. van den Berg. Understanding mild cell disintegration of microalgae in bead mills for the selective release of biomolecules.

Abstract.

Cell disintegration is, in general, the first step in the biorefinery of algae, since it allows the release of biomolecules of interest from the cells into the bulk medium. For high value commercial applications, the disintegration process must be selective, energy efficient and mild. Developing a process with such features would demand extensive experimental effort. In the present study, we attempt to provide a tool for developing an efficient disintegration process via bead milling, by proposing a modelling strategy that allows the prediction of the kinetics of cell disintegration while having as input not only process parameters, but also strain-specific parameters like cell size and cell-wall strength. The model was validated for two different algal strains (*Tetraselmis suecica* and *Chlorella vulgaris*), at various values of bead size (0.3-1 mm) and bead fillings (2.5 – 75 %) and at two different scales of 80 and 500 mL. Since the kinetics of disintegration is proportional to the kinetics of release of biomolecules, the model can be further used for scale-up studies and to establish a window of operation to selectively target cells or metabolites of interest. Furthermore, the energy consumption in the mill was evaluated and it was found that operating at high bead fillings (> 65 %) is crucial to ensure an energy efficient process.

1. Introduction:

Microalgae have gained attention in the last years due to their rich composition and sustainable attributes. No fresh water and arable land are required for algae cultivation and the areal productivities are in general superior to typical crops (Draaisma et al., 2013). Algae can accumulate a variety of biomolecules, which can serve multiple industries: proteins for food/feed applications (Vanthoor-Koopmans et al., 2013), carbohydrates for materials and biofuels (Wijffels et al., 2010), lipids for nutraceuticals and biofuels (Adarme-vega et al., 2012), pigments and specialty chemicals (Cuellar-Bermudez et al., 2015) for high end markets, just to name the most common applications. However, in order to recover the valuable biomolecules from algae, it is necessary to access the cell wall and/or membrane under mild conditions. To achieve this, several methods have been reported in literature, including physical, biological and chemical treatments (Dixon and Wilken, 2018; Günerken et al., 2015; Phong et al., 2018b). Among these, bead milling has been proposed as an energy efficient, mild technology leading to complete cell disintegration and selective release in a short time (Suarez Garcia et al., 2018a).

Bead mills have been extensively studied for applications in mineral processing and biotechnology (Kwade et al., 1996; Kula and Schütte 1987). However, investigations regarding microalgae biorefinery have been limited to disintegration studies (Postma et al., 2015) using statistical tools, residence time distribution analysis and kinetic studies (Montalescot et al., 2015) and application of the stress model (Montalescot et al., 2015; Postma et al., 2017; Zinkoné et al., 2018). The stress model developed by Blecher et al., (1996) and Kwade et al., (1996) for the comminution of minerals, is based on the existence of stress events that lead to shear and eventual disintegration. Both the intensity and the frequency of such events are taken into account to quantify the power transferred to the product and the corresponding comminution (crystalline materials) or disintegration extent (agglomerates and cells). However, in the case of cells, the model does not include cell properties and assumes that the beads move at

a speed proportional to the tip speed. This is an important disadvantage as the beads develop a velocity profile in the milling chamber (Yamamoto et al., 2012).

A more complete theoretical understanding of the disintegration of microalgal cells in bead mills is lacking. It is important to take into consideration the mechanical properties of the cells (i.e., cell size, cell-wall toughness, biomass composition) as well as equipment characteristics and process variables (e.g., bead size, bead filling ratio, agitation speed, flow rate). In addition, as the release of biomolecules -proteins, carbohydrates and pigments- is linked to the kinetics of cell disintegration (Postma et al., 2017; Suarez Garcia et al., 2018a), a more clear understanding of the cell disintegration process can contribute to the design, operation, optimization and scale-up.

The present study aims at developing a modelling strategy for the disintegration of microalgae cells in bead mills. The model takes into consideration the mechanical properties of the cell as well several process and equipment variables. We have included the concept of effective disruption energy and have considered variable energy release as function of the mill radius. The model is validated with experimental data at various bead sizes and bead fillings, at two different scales and for two microalgae strains. We also propose that the kinetic constants can be used as a key parameter in process design studies, performance indicator, optimization and for scale-up purposes.

2. Material and methods

Microalgae cultivation and harvesting. Tetraselmis suecica (UTEX LB2286, University of Texas Culture Collection of Algae, USA) was cultivated using two different systems. For lab scale experiments, cultivation took place in a 25 L flat panel photo-bioreactor. Ten fluorescent lamps (Philips 58W/840) provided a continuous incident light of 373 ± 18 µmol m^{-2} s^{-1}. Mixing and pH ~ 7.5 were maintained by sparging gas (0.254 vvm) composed of a mix of air and 5 % v/v CO_2. For semi-pilot scale experiments, cultivation was done in a 300 L tubular horizontal photo-bioreactor. The system was subjected to

artificial light by 7 halogen lamps with a total incident light of 312 ± 25 µmol m^{-2} s^{-1} and a light:dark regime of 20:4 h. pH ~ 7 was controlled by sparging a blend of air and 7% (v/v) CO_2 at 1.07 mL min^{-1}. The culture was thoroughly mixed by continuous recirculation at a rate of 30 L min^{-1}. For both systems Walne medium was supplied at a ratio of 8.8 mL L^{-1} culture (Michels et al., 2014b). Temperature was maintained at 20°C via inner coils controlled by an external cooling unit. The photo-bioreactors were located in a greenhouse in AlgaePARC, Wageningen - The Netherlands. Cultures were harvested by centrifugation (80 Hz) using a spiral plate centrifuge (Evodos 10, Evodos, The Netherlands). After centrifugation, the biomass paste was stored in dark at 4°C. *Chlorella vulgaris* UTEX 2714 was kindly provided by Dr. Dorinde Kleinegris (UniResearch, Bergen-NO) and Jeroen de Vree (University of Bergen, Bergen-NO).

Algae disintegration. Prior to the disintegration experiments, the algae paste was re-suspended in phosphate-buffer saline (PBS: 1.54 mM KH_2PO_4, 2.71 mM $Na_2HPO_4 \cdot 2H_2O$, 155.2 mM NaCl at pH 7.0) to obtain the desired biomass concentration. Disintegration experiments were conducted in batch recirculation mode (Fig. 1A) using two horizontally oriented bead mills (Willy A. Bachofen AG Maschinenfabrik, Muttenz, Switzerland). Laboratory scale studies were conducted in a 0.079 L mill (DYNO-Mill Research Lab). To test the effect of the shear generated by the agitator on the cells, the mill was run without beads at 1500, 3500, and 5500 rpm and slurry concentrations of 30, 93, and 155 g kg_{DW}^{-1}. Additionally, disintegration studies were performed at bead filling ratios of 2.5, 10, 45, 65 and 75 %. These correspond to the percentage of the maximum achievable packing. Semi-pilot experiments were conducted in a 0.5 L mill (DYNO-Mill Multilab) at 75 % bead filling ratio and 1800 rpm. Both milling systems contained 0.5 mm Yttria-stabilised ZrO_2 beads (Tosoh YTZ®). Temperature was controlled at 25^{o}C by external cooling units fitted to the mill's cooling jacket. Equipment details are given in Table 1.

Power consumption and heat dissipation. Power consumption was estimated from the actual torque and agitator's speed used by the mill during operation. Heat dissipation

was assessed by running the mill (65 % of 0.5 mm beads, 100 g L^{-1} biomass slurry) without external cooling and by recording the temperature increase over a period of 20 min. The corresponding power was estimated from the temperature increase using as specific heat 3.87 J kg^{-1} K^{-1} and density of 1200 kg m^{-3} (Schneider et al., 2016).

Table 1. Dimensions of bead mills used for the disintegration experiments.

Section	unit	Laboratory	Semi-pilot
Chamber volume	mL	79.6	500
Chamber radius	mm	29.5	38.5
Accelerator radius	mm	25	31.8
Number of accelerators		1	3
Shaft radius	mm	15	13.3
Chamber length	mm	38.5	139.1
Accelerator length	mm	22	99.1
Shaft length	mm	7	40.0

Sample collection for kinetic studies. For each experiment, samples were collected at different times directly from the feeding chamber (Fig. 1A). The volume of the total samples never surpassed 5 % of the feed volume. After collection, samples were centrifuged at 20,000 RCF and 20°C for 20 min. The supernatants were separated and stored at 4°C prior to analysis.

Sample analysis. Dry weight was determined gravimetrically after drying for 24 hours to constant weight using a Sublimator 2x2x3 (Zirbus technology, GmbH). Analysis of the soluble phase was conducted as described by (Postma et al., 2017). In short, protein content was determined following the method of Lowry (Lowry et al., 1951) using Bovine serum albumin as protein standard. Carbohydrates were measured via the phenol-sulfuric acid method (Dubois et al., 1956) using glucose as standard.

Cell sizing and disintegration. Cell size was estimated with a Beckman Coulter Multisizer 3 (Beckman Coulter, Fullerton USA) with a fixed aperture of 50 μm. Samples were diluted with Coulter Isoton® II prior to analysis. The size distribution of

microalgae cells shows a peak at ~ 1-2 μm which corresponds to flagella, cell debris and bacterial contamination. In this study we report only the mean of the second peak, which correlates to intact cells. The disintegration analysis was conducted as presented in our previous publication (Postma et al., 2017) using a flow cytometer (BD Accuri® C6). Samples were diluted with PBS buffer prior to analysis and measured at fluidics rate of 35 μL min^{-1} and a constant volume of 15 μL. Forward scattering data was used to quantify the degree of disintegration over time.

Viscosity. The viscosity of the biomass slurries was determined using a dial reading viscometer Brookfield® LVT (AMETEK.Inc., USA). Measurements were conducted at ambient conditions.

Statistics. Until otherwise noticed, all experiments were performed in duplicates. Statistical analysis at 95 % confidence level was conducted using R (V 3.4.0). Significance was evaluated applying one way ANOVA. To compare significantly different means, a Tukey's Honest Significant Tests (HSD) was applied.

3. Model development

A schematic representation of the milling system under batch recirculation mode is shown in Fig. 1. A suspension containing alga cells n_x is fed from a hopper to the milling chamber via a conveying screw and recirculated back at a constant rate *F*. In the milling chamber, disintegration takes place as a result of the shear caused by colliding beads. The following assumptions are made:

i. As shown in Fig. 1A, an external stirrer is placed in the feeding hopper and thus, ideally mixed conditions are assumed (Eq. 1). The conveying screw forces the fluid through the milling chamber where strong mixing takes place, pushing the fluid back to the feed section. Here, ideally mixed conditions are considered (Montalescot et al., 2015) (Eq. 2):

$$V_f \, dn_{X,f} = F(n_{X,out} - n_{X,f})dt \qquad (1)$$

$$Fn_{X,out} = Fn_{X,f} - n_{X,out} \, k_D V_{ch} \qquad (2)$$

$$V_f = V_{susp} - (1 - \alpha * (1 - \varepsilon))V_{ch} \qquad (3)$$

Where ε is the porosity of the bead porosity due to packing, V_{ch} is the volume of the mill chamber, α is the bead filling ratio, $n_{X,f}$ and $n_{X,out}$ are the cell concentrations in the feed and mill respectively, and V_f the volume of feed. In Eq. 2, k_D [s^{-1}] is a constant given by:

$$k_D = \frac{V_x}{V_{ch}} \eta \frac{E}{E_X} \qquad (4)$$

Where V_X is the volume of a single cell, E is the total energy resulting from collisions in the mill and E_X the energy required to break a single cell. The fraction $V\,V_{ch}^{-1}$ represents the probability of cells to be hit by collisions in the mill while the fraction $E\,E_X^{-1}$ accounts for the excess of energy of collisions in the mill. While k_D can be seen as a constant accounting for cell death, η represents the "effective disruption energy" and gives an indication of the energy losses for other purposes rather than cell disintegration.

ii. In the mill chamber the accelerator rotates at a constant speed ω and transfers momentum to the fluid and to beads of equal size d_b (Fig. 1B). The movement of the beads is governed by several forces, including gravity, drag and buoyancy (Fig. 1C). By applying a force balance on an individual bead, the resultant bead velocity is given by:

$$u_b = u_L \left(1 - \exp\left(-\frac{18\,\mu}{\rho_b d_b^2}\, t\right)\right) \qquad (5)$$

Where μ is the liquid viscosity and ρ_b is the bead density. In Eq. 5 it was assumed that the effects of gravity and buoyancy cancel out at the opposite positions in the circular coordinate. In addition, centrifugal force, hydrodynamic lift, Coriolis force and bead rotation are neglected. This allows us to formulate bead velocity as function of the frictional force or Stokes' drag (Dogonchi et al., 2015). Eq. 5 predicts that $u_b \approx u_L$ even for very short times due to the small bead size. We therefore assume that the fluid and the beads are traveling at equal speeds. Consequently, u_b is a function of the radial position as there is a distribution of velocities between the accelerator and the

chamber wall. Furthermore, we consider beads to be homogeneously distributed in the mill and stacked in layers (Fig. 1B).

iii. The stacking of beads in layers has also been used by Doucha and Lívanský (2008) and allow us to have a distribution of number of beads and their velocities by layers (J to J_m), i.e., there are less beads close to the accelerator traveling at maximum speed (speed of the accelerator) and more beads close to the wall moving at low speeds or static. This also means that more layers are available for beads of smaller size. Computational estimations by Yamamoto et al., (2012) confirm these assumptions.

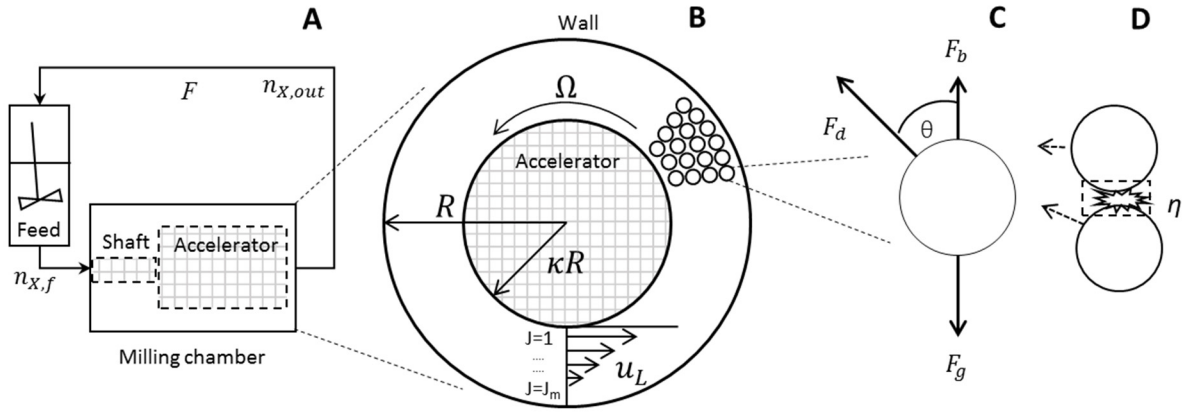

Figure 1. Schematic representation of the bead milling system. **A:** Milling chamber under batch recirculation mode. **B:** Frontal view of milling chamber with velocity profiles and bead stacking in layers. **C:** Force balance on a single bead (F_d=Drag, F_b=Boyancy, F_g=Gravity). **D:** Colliding beads and effective disruption energy η.

iv. The alga slurry behaves like a Newtonian fluid. Preliminary experimental data revealed negligible changes in viscosity during bead milling (data not shown). Thus, the *Navier-Stokes* equation in *Couette* flow (Bird et al., 2002) can be used to describe the fluid velocity distribution u_L in the annular section (Fig. 1B). The effect of gravity on the flow distribution and the axial velocity component are deemed negligible. Under these conditions, the velocity profile and shear rate ($\dot{\gamma}$) in the mill are given by (Gers et al., 2010; Michels et al., 2016; Yamamoto et al., 2012):

$$u_L = \frac{\Omega\kappa^2}{1-\kappa^2}\left(\frac{R^2}{r} - r\right) \qquad (6)$$

$$\dot{\gamma} = \frac{2\Omega\kappa}{1-\kappa^2} \qquad (7)$$

Where κ is the ratio of the radius of accelerator and mill chamber (R), Ω is the angular velocity and r is the radial position inside the mill. Correspondingly, the shear stress can be estimated by multiplying the shear rate and the fluid viscosity (Bird et al., 2002; Geankoplis, 1993; Michels et al., 2010). Moreover, Eq. 5-6 were applied to the two sections of the milling chamber: shaft and accelerator.

v. The moving beads carry kinetic energy which is released upon collisions (Fig. 1D). The frequency of collisions per unit volume (z) was estimated according to the kinetic theory of gases (Atkins and Paula, 2006) as proposed by Melendres et al., (1991b):

$$z = \frac{\sqrt{2}}{2} u_b \pi d_b^2 n^2 \qquad (8)$$

Where n is the number density of beads (amount of beads per unit volume). Since there is a distribution of velocities for the beads, Eq. 8 leads to a distribution of frequency of collisions as function of the mill radius.

vi. Several types of interactions can take place among moving beads, including impact, torsion, shearing and rolling (Beinert et al., 2015). Similarly, the interaction of colliding beads and cells can result in shear forces, compressive forces and impact forces (Pan et al., 2017). It was assumed that all the energy is released after single collision impacts (Fig. 1D) and that their energy is equivalent to the kinetic energy carried by the beads:

$$E_b = \rho_b V_b u_b^2 \qquad (9)$$

Where ρ_b and V_b are the density and volume of the bead, respectively. The total energy released by colliding beads (E) is therefore calculated as the product of the energy and frequency of collisions (Kwade and Schwedes, 2002):

$$E = \sum_{j=1}^{jm} E_{b,j} * z_j * V_j \qquad (10)$$

Where the subscript *j* refers to the radial stream layers in which the beads are moving in the milling chamber (Fig. 1B).

vii. The specific disruption energy E_X depends on the physiological structure of each species and on the media osmolality. The corresponding values for *T. suecica* (17.4 pJ) and *C. vulgaris* (22.8 pJ) were taken from Lee et al., (2013) and Günther et al., (2016) and corrected by the osmolality of the media (PBS buffer). Although cell disintegration can also take place as result of cumulative damage, such effects were not taken into consideration.

viii. Several authors have recognized the existence of a region between colliding beads in which disintegration effectively takes place (Bunge et al., 1992; Kwade and Schwedes, 2002; Melendres et al., 1991). We have introduced the concept of "effective disruption energy" η to account for the energy released after collisions that reaches the cells to cause damage or disintegration (Fig. 1D). Suarez Garcia et al., (2018) presented an overview of the specific energy consumption (E_m) of several bead milling processes reported in literature for microalgae disintergation; the average experimental value was $E_{m,exp}$ = 11.8 kWh kg_{DW}^{-1}. On the other hand, the average experimental energy for disintegration is E_x = 1.35x10^{-3} kWh kg_{DW}^{-1}. η was therefore calculated as $\eta = E_X/E_{m,Exp}$ =1.15x10^{-4}.

ix. Eq. 1 and Eq. 2 can be solved in order to estimate the amount of cells that are leaving the milling chamber $n_{x,out}$:

$$\frac{dn_{X,out}}{dt} = -k_{dis}\, n_{X,out}\ ;\ \ k_{dis} = \frac{F}{V_f}\left(\frac{F}{F+k_D V_{ch}} - 1\right) \quad (11)$$

Eq. 11 corresponds to a first-order kinetic model, as several authors have implemented to describe the disintegration kinetics of bacteria, yeast and microalgae in bead mills (Doucha and Lívanský, 2008; Kula and Schütte, 1987; Middelberg, 1995; Zinkoné et al., 2018).

Model solution. The values of k_{dis} for several experimental and processing conditions were estimated by solving equations 3 - 11 using Matlab® R2015b.

4. Results and Discussion

Cell damage and disintegration occur as result of the cumulative intensity of the forces that effectively reach the cells. The nature of such forces and their effect on the cells depend on the type of disintegration method. In general, differences in osmotic pressure, electric fields, eddy diffusion, turbulence, cavitation, hot spots and/or shear caused by mechanical elements are believed to be the responsible mechanisms of damage on the cell structure (Brookman, 1974). The rigidity of the cell envelope also plays a critical role to withstand shear forces, temperature or extreme local pressure gradients. Cell strength varies greatly depending on the microalgae strain and the cell physiology. Wang and Lan, (2018) reported critical stress values (i.e., pressure limit to ensure cell viability) for several algae species in the range $1.6x10^{-4}$ to 88 Pa. Low critical values are often occurring in strains lacking of a defined outer cell wall, and instead have peptidoglycan layers, plasma membranes or polysaccharides which can dissolve in the culture medium (Geresh et al., 2002). On the contrary, strains with a cell wall rich in polymers like cellulose or sporopollenin (Hagen et al., 2016), are highly resistant to stress and chemical treatments. *Tetraselmis suecica's* cell wall rich in a pectin-like polysaccharide (Kermanshahi-pour et al., 2014), which confers it relative resistance to shear stress (Michels et al., 2016). *Chlorella vulgaris* is believed to contain a cell wall rich in cellulose and hemicellulose (Abo-Shady et al., 1993) and therefore displays a superior resistance against external stress. In a milling chamber, however, shear can be originated from collisions, from friction between beads or from the turbulence generated nearby the accelerator or close to the wall. Several experiments were

therefore conducted in order to assess the effect of shear caused by agitation without beads.

4.1. Effect of shear on cell disintegration

The shear generated by the rotation of the agitator without beads, in the range 1500 to 5500 rpm, has a negligible effect on the cells of *T. suecica*. This was confirmed by measuring the percentage of cell disintegration and the amount of released proteins and carbohydrates after 20 min of operation. As presented in Fig. 2A, cells remain practically intact and the amount of released biomolecules varies only marginally ($p > 0.05$). Even after 1 h of operation, no significant effect was noted (data not shown). Under these operational conditions, the alga cells were exposed to theoretical shear forces up to 5.5 kPa (Eq. 7), which is well above the critical stress level of 88 Pa reported by Michels et al., (2016). However, 88 Pa may represent a stress condition rather than a cell damage threshold. In fact, Lee et al., (2013) reported a minimum experimental energy required to disrupt a cell of *T. suecica* of 7.1 ± 3.5 μN. By considering this force acting on the surface of a cell with an average diameter of 7 μm, the minimum theoretical force required to cause disintegration varies from 23.4 to 68.8 kPa. This confirms that agitation alone is insufficient to induce cell disintegration or release of proteins and carbohydrates from the alga under study.

Simulations of the fluid and bead flow profiles were conducted at agitation speeds of 1500 to 5500 rpm, bead sizes of 0.3-1 mm and fluid viscosities of $1x10^{-3}$ to 1.6 Pa s. It was found that the flow profile for the beads deviates significantly from the ideal *Couette* flow (Eq. 6) only at low viscosity values ($\mu < 0.01$ Pa s) and short times ($t < 0.1$ s). Since all disintegration experiments were conducted with biomass slurries displaying viscosities above 0.017 Pa s, significant differences in fluid and bead velocity are only taking place at $t < 0.05$ s. It is therefore assumed that $u_b = u_L$. It is worth noticing that in reality the flow patterns in agitated mills is greatly complex (Blecher et al., 1996) and depends on several variables. Our oversimplification, however, makes possible to

have an estimate of the velocity profiles which is used to calculate the energy released from the colliding beads.

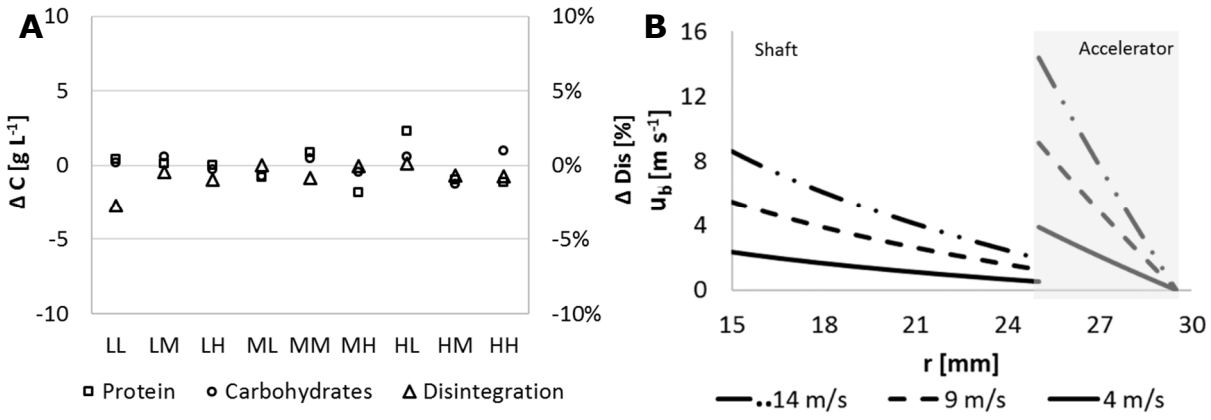

Figure 2. A. Variation in the percentage of disintegrated cells and released proteins and carbohydrates after 20 min stirring without beads. Letters in the y-axis refer to the operating conditions (L: Low, M: Medium, H: High) for biomass concentration: 30, 93, 155 g L^{-1}, and agitation: 1500, 3500, 5500 rpm**. B.** velocity profiles of beads in the milling chamber at several tip speeds [m s^{-1}].

The bead velocity profiles developed in the milling chamber at several agitation speeds in both the shaft and accelerator regions are shown in Fig. 2B. The simulations show that the beads acquire the tip velocity in the vicinity of the shaft or accelerator, and become nearly static at the chamber's wall. As expected, beads reach a superior speed over the accelerator where maximum energy densities are expected. Computational simulations conducted by Yamamoto et al., (2012) on horizontally oriented mills confirm our simulations: beads nearby the agitator move at maximum speeds while a larger number of beads are located around the proximity of the wall, moving at low speeds or almost static. Within the range of experimental conditions tested in the present study for cell disintegration, the Reynolds number (Eq. 12) varies in the interval $1x10^3 \leq Re \leq 9x10^3$ which corresponds to the Doubly periodic flow regime (Bird et al., 2002). This is a complex flow regime involving periodic waves traveling in the tangential direction. Only for slurries with a viscosity of 1.6 Pa s, Re ≈ 100, under which laminar flow can be considered. As the description of the flow under the actual regime is overly complex or unknown, the simplification to laminar regime is required.

$$Re = \Omega \rho_L (\kappa R)^2 \mu_L^{-1} \qquad (12)$$

4.2. Power consumption in the milling chamber

Experimental evidence indicated that shear from the accelerator alone -without beads- is not responsible for cell damage or disintegration during bead milling. In this regard, cell rupture takes place as a result of the energy released by colliding beads. This energy depends on the kinetic energy carried by the beads but also on the probability of the cells to be trapped in between colliding beads, where shear is strong enough to cause disintegration (Kula and Schütte, 1987). To further understand the energy distribution in the mill and its effect on cell disintegration, the power consumption of the laboratory scale mill under several conditions was measured and the results compared in Fig. 3A.

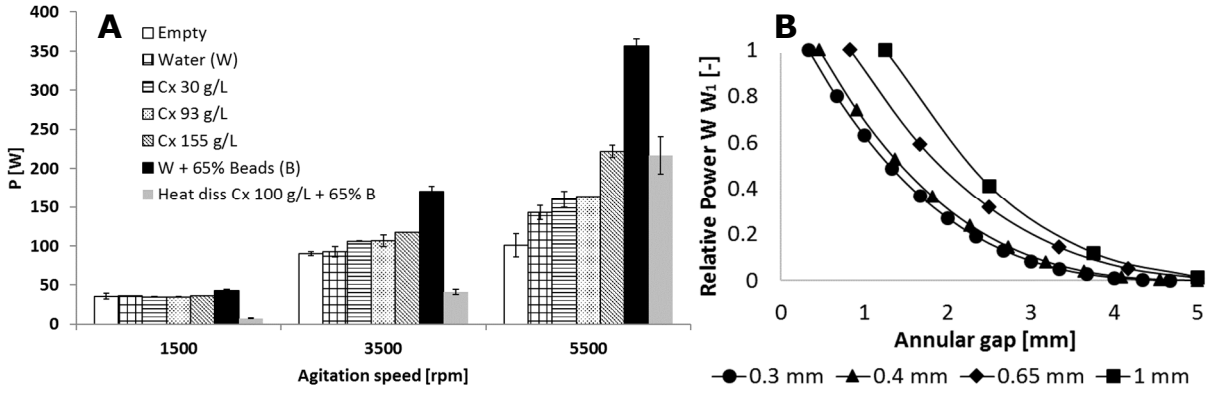

Figure 3. A. Power consumption for the laboratory scale mill under several processing conditions. **B.** Theoretical power released by colliding beads over the accelerator region for different bead sizes.

As can be seen, for a stirring speed of 1500 rpm, the power consumption remains practically stable even if the mill runs empty or with beads (65 %) and biomass slurry (155 g L^{-1}). The corresponding measured heat dissipation at this speed reaches 17.8 % of the total power spent. The power consumption further increases following an exponential tendency as the agitation speed augments to 3500 and 5500 rpm. This can be the result of the chaotic movement of the beads which forces the accelerator to demand higher power in order to keep a constant stirring speed. Under 3500 and 5500

rpm, the measured power dissipated as heat reaches 24.2 % and 60.8 % of the total respectively, confirming excessive shear generation. Furthermore, the simulations indicate that approximately 95 % of the total energy released from collisions in the mill is occurring in the region of the accelerator. This suggests the existence of a zone of high energy surrounding the accelerator and a zone of low energy located around the shaft and close to the wall. In Fig. 3B the theoretical energy released as a result of collisions over the accelerator is plotted against the radial position for several bead sizes and a constant stirring speed of 3500 rpm (Re≈5000). Indeed, at the vicinity of the accelerator, there is a high energy density which falls exponentially to the proximity of the wall. Blecher et al., (1996) also proposed an energy density distribution in agitated mills which is mainly determined by the velocity gradients of the fluid. Their simulations, however, predicted the existence of two high energy zones: Close to the agitator disc and close to the wall. Similarly to our predictions, the regions of high energy account for about 90 % of the total energy dissipated in the mill.

4.3. Simulation of disintegration rates

Experimental data and simulations show that colliding beads are required to cause cell disintegration and that the region surrounding the accelerator accounts for almost all (> 95 %) the energy released in the milling chamber. This energy is used to calculate the disintegration kinetics constants (k_{dis}) according to Eq. 11. The simulated k_{dis} as function of the accelerator's tip speed, cell size and cell strength are displayed in Fig. 4. As expected, the kinetic rates decrease as the cell strength increments from 5 to 80 pJ. This range covers a broad range of microorganisms and algae strains. For instance, the force required to break mammalian cells ranges from 1.5 to 4.5 µN (Mashmoushy et al., 1998), while for bacteria and yeast the ranges are 3 to 34 µN (Shiu et al., 2002) and 55 to 175 µN (Mashmoushy et al., 1998) respectively. *T. suecica* demands a force of 7.4 µN (17 pJ) (Lee et al., 2013) whereas for *C. vulgaris*, the force can increase 5 fold for high medium osmolality which directly affects the cell's turgor pressure (Günther et al., 2016).

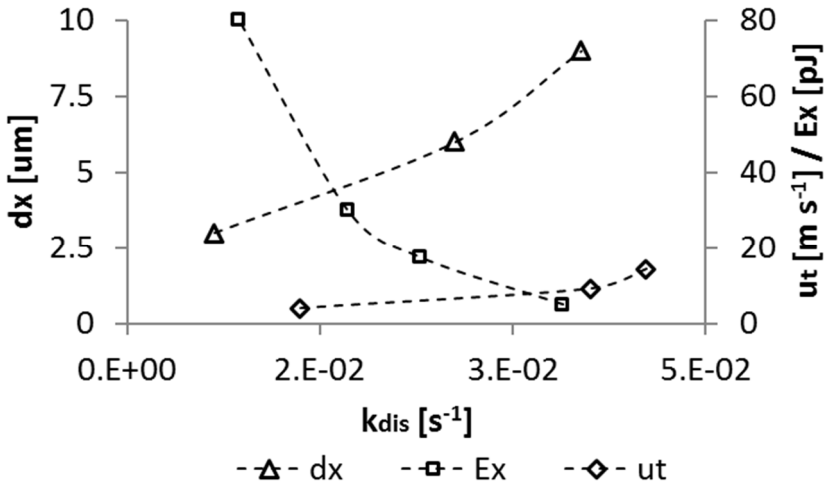

Figure 4. Predicted disruption rates k_{dis} [s^{-1}] at fixed bead size (0.5 mm) and bead filling (65 %) as function of cell size (d_X), cell strength (E_X) and tip speed (u_t). The standard value of the parameters are u_t = 6.8 m s^{-1}, E_X = 17.4 pJ and d_X = 6 um.

From Fig 4. it is also clear that Eq. 11 predicts an increment in k_{dis} as the cell size or the tip speed increases. This means that larger cells are more likely to be trapped in between colliding cells, which will result in higher degrees of disruption. Similarly, at larger agitation speeds both the frequency and intensity of collisions are superior and so does the energy available for disintegration. Tip speed, however, appears to have a marginal effect on the kinetic rates above 3500 rpm (u_t >9.6 m s^{-1}). This resembles what Kwade and Schwedes, (2002) defined as optimal stress intensity (SI_{opt}), a limit above which an additional energy input has a negligible effect on the comminution process. As also observed in Fig. 3A, heat dissipation becomes excessive beyond 3500 rpm, which will have an impact on product quality and operation costs. The model predictions can therefore serve to establish a window of operation to maximize disintegration and reduce costs. The tendencies simulated for d_X vs k_{dis} (Fig. 4) were experimentally observed by Zinkoné et al., (2018) and Montalescot et al., (2015) on a continuously operated bead mill for several algae strains of sizes ranging from 3 to 9 µm. The authors indicated that bigger cells are disintegrated more rapidly as the probability of larger cells to be trapped in between colliding beads is higher. On the contrary, smaller cells offer a higher resistance to disintegration, but recognized that the influence of cell strength was not assessed. Postma et al., (2017) also reported k_{dis}

for three different algae strains of sizes ranging from 3.1 to 7.6 µm; similar observations were made, but the results were explained considering differences in cell strength rather than on cell size. To our knowledge, the present study is the first attempt to incorporate cell strength to predict disintegration rates for microalgae in bead mills.

4.4. Model validation

Model predictions as given by Eq. 11 were validated against experimental data collected in this investigation along with data published by Postma et al., (2015) and Postma et al., (2017). In all cases the same bead mill and operation mode were used. In Fig. 5, the kinetic constants reported by Postma et al., (2015) for the disintegration of *C. vulgaris* as function of tip speed (u_t) and biomass concentration (C_X) are compared against the model estimations. The model predicts that k_{dis} increases at higher u_t, which is due to a superior kinetic energy delivered by the colliding beads, and remains practically stable at various C_X. In this regard, the published data is contradictory and appears to depend on the system under investigation. Some studies find a positive effect of C_X on k_{dis} while others report an optimal, negative or negligible effect for algae and yeast (Doucha and Lívanský, 2008; Montalescot et al., 2015). It appears that biomass concentration is important mainly to ensure low specific energy consumptions.

The data from Postma et al., (2015) show a slight increase of k_{dis} as function of u_t, and a more pronounced increment of k_{dis} at higher values of C_X. Considering the uncertainty associated with the experimental data (≈21 %) the model shows acceptable predictions, except at u_t =12 m s^{-1} where deviations are significant. This indicates that the energy dissipated at high agitation rates is larger in practice than estimated in the model and thus, it suggests that a smaller value of η is needed for such conditions.

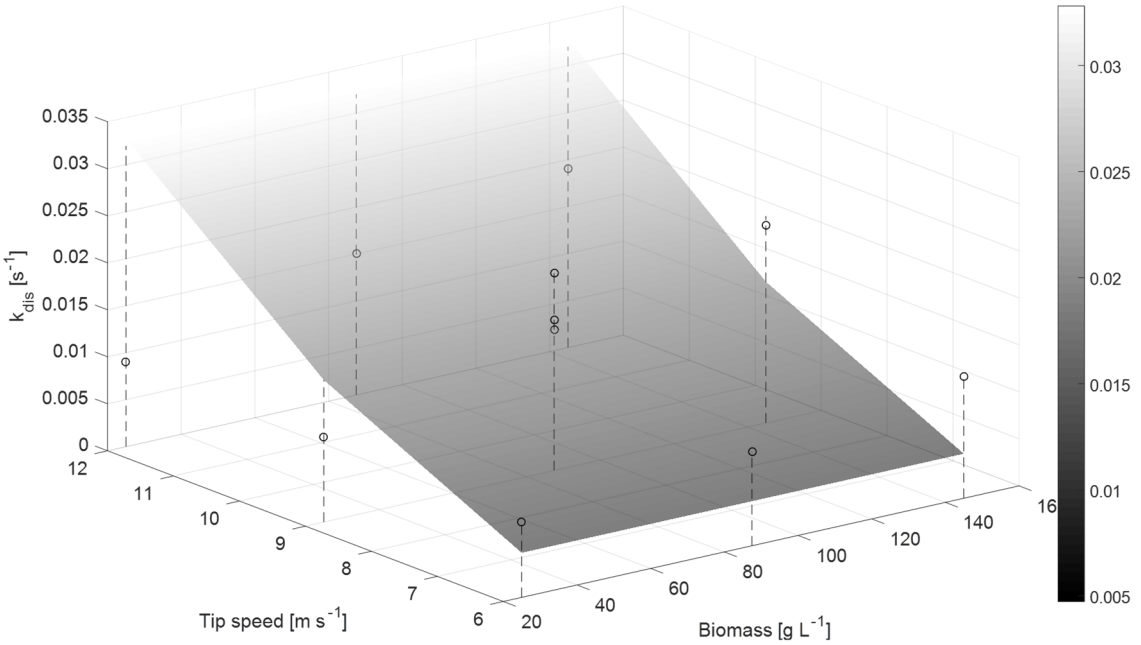

Figure 5. Comparison of model predictions (surface) with data published by Postma et al., (2015) (open markers) for *C. vulgaris*. Dashed lines are a guide to the eye.

Bead size and bead filling are crucial parameters since they are directly related to the total energy that can be released in the milling chamber. Several investigations have addressed the influence of bead size on the k_{dis} of algae in bead mills. Superior disintegration has been reported for the microalgae *Scedenesmus sp*., *Nannochloropsis oculata*, and *Chlorella sorokiniana* as the bead size decreases, in particular for beads in the range 0.2-0.6 mm (Hedenskog et al., 1969; Montalescot et al., 2015; Zinkoné et al., 2018). The bead material has also a direct effect on the disintegration of algal cells (Montalescot et al., 2015). It has been reported that superior disruption levels are obtained with zirconia beads in comparison to glass beads probably due to their higher density which results in enhanced kinetic energy at constant speeds (Doucha and Lívanský, 2008). In Fig. 6A-B, the corresponding k_{dis} for two algal strains reported by Postma et al., (2017) using zirconia beads at 65 % filling rate are compared with the model calculations. The model accurately predicts the trends for *T. suecica* (Fig 6A) and *C. vulgaris* (Fig. 6B). For the former, no significant variation of k_{dis} was obtained at different values of d_b. This can be explained by its relatively weak cell wall which can be disintegrated at comparable rates regardless of the bead size. For *C. vulgaris*, the model captures the general expected behaviour: k_{dis} decreases as the bead size

increases, confirming previous studies. Although with smaller beads the kinetic energy carried per bead is lower, the number of beads and therefore number of collisions that take place in the milling chamber is superior, suggesting that the frequency and not intensity of the collisions is the rate controlling factor during bead milling. Zinkoné et al., (2018) found a linear correlation of stress frequency with k_{dis} for *C. sorokiniana* in a continuously operated bead mill.

The effect of bead filling (α) on the disintegration of algal cells is often overlooked. Montalescot et al., (2015) evaluated disintegration rates for *P. cruentum* from 35 to 65 % and Doucha and Lívanský, (2008) presented data for several milling systems in the range 60-85 %. In both cases it was reported superior disintegration rates at higher α. In Fig. 6C, experimental data and model results for *T. suecica* at α from 2.5 to 75 % are shown. The predicted data accurately describe the experimental values, reflecting that as α increases, the number of beads and the frequency of collision becomes larger, therefore disrupting more cells per unit time. At low α, the frequency of collisions is low, requiring remarkably long residence times to achieve complete cell disintegration. This, in turn, implies large equipment volumes and consequently high capital expenses. As the value of α increases, the energy released by colliding beads becomes larger, and complete disintegration is obtained in short times. The corresponding specific energy consumption to reach 95 % disintegration (E_m) as function of the bead filling is presented in Fig. 6D. As shown, there is a clear reduction in E_m mainly due to the impact on residence time. Furthermore, as the data presented in Fig. 6D was collected at moderate agitation speeds (2039 rpm), it is expected that no significant additional power will be consumed as a result of the presence of the beads (Fig. 3A). Operating the mill at α= 65 to 75 % will guarantee that the target for energy consumption for the extraction step within an algae biofuel biorefinery $E_{m,Extr}$ = 0.6 kWh $kgDW^{-1}$ (Coons et al., 2014) is achievable.

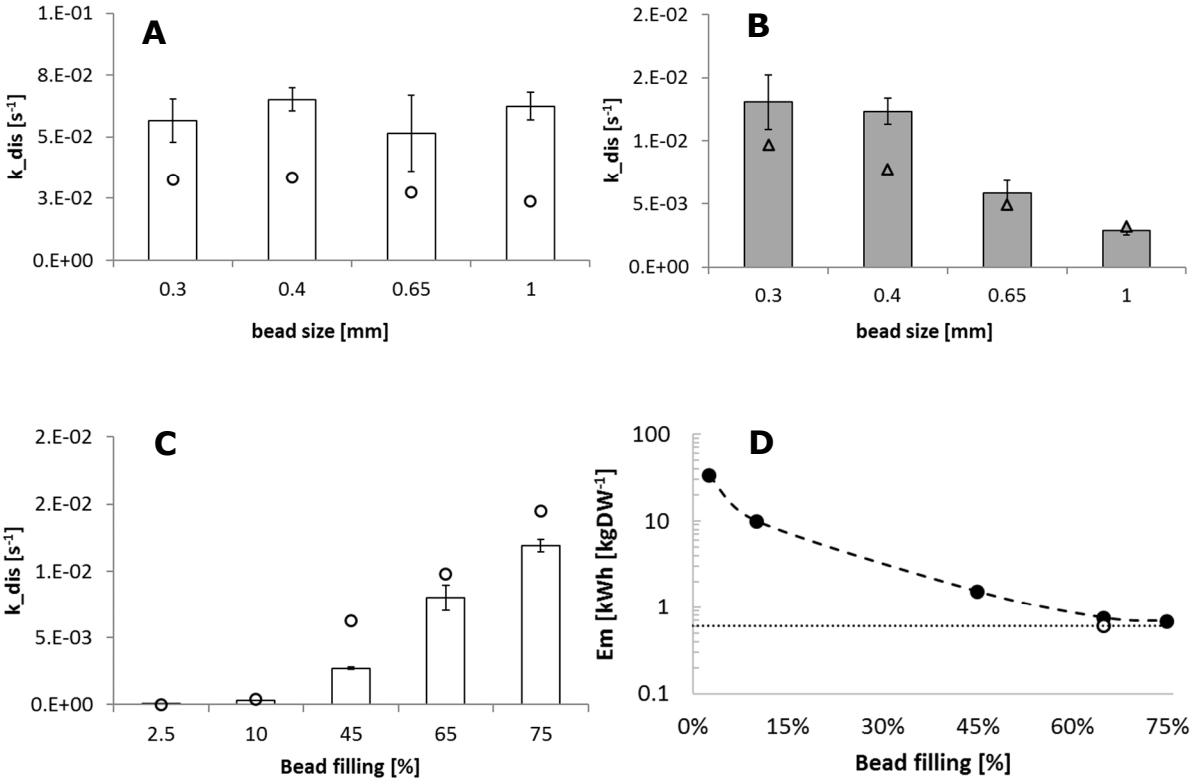

Figure 6. (A-B) Disintegration rates for two algae strains at different bead sizes. Experimental data from Postma et al., (2017). **A.** *T. suecica* (o). **B.** *C. vulgaris* (Δ). **C.** Disintegration rates at different bead fillings for *T. suecica* (o). Columns: experimental data. Markers: model predictions. **D.** Specific energy consumption (E_m, Log scale) as function of the bead filling to reach 95 % cell disintegration. Open marker: Experimental data (Suarez Garcia et al., 2018). Dotted line: E_m for extraction (Coons et al., 2014).

The development of mild and energy efficient disintegration processes is crucial to ensuring the extraction of functional biomolecules from algae and to realise algae based processes at large scale (Suarez Garcia et al., 2018a). In this regard, the modelling approach presented in this investigation allows the study of the disintegration of several microalgae species when information on the cell-wall strength and size are known. Moreover, the model makes possible the selection of an operational window depending on the biorefinery needs. Agitation speed, bead filling, bead size and flow rate can be estimated to target specific groups of cells within a population. For example, cells that accumulate preferentially a metabolite of interest and therefore appear larger (Cabanelas et al., 2016) or cells displaying a stiffer cell-wall

because they are undergoing a different stage in the cell cycle as demonstrated by de Winter et al., (2013), cells accumulate first proteins and pigments and later carbohydrates and lipids during the growth phase of synchronized cultures. This can be exploited in order to release selectively metabolites during bead milling and to obtain crude fractions with higher purities. Also, in case of a mixed algae population, the operational parameters of the mill can be tuned to operate within a range of energy values (energy released in the milling chamber) to selectively release high value biomolecules that are produced by a certain strain only. A more extensive knowledge on the cell-wall composition and the energy required to disrupt a single cell is therefore needed (Alhattab et al., 2018).

4.5. Effective disruption energy

We have introduced the term effective disruption energy η as a factor that indicates the fraction of energy that is dissipated into the medium, without effectively reaching the cells. A significant portion of the total available energy is spent in providing momentum to the mechanical elements of the mill as well as to the biomass slurry and the beads. It was determined that as the agitation speed increases, the energy demand and heat dissipation becomes significant (Fig. 3A), which is probably due to the complex nature of the collisions occurring in the mill. We have assumed perfectly elastic collisions occurring at a frequency similar to that of gas molecules. However, the real nature of the collisions, flow regimes and the actual gradients of speeds at which collisions are taking place are unknown (Becker et al., 2001). For instance, the restitution coefficient (ratio of post- to pre-impact bead velocity) for 0.5 mm beads at α = 65 % for the system under investigation is 0.9 (Beinert et al., 2015). This means that < 1 % of the energy of collisions is dissipated to the fluid. For the estimation of the collision frequency, the kinetic theory of gases was used, but this requires particles with negligible volume, which does not hold for the system under study, in particular at high filling ratios. The values of E_X were taken from studies in which nano-indentation was used. However, during bead milling the beads have a typical diameter of 10^2-fold larger than the cell diameter. Since the contact area provided by the needle

during indentation is much smaller than the area of a bead in contact with a cell, a stronger force is needed from the beads to attain the same pressure. Also, there are physiological variations for the same strain due to culture conditions and random mutagenesis, which have a direct effect on the values of E_X.

4.6. Selective release of biomolecules

The comminution process of microorganisms cannot be defined by the fineness of the cell debris but from the cell rupture and consequent release of biomolecules into the surrounding fluid. In this regard, cell disintegration and release of biomolecules are proportionally correlated. We have analysed the experimental data reported by Postma et al., (2017) for the release of proteins and carbohydrates from three microalgae species and found that protein and carbohydrate release can be estimated directly from the rates of disintegration. In other words, with a confidence level of 95 %, the kinetic rates of proteins and carbohydrate release are proportional to k_{dis}. The rates of pigment release also appear to be dependent on the cell comminution rate as pigments are normally located in the chloroplast or in internal storage organelles (de Winter et al., 2013; Suarez Garcia et al., 2018a). Therefore, the accurate estimation of the disintegration rates not only provides crucial information for the design and optimization of the disruption processes, but also for the fractionation and purification steps downstream. A clear example of this is that differences in kinetic rates can be exploited to selectively enrich the extract phase with a metabolite of interest, which can favour both the yields and purities (Suarez Garcia et al., 2018a).

4.7. Scale up

The predictive capabilities of Eq. 11 were also evaluated for a system at semi-pilot scale as described in section 2 and Table 1. The experimental disintegration rate for *T. suecica* was 1.29 ± 0.08 $x10^{-2}$ s^{-1} and that for *C. vulgaris* was 4.14±0.09 $x10^{-3}$ s^{-1}. The simulated rates were 7.86$x10^{-3}$ s^{-1} and 3.58$x10^{-3}$ s^{-1} respectively. The corresponding kinetic curves are shown in Fig. 7. As expected, higher disintegration rates are obtained for *T. suecica* as its cell wall is weaker and thus, the energy released in the bead mill is

sufficient to break more cells per unit time. The model presented in this investigation can potentially be used for scale up purposes. By keeping the rates of disintegration k_{dis} uniform at different scales, the model can be solved to estimate the corresponding rotational speeds, bead size, bead filling and geometrical dimensions of the mill at a larger scale. This can be made strain-dependent or can be aimed at multi-strain and multiproduct biorefinery process. Such scale-up procedure can be considered as a combination of rate of production, and sizing by energy (Austin, 1973), since it involves equating k_{dis} for two scales and incorporating the energy consumption as function of operational parameters.

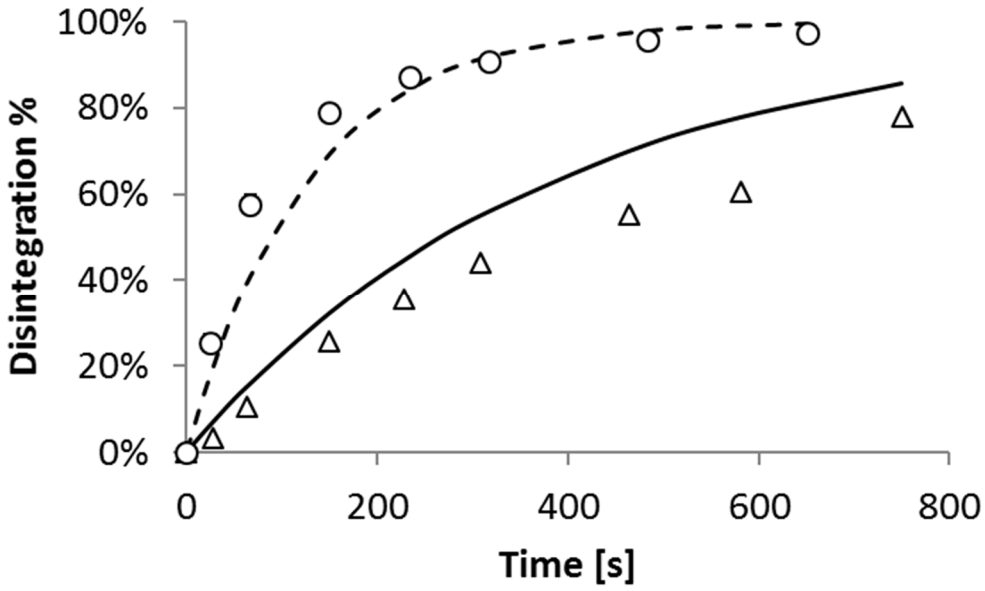

Figure 7. Disintegration profiles for *T. suecica* (o) and *C. vulgaris* (Δ) for a semi-pilot scale bead mill. Dashed and solid lines are model predictions for the respective strains.

Equipment design and optimization studies can also be conducted by solving the model to reach a particular range of values of k_{dis} and determining the values of operational parameters and equipment dimensions. This will ensure not only precise rates of disintegration and release of biomolecules, but also minimum levels of energy consumption and costs. By controlling the disintegration times, it is possible to modify the overall composition of the resulting algae extracts, their properties and their market potential (Suarez Garcia et al., 2018a). The applicability of the model is limited by the major assumptions made in terms of hydrodynamics and mechanism of bead

collision. However, it can be made extensive to other microalgal cells if information on the size and cell strength is readily available. In other words, the modelling approach presented in this report can find application in multi-feed multi-product microalgae biorefineries.

5. Conclusions

The disintegration of microalgae in bead mills have been studied by means of a modelling approach that involves process and equipment parameters to estimate the theoretical energy released in the mill, and cell parameters to account for the energy needed to disrupt a cell. This allowed us to accurately predict the kinetic rates of disintegration of two microalgae species over a broad range of bead sizes and bead fillings, and for two different bead mill scales. Furthermore, we propose that such modelling approach can support development, optimization and scale up studies and can allow the determination of operation windows to achieve energy efficient, selective and mild disintegration processes for the biorefinery of microalgae.

Acknowledgements

This study was financed by the Dutch Technology Foundation STW under the project AlgaePro4You, nr. 12635. From January 2017, STW continued its activities as NWO (Dutch national science foundation) Applied and Engineering Sciences (TTW). The authors are grateful to Dorinde Kleinegris (UniResearch Bergen, Norway) and Jeroen de Vree (University of Bergen, Norway) for providing *Chlorella vulgaris* for the disintegration experiments.

Nomenclature

Symbols

A	Cross sectional area of the gap between the accelerator and chamber wall [m]
C_X	Algal biomass concentration in the suspension [g/kg]
d_b	Bead diameter [m]
d_X	Cell diameter [m]
E	Total energy released by collisions [J s^{-1}]
E_b	Energy released in a single impact event [J]
E_b	Specific energy consumption [kWh $kgDW^{-1}$]
E_X	Specific energy required to disrupt a single cell [J/cell]
F	Recirculation flowrate [m^3/s]
k_{dis}	Disintegration kinetic constant [s^{-1}]
L	Effective length of chamber mill, compensating the area "inside" the accelerator [m]
n	Number density of beads [bead/m^3]
n_X	Number density of cells [cell/m^3]
n_{Xf}	Number density of cells in the feeding compartment [cell/m^3]
$n_{X,out}$	Number density of cells in the recirculation flow [cell/m^3]
u_b	Bead velocity [m/s]
u_L	Liquid velocity [m/s]
u_θ	Azimuthal component of liquid velocity [m/s]
P	Volumetric energy supply due to collisions [J m^{-3} s^{-1}]
R	The radius of milling chamber [m]
r	Radial position inside the mill chamber [m]
r_b	Bead radius [m]
r_j	Radial position of the centre of mass of bead at layer j [m]
t	Time [s]
V_b	Volume of a single bead [m^3]
V_{ch}	Volume of grinding chamber [m^3]
V_f	Remaining volume of suspension inside the feeding chamber [m^3]
V_{susp}	Total volume of suspension [m^3]
V_X	Volume of a single cell [m^3]
T	Throughput of a bead mill [m^3/h]
z	Collision frequency of beads per unit volume [m^{-3} s^{-1}]

Greek symbols

α	Bead filling percentage
$\dot{\gamma}$	Shear rate [s^{-1}]
ε	Bead porosity due to packing
η	Effective disruption efficiency constant
κ	The ratio between the accelerator radius and the mill radius
μ	Liquid dynamic viscosity [kg s^{-1} m^{-1}]
ρ_b	Bead density [kg/m^3]
ρ_L	Liquid density [kg/m^3]
Ω	Angular velocity of the accelerator [s^{-1}]

Chapter 4

Techno-functional properties of crude extracts from the green microalga *Tetraselmis suecica*

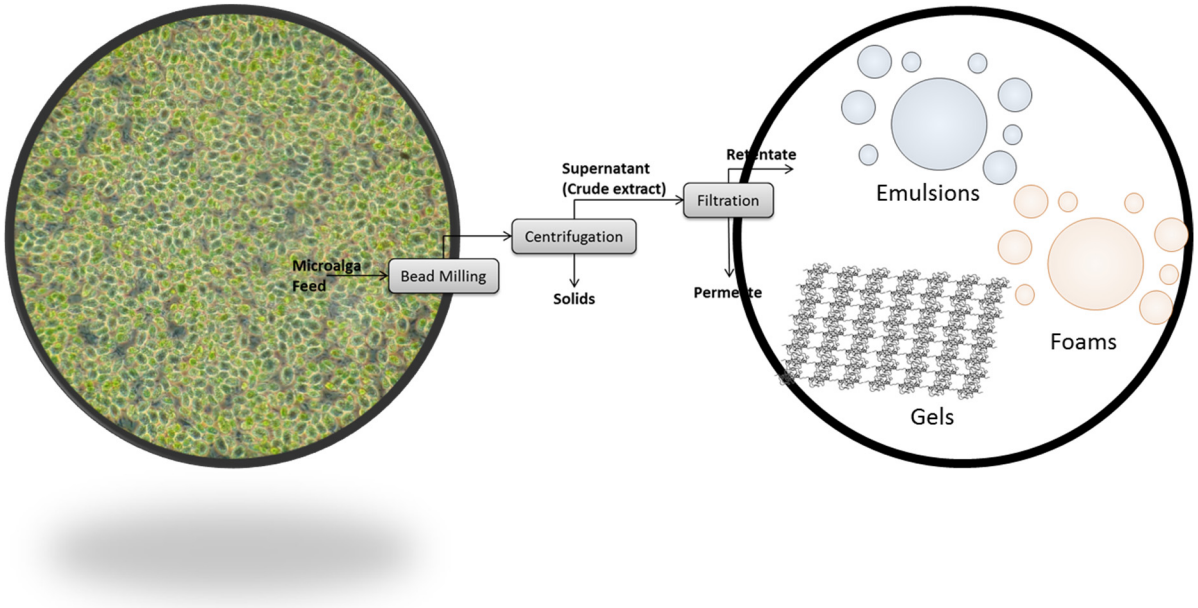

Published as :

E. Suarez Garcia, J.J.A. van Leeuwen, C. Safi, L. Sijtsma, L..A.M. van den Broek, M.H.M. Eppink, R.H. Wijffels, C. van den Berg. Techno-Functional Properties of Crude Extracts from the Green Microalga *Tetraselmis suecica.* Journal of Agricultural and Food Chemistry 2018 66 (29), 7831-7838.

Abstract:

A mild fractionation process to extract functional biomolecules from green microalgae was implemented. The process includes bead milling, centrifugation and filtration with several membrane cut-offs. For each fraction, the corresponding composition was measured and the surface activity and gelation behaviour were determined. A maximum protein yield of 12 % was obtained in the supernatant after bead milling and between 3.2-11.7 % after filtration. Compared to whey protein isolate, most of the algae fractions exhibited comparable or enhanced functionality. Surface activity for air-water and oil-water interfaces, and gelation activities were notably superior for the retentate fractions compared to the permeates. It is proposed that such functionality in the retentates is due to the presence of hydrophobic compounds and molecular complexes exhibiting a similar behaviour as Pickering particles. We demonstrated that excellent functionality can be obtained with crude fractions, requiring minimum processing and thus, constituting an interesting option for commercial applications.

1. Introduction

Algae have been recognized as a promising renewable feedstock for the production of fuels and bulk chemicals, pigments and particularly food and feed ingredients (Vigani et al., 2015). To obtain such products, an intricate series of unit operations is often needed, involving cell disintegration, extraction, and purification. Algae biorefinery is therefore associated with multiple downstream processing steps that result in several highly pure products (Ruiz Gonzalez et al., 2016). For some applications, however, product functionality must be the determining criterion, rather than product purity (Kiskini et al., 2015). The functional properties of a certain product (e.g., foaming, emulsification and gelation) is determined by the presence of proteins, carbohydrates and lipids and the interactions among them (Kiskini et al., 2015). It is therefore expected that complex mixtures also show certain functionality. In other words, impure fractions can be potentially marketed as functional ingredients.

The functionality of algae proteins has been investigated in several publications. Excellent gelling properties were observed for proteins extracted from the cyanobacteria *Arthrospira platensis* (Chronakis, 2001). A soluble protein isolate (ASPI) from the microalga *Tetraselmis sp.* was prepared by Schwenzfeier et al., (2011). The ASPI, containing 64 % proteins and 24 % carbohydrates, showed complete solubility at a pH above 5.5, the formation of stable emulsions at pH 5-7 (Schwenzfeier et al., 2013a) and superior foam stability at pH 5-7, compared to whey and egg protein isolates (Schwenzfeier et al., 2013b). The authors argued that the presence of charged sugars contributed to the foaming and emulsifying properties of the algae protein isolate (Schwenzfeier et al., 2014). Proteins from the microalga *Chlorella vulgaris* were extracted after a process of homogenization, pH shift and ultrafiltration (Ursu et al., 2014). Only the permeate fractions obtained under neutral conditions showed higher emulsifying capacity and stability than commercial sodium caseinate and soy protein isolate. Similarly, water soluble proteins from *Haematococcus pluvialis* were extracted using high pressure homogenization, centrifugation and pH shift. The resulting supernatants were rich in proteins (26-44 dw %), carbohydrates and lipids, and

exhibited superior emulsifying stability and activity index in comparison to sodium caseinate. Emulsification capacity, however, was lower (Ba et al., 2016).

A protein isolate (70 dw % proteins) obtained from *Arthrospira platentis* was evaluated for several functional properties (Benelhadj et al., 2016). it was found that emulsification and foaming are highly dependent on the pH and correlate directly with protein solubility. Under the presence of a plasticizer, the fractions were able to form stable gels. Isoelectric precipitation was applied to extract proteins from bead milled *Nannochloropsis oculata* (Cavonius et al., 2015). the extract, containing 23 % proteins and 15 % lipids (dw) was proposed as an interesting functional ingredient for food and feed. Extraction and precipitation of proteins from *Nannochloropsis spp*. after thermal treatment and pH shift was reported by Gerde et al., (2013). Although the extraction conditions were harsh, the authors pointed out that the high degree of glycosylation of the protein extract could have led to unique functional properties. Waghmare et al., (2016) employed a three-phase system to concentrate proteins from *Chlorella pyrenoidosa*, and obtained a concentrate with 78 % (dw) proteins, exhibiting excellent foaming and good oil holding capacities.

The present study presents an overview of the functional activity (surface activity and gelation behaviour) of extracts obtained under mild conditions from the marine microalga *Tetraselmis suecica.* The fractionation process consists of bead milling, centrifugation and filtration, which are simple and standard technologies in downstream processing and thus with high potential to be scalable. The effect of the membrane cut-off on the composition and functionality of the permeates and retentates was also investigated. The main objective of this research was to demonstrate a simple fractionation strategy to recover algae fractions and to show that crude extracts display comparable or superior functionality than commercial protein isolates.

2. Material and methods

2.1. Alga cultivation and harvesting

Tetraselmis suecica (UTEX LB2286, University of Texas Culture Collection of Algae, USA) was cultivated and harvested as described by Postma et al., (2017). In short, the cultures where maintained in a greenhouse (AlgaePARC, Wageningen - The Netherlands) at 20 ^{o}C under 0.254 vvm (5 v% CO_2) sparging gas and 373 µmol m^{-2} s^{-1} of continuous artificial incident light. The cultures were harvested and centrifuged and the resulting biomass was kept at 4 ^{o}C until further use.

2.2. Preparation of algae fractions

A simple fractionation process is proposed, involving the steps of bead milling, centrifugation and filtration (Fig. 1). After separation, every fraction (crude extract, solids, permeate and retentate) was collected and analysed independently.

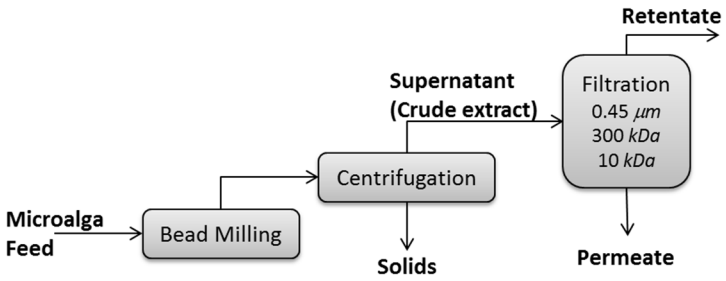

Figure. 1. Fractionation strategy of bead milled algae suspensions.

Bead milling and centrifugation. Disruption experiments were conducted in a horizontal 0.075 L bead mill (Dyno-Mill Research Lab, Willy A. Bachofen AF Maschinenfabrik, Switzerland) operated in batch recirculation mode. Algae suspensions containing ~100 g L^{-1} biomass were prepared in phosphate saline buffer pH 7 (1.54 mM KH_2PO_4, 2.71 mM $Na_2HPO_4.2H_2O$, 155.2 mM NaCl). All runs were conducted for 1 h, under the same conditions as presented before (Postma et al., 2017), except bead size, which was kept constant at 0.4 mm. Bead milled suspensions were centrifuged at 20000 x g and 20 ^{o}C for 30 min and the supernatants and pellets were stored separately at -20 ^{o}C for further analysis.

Filtration. Ultrafiltration experiments were conducted on a LabscaleTM TFF system (Millipore, Billerica, MA) fitted with membrane cassettes with a filtration area of 50 cm^2 and cut-offs of 300 *kDa* or 10 *kDa* (Pellicon XL Ultrafiltration Ultracell) at a fixed average transmembrane pressure (TMP) of 2.07 bar. Microfiltration was performed by manually pressing feed (crude extract) through 0.45 *μm* dead-end cellulose filters (Sartorius). Permeates and retentates were stored at -20 ^oC until analysis.

2.3. Analytical methods

Biomass characterization. Dry weight (DW), proteins, carbohydrates and starch analysis were conducted as described by Postma et al., (2017). To summarize, dry weight was estimated gravimetrically, proteins and carbohydrates were measured with the methods of Lowry[1] and Dubois (Dubois et al., 1956) respectively. Total lipids were measured with the method of Folch (Folch et al., 1957) and starch with the total starch assay kit of Megazyme®. Total ash was determined gravimetrically by burning a known amount of freeze dried biomass in an oven at 575 ^oC and regarding the remaining material as ash.

Mass yields. Mass yields per component (Y_i) were estimated according to:

$$\mathbf{Y_i}\ \% = \frac{\boldsymbol{m_{i,j}}}{\boldsymbol{m_{i,b}}} \times \mathbf{100} \qquad \text{Eq. 1}$$

Where m_i is the mass of component *i* (protein, carbohydrates, lipids, ash and starch). Subscripts *j* and *b* refer to each fraction evaluated (crude extract, permeate, filtrate, etc.) and initial biomass, respectively.

Acrylamide native gel electrophoresis. Protein samples were prepared in Milli-Q® water and diluted with native buffer (Biorad) at a ratio 1:0.8 v/v. 25 µL of the resulting solution were loaded per lane in a 4–20% Criterion TGX gel (Biorad). NativeMark™ (Life Technologies) was used as marker. Electrophoresis was run at 125 V constant for 75 min using Tris-Glycine (Biorad) as running buffer. Staining of the gels was performed with Bio-Safe Coomassie blue (Biorad) for 2 h. Gels were left overnight after abundant washing with demineralized water to further develop the bands before scanning.

Particle size: Particle size distributions of solutions containing algae extracts (0.1% w/v protein basis) were determined using a Nanosizer-Zetasizer Malvern ZEN 5600SN (Malvern Instruments Ltd, Malvern, UK) at room temperature and pH 7.

2.4. Techno functional properties

Protein solutions. Before determining techno functional properties, samples were lyophilised for at least 27 h using a Sublimator 2x3x3 (Zirbus Technology GmbH) and stored air-tight at room temperature until use. The corresponding amount of algae fraction was weighted and dissolved in distilled water in order to obtain a desired protein concentration. The resulting solution was adjusted to pH 7 with NaOH 0.1 M before each analysis.

Whey protein Isolate (WPI). Whey Protein Isolate (BiPRO, Davisco Foods international) containing 97.6 % protein and 2 % ash (DW) and 5 % moisture content, was used as reference commercial standard.

Surface activity. The ability of the fractions to influence surface tension was determined by recording the interfacial tension of static controlled droplets using an Automated Drop Tensiometer (ADT Tracker®, Teclis Scientific, France). The ADT measures surface tension according to the Young-Laplace theory (Berry et al., 2015). Foaming and emulsification behaviour were derived from static drop experiments as presented below. All experiments were conducted at room temperature.

Foaming. surface activity for air-water interface was studied from air-water droplets. Each droplet was formed with 11 µL of suspension containing 0.1 % protein (w/v). The droplet was kept hanging from a needle while subjected to a stream of saturated air flowing vertically in a 5 mL cuvette. Surface tension of the droplet was recorded for a period of 36 min.

Emulsification. Studies of surface activity for oil-water interface were conducted on 20 µL static drop of hexadecane (Anhydrous, > 99%, Sigma Aldrich) submerged in a 5 mL 0.1 % protein solution (w/v). surface tension was recorded for 60 min. After

equilibrium is reached, perturbations on the droplet's volume were enforced by adding 1 µL solvent, 5 times in 10 s, ensuring variations in surface area lower than 10 %. Fourier analysis was conducted on the dilation data, resulting in the elastic modulus ϵ (mN m^{-1}).

Gelation. Gelation tests were conducted according to Martin et al., (2014) using an Anton Paar MCR 302 (Modular Compact Rheometer) with a heating rate of 5 ^{o}C min^{-1} in the range 25 to 95 ^{o}C.

2.5. Statistics

All experiments were conducted in duplicates from independent experiments. Statistical analysis at 95 % confidence level were conducted using R (V 3.2.2). Significance was evaluated applying one way ANOVA. To compare significantly different means, a t-test or a Tukey's Honest Significant Tests (HSD) was applied.

3. Results and Discussion

3.1. Fractionation process.

The complete mass balance and corresponding compositions and mass yields per component, according to the fractionation process depicted in Fig. 1., are presented in Table 1. and Fig. 2A. The carbohydrates content in the initial biomass (41 % dw) was significantly higher compared to the values reported by Schwenzfeier et al., (2011) for *Tetraselmis sp* (24 % dw) while the protein content was similar (~ 37 % dw). The high content of carbohydrates can be due to the accumulation of starch granules and seasonal variation as noted by Michels et al., (2014a) for cultures of *Tetraselmis suecica* maintained in green houses.

During bead milling, the shear caused by bead-bead collisions leads to the release of intracellular components. Proteins are released quickly, reaching a maximum concentration at short milling times. Carbohydrates, on the contrary, display a gradual increasing trend as noted in our previous study (Postma et al., 2017). After bead milling, over 30 % of the total sugars and only 12 % of the proteins were found in the

Table 1. Compositions [g kg^{-1}] of fractions after bead milling and filtration. The data presented is the average of duplicates and corresponding standard deviations. Values in parenthesis indicate mass yields according to Eq. 1. Low case and capital letters show significantly equal means -per compound- for permeates and retentates respectively ($p < 0.05$).

	Feed	Bead milling		Filtration				
		Pellet	Supernatant	0.45 µm	300 kDa		10 kDa	
				Permeate	Permeate	Retentate	Permeate	Retentate
Dry mass	129.2 ± 6.6	156.5 ± 10.5	62.1 ± 7.3	52.7 ± 0.2^{a,b}	45.4 ± 4.4^{a}	97.5 ± 9.9^{A}	55.0 ± 0.2^{b}	94.9 ± 0.6^{A}
Protein	43.4 ± 2.0	58.9 ± 9.1 (77.7)	12.1 ± 0.7 (11.9)	12.2 ± 0.7 (11.7)	3.9 ± 1.2 (3.2)	19.6 ± 3.2^{A} (4.4)	7.8 ± 0.5 (6.1)	17.3 ± 1.9^{A} (3.4)
Carbs	47.2 ± 4.7	50.6 ± 11.7 (61.4)	34.3 ± 1.5 (31.0)	21.4 ± 1.0^{a} (18.9)	24.6 ± 5.9 ^{a} (18.2)	55.4 ± 7.8^{A} (11.4)	26.1 ± 2.5^{a} (18.9)	54.5 ± 5.2^{A} (9.9)
Lipids	28.2 ± 2.8	47.3 ± 8.2 (96.1)	2.9 ± 1.3 (4.4)	2.3 ± 0.7^{a} (3.4)	1.5 ± 0.8^{a,b} (1.9)	7.2 ± 3.0 (2.5)	1.1 ± 0.2^{b} (1.3)	3.2 ± 0.7 (1.0)
Ash	10.3 ± 1.2	8.4 ± 1.4 (46.3)	9.8 ± 1.6 (40.4)	11.9 ± 0.9^{a} (47.8)	6.9 ± 1.1 (23.5)	10.1 ± 1.0^{A} (9.6)	10.2 ± 0.1^{a} (33.8)	9.0 ± 1.8^{A} (7.5)
Starch	25.8 ± 1.2	8.9 ± 3.3 (19.9)	1.0 ± 0.6 (1.6)	1.5 ± 0.2^{a} (2.5)	1.7 ± 0.2^{a} (2.3)	1.1 ± 0.7^{A} (0.4)	1.7 ± 0.1^{a} (2.2)	1.9 ± 0.2^{A} (0.6)

soluble phase or “Crude Extract (CE)” (Fig. 2B). This indicates than only a small fraction of the total proteins in *T. suecica* is soluble and can be extracted in the aqueous phase after complete mechanical disintegration. Postma et al., (2017) and Schwenzfeier et al., (2011) reported yields of soluble proteins of approximately 20 % for *Tetraselmis* species after bead milling. This higher yield can be due to differences in biomass composition and in the calculation method, as we are reporting mass yields according to Eq. 1. The insoluble phase (solids) contains almost equal proportions of proteins, carbohydrates and lipids, in addition to 5.3 ± 0.9 % (dw) ash (Fig. 2A). It constitutes an interesting material for the preparation of feed formulations for livestock, poultry and aquaculture (Barron et al., 2016).

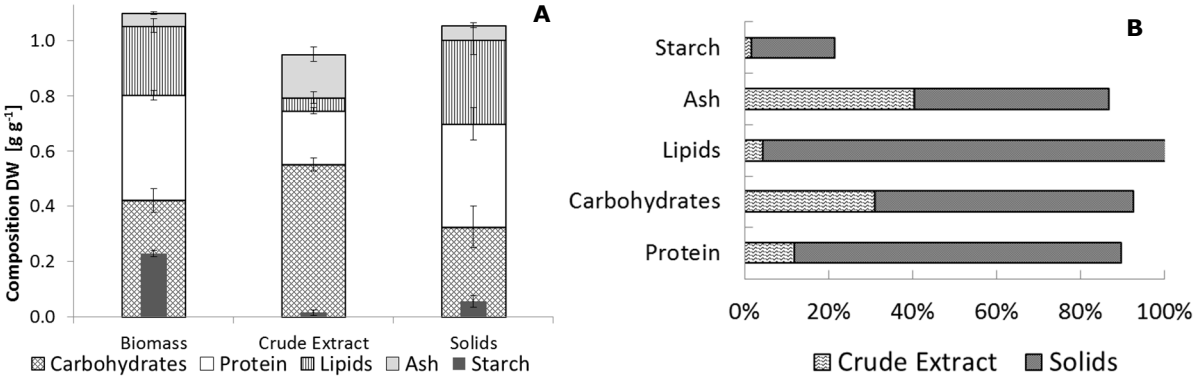

Figure. 2. (A) Dry weight composition of crude extract and solid fractions after bead milling and centrifugation and (B) corresponding mass yields (Eq. 1). Error bars represent standard deviations of four independent experiments and measurements in duplicates.

The effect of the membrane cut-off on the fractionation yields and functionality was further investigated. Sequential filtration has been applied for algae biorefinery (Safi et al., 2017b, 2014b), but the study of the functionality of the resulting fractions remains elusive. For each membrane cut-off, the content of proteins, carbohydrates, lipids and ash were quantified and the results are presented in Table 1. The corresponding mass yields are also given. The permeate fraction after microfiltration (0.45 *µm* membrane) resulted in the highest yields for all components. This is anticipated as this membrane removes only large particles, yielding a permeate containing nearly 97 % of the total feed. Unexpectedly, the protein yield in the

permeate of the 10 *kDa* membrane doubles that of the 300 *kDa*. This can be due to fouling for the 300 *kDa* membrane, preventing a significant fraction of proteins to migrate to the permeate. The same phenomena was observed by Safi et al., (2017b) who noted a higher degree of membrane fouling for higher cut-offs and attributed this to the formation of polarization layers and to the adsorptive fouling during the filtration of algae suspensions. Such fouling can also explain why the retentate of the 300 *kDa* membrane shows a higher amount of total lipids compared with the 10 *kDa*.

The permeates of the 300 and 10 *kDa* appeared clear, indicating complete removal of pigments. This was also observed in other study (Safi et al., 2017b) for extracts from *Nannochloropsis gaditana* using polyethersulfone membranes of 1000, 500 and 300 *kDa*. Pigments are recovered in the retentate phase due mainly to the hydrophilic nature of the membrane materials used in both studies. Regarding starch, we measured concentrations in the range 1.1-1.9 g kg^{-1} in both the permeate and retentate fractions (Table 1). This contradicts the results of Safi et al., (2017b, 2014b) who reported complete retention of starch for membranes ranging from 1000 to 10 *kDa*. This difference can be due to a lesser extent of fouling for the cellulose-based membranes used in our research compared to polyethersulfone-based membranes used by Safi and co-workers, allowing starch fragments to also migrate to the permeate phase.

Besides a strong green colour, the retentate fractions showed a significantly higher content of proteins, carbohydrates and lipids (Table 1). This suggests that proteins are associated with pigments and polysaccharides. In fact, it has been reported that proteins in green microalgae are often covalently bound to lipids (Palsdottir and Hunte, 2004), polysaccharides and sugars (Heaney-Kieras et al., 1977; Schwenzfeier et al., 2014, 2011), and pigments (Knoetzel et al., 1988), forming molecular complexes that can easily be retained by membranes during ultrafiltration. The fractionation process presented in this investigation was conducted under mild conditions (room temperature and native pH of 5.7 ± 0.2) and without the addition of chemicals. Native

gel electrophoresis (Fig. 3) shows the expected bands for *T. suecica* (Postma et al., 2017) and demonstrates that after bead milling and filtration, the main protein bands are maintained. In addition, it is confirmed that the permeate of the 10 *kDa* only contains low molecular weight proteins. A maximum overall total protein yield of 6.1 % was observed after filtration (Table 1). This is comparable with a 7 % yield reported for *Tetraselmis sp* under a process involving bead milling, dialysis, chromatography and precipitation (Schwenzfeier et al., 2011). On the contrary, Ursu et al., (2014) found a yield of 87 % for *Chlorella vulgaris* after filtration over a 300 *kDa* membrane. The authors attributed this to the fact that proteins from the algae extracts exists as large macromolecular aggregates with molecular weights above 670 *kDa*, thus the majority of the proteins are retained. The corresponding protein yields for the filtration step in the present investigation are 40.1 % and 26.9 % for the retentates of the 300 and 10 *kDa* membranes respectively. The lower yields are an indication of a more diverse range of proteins and macromolecular complexes in the extracts from *T. suecica*. Such diversity may lead to a richer technical functionality.

3.2. Techno-functional properties

3.2.1. Surface activity: foaming and emulsification

Surface activity - foaming and emulsification - refers to the ability of certain compounds to form and stabilize air-water (awi) or oil-water (owi) interfaces. Such stabilization takes place due to the formation of network-like structures around a clean surface, which effectively lowers its surface tension. This requires surface active molecules to be soluble, to diffuse to, and to adsorb on an interface (Serrien et al., 1992). Furthermore, molecular rearrangements and interactions among molecules adsorbed on the surface also lead to variations of the surface tension (Tornberg, 1978). In this regard, functionality is not limited to proteins but can be enhanced by the presence and chemical nature of other biomolecules, and their ability to interact (Kiskini et al., 2015).

The dynamic surface tension (γ [mN m^{-1}]) of samples containing extracts from *T. suecica* and whey protein isolate (WPI) as reference protein is presented in Fig. 3A for awi and Fig. 3B for owi. For both cases, the surface tension decreases sharply and reaches slowly an equilibrium level. This behaviour is typical for surface active molecules and reflects the basic mechanisms mentioned before. For a theoretical treatment of the experimental data presented in Fig 3, the reader is referred to the Appendix.

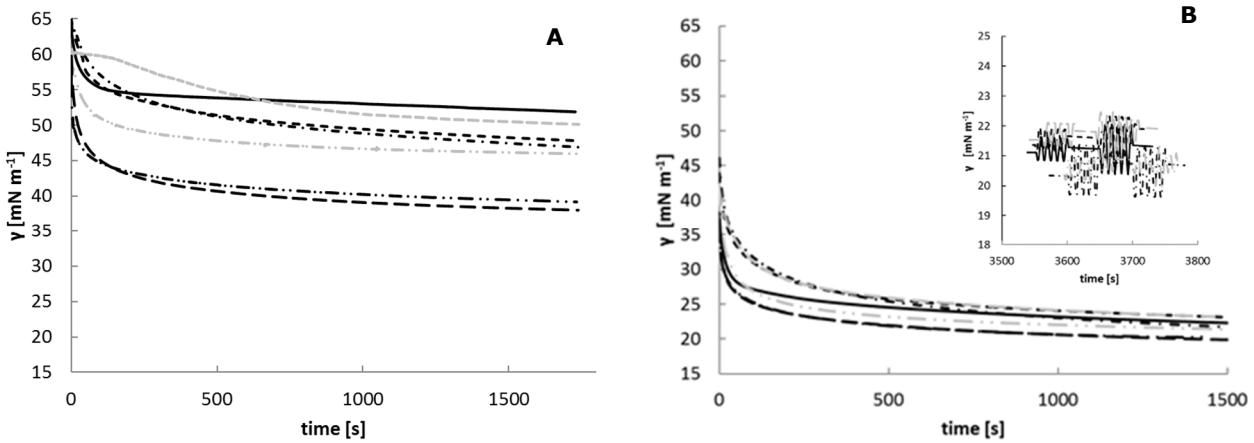

Figure. 3. Surface tension as function of time for (A) air-water and (B) hexadecane-water interfaces; Inner graph shows dilation responses. — WPI, ···· CE, —· 0.45 *μm* P, —·· 300 *kDa* R, —·· 300 *kDa* P, — — 10 *kDa* R, — — 10 *kDa* P. (R=Retentate, P=Permeate).

The surface activity of alga extracts in awi showed a comparable or superior performance than samples prepared with WPI. This can be seen in Fig. 3A by comparing the slopes (reflecting the rates of diffusion, adsorption and stabilization) and the surface tension at equilibrium conditions, which reflects the extent of surface activity. The retentate fractions from the 10 and 300 *kDa* membranes resulted in the strongest activities. On the contrary, the permeate from the 10 *kDa* membrane showed the poorest performance. This clearly demonstrates the effect of the fractionation strategy. The retentate fractions are rich in pigments and lipids, contain larger particles and a wider range of proteins (Fig. 4). On the contrary, the permeate fractions are depleted of pigments, contain only small particles and, for the case of the 10 *kDa*

membrane, lack of large molecular weight proteins (Fig. 4A). The presence of larger macromolecular complexes appear to favour the stabilization process. It is therefore not surprising that the alga extracts, containing a mixture of compounds, presented a higher activity than a pure protein isolate. This has been attributed not only to proteins and glycoproteins (Gerde et al., 2013; Schwenzfeier et al., 2014; Waghmare et al., 2016) but to charged sugars (Schwenzfeier et al., 2013a) and pigments (Chronakis, 2001).

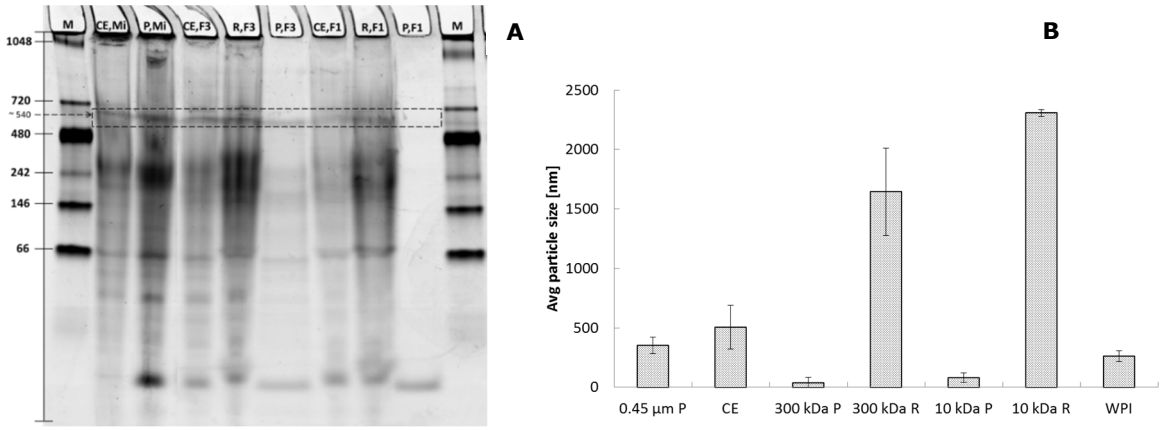

Figure. 4. A) Native gel analysis of fractions before and after filtration (M: Marker. CE: Crude Extract. R: Retentate. P: Permeate. Mi: 0.45 *µm* microfiltration. F3: 300 kDa filtration. F1: 10 kDa filtration). Dotted arrow and square indicates the expected band of Rubisco (~ 540 *kDa*). **B)** Average particle size for several alga fractions after Ultrafiltration.

The surface activity in owi presented a similar behaviour: a sharp decline of γ followed by a slow decrease to reach a plateau phase (Fig. 3B). All samples containing alga extracts showed a comparable performance as WPI. Other studies have also found a similar or superior emulsification activity of algae proteins in comparison with commercial protein isolates. The superior performance has been attributed to the activity of the proteins present in the extracts (Ba et al., 2016), but also to the interactions and favourable effect of other biomolecules present in the extract such as sugars (Schwenzfeier et al., 2013a), chlorophyll and lipids (Ursu et al., 2014). Emulsion stabilization takes place because of the development of steric forces around the

surfaces which limit the extent of coalescence and emulsion degradation (Ba et al., 2016).

For the retentate fractions (10 and 300 *kDa*) measurements of γ could not continue beyond 1500 s (data not shown) due to the sudden detachment of the hexadecane drop from the measurement device. This suggests a remarkable surface stabilization, probably brought about by the presence of pigments and higher lipid content (Table 1) which allows a stronger interaction with the hexadecane. For the remaining fractions, surface activity was further studied by imposing periodic expansions and compressions on the droplet's surface area (Fig. 3B). As can be seen, all samples recovered their original surface tension without appreciable deformation, indicating a high degree of stability. A measure of such stability during perturbation is obtained with the elastic modulus ϵ. The values of ϵ for samples containing alga extracts varied between 35-41 mNm^{-1} while that for WPI was nearly 40 mNm^{-1}. This elastic behaviour is typical of molecules which can store energy, such as proteins (Dimitrova and Leal-Calderon, 2001).

Contrary to our findings, Ursu et al., (2014) observed better emulsification activity for the permeates of a 300 *kDa* (polyethersulfone) filtration process. The authors argued that after the extraction process proteins were denatured and formed aggregates, which were later recovered in the retentate fractions. Such aggregates therefore displayed inferior functionality. As indicated by native gel analysis (Fig. 4A), the fractionation process employed in the present research did not lead to appreciable protein denaturation nor aggregation and thus, both fractions are enriched with functional molecules.

3.2.2. Gelation

The textural attributes of several food products result from the development of stable gels. In general terms, gels are formed after a two steps process. In the first step the functional groups of the active molecules are exposed due to thermal or chemical denaturation. Later, the exposed functional groups interact with specific regions of

neighbouring molecules, creating a network like structure. Furthermore, cross links are developed, leading to a three-dimensional assembly with specific viscoelastic properties (Dissanayake et al., 2010). Only few studies have addressed the gelation properties of algae proteins. In all cases, proteins from *Spirulina platensis* have been investigated (Benelhadj et al., 2016; Chronakis, 2001; Lupatini et al., 2016).

To study the gelation activity of alga extracts, the storage modulus *G'* [Pa] was measured during a defined heating – cooling profile. The storage modulus indicates the force required to deform certain material and thus, it serves as a quantitative measure of the strength of the formed gels. The results are presented in Fig. 5A for alga extracts prepared in this study, and in Fig. 5B comparing with data published for Rubisco from spinach and two commercial protein isolates (WPI and Egg White Protein EWP) (Martin et al., 2014). At first, all fractions were prepared at 5 % protein content. However, due to solubility constrains, only two fractions could be prepared at 10 % protein content: CE and 0.45 *µm* P. WPI did not show any gel-like behaviour at 5 nor at 10 % protein content, which was also observed by Martin et al., (2014).

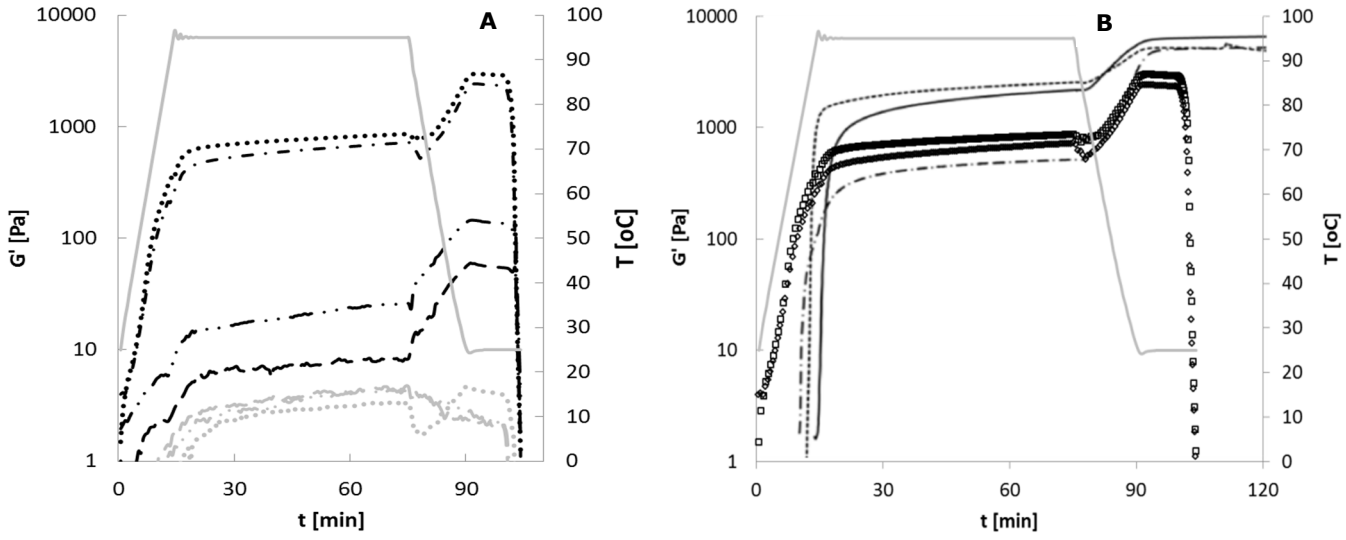

Figure. 5. A) Storage modulus (G' [Pa]) as function of time and temperature (—) for algae fractions: ···· CE 10 %, —· 0.45 *µm* P 10 % **,** ···· CE 5 %, —·· 300 kDa R 5 %, —·· 300 kDa P 5 %, — — 10 kDa R 5 %, — — 10 kDa P 5 %). **B)** comparison of algae fractions: □□□□ CE 10 %, ○○○○ 0.45 *µm* P 10 %, and commercial proteins(Martin et al., 2014): – · – 2.5% RuBisCO, — 10% EWP, - - - 12.5% WPI.

During the heating phase (25 to 95 °C) the onset of gelation (t_g) marks the time at which *G'* starts increasing, and reflects the thermal stability of the molecules in the sample. Rubisco, WPI and EWP are stable at temperatures below 65 °C (Libouga et al., 1996), 77 °C and 84 °C (Berry et al., 2009) respectively and therefore long t_g are expected. For instance t_g of 10, 12, 15 min are reported for gels formed with three different isolates containing 2.5–12.5 % protein (Fig. 5B) (Martin et al., 2014).

For alga extracts containing 10 % proteins (CE and 0.45 *µm P*), *G'* raised rapidly approximately 1 min after heating was initiated, which suggests low thermal stability. It appears that proteins denature quickly and readily form gels. On the contrary, for samples containing 5 % proteins, the onset of gelation took place at longer times (2-15 min). This reflects the effect of concentration on the development of stable gels. In fact, gels are formed only above a critical concentration specific for each protein (Banerjee and Bhattacharya, 2012). For example, Rubisco can form gels at concentrations as low as 0.5 % (Libouga et al., 1996). On the contrary, Proteins from *Arthrospira platensis* could only form gels from 1.5-2.5 % w/w (Chronakis, 2001) and 12 % (Lupatini et al., 2016).

Gels formed with 10 % proteins show a strong increase in *G'* followed by a plateau at 95 °C (*G'∞)*. A similar trend but with a moderate slope was observed for fractions containing 5 % proteins (Fig. 5A). This is possibly due to a lower availability of interacting molecules at 5 %, which reduces the probabilities of forming new bonds upon heating. The values of *G'∞* for all samples are presented in Table 2. Interestingly, gels prepared with CE (10 % protein) showed superior gel strength after the heating phase compared to 2.5 % Rubisco (Fig. 5B), 10 % soy (G′∞ = 400 Pa), and 21.5 % lupine (G′∞ = 340 Pa) protein isolates (Martin et al., 2014). WPI (12.5 %) and EWP (10 %) form substantially stronger gels, which may be due to the prevalence of non-covalent interactions which render them as rigid and brittle gels (Havea et al., 2002).

When the samples are cooled down to room temperature, a further increase in *G'* is observed for most fractions, except for the permeates of 300 and 10 *kDa* (Fig. 5A).

Martin et al., (2014) postulates that during this phase, hydrophobic interactions and hydrogen bonds are primarily responsible for the development of a stronger gel network. Weak or lack of hydrophobic interactions in the permeates can indeed occur due to the hydrophilic nature of the membrane materials used during fractionation. When the temperature is sustained at 25 ^{o}C, a new plateau is reached (Fig. 5) corresponding to G'_{max} (maximum gel strength). In Table 2 the values of G'_{max} are tabulated. Once more, gels prepared with CE or 0.45 μm at 10 % protein registered the highest values, only comparable with 10 % soy (G'_{max}=1500 Pa) and 17.5 % pea (G'_{max}=3100 Pa) isolates (Martin et al., 2014). Gels formed with WPI and EWP greatly surpass the strength of the fractions investigated in this study (Fig. 5B).

Table 2. Values of t_g, G'∞, G'_{max} and corresponding standard deviations for several alga fractions. Letters show significantly different means (p < 0.05) according to t-test (samples at 10%) and Tukey's HSD test (samples at 5%).

Sample	t_g [min]	G'∞ [Pa]	G'_{max} [Pa]
CE 10%	1.2 ± 0.0	862.5 ± 133.6	2985.0 ± 473.8[a]
0.45 µm P 10%	1.5 ± 2.0	723.5 ± 125.2	2430.0± 424.3
CE 5%	14.5 ± 0.8	3.4 ± 0.6[a]	4.5 ± 1.1[a]
300 kDa R 5%	2.0 ± 1.2[a]	26.1 ± 4.2[a]	145.5 ± 19.1[a]
10 kDa R 5%	8.8 ± 6.6	8.6 ± 0.6[a]	60.0 ± 9.4[a]

3.3. Functional activity and purity

We have shown that all alga extracts display a similar or superior functionality compared to the commercial protein isolate WPI. In addition, we observed that the retentate fractions presented better functionality compared to the crude fractions or permeates. This can be due to:

i. Pigment-protein complexes, which in algae extracts have been found to stabilize emulsions and to form stable gels (Chronakis, 2001). The strong green colour and a higher amount of total lipids (Table 1) indeed confirm that virtually all pigments are recovered in the retentate phase. In addition, due the hydrophilic nature of the membrane used in this research, the permeate fractions are expected to be depleted

of hydrophones. Under this condition, hydrophobic interactions in the permeates are limited, which in turn results in a poorer functional activity.

ii. The permeate fractions perform as soft particles or Pickering stabilizers (Dickinson, 2010). As presented in Fig. 4B, the average particle size in the retentate fractions is significantly higher. Such particles correspond to large molecular aggregates or fragments of cell wall, membranes and other cellular structures. Tenorio et al., (2017) studied the interfacial properties of thylakoid membrane fragments obtained from leaves and suggested as well that their functionality resembles that of Pickering stabilizers.

iii. Divalent cations. As mentioned before, the renteate fractions are likely to be enriched with cell fragments originated from the cell wall. The cell wall of *Tetraselmis* species have been found to contain approximately 4 % of Ca^{2+} (DW) (Becker et al., 1998). Divalent cations, like Ca^{2+}, contribute to the development of bridges among charged sites of active molecules, therefore enhancing the strength of films around surfaces and networks within gels (Havea et al., 2002).

Besides the remarkable functional activity displayed by extracts obtained from green microalgae, their potential application as food ingredients is still constrained by the solubility, strong green colour, risk of off-flavour and economics. We have studied samples containing 0.1, 5 and 10 % proteins, which are ranges commonly found in literature. However, further exploration on how solubility is affected by pH, ionic strength and concentration could provide more specific information on the possible applications in foods. For specific markets and products, the characteristic colour and organoleptic properties of the retentate fractions or crude extract may impede their applicability. In terms of protein recovery, we have observed total yields of soluble proteins of about 12 % after bead milling and 3-6 % after filtration. Although the published yields of water soluble proteins varies considerably (5 - 55 %) depending on

the algal strain and separation method (Safi et al., 2014a, 2014c) , it is clear that the recovery of functional proteins from the insoluble phase is still the most important challenge.

The concept of functionality linked with purity and native conformation needs to be critically evaluated. Waghmare et al., (2016) observed excellent foam properties of the protein extracts obtained after a harsh process in which proteins were mostly denatured. Our research showed that excellent functionally can be obtained with crude samples, even after minimal separation steps (crude extract, Fig. 1). This fraction therefore represents a more interesting option in terms of processing costs. In fact, techno-functional properties can be improved by exploiting other compounds present in algae, without the need of numerous purification steps. The presence of side products or impurities can actually enhance activity. Carbohydrates[9,4], pigments and lipids (Ba et al., 2016; Chronakis, 2001; Tenorio et al., 2017), ash (Havea et al., 2004, 2002) and starch (Asghari et al., 2015), have been found to improve functional properties. Even whole biomass could be used as functional ingredients for some applications (Batista et al., 2012; Guil-Guerrero et al., 2004). This in turn will result in simpler and more compact downstream processing and therefore, more cost competitive processes.

4. Conclusions

The resulting crude fractions displayed comparable or superior functionality to whey protein isolate, for surface activity (foaming and emulsification). It was observed that the retentate fractions after ultrafiltration displayed superior functionality in all cases. Gels formed with 10% protein crude extract present a comparable behavior as gels formed with 2.5% (pure) Rubisco. We propose that the presence of large molecular size complexes of protein-saccharides-pigments, and the low ash content in these fractions are responsible for the enhanced functionality. In this regard, we hypothesize that the retentate fractions behave like Pickering particles.

Acknowledgements

This project is financed by the Applied and Engineering Sciences domain (TTW, former STW) of the Dutch national science Foundation (NWO) under the project AlgaePro4You, nr. 12635. The authors would like to thank Rebecca Zettwoog (Wageningen Food and Biobased Research) for her contribution during the preliminary phase of experiments.

Appendix.

A1. Static drop experiments

In this investigation, static drop experiments on air water (awi) and oil water (owi) interfaces containing 0.1 % protein from several alga fractions were conducted. The experimental data was fitted to a mixed adsorption-kinetic model described by Serrien et al., (1992) and given in Eq. S1:

$$\boldsymbol{\gamma = \gamma_e + \left(\alpha e^{-\left(\frac{4t}{\pi\tau}\right)^{0.5}} + \beta \right) e^{-kt}} \qquad \text{Eq. A1.}$$

Where:

γ, γ_e [$mN\ m^{-1}$]: Surface tension and equilibrium surface tension respectively.

α [$mN\ m^{-1}$], β [$mN\ m^{-1}$]: parameters such that $\alpha+\beta = \gamma_o+\gamma_e$ (γ_o is the surface tension of the solvent).

τ [s]: Diffusion relaxation time, which depends on the diffusion coefficient.

k [s^{-1}] : rate constant for the transformation between native and unfolded states.

All the experimental data could be described satisfactory by Eq A1. (r2>0.99). The values of initial surface tension (γ_o) for all samples in awi was in good agreement with the values reported by Serrien et al., (1992) (γ_o=63 $mN\ m^{-1}$). For owi, on the other hand, γ_o significant differences were obtained for the surface tension of the clean surface (γ_o), and notably lower (~38-46 mNm^{-1}) than the published value for water-hexadecane systems (53.5 $mN\ m^{-1}$) (Wu and Hornof, 1999). The observed variability could be due to the delay between bubble formation and the actual measurement of γ at $t = t_o$.

The first term of Eq. A1 -containing τ- accounts for the diffusion process while the last term –containing k- gives information on the molecular reorientation process. τ is inversely proportional to the molecular diffusivity and thus, indicates the rates of migration of surface active molecules to the interface. This was the case for the

retentates (300 and 10 *kDa*) and WPI in awi, for which the steepest curves $\gamma\ \gamma_o^{-1}$ vs t were measured and correlated well with lower values of τ.

Surfactants in their native state are transferred to a clean surface where they experience unfolding (surface denaturation). An equilibrium is then stablished between the native and unfolded states (Serrien et al., 1992). Such equilibrium corresponds to γ_e, and reflects the extent of surface tension modification. This parameter was, for the case of awi, lowest for the retentates of the 300 and 10 *kDa* membranes (~39 mNm^{-1}) compared to WPI (~52 mNm^{-1}). For the other samples, γ_e was statistically equal (~47 mNm^{-1}). For owi also a sharp decline in the surface tension was observed, suggesting high rates of diffusion and adsorption. This feature resembles the functioning of hydrophobins, a remarkable surface active protein produced by fungi (Green et al., 2013). Moreover, the magnitude of γ_e was statistically comparable for all cases.

All samples were prepared to obtain 0.1 % (w v^{-1}) protein. Due to the composition of the fractions, also carbohydrates, lipids and ash were present. For example, samples of CE contained nearly three times more carbohydrates than proteins. On the contrary, WPI contains virtually only proteins.

Table A1. Fitted parameters according to Eq. A1 for surface activity of air-water interfaces containing 0.1 % (w v^{-1}) protein fractions with standard deviations. Letters show significantly different means ($p < 0.05$) according to Tukey's HSD test. Experiments run in duplicates.

Fraction	γ_0 [mN m^{-1}]	γ_e [mN m^1]	α [mN m^{-1}]	β [mN m^{-1}]	k [s^{-1}]	τ [s]	r^2
WPI	64.6 ± 4.2	51.9 ± 3.0^{a}	9.6 ± 0.5^{a}	3.1 ± 1.0^{a}	1.2E-03 ± 4.3E-05^{c,d,e}	26.1 ± 7.2	0.972 ± 0.003
CE	64.4 ± 7.7	47.7 ± 5.9	11.3 ± 0.4	5.4 ± 2.2	1.3E-03 ± 1.3E-04^{a}	250.6 ± 251.9	0.977 ± 0.030
0.45µm P	65.3 ± 8.5	46.8 ± 5.4	11.8 ± 1.9	6.6 ± 3.3	1.4E-03 ± 3.2E-04^{b}	320.6 ± 200.0	0.994 ± 0.002
300kDa P	60.2 ± 0.2	46.0 ± 0.3	10.7 ± 0.5	3.6 ± 0.6	1.7E-03 ± 1.6E-04^{d}	67.5 ± 15.4	0.992 ± 0.001
300kDa R	56.8 ± 0.01	39.3 ± 0.05^{a}	11.6 ± 0.2	5.9 ± 0.2	1.9E-03 ± 2.7E-05^{a,e}	15.4 ± 1.2	0.996 ± 0.000
10kDa P	60.2 ± 0.3	50.2 ± 0.3	0.0 ± 0.0^{a}	10.0 ± 0.04^{a}	1.7E-03 ± 1.2E-04	93.2 ± 23.5	0.960 ± 0.012
10kDa R	59.7 ± 0.1	38.2 ± 0.2^{a}	15.4 ± 0.3^{a}	6.2 ± 0.5	1.9E-03 ± 4.9E-05^{a,b,c}	35.0 ± 0.8	0.996 ± 0.000

Table A2. Fitted parameters, with standard deviations, according to Eq. A1 for surface activity of oil-water interfaces containing 0.1 % (w v^{-1}) protein fractions. Letters show significantly different means ($p < 0.05$) according to Tukey's HSD test. Experiments run in duplicates.

Fraction	γ_o [mN m^{-1}]	γ_{eq} [mN m^{-1}]	α [mN m^{-1}]	β [mN m^{-1}]	k [s^{-1}]	τ [s]	r^2	t_d [s]	ϵ [m Nm^{-1}]
WPI	38.3 ± 2.5^{a,b,c}	21.7 ± 0.1	11.3 ± 2.1^{a,b,c,e}	5.3 ± 0.5	1.3E-03 ± 4.2E-05^{d,e,f}	21.8 ± 0.02^{a,b,c}	0.995 ± 0.002	ND	40.6 ± 1.6^{c}
CE	43.9 ± 0.1^{a}	21.6 ± 0.4	17.7 ± 0.5^{a}	4.7 ± 0.8^{a}	7.3E-04 ± 2.8E-05^{a}	95.2 ± 2.9^{a}	0.994 ± 0.002	ND	41.2 ± 1.6^{a}
0.45 µm P	46.3 ± 0.7^{b}	20.5 ± 2.6	17.7 ± 1.7^{b}	8.1 ± 1.6^{a,b}	1.3E-03 ± 3.8E-04^{b}	70.8 ± 8.8^{b}	0.999 ± 0.000	ND	38.9 ± 3.0
300 kDa P	42.0 ± 0.9^{b,d,e}	21.5 ± 0.1	16.0 ± 0.8^{d,e}	4.4 ± 0.02^{b}	2.2E-03 ± 4.3E-05^{a,b,e}	34.4 ± 0.5^{a,c}	0.993 ± 0.001	ND	35.9 ± 0.6^{a,b,c}
300 kDa R	37.4 ± 0.2^{a,b,c,e}	20.3 ± 0.4	11.4 ± 0.3^{a,b,c,e}	5.7 ± 0.02	2.6E-03 ± 1.9E-04^{a,b,c,f}	19.1 ± 0.5^{a,b,c}	0.998 ± 0.001	1710 ± 325	--
10 kDa P	42.2 ± 0.8^{c}	23.3 ± 0.1	16.0 ± 0.8^{c}	4.6 ± 1.1^{b}	1.9E-03 ± 3.2E-05^{a,c}	129.6 ± 22.6^{a,b,c}	0.988 ± 0.003	ND	41.9 ± 0.3^{b}
10 kDa R	36.7 ± 0.1^{a,b,c,d}	20.2 ± 0.1	11.0 ± 0.2^{a,b,c,d}	5.5 ± 0.2	2.4E-03 ± 1.5E-04^{a,b,d}	19.2 ± 2.3^{a,b,c}	0.996 ± 0.001	2180 ± 594	--

ND: Not Detected.

A2. Strain sweep

Additional tests were conducted to characterize the gels produced with alga fractions. After the heating and cooling steps, the samples were subjected to a small amplitude oscillatory shear in the range 0.001 to 10. This allows the study the rigidity and breakdown behaviour of the formed gels. The results are presented in Fig. A2. For each fraction the same tendency of G′ was observed. First a linear period, followed by a deformation and a sharp decline. The point of steep decrease in G′ (critical strain γ_c) was noted for every case (Table A3) . Low values of γ_c indicates a rather brittle material, as obtained by Martin et al., (2014) for gels containing 2.5-10 % Rubisco (γ_c ~0.037-0.044). The gels prepared in this research showed larger values of critical strain (γ_c ~0.1-1.3), suggesting a more flexible character.

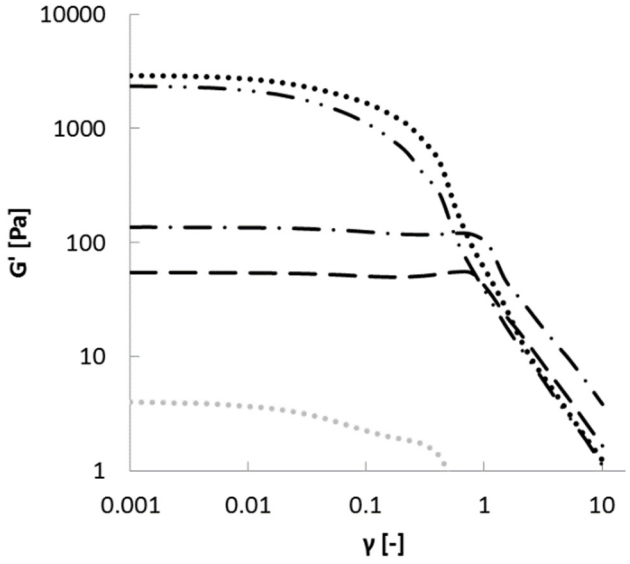

Figure A2. Strain sweep for fractions containing 10 % (···· CE, — ·· 0.45 *μm* P) and 5 % (— · 300 *kDa* R, — — 10 *kDa* R, ···· CE) proteins. P=Permeate, R= Retentate.

Table A3. Critical strain for gels containing alga fractions.

Sample	γc [-]
CE 10%	0.19 ± 0.04[a]
0.45 µm P 10%	0.10 ± 0.02[a]
CE 5%	0.0098± 0.004[a]
300 kDa R 5%	1.30 ± 0.29
10 kDa R 5%	1.31 ± 0.29

Chapter 5

Selective and energy efficient extraction of functional proteins from microalgae for food applications

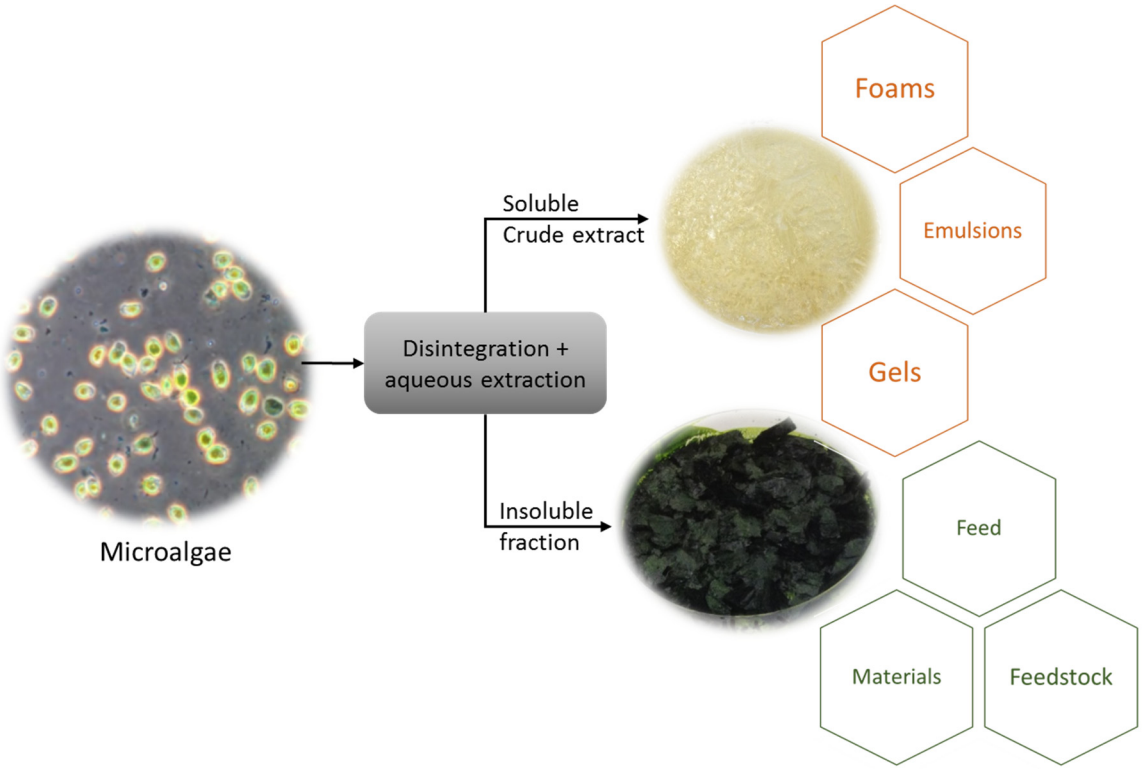

Published as:

E. Suarez Garcia, J.J.A. van Leeuwen, C. Safi, L. Sijtsma, M.H.M. Eppink, R.H. Wijffels, C. van den Berg (2018). Selective and energy efficient extraction of functional proteins from microalgae for food applications Bioresource Technology 268, 197-203.

Abstract

The use of a single controlled bead milling step of the microalga *Tetraselmis suecica* resulted in a soluble fraction, rich in functional proteins. This was achieved by fine-tuning the processing time, thereby exploiting the difference in rates of protein and carbohydrate release during milling. Soluble proteins were extracted under mild conditions -room temperature, no addition of chemicals, pH 6.5, with a yield of 22.5 % and a specific energy consumption of 0.6 kWh kg_{DW}^{-1}, which is within the recommended minimum energy for an extraction step in a biorefinery process. The resulting protein extract contained 50.4 % (DW) of proteins and 26.4 % carbohydrates, showed light green color and displayed superior surface activity and gelation behavior compared to whey protein isolate. The proposed process is simple (only one bead milling step), scalable, and allows the mild extraction of functional proteins, making it interesting for industrial applications in the food industry.

1. Introduction:

Microalgae have been considered a promising feedstock for the feed and food industries due to their rich composition (broad range of biomolecules of diverse chemical nature), superior areal productivities compared to traditional crops and no dependence on fresh water and arable land (Draaisma et al., 2013). However, the implementation of algae fractions as functional ingredients in food products remains largely unexplored.

The fractionation and purification of biomolecules –in particular proteins- from algae is not trivial. The first step, for most algae strains, involves cell disruption in order to release intracellular components into the bulk medium. For this, several technologies have been successfully employed, including bead milling, ultrasonication, enzymatic hydrolysis among others (Gunerken et al., 2015, Phong et al., 2018). After cell disintegration, the resulting suspension is subjected to several separation steps which can be grouped into precipitation, filtration, extraction or combinations of these processes. Precipitation methods take advantage of the solubility and isoelectric point of the target molecules in order to induce selective precipitation. The method is commonly referred as pH-shifting and involves a broad range of pH adjustment to maximize protein solubility followed by precipitation at the isoelectric point (Ba et al., 2016; Benelhadj et al., 2016; Cavonius et al., 2015; Gerde et al., 2013). Filtration methods make use of differences in the polarity and molecular size of the components in suspension to obtain fractions rich in the molecules of interest (Safi et al., 2017, 2014). More elaborated processes involving three phase partitioning (Waghmare et al., 2016), extraction + precipitation + filtration (Chronakis, 2001; Ursu et al., 2014) or precipitation + dialysis + adsorption (Schwenzfeier et al., 2011) have also been investigated to purify proteins from algae. In these cases, higher purities are obtained at expenses of intricate and costly processing steps.

As indicated by Ruiz Gonzalez et al., (2016), algae products for the food market will be profitable within the next decade if further cost reductions in both cultivation and

downstream processing are achieved. This could be attained by reducing the amount of unit operations (process integration) while keeping the final products in a high-end market segment (functional ingredients) (Cuellar-Bermudez et al., 2015). In spite of the several studies dealing with protein fractionation and purification, little attention has been paid to simple processing and to product functionality for food applications. In previous research (Postma et al., 2016) it was observed that the release of soluble proteins from microalgae already reaches a maximum at early stages of bead milling, and that the rates of protein release are significantly superior compared to the rates of carbohydrate release. It appears that controlling the residence time during bead milling allows the selective fractionation of proteins from carbohydrates.

The aim of this study was to demonstrate that with a simple process strategy (one unit operation, low energy consumption) it is possible to selectively concentrate proteins from green microalgae in a crude extract. Furthermore, the techno-functional properties (foaming, emulsification, gelation) of the resulting crude extract were determined and compared to the commercial standard whey protein isolate.

2. Material and methods

2.1. Algae cultivation, harvesting and fractionation

Cultivation. Tetraselmis suecica (UTEX LB2286, University of Texas Culture Collection of Algae, USA) was cultivated in 25 L flat panel photo bioreactors (AlgaePARC, Wageningen - The Netherlands) located in a green house. The cultures were supplied with artificial light, CO_2 and nutrients as described by Postma et al., (2016). The biomass was harvested via continuous centrifugation (E10, Evodos, NL) at 80 Hz and concentrated to ~ 20 % dry weight (dw). This suspension was stored at 4^{o}C in the dark for up to 7 days until disruption experiments, in order to limit the extent of biomass decay due to bacterial growth.

Fractionation. A fresh algal suspension (biomass) is fed to a bead milling where both cell disintegration and aqueous extraction are taking place. The bead milled suspension

is centrifuged (14000 rpm, 30 min, 20°C) and the resulting fractions regarded as soluble crude extract and insoluble fraction.

2.2. Algae disruption and aqueous extraction

Bead milling. Algae suspensions containing about 100 g_{DW} L^{-1} were prepared in distilled water and used as feed for the disruption experiments. Disruption was conducted in a horizontal 0.075 L bead mill (Dyno-Mill Research Lab, Willy A. Bachofen AF Maschinenfabrik, Switzerland) containing 0.4 mm Y_2O_3 stabilized ZrO_2 beads at 65 % filling percentage. The system was operated in batch recirculation mode, with a constant agitation speed of 2039 rpm. Temperature of the suspension was controlled at ~ 25 °C with an external cooler (FP40-HE, Julabo® GmbH).

Sample collection. Samples from the feed chamber were collected at different time intervals and used for the estimation of the disintegration rates and for the quantification of component release. For the latter, the samples were centrifuged and the supernatants and pellets analyzed separately.

2.3. Analytical methods

Cell disintegration. Cell disintegration was quantified in a flow cytometer (BD Accuri C6®). In this technique, forward scattering data was used to estimate the number of intact cells remaining at every time step compared to the initial amount of intact cells (Postma et al., 2016).

Biomass characterization. Dry weight and total ash were estimated gravimetrically after drying in oven at 100°C for 24 h and burning in a furnace at 575°C respectively. Proteins were measured with the method of Lowry (Lowry et al., 1951), total carbohydrates with the method of Dubois (Dubois et al., 1956) and total lipids with the method of Folch (Folch et al., 1957). Starch content was estimated with a commercial kit (Total Starch, Megazyme® International, Ireland).

Pigment release. The release of pigments was determined by measuring the UV-spectra of supernatants at several times using an UV-Vis spectrophotometer DR 6000

(Hatch Lange, The Netherlands). The wavelengths 430 nm, 450 nm and 660 nm were selected as representative for total pigments (Chlorophyll a and b).

Mass yields. Mass yields per component (Y_i) were estimated according to:

$$\mathrm{Y}_i\ \% = \frac{m_{i,j}}{m_{i,b}} \times 100 \qquad \text{Eq. 1}$$

Where m_i is the mass of component *i* (protein, carbohydrates, etc.). Subscripts *j* and *b* refer to each fraction evaluated (supernatant, pellet) and initial biomass, respectively.

Acrylamide native gel electrophoresis. Protein samples were diluted with native buffer (Biorad) at a ratio 1:0.8 v/v. 25 µL of the resulting solution was loaded per lane in a 4–20% Criterion TGX gel (Biorad). Electrophoresis was run at 125 V for 75 min using Tris-Glycine (Biorad) as running buffer. Gels were stained overnight with Bio-Safe Coomassie blue (Biorad).

2.4. Techno functional properties

Prior to the evaluation of the techno functional properties, samples were freeze dried during 24 h in a Sublimator 2x3x3, Zirbus Technology® GmbH, and stored at 4°C in sealed bags. Unless otherwise noticed, all experiments were conducted at room temperature (~ 23°C); all runs were performed in duplicate.

Whey protein Isolate (WPI). Whey protein isolate (BiPRO, Davisco Foods international) with a purity of 97.6 % was used as commercial reference protein.

Surfactant activity. Surface activity of samples containing alga proteins was determined via static drop experiments in an Automated Drop Tensiometer (ADT Tracker®, Teclis Scientific, France). With this technique, the surface tension of individual drops created automatically are monitored over time. Two distinct set ups were used to assess foaming and emulsification activity.

To investigate foaming activity, algae samples were dissolved in MilliQ® water to obtain solutions containing 0.1 % (w/v) protein at pH 7. A single drop containing 11 µL of protein solution is formed and held hanging, while subjected to a stream of saturated

air flowing vertically in a 5 ml cuvette. Emulsification studies were conducted on a 20 µL drop of hexadecane (Anhydrous, > 99%, Sigma Aldrich) submerged in 5 ml of a 0.1 % (w/v) protein solution.

Gelation. Gelation tests were conducted according to Martin et al., (2014), using an Anton Paar MCR 302® (Modular Compact Rheometer). Solutions containing 10 % protein (w/v) were prepared in MilliQ® water and adjusted to pH ~ 7. Gel strength was measured in terms of the storage modulus of the sample (G' [=] Pa), which represents its elastic behavior. G' was recorded along a heating – cooling profile in the range 25 to 95^{o}C, using a heating rate of 5^{o}C min^{-1}.

3. Results and Discussion

3.1. Bead milling and component release

The kinetics of cell disintegration and component release during bead milling of microalgae was investigated by Postma et al., (2016) at different bead sizes (0.3 to 1 mm). For the case of *T. suecica*, it was observed that the same kinetic rates were obtained regardless of the bead size. In addition, the rates of protein release were over 6 times higher than those of carbohydrate release. The authors argued that the slow release of sugars is due to the solubilization of saccharides from the cell wall and starch granules. To further confirm this reasoning, a complete analysis of component release during bead milling was conducted for a period of 3 h. The results for disintegration, proteins, carbohydrates and starch are presented in Fig. 1A. In accordance with our previous findings, proteins are quickly released into the bulk medium, reaching a plateau phase after ~ 10 min. Cell disintegration takes place at lower rates, but the disintegration profile flattens out after ~ 30 min. This can be explained considering a two-steps disintegration process: Cell bursting, where the intracellular content is released without tearing the cells, and comminution, where the cells are fragmented over time into smaller debris. The method used to quantify intact cells (section 2.3) is based on particle size and thus, cells are counted as intact even if the cell wall has received damage without fragmentation.

The rates of carbohydrate release (i.e., total sugars in the soluble phase) and the fraction of starch loss (i.e., total starch in the insoluble phase) were also quantified (Fig. 1A). In both cases, the experimental data follow a first order model ($r^2 > 0.96$) with corresponding kinetic constants of $5.9x10^{-3} \pm 2.7x10^{-4}$ s^{-1} and $3.6x10^{-3} \pm 1.6x10^{-4}$ s^{-1} for carbohydrates and starch respectively. This suggests that the enrichment of sugars in the soluble phase can be explained in part by the loss of starch from the insoluble phase. In fact, starch dextrinization, which is the process of partial de-polymerization, can occur under intense shear conditions (Sarifudin and Assiry, 2014) as occurring in the bead mill. Additional tests were conducted in order to rule out the possibility of starch degradation due to intracellular enzymes (data not shown). In line with the kinetic data published for *T. suecica*, our observations confirmed that ~ 8 min processing time is sufficient to release nearly 95 % of the maximum achievable amount of proteins in the soluble phase. Although not confirmed experimentally, it is expected that a shorter bead milling time leads to larger fragments of cell debris which are less stable in the soluble phase and thus, their removal becomes easier.

In Fig. 1B, the corresponding composition of the insoluble (pellet) and soluble fractions (supernatant) after bead milling are presented. The protein content in the biomass is 54.0 ± 4.0 %, significantly higher compared with ~ 30 - 43 % (dw) published for the same strain (Postma et al., 2016) and ~ 35 % (dw) for *Tetraselmis sp*. (Schwenzfeier et al., 2011). This can be due to variations in light supply as the alga cultures were kept in a green house. Michels et al., (2014) reported values of protein content fluctuating from 35 to 55 % (dw) for *T. suecica* in the period February to March, for cultures maintained in green houses.

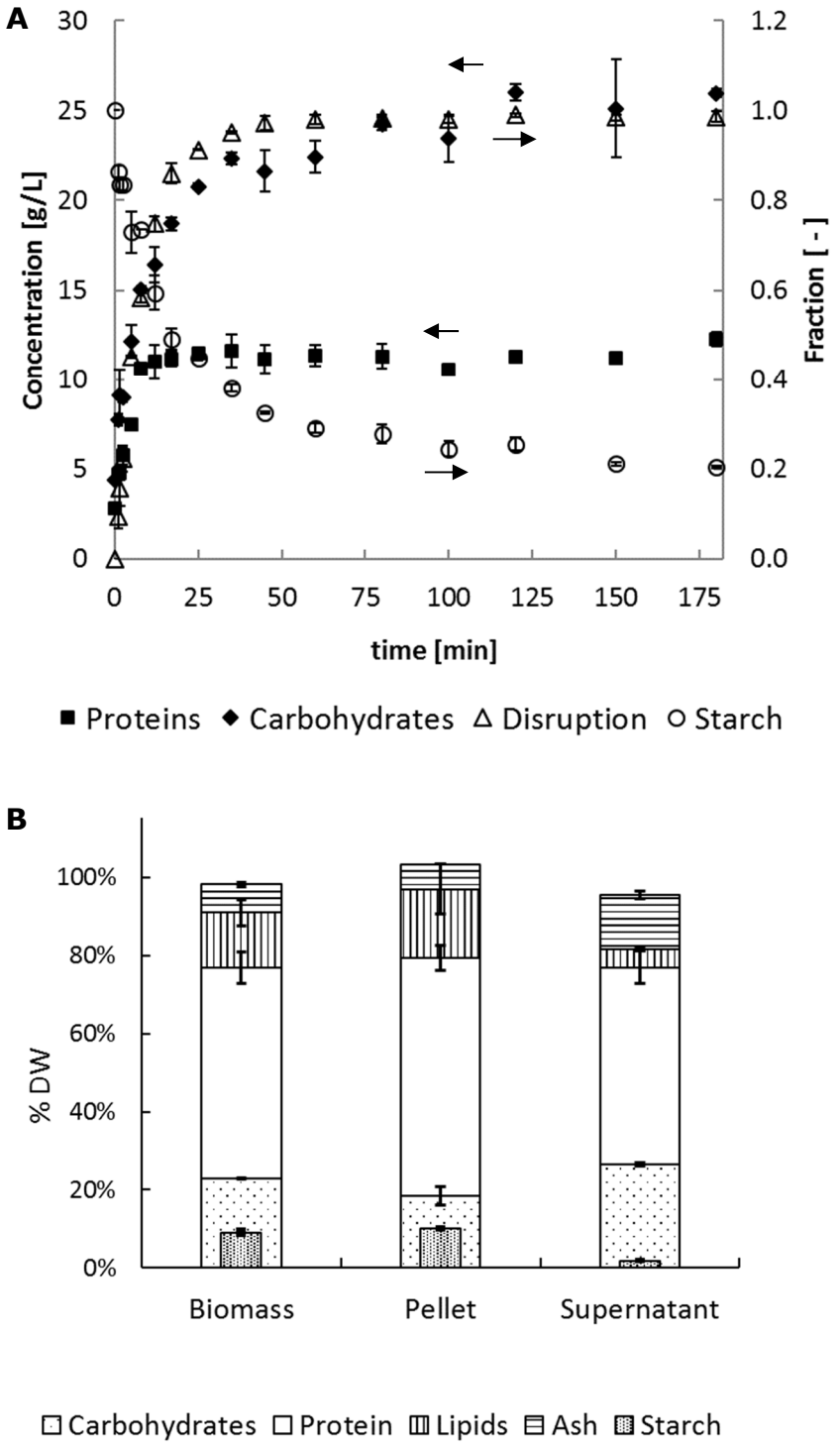

Figure 1. A. Overview of cell disruption (fraction of disintegrated cells), protein and carbohydrate concentration (in the soluble phase), and starch content (fraction remaining in the insoluble phase compared to initial biomass content) during 3 h bead milling of *T. suecica*. Arrows point to the corresponding axis for each curve. **B.** dry weight compositions of fractions after 8 min bead milling and centrifugation.

As displayed in Fig. 1B, the content of proteins and carbohydrates changes marginally from biomass to pellet and supernatant. The pellet phase, nonetheless, is richer in lipids (17.6 % ± 6.5 %) and contains a small fraction of ash (6.3 ± 0.1 %), making it an interesting feedstock for feed formulations. Although whole microalgae cells have long been used as feed in aquaculture (Shields and Lupatsch, 2012), the pellet phase represents a more attractive alternative for various reasons. First, its high protein and lipid content and the low amount of ash resembling typical diets in fish trials (Sorensen et al., 2016). Second, *T. suecica* has been reported to contain polyunsaturated fatty acids, in particular Eicosapentanoic acid (EPA) (Abiusi et al., 2014), which is a crucial ingredient to develop feed formulations devoid of fish meals. Moreover, since the pellet phase contains mostly cell debris, it is expected that nutrient accessibility is superior, leading to enhanced digestibility (Teuling et al., 2017). Other applications of the insoluble fraction include bio-based materials or feedstock for other industries.

3.2. Protein yields and energy consumption

The kinetics of protein and carbohydrate release for *T. suecica* during bead milling (Fig. 1A) was exploited in order to limit the enrichment of carbohydrates and pigments in the soluble phase. After short bead milling (8 min), the ratio of proteins to carbohydrates was 3.31 g g^{-1}, significantly higher compared to 0.45 g g^{-1} when disintegration is run for 3 h (Fig. 1). Also the amount of released pigments is reduced. This was confirmed by visual inspection of the samples and by determining the amount of pigment released in the soluble phase (Fig 2A). Pigments migrate to the soluble phase at slower rates compared to the rates of disintegration and protein release (Fig 1A) as also observed by Postma et al., (2015). This is expected as pigments are usually located in the chloroplast as part of the light harvesting mechanism of the cells (Knoetzel et al., 1988) and therefore not freely available upon cell disintegration. We have found that the kinetics of pigment release does not clearly follow a first-order model (r^2>0.85). Fig. 2A shows that beyond 120 min bead milling time, the amount of released pigments follows a linear trend, implying a two-steps mechanism. An overall kinetic constant of $8.1x10^{-4}$ ± $3.9x10^{-4}$ s^{-1} was estimated as representative for all

pigments. This value is up to 2 orders of magnitude inferior than the kinetic constants reported by Postma et al., (2015) for pigments from the microalgae *C. vulgaris*, which can be the result of physiological differences among the two algal species.

The corresponding mass yields in the supernatant fraction are 22.5 % for proteins, 27.7 % for carbohydrates, 8.1 % for lipids and 45.5 % for ash. The bead milling process can be considered as an aqueous extraction process and thus, the largest fraction of lipids remains in the pellet phase due to their hydrophobic nature and density. The small amount of total lipids in the soluble phase corresponds to phospholipids, prosthetic groups (e.g., porphyrins) (Schwenzfeier et al., 2013b), lipoproteins and pigments. Similarly, the largest fractions of carbohydrates and proteins remain in the insoluble phase. Starch, which accounts for almost 40 % of the total carbohydrates, is insoluble at room temperature. The rest of the carbohydrates in the pellet phase correspond to cell wall fragments (Becker et al., 1998) and other insoluble cell debris.

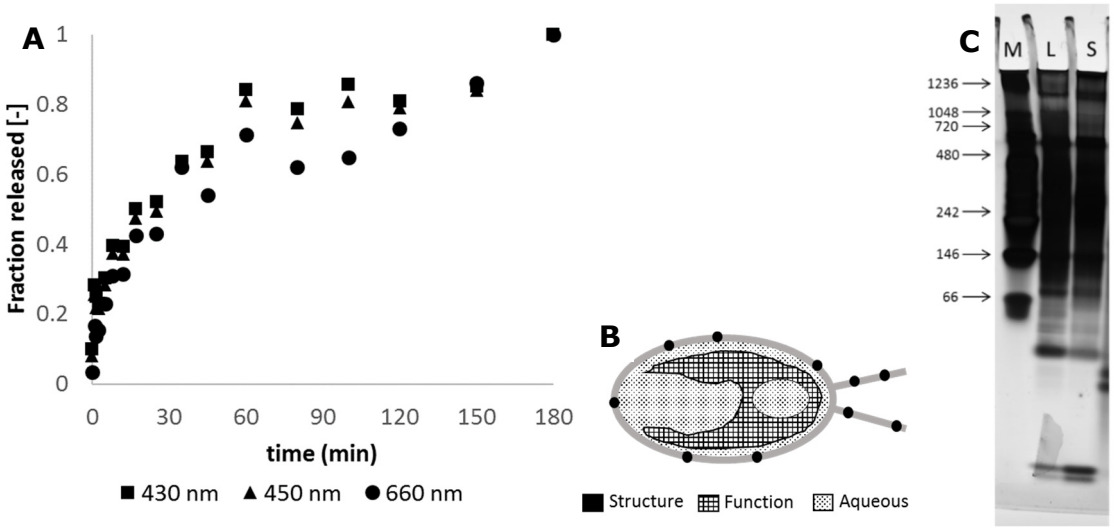

Figure 2. A. Absorbance of soluble phases during bead milling. . **B.** Schematic representation of hypothetical protein pools in *T. suecica.* **C.** Native gel electrophoresis (M, marker) of samples after long (L, 3h) and short (S, 8 min) bead milling.

Regarding proteins, previous studies have found yields in the soluble phase of 21 to 24 % for *Tetraselmis* species after mechanical disintegration (Postma et al., 2016; Schwenzfeier et al., 2011). Such low yields can be explained considering the characteristics of the extraction process (aqueous buffer, native pH~6.5, room

temperate) and the nature of the proteins in green microalgae. We hypothesize that for *T. suecica* proteins are present in pools (Fig. 2B). A first pool (Aqueous) corresponds to proteins that exist in the cytosol and in internal organelles like the pyrenoid (González et al., 2015). Upon cell rupture, those proteins migrate rapidly to the bulk fluid due to a concentration gradient. A second pool (Structure) are proteins which have a more structural role, for instance proteins in the cell wall and membrane, and in the flagella. The extraction of such proteins has been reported using detergents (Becker et al., 1998; Gödel et al., 2000). Another major pool (Function) corresponds to proteins which are present in the chloroplast and are involved in the light harvesting system of the cells. Such proteins are non-covalently bound to an intricate assembly of pigments and have been shown to be soluble in detergents (Knoetzel et al., 1988). It becomes evident that the proteins present in the pellet phase (72 % of the total) could only be extracted under detergent conditions, or using methods in which the insoluble structures, in which proteins are entangled, are solubilized. For the present case, mechanical shear caused by bead milling is insufficient to induce such solubilization.

Several extraction methods have been proposed in literature for the extraction of soluble proteins from microalgae. Those methods can be divided into physical and chemical. Physical methods involve mechanical shear (bead milling, high pressure homogenization, ultrasonication, explosive decompression, microfluidization), electric fields and thermal treatments (thermal shock, microwaves). Chemical methods include solvents, ionic liquids, pH shifts and enzymatic hydrolysis (Günerken et al., 2015; Phong et al., 2018b). The extent of cell damage and consequently the resulting protein yields depend greatly on the algal strain and on the amount of energy that can be effectively transferred to the cells. In Fig. 3 several physical processes reported in literature for the extraction of proteins from microalgae are compared in terms of yield and specific energy consumption (*Em* [kWh kg^{-1}_{DW}]). Two reference levels are indicated: the minimum experimental specific energy (Em_{min}) required to break a cell of *T. suecica* (Lee et al., 2013) and *C. vulgaris* (Günther et al., 2016) which varies from $1.9x10^{-4}$ to $2.5x10^{-3}$ kWh kg_{DW}^{-1} depending on the strength of the cell wall and on the osmolality,

and the maximum specific energy (Em_{ext}) recommended for the extraction step within a biorefinery, which is estimated at 0.6 kWh kg_{DW}^{-1} and equivalent to ~ 10 % of the energy content in microalgae (Coons et al., 2014; Illman et al., 2000). It is remarkable that all the reported methods require at least 100 times more energy than Em_{min}. This is due to energy losses and dissipation to the bulk media, in other words, energy that is not effectively applied on the cells. From Fig. 3, only mechanical methods namely bead milling and high pressure homogenization resulted in acceptable yields (> 20 %) and energy consumptions below the target Em_{ext}. In the present study we measured a protein yield of 22.5 % and an E_m of 0.607 ± 0.002 kWh kg_{DW}^{-1}. Safi et al., (2017a) reported yields from 23 to 51 % and corresponding energy consumptions of 0.1 to 0.6 kWh kg_{DW}^{-1} for the microalgae *Nannochloropsis gaditana* using bead milling and high pressure homogenization. Such high yields reflect structural differences between the two algae strains, since both works implemented comparable operation conditions for the case of the bead milling (BM) process.

In general, the application of electric fields leads to low yields even at high energy consumptions. This is due to the presence of a cell wall, which remains practically unaffected by electric fields (’t Lam et al., 2017). Parniakov et al., (2015) reported protein yields of nearly 15 %, but the process involved pulsed electric fields at pH 8.5, thus a synergistic effect is likely. Ultrasound, which mechanism of action on the cells involves shear caused by cavitation, can lead to appreciable protein yield at expenses of a high energy consumption. This is the case of the work of Safi et al., (2014c) who reported protein yields ranging from 8 to 67 % for several algae strains under the same processing with a consequent specific energy consumption of *Em* ~187 kWh kg_{DW}^{-1}. Worth noticing, several works in which thermal treatments were implemented reported energy consumptions of the order of 3 kWh kg_{DW}^{-1} with protein yields ranging from 1.5 to 35 %. It is not surprising to obtain low yields of soluble proteins under thermal processing, due to denaturation and consequently thermal coagulation. However, a 35 % yield reported by Jazrawi et al., (2015) after processing *Chlorella vulgaris* at 200 ^{o}C suggests instead a high degree of protein denaturation via hydrolysis,

rendering the extract phase rich in small protein fragments. The effect of the extraction process on the protein conformation is rarely studied. As shown in Fig. 2C, all the protein bands expected for *T. suecica* (Postma et al., 2016) are preserved, confirming the mildness of the present extraction process.

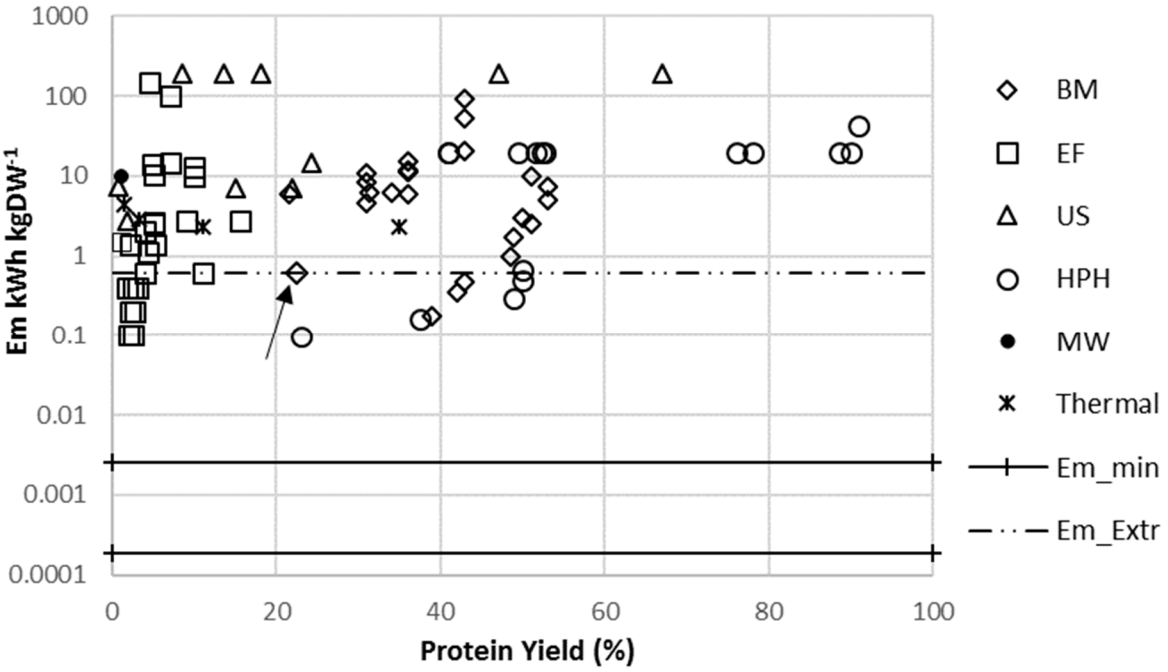

Figure 3. Overview of specific energy consumption (***Em*** [kWh kg^{-1}_{DW}]) for algal disintegration and corresponding protein yields. **BM:** Bead milling (arrow: present study, (Postma et al., 2016; Postma et al., 2015; Safi et al., 2017a)), **EF:** Electric Fields ('t Lam et al., 2017; Grimi et al., 2014; Parniakov et al., 2015; Postma et al., 2016; Safi et al., 2017a), **US:** Sonication (Grimi et al., 2014; Parniakov et al., 2015; Passos et al., 2015; Safi et al., 2014c; Wenjuan et al., 2013), **HPH:** High Pressure Homogenization (Grimi et al., 2014; Safi et al., 2017a, 2014a, 2014c), **MW:** Microwaves (Passos et al., 2015), **Thermal** processing (Jazrawi et al., 2015; Passos et al., 2015), ***Em_{min}*:** Minimum specific energy for cell rupture (Günther et al., 2016; Lee et al., 2013), ***Em_{Ext}*:** Target maximum specific energy for extraction (Coons et al., 2014; Illman et al., 2000).

3.3. Techno-functional properties

Despite its importance, the techno-functionality of algae proteins is often overlooked. Most studies focus on presenting yields or extraction efficiencies, without addressing potential applications beyond a mere amino acid profile analysis. The issue of purity is also frequently neglected. In general, for a given separation process, purity and yield

are inversely related. In other words, higher yields can be achieved at expenses of low purities. Cavonius et al., (2015) and Ba et al., (2016) reported a process of high pressure homogenization and pH-shifting which resulted in protein yields of 68 to 84 % with purities of 26-44 % (DW). On the contrary, high purities can be obtained by implementing several unit operations, but having as consequence low yields. This is the case of the process presented by Schwenzfeier et al., (2011), in which bead milling, adsorption, precipitation and dialysis yield 7 % of the total protein in the soluble phase with a purity of over 64 % (DW). Similarly, two processes leading to protein purities above 78 % (Chronakis, 2001; Waghmare et al., 2016) are complex, requiring multiple and expensive unit operations, thereby unsuitable for large scale applications. It is also clear that pH-shifting is the most common method to extract proteins (Benelhadj et al., 2016; Gerde et al., 2013; Ursu et al., 2014). However, this requires the addition of chemicals, which is economically undesirable and can lead to protein denaturation. The present research involves a single unit operation and leads to a protein yield of 22.5 % and purity of 50.6 % (DW).

The functional activity of the crude protein extracted after short term bead milling was further investigated in terms of surface activity and gelation behavior. Samples were compared with whey protein isolate. Dynamic surface activity for air water interfaces (foaming) and oil water interfaces (emulsification) showed the expected tendencies (Fig. 4A): a sharp decline in surface tension followed by a slow decrease to reach an equilibrium value. This behavior reveals three basic mechanisms namely diffusion towards the surface, adsorption and molecular reorientation (Serrien et al., 1992). Hence, superior surface activity is reflected in a curve with a higher slope and a lower value of surface tension at equilibrium. From Fig. 4A it is clear that the crude protein fraction presented a higher surface activity than whey protein isolate (WPI) for foaming and emulsification. This superior performance can be due to the presence of charged carbohydrates and glycoproteins as hypothesized by Schwenzfeier et al., (2014). In addition, the presence of lipids (8 % by weight) in the crude extract could have

contributed to the development of more stable interactions around the surfaces (Gerde et al., 2013).

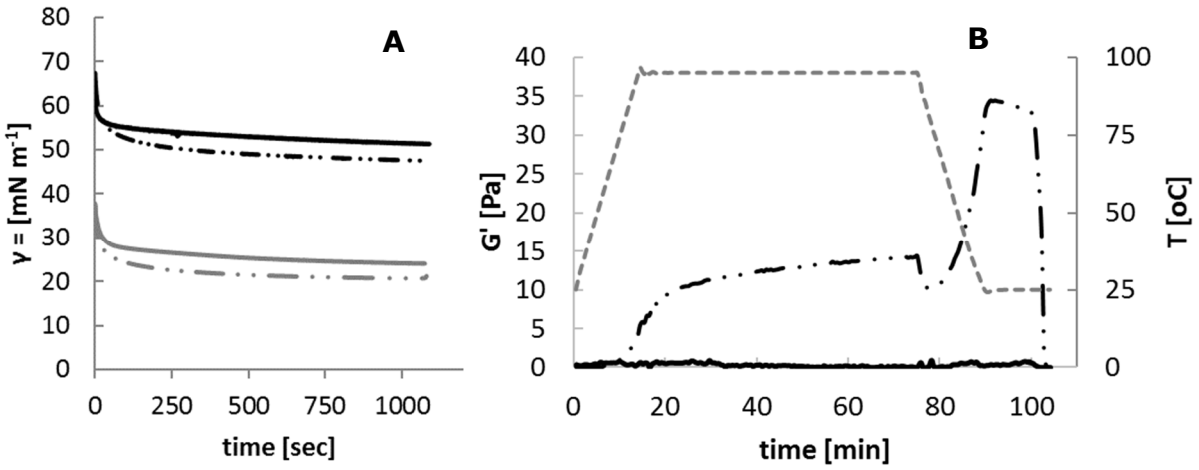

Figure 4. A. Surface activity for algae samples (·· –) and Whey Protein Isolate WPI (–) for foaming (black) and emulsification (grey). **B.** Gelation of alga samples and corresponding temperature (– –).

The gelation behavior was studied by measuring the storage modulus (G' [Pa]) during a defined heating-cooling profile (Fig. 4B). During the heating phase (25-90 ^{o}C) proteins unfold, exposing their functional groups. This makes possible the formation of covalent bonds with neighboring molecules, which result in the development of a film-like structure. During the cooling phase (90 -25 ^{o}C) the gel further hardens due to the formation of non-covalent interactions such as hydrogen bonds and hydrophobic interactions (Martin et al., 2014). WPI did not show gel-like behavior at 10 % protein content. WPI is composed of small globular proteins and thus, steric repulsion may prevent the formation of a stable network during the heating-cooling treatment. On the contrary, the algae extract contains proteins of a broad range of sizes (Fig. 2C) in addition to sugars, lipids and ash, which may be contributing not only to forming new bonds during the heating phase but to enhancing the rigidity of the gel network. Chronakis, (2001) suggested that hydrophobic interactions are mainly responsible for molecular association and aggregation. It was also argued that, for the case of proteins

extracted from cyanobacteria, gelation properties are controlled from protein complexes rather than from individual proteins.

4. Conclusions

In this study it was shown that the soluble extract from green microalgae can be significantly enriched with proteins by performing cell disintegration –via a single bead milling step- for short times. This also ensures low specific energy consumptions, well below other disintegration methods like ultrasonication and electric fields. The resulting crude protein extract displayed excellent surface activity and gelation behavior, superior to whey protein isolate. The proposed process is easily scalable, does not require the addition of chemicals or expensive unit operations and lead to a product with potential application as functional ingredient in foods.

Acknowledgements

This project is financed by the Dutch Technology Foundation STW under the project AlgaePro4You, nr. 12635. From January 2017, STW continued its activities as NWO (Dutch national science foundation) Applied and Engineering Sciences (TTW).

Appendix

Table A1. Overview of fractionation processes of microalgae products with focus on product functionality, and composition (% dw) of selected fractions (Prt: Proteins, CH's: Carbohydrates, Lip: Lipids).

Reference	Algal Strain / Functional Property	Process	Y_P %	Prt.	CH's	Lip.	Ash
Present study	*Tetraselmis suecica* Surface activity: Foaming Emulsification Gelation	Bead milling (8 min)	22.5	50.6	26.4	4.7	13.7
(Garcia et al., 2018)	*Tetraselmis suecica* Surface activity: Foaming Emulsification Gelation	Bead milling (BM) + filtration (0.45 µm)	11.7	25.5	44.9	4.8	24.8
		BM + Ultrafiltration (UF) (Retentate, 300 kDa)	4.4	21.3	60.0	7.8	11.0
		BM + UF (Retentate, 10 kDa)	3.4	20.6	64.9	3.8	10.8
(Ba et al., 2016)	*Haematococcus pluvialis.* Emulsification	High pressure homogenization + pH shift (pH 5.7)	64	26	37	18	n.a.
		High pressure homogenization + pH shift (pH 7)	73	44	26	16	n.a.
(Waghmare et al., 2016)	*Chlorella pyrenoidosa* Foaming Water/oil absorption	Precipitation in three phase system + enzyme hydrolysis + Dialysis + precipitation	n.a.	78.3	12.8	4.1	4.1
(Benelhadj et al., 2016)	*Arthrospira platensis* Water/oil absorption Emulsification Foaming	Biomass dissolution + Isoelectric precipitation (pH 3)	n.a.	69.6	8.9	3.7	17.8

(Cavonius et al., 2015)	*Nannochloropsis oculata.* Enriched Food/Feed	Homogenization + pH shift (pH 7→3, Pellet) Homogenization + pH shift (pH 10→3, Pellet)	86 72	23 24	42 58	12 13	25 28
(Ursu et al., 2014)	*Chlorella vulgaris* Emulsification	Homogenization + pH shift (pH 12-4) Homogenization (pH 12) + Ultrafiltration	40 50	n.a n.a.	n.a. n.a.	n.a. n.a.	n.a. n.a.
(Gerde et al., 2013)	*Nannochloropsis spp* Enriched Food/Feed	Extraction (pH 11) + precipitation (pH 3) Extraction (pH 11) + precipitation (pH 3) (defatted)	35 16	41 53.5	5.6 6.7	20.5 n.a.	7.3 8.2
(Schwenzfeier et al., 2014, 2013b, 2013a, 2011)	*Tetraselmis sp.* Foaming Emulsification	Bead milling + Adsorption + precipitation + dialysis.	7	64.4	23.8	n.a.	n.a.
(Chronakis, 2001)	*Spirulina platensis* Gelation	Extraction + precipitation (pH 10/3) + dialysis + defatting	n.a.	78.6	n.a.	n.a.	n.a.

n.a.: Not available.

Chapter 6

Fractionation of proteins and carbohydrates from crude microalgae extracts using an Ionic liquid based-Aqueous Two Phase System

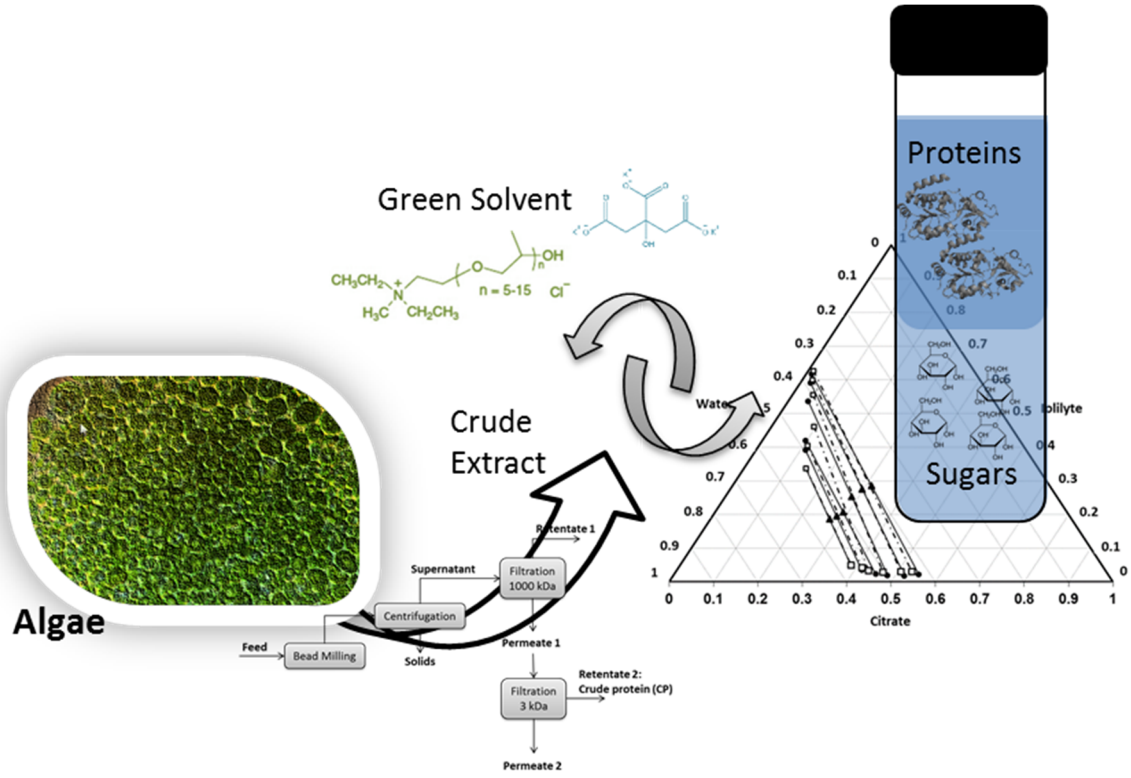

Published as:

E. Suarez Garcia*, C. Suarez Ruiz*, M.H.M. Eppink, R.H. Wijffels, C. van den Berg (2018). Fractionation of proteins and carbohydrates from crude microalgae extracts using an Ionic liquid based-Aqueous Two Phase System. Separation and Purification Technology 204, 56-65.

* Equal contribution

Abstract

Mild, simple and efficient recovery methods are required to obtain high-value microalgae proteins. As a promising extraction method, an Aqueous two phase system (ATPS) was used to partition proteins from crude microalgae extracts obtained from two green microalgae of industrial interest: *Neochloris oleoabundans* and *Tetraselmis suecica*. Furthermore, the Non-Random Two Liquids model (NRTL) was applied to describe both the phase diagram and the partition coefficient of total protein. It was observed that total protein preferentially concentrates in the top phase. Additionally, no significant effect on partition or extraction efficiency was noted at different tie lines. Experimental data indicate that proteins and sugars are selectively fractionated in top and bottom phases respectively. The model provided a good representation of the experimental data for the liquid-liquid equilibrium. Moreover, the model also led to a good representation of the partitioning data for two reference proteins, Rubisco and Bovine Serum Albumin (BSA), as well as for total protein from crude microalgae extracts.

1. Introduction

Due to their rich composition, microalgae are a potential source of biomolecules for food, feed, chemical and pharmaceutical products, of which proteins are of paramount industrial relevance. Microalgae can accumulate up to 60% protein under different cultivation conditions (Draaisma et al., 2013). Because of their sustainability, techno-functionality and broad range of applications, algae proteins have been in the spotlight of numerous studies (Samarakoon and Jeon, 2012). However, microalgae proteins are often present intracellularly or forming complexes with pigments and polysaccharides and thus, their recovery and purification still represents a challenge (Chronakis et al., 2000). Several processes have been developed for the extraction and fractionation of proteins from microalgae. pH-shifting, filtration and adsorption are commonly reported (Lupatini et al., 2017). However, such processes, are often characterized by low yields, poor selectivity and harsh conditions. Further research on alternative separation methods is therefore required.

Aqueous two-phase system (ATPS) is a liquid-liquid extraction method that has been presented as a mild, easily scalable, efficient and cost competitive technology for the recovery of a broad range of biomolecules (Rosa et al., 2011). Although large scale applications are reported (Glyk et al., 2015), its widespread implementation has been constrained by the poor understanding of the partitioning mechanism and by the selection of the phase forming components, in terms of sustainability, recyclability and costs. Ionic liquids (ILs) have gained significant attention in the last decades as phase forming components in ATPS due to their chemical versatility and physicochemical properties. They are non-flammable and non-volatile. Moreover, their physicochemical properties (e.g. polarity, viscosity, miscibility) can be tuned by manipulating their cations and anions, allowing the tailor-made design of extraction processes (Ventura et al., 2017). Ionic liquid-based ATPS have been studied by several authors for the extraction of lipids proteins (Lee et al., 2017a). High extraction efficiencies and partition coefficients 3-4 times higher can be achieved in comparison with traditional polymer-salt systems (Desai et al., 2014).

Partitioning of proteins in IL-based ATPS is a complex phenomenon. It depends on several factors including type and concentration of phase-forming components, pH, temperature, ionic strength and chemical nature of the target molecule(s) (Ventura et al., 2017). In the case of proteins, hydrophobicity, isoelectric point, molecular weight and conformation play a critical role (Dreyer et al., 2009). Significant progress has been made in the theoretical understanding of the underlying mechanisms of protein partitioning as well as phase equilibrium in ATPS. For the latter, several thermodynamic models have been successfully implemented for systems containing polymers (Wu et al., 1998), salts (Perez et al., 2013) and ILs (Simoni et al., 2008). Thermodynamic models have also been used to describe and predict the partition coefficients of model proteins in ATPS; satisfactory estimations are reported for polymer/salt systems using an extension of the Pitzer's model (Perez et al., 2013) and multicomponent Wilson model (Madeira and Xu, 2005). For polymer-polymer systems, modifications of the Pitzer's model (Lin et al., 2003), Flory Huggins theory (Diamond and Hsu, 1990) and UNIQUAC model (Hartounian et al., 1994), have been successfully implemented. A correct understanding and prediction of equilibrium and partitioning can lead to further developments in design, scale up and process optimization.

Despite the large number of publications in the field of ILs and protein extraction (Du et al., 2007; Lee et al., 2017a), the application of ATPS for the extraction of microalgae proteins and in particular for crude microalgae extracts is limited. The published research have centred mostly on extracting *C-phycocyanin* from *Spirulina* strains (Luo et al., 2016), *B*-phycoerythrin from *Porphyridium cruentum* (Benavides and Rito-Palomares, 2006) and proteins from *Chlorella pyrenoidosa* (Waghmare et al., 2016) and *Chlorella sorokiniana* (Phong et al., 2017). Combination of several disintegration-extraction methods have also been described. Lee and co-workers (Lee et al., 2017b) extracted proteins from *Chlorella vulgaris* using ultrasound and IL-based buffers, proving that the IL aids in the disintegration process. This was also demonstrated by Orr et al. (Orr et al., 2016) for the extraction of lipids from wet microalgae.

In the present investigation, we study the equilibrium of an IL-based ATPS and the partitioning of crude protein extracts obtained from two green microalgae: *Neochloris oleoabundans* and *Tetraselmis suecica*. *N. oleoabundans* have been extensively investigated and it is considered a promising industrial strain due to its versatility, high growth rate, and biomass composition (Abu Hajar et al., 2017). *T. suecica* has been traditionally used in aquaculture (Gladue and Maxey, 1994) and recently it has been highlighted due to the techno-functional properties of its proteins (Schwenzfeier et al., 2014). In addition, the Non Random Two Liquids (NRTL) model is used to describe equilibrium and partition coefficients. The NRTL model was selected because of its flexibility to describe systems of different chemical nature, including electrolyte solutions and IL (Simoni et al., 2008), and because of its simplicity compared with models like UNIQUAC or UNIFAC (Renon and Pruasnitz, 1968). To our knowledge, this is the first attempt to describe the partitioning of crude microalgae proteins in ATPS containing ILs using thermodynamic models.

2. Experimental Section

2.1. Materials

The Ionic liquid Iolilyte 221PG (> 95 %) was purchased from Iolitec®. Citric acid monohydrate (> 99.0 %) was purchased from Merck Millipore®. Bovine serum albumin (BSA, > 96 %, 66.4 kDa), potassium citrate tribasic monohydrate (> 99.0 %) and D-Ribulose 1,5- diphosphate carboxylase (Rubisco, ~ 540 kDa), a partially purified protein from spinach, were purchased from Sigma-Aldrich®. Potassium citrate buffer stock solution was prepared by weighing and mixing 60 % (w/w) citric acid monohydrate with 60 % (w/w) potassium citrate tribasic until pH 7 was reached.

2.2. Microalgae cultivation and harvesting.

Two microalgal strains were used for this study: *Neochloris oleoabundans and Tetraselmis suecica*. *N. oleoabundans* (UTEX 1185, University of Texas Culture Collection of Algae) was cultivated in fresh water using a fully automated 1400 L vertically stacked tubular photobioreactor supplied with Bold's basal medium (Postma et al., 2017). *T. suecica* (UTEX LB2286, University of Texas Culture Collection of Algae,

USA) was cultivated in 25 L flat panel photobioreactors in sea water supplied with Walne medium. Cultivation details are given elsewhere (Postma et al., 2017). Both photo-bioreactor systems were located in AlgaePARC (Wageningen, The Netherlands). After harvesting, biomass was stored at 4 ^{o}C until further use.

2.3. Fractionation Process

The harvested microalgae were suspended in MilliQ® water to obtain a biomass concentration of ~ 90 g L^{-1}. The microalgae suspension was disrupted in a horizontal stirred bead mill (Dyno-Mill Research Lab, Willy A. Bachofen AF Maschinenfabrik, Switzerland) using 0.5 mm beads as described by Postma et al. (Postma et al., 2017). The milled suspension was then centrifuged at 14000 rpm and 20 ^{o}C for 30 min in a Sorval® LYNX 6000® centrifuge (ThermoFisher Scientific®). The supernatant was recovered and subjected to a two steps filtration process. First, ultrafiltration was conducted on a laboratory scale tangential flow filtration (TFF) system (Millipore®, Billerica, MA) fitted with a membrane cassette with a filtration area of 50 cm^2 and a cut-off of 1000 kDa (Pellicon® XL Ultrafiltration Biomax®). The process was run at constant transmembrane pressure until a 5x concentration factor was achieved. The resulting permeate was then filtered three times over a 3 kDa Ultracel® Amicon® Ultra centrifugal filter (Millipore®, Tullagreen, IRL). Each run was performed for 20 min at 4000 xg and 20 ^{o}C; MilliQ® water was used as feed for the second and third run. The resulting retentate, regarded as crude protein (CP), was stored at -20^{o}C until further use.

2.4. Characterization of the crude protein extract

The crude protein (CP) extract was characterized based on proteins, carbohydrates, lipids and ash content. Soluble proteins were quantified using the DC Protein assay (Bio-Rad), which is based on the Lowry assay (Lowry et al., 1951). Bovine serum albumin (Sigma–Aldrich) was used as protein standard and absorbance was measured at 750 nm using a microplate reader (Infinite M200,Tecan, Switzerland).

Total carbohydrates content was determined by the method of Dubois (Dubois et al., 1956), which is based on a colorimetric reaction in phenol-sulfuric acid which is

measured at 483 nm. Glucose (Sigma–Aldrich) was used as standard. Total lipids were analysed following the method of Folch (Folch et al., 1957). Lipids were extracted three times with chloroform/methanol/Phosphate buffer saline (1:2:0.8 v/v). After extraction, the excess of solvent was removed in a vacuum concentrator (RVC 2-25 CD+, Christ GmbH) and total lipid content was determined gravimetrically. Ash content was measured gravimetrically after burning in a furnace at 575 ^{o}C. Free glucose was determined as described below.

2.5. Electrophoresis

To investigate the native conformation of the microalgae proteins before and after partitioning in the ATPS, the samples were analysed by native gel electrophoresis. The samples were diluted with native sample buffer at a ratio 1:2 and applied on a 4-20 % Criterion TGX (Tris-Glycine eXtended) precast gel. The gel was run in 10x Tris glycine native buffer at 125 V for 75 min. The native gel was stained using the Pierce Silver Stain Kit from Thermo Scientific®. The precast gels and buffers were procured from Bio-Rad®.

2.6. Aqueous two phase systems, tie lines and protein partitioning

The aqueous two phase system Iolilyte 221PG (1) - citrate (2) - water (3), further regarded as Iol-Cit, was selected to study the partitioning of proteins. This system was chosen from several ionic-liquid based ATPS (data not shown) due to its strong ability to form two phases and to partition proteins, biocompatibility and mild interaction with proteins; furthermore, the corresponding phase diagram and 4 tie lines are readily available as described by Suarez Ruiz et al., (2017). To study the partitioning behaviour of the model proteins BSA and Rubisco, four tie lines were selected. For the CP, two tie lines more were constructed to assess in total six tie lines. Along each tie line, a sole point was selected where the volume of top and bottom phases are equal. The final protein concentration in the system was ~ 0.3 mg g^{-1}. The mixture was stirred in a rotary mixer for 10 min. Subsequently, bottom and top phases were separated by centrifugation at 2500 rpm for 5 min and transferred to separate flasks. Experiments were conducted at room temperature and pH 7.

2.7. Protein determination

Reference proteins BSA and Rubisco were quantified by measuring the absorbance at 280 nm using a Tecan infinite M200® plate reader. The CP from both strains were quantified with bicinchoninic acid using the Pierce BCA protein assay kit from Thermo Scientific®. For both methods, BSA was used as protein standard. Sample blanks (ATPS without protein) were prepared to correct for the influence of solvent composition. Because of the strong interference of the phase forming components in the top phase and the protein determination methods, the concentration of the protein in the top phase was calculated as function of the total protein fed in each tie line and the protein concentration in the bottom phase.

2.8. Free glucose determination

Soluble glucose in the ATPS was determined by reaction with a solution containing *p*-hydroxybenzoic acid, sodium azide (0.095 % w/v), glucose oxidase plus peroxidase and 4-aminoantipyrine (GOPOD reagent) from Megazyme®. Samples were mixed with the reagent at a ratio 0.1:3 (v/v) and incubated at 50 °C for 30 min. After cooling down to room temperature, quantification was conducted by measuring absorbance at 510 nm using a Tecan infinite M200® plate reader. GOPOD reagent and glucose were used as blank and standard respectively.

2.9. Partition coefficients and extraction efficiencies

The partition coefficient for proteins (k_p) between top (T) and bottom (B) phases was estimated according to Eq. 1 where x_p is the mole fraction of protein in each phase. Additionally, the extraction efficiencies for proteins EE_p and for free glucose EE_g were calculated as shown in Eq. 2. EE% indicates the extent of extraction of a compound in the top phase compared to the total feed.

$$k_p = \frac{x_{p,T}}{x_{p,B}} \qquad (1)$$

$$EE\% = \frac{C_T * V_T}{C_B * V_B + C_T * V_T} * 100 \qquad (2)$$

Where *C* stands for concentration and *V* stands for volume in each phase.

2.10. Statistics

All experiments were conducted in duplicates. Statistical analysis was performed using R (V 3.4.1). One way ANOVA and Tukey HSD tests were implemented at 95 % confidence level to assess significant differences among treatments.

2.11. Thermodynamic framework

In this investigation, the NRTL model was implemented for the description of phase equilibrium and protein partitioning in the ATPS. Although this model was not developed for electrolyte solutions, it has been shown to accurately calculate equilibrium data of systems containing salts and ILs (Simoni et al., 2008). With this model, we assume that the ILs and salts do not dissociate; this means that each pair cation-anion is treated as a single molecule. The NRTL model assumes that the liquid is made up of molecular "cells" in a binary mixture. Each cell comprises a central molecule interacting with its neighbouring molecules (Renon and Pruasnitz, 1968). Such interaction is characterized by the parameter g_{ij}, which accounts for the interaction energy between the pair *i-j*. The model details are given in Appendix A.

Liquid-liquid equilibrium was estimated assuming constant pressure and temperature (isothermal flash calculation) as described by Denes and Lang, (2006) In this approach, equality of activities for component *i* in both phases (Eq. 3) and mass conservation equations are coupled with the activity coefficient model.

$$(\gamma_i x_i)_{Top} = (\gamma_i x_i)_{Bottom} \quad (3)$$

Where x_i and γ_i are the mole fraction and activity coefficient of component *i* in each phase.

Experimental equilibrium data collected for the characterization of the system Iol-Cit (Suarez Ruiz et al., 2017) was used to estimate the corresponding interaction parameters τ_{ij} via model regression. First, the non-randomness parameter α was fixed between 0.1-0.3 (Renon and Pruasnitz, 1968). The three remaining parameters were

correlated following the solution algorithm proposed by Haghtalab and Paraj, (2012) and described in Appendix B. To summarize, two objective functions involving molar compositions and activities are minimized in order to find the best set of integration parameters τ_k (IP) that correlate best the experimental data.

To describe the partitioning of crude proteins in the system Iol-Cit, the following assumptions are made:

i. The proteins in the CP behave like a single molecule. This implies that the presence of other components (carbohydrates, lipids, ash) do not affect the protein's partitioning behaviour; LLE is also unaltered.
ii. The CP does not affect the system equilibrium. In other words, the interaction parameters for components 1, 2 and 3 remain unaltered by the presence of small amounts of CP. In the present study, a maximum CP concentration of ~ 0.3 mg g^{-1} was used. This assumption has been already implemented by Hartounian et al., (1994) and Perez et al., (2013), and allow us to treat LLE and protein partitioning separately.
iii. The protein partition coefficient (k_p) is calculated as follows:

$$k_p = \frac{x_p^T}{x_p^B} = \frac{\gamma_p^B}{\gamma_p^T} \qquad (4)$$

Where x_p and γ_p are the molar fraction and activity coefficient of the pure (reference protein) or crude protein (CP) in each phase.
iv. γ_p can be estimated using the NRTL model.
v. Although the CP is a mixture of proteins of different molecular weight and chemical nature, no distinction is made on the type of protein that is present in each phase. In this regard, x^T_p and x^B_p refer to total protein found in top and bottom phase respectively. To estimate the corresponding molar fractions, the molecular weight of Rubisco was selected to represent all proteins present in the crude extract.
vi. Furthermore, we assume that the protein remains in solution, without aggregation or precipitation. We also ignore protein-protein interactions.
vii. The partitioning process takes place at constant pressure and temperature.

It was assumed that the presence of protein is not altering the established equilibrium of the system Iol-Cit. If we consider a fourth component (CP or pure protein), the interaction parameters $\tau_{p\text{-}lolilyte}$, $\tau_{p\text{-}citrate}$ and $\tau_{p\text{-}water}$ can be calculated by experimentally measuring x^T_p and x^B_p, and by an optimization procedure adopted by Perez et al., (2013). In this procedure, the interaction parameters are obtained by minimization of two objective functions (Appendix B).

3. Results and Discussion

Since retaining the native conformation and the stability of valuable proteins is crucial for a variety of industrial applications, we selected the ionic liquid Iolilyte 221PG based on a previous screening (Suarez Ruiz et al., 2017). The screening was conducted over 19 ILs of different chemical nature and included aspects like ability to form two phases and the IL effect on protein stability. Iolilyte 221PG did not significantly affect the native conformation of Rubisco (present in microalgae) and other reference proteins (BSA and IgG1) up to a 50% concentration of IL (Desai et al., 2014; Dreyer et al., 2009). Citrate was selected as phase forming component due to its strong salting out character, and because it has a more environmentally friendly character as opposed to inorganic phosphate salts (Sinha et al., 2014). The system Iolilyte 221PG-Potassium citrate showed outstanding extraction efficiencies in the partitioning of Rubisco compared to the commonly used polymer/salt systems.

The phase diagram for the system Iol-Cit is presented in Fig. 1. Equilibrium compositions mark the transition from single to two phases, and are linked from top to bottom with tie lines. The points linked by a tie-line represent the composition of the existing phases, which are identical along a tie line. We have studied the partitioning of CP in an area covering six tie lines, with compositions of IL ranging from 2 to 60% (w/w) and salt concentrations from 1 to 55% (w/w). Furthermore, the NRTL model was implemented in order to describe the experimental data.. The experimental equilibrium compositions, extended from four tie lines (Suarez Ruiz et al., 2017) to six tie lines and the corresponding model estimations are shown in Fig. 1. The resulting

interaction parameters are listed in Table 1. A good representation of the experimental data is achieved in both cases, demonstrating the flexibility of the NRTL model and its applicability to systems containing IL and salts, as indicated in other studies (Simoni et al., 2008)

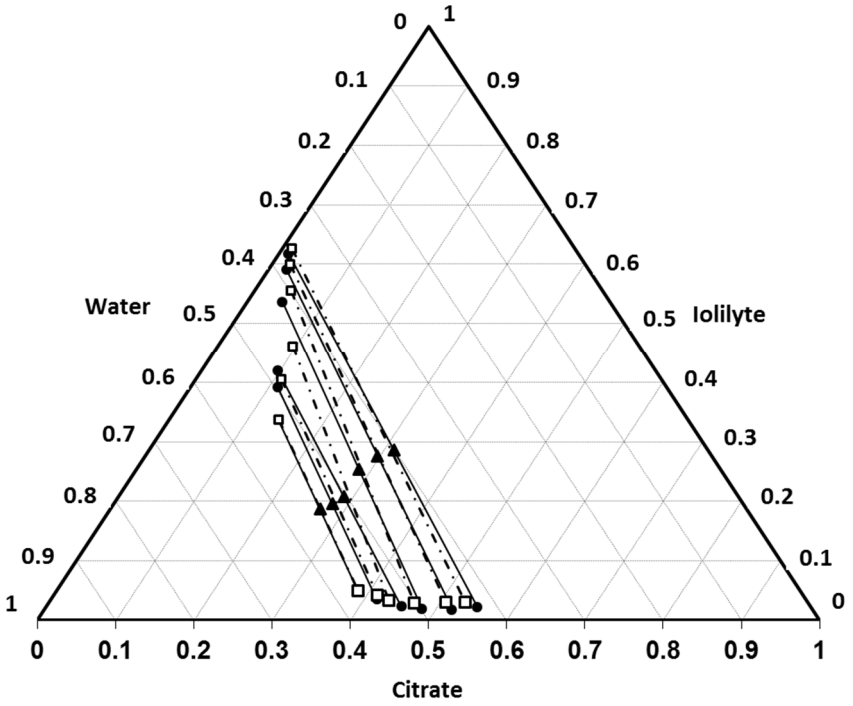

Figure 1. Phase diagram (% w/w) for the system Iolilyte (1) - Citrate (2) - Water (2). Experimental data (filled symbols and solid line for tie lines, ▲ for feed compositions) and model estimation (open symbols and dashed line for tie lines).

3.1. Protein partitioning

The equilibrium data and interaction parameters for the system Iol-Cit (Fig. 1 and Table 1) were used to evaluate the partitioning of proteins. Two reference proteins, BSA (~ 67 kDa) and Rubisco (~ 540 kDa), were assessed in the system with four tie lines and microalgae proteins (CP) were assessed with six tie lines. For each case, the Tie Line Length (TLL) was calculated according to Eq. 5. TLL is proportional to the concentration of the phase forming components and thus, it reflects the effect of the system components on the fractionation process. Higher values of TLL correspond to tie lines farther away from the origin (Fig. 1).

$$TLL = \left(\frac{\Delta x_1^2}{\Delta x_2^2} \right)^{1/2} \quad (5)$$

Where subscripts 1 and 2 stand for Iolilyte and citrate respectively, and Δ refers to the difference between top and bottom composition for each tie line.

The experimental partition coefficients presented in Fig. 2A indicate that the proteins are preferentially concentrated in the IL-rich phase. A notably high standard deviation occurs for TLL 53 %, which can be due to the inherent stability of Rubisco in Iolilyte 221PG. At a TLL of 53 %, the concentration of IL in the top phase is ~ 42 % (w/w). This appears to be a turning point for the molecular stability of Rubisco, leading to strong responses in solubility and therefore uncertainties in the analytical determination. In fact, Desai et al., (2014) found that the molecular conformation of Rubisco in the same IL changes already from 30 % IL but becomes significant at 50 % IL. This was also observed in our earlier publication (Suarez Ruiz et al., 2017). Partition coefficient results are in agreement with studies on protein partitioning in ATPS containing the same ionic liquid (Desai et al., 2014; Dreyer et al., 2009; Suarez Ruiz et al., 2017). Dreyer et al., (2009) postulated that molecular weight and net protein charge are the most important factors explaining the enrichment of proteins in the IL-rich phase. When comparing the partition coefficients of BSA and Rubisco, no significant differences were found ($p > 0.05$). Considering the remarkable difference in size of these reference proteins, molecular weight does not seem to play a relevant role in our case. On the other hand, the system pH (~6.5) is higher than the isoelectric point (pI) of Rubisco (pI ~ 5.5) (Martin et al., 2014) and BSA (pI ~ 4.7) (Desai et al., 2014), which means that both proteins are negatively charged in the ATPS. Electrostatic interactions between the negatively charged protein and the ionic liquid cation influence positively the concentration of the protein in the ionic liquid-rich phase. We also propose that the citrate anion plays an important role in the partitioning of the proteins to the top phase. Citrate is a highly hydrated anion with a strong salting out capability (Silvério et al., 2013) and therefore proteins in the CP migrate to the IL rich phase in which the

charge density is lower. Thus, it appears clear that the protein net charge in the ATPS is an important driving force for the preferential concentration of proteins in the IL-rich phase (Hartman et al., 1974).

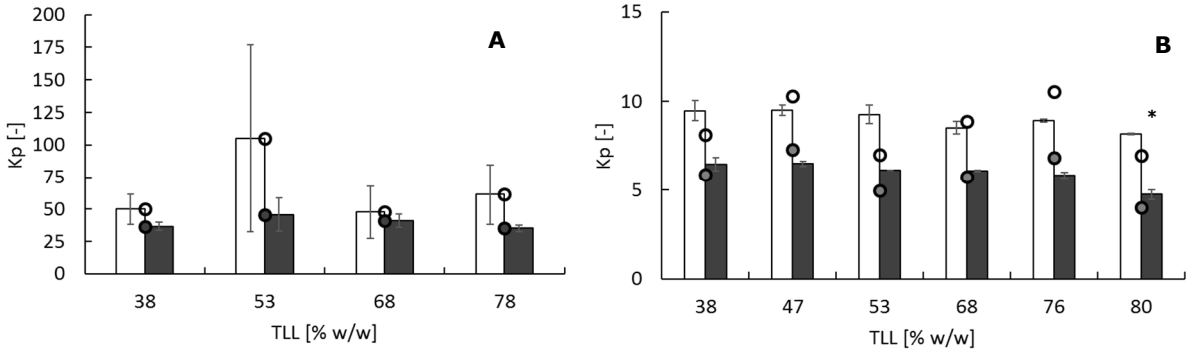

Figure 2. Partition coefficients as function of tie line length in the system Iolilyte (1) - citrate (2) - water (3). Experimental data is shown in bars and model estimations with markers. **(A)** Rubisco (open marker and bars) and BSA (filled bars and marker). **(B)** Crude protein from *N. oleoabundans* (open marker and bars) and *T. suecica* (filled marker and bars). Error bars indicate standard deviation. * Significant difference ($p < 0.05$).

Fig. 2B displays the partition coefficient of total protein from the CP derived from *N. oleoabundans* and *T. suecica.* Although a slight decreasing trend is observed, statistically only the k_p for the tie line length (TLL) 80 % is significantly lower ($p < 0.05$). A decrease of k_p with TLL have been previously reported by other authors (Boaglio et al., 2006; Patil and Raghavarao, 2007). The TLL changes the free volume available, therefore, the migration of the protein to the opposite phase seems to be consequence of the high concentration of the ionic liquid in the top phase which reduces the free volume available for the protein. This was the case for the CP from both microalga strains. The statically lower value of k_p at TLL 80 % can be due to protein loss as result of the high concentration of IL at TLL 80 %, which reaches nearly 62 % (w/w). At such concentrations, some proteins from the CP are excluded from the top phase into the bottom phase or interphase. Although we expected protein loss already from TLL 68% (where the concentration of IL is higher than 50 % (Desai et al., 2014)), it appears that above 60 % IL the effect becomes significant. The corresponding k_p for TLL from 38 to

76 % confirm the observations for the reference proteins (Rubisco and BSA) presented in Fig. 2A, in which the partition coefficients remained statistically stable through the different tie lines. In this regard, the proteins present in the CP are of different molecular size (Schwenzfeier et al., 2011) and their chemical nature is unknown, which makes it challenging to predict accurately the mechanism of partitioning. Furthermore, when increasing the tie line length, the concentration of phase forming components also increases, making the upper phase richer in IL and the lower phase richer in salt. Hence, composition difference between phases becomes larger. In the system studied, however, the conductivity of the top phase varied between 81.3-89.2 mS cm^{-1} while that of the bottom phase reached 5.1-8.7 mS cm^{-1} depending on the tie line. This narrow range gives additional insights in how to explain the constant trend observed for k_p at different TLL.

The effect of TLL on protein extraction appears to be minor. Similar observations have been made for proteins from microalgae. Zhao et al. (Zhao et al., 2014) noted a slight effect on protein yield when the TLL varied from 20 to 33 %, while Patil and Raghavarao, (2007) observed an increase in protein yield from 90 to 97 % when the TLL changed from 13 to 33 %. In both cases, c-phycocyanin was extracted from *Spirulina platensis* in a system containing Polyethylene glycol and phosphate. Suarez Ruiz et al., (2017) found a small increase in *EE* for Rubisco (91 to 98 %) in the system Iol-Cit for TLL in the range 37 to 80 %.

After microalgae cultivation and harvesting, a fractionation process involving bead milling, centrifugation, filtration and diafiltration was implemented to produce a crude protein extract from two microalgae strains. The composition of the resulting CP extracts is presented in Fig. 3A. The protein content reached 43.5 ± 2.7 and 48.1 ± 1.8 % (dw of the CP) for *N. oleoabundans* and *T. suecica* respectively. These values are in good agreement with protein extracts obtained from several microalgae strains using various separation processes (Safi et al., 2014c). As expected, a higher value of ash was observed for the marine strain *T. suecica* (18.5 ± 0.5 % dw) compared to *N.*

oleoabundans, which was grown in fresh water. A maximum lipid content of ~ 2 % dw was found for both strains; these are probably prosthetic groups (e.g., porphyrins) and lipoproteins (Schwenzfeier et al., 2013b).

The carbohydrates content in the CP is notably high, in particular for *N. oleoabundans* (~ 40 % dw) This could be due to an elevated carbohydrates content in the initial biomass. Since both microalgal strains used in this investigation can accumulate starch during cultivation, we anticipate that glucose is the most abundant sugar. In fact, Brown, (1991) measured the sugar composition of 16 species of microalgae including the classes *Chlorophyceae* and *Prasinophyceae*, finding that glucose accounts for 55.2 to 85.3 % of the total carbohydrates content. The fraction of free glucose to total carbohydrates in the CP is 21.49 ± 0.55 % and 36.47 ± 1.28 % for *N. oleoabundans* and *T. suecica* respectively.

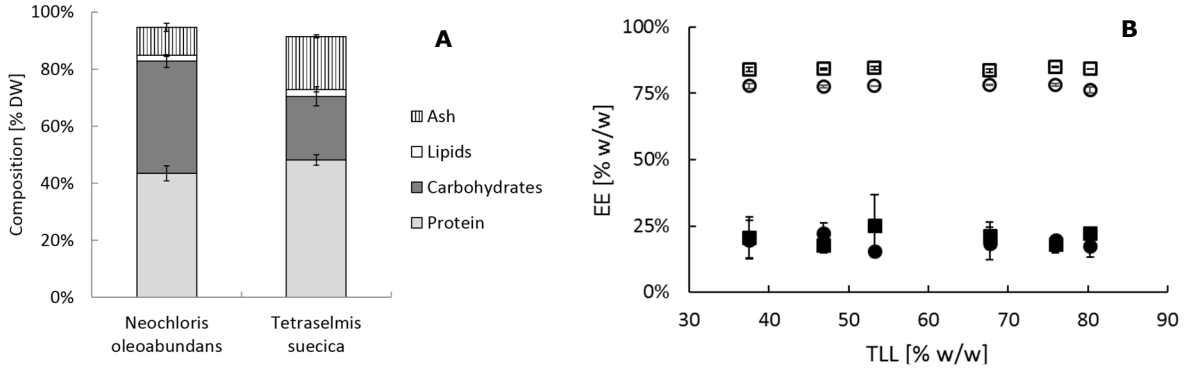

Figure. 3. (A) Overall composition (% dw) of crude protein extract from *T. suecica* and *N. oleoabundans*. Error bars indicate standard deviation. Experiments run in duplicate. **(B)** Extraction efficiencies for proteins (open symbols) and free glucose (filled symbols) for *T. suecica* (circles) and *N. oleoabundans* (squares).

The corresponding extraction efficiencies (*EE*) for total protein and free glucose, according to Eq. 2, are presented in Fig. 3B for different tie lines. We have determined free glucose as an indirect measure of carbohydrates in the ATPS, as the common methods for the quantification of total sugars show strong interference with Iolilyte 221PG. It is clear that proteins are preferentially accumulated in the top phase while sugars are mostly concentrated in the bottom phase. The high affinity of sugars for

water and their lack of charge seems to be responsible for their separation into the most hydrated phase (bottom phase). This confirms that the system Iol-Cit effectively fractionate proteins from sugars in a single step. Only few studies have demonstrated the separation of proteins from saccharides in ATPS containing IL (Lee et al., 2017a); the reported extraction efficiencies (> 82 % for proteins and < 100 % for saccharides) are in good agreement with our findings. Furthermore, to our knowledge, the present research is the first evidence of extraction of proteins and carbohydrates from microalgae crude extracts in an IL based ATPS. Moreover, there is no significant difference ($p > 0.05$) in the values of *EE* for *N. oleoabundans* and *T. suecica*. This is unexpected, but indicates that the chemical nature of the proteins and sugars from both microalgal strains are comparable.

3.2. Protein conformation

Previous research conducted on several ionic liquids-salt pairs (data not shown) revealed that Iol-Cit forms two phases at relatively low concentrations of IL. This is important considering protein stability; Desai et al., (2014) studied the stability and activity of Rubisco in Ioliliye 221 PG and found that above 30 % IL there is aggregation and significant loss of enzyme activity but no signs of protein fragmentation. In our experiments, the highest concentration of IL was 60 % (w/w), and occurs in the top phase of the sixth tie line. Visually, we did not identify aggregation or the formation of precipitates. In order to evaluate protein conformation, native gel electrophoresis was performed for each tie line in the top phase and the resulting protein bands are presented in Fig. 4. The expected protein band for Rubisco (~540 kDa) is observed for all tie lines, with a gradual decrease in band intensity at higher values of tie lines for *N. oleoabundans*. There is a clear loss of distinctive protein bands in the range < 20 kDa for both microalgal strains (dotted squares). We hypothesize that these proteins could have suffered denaturation due to the presence of IL and thus they migrated to the bottom phase. To understand the partitioning of all proteins present in microalgae, their chemical nature should be investigated.

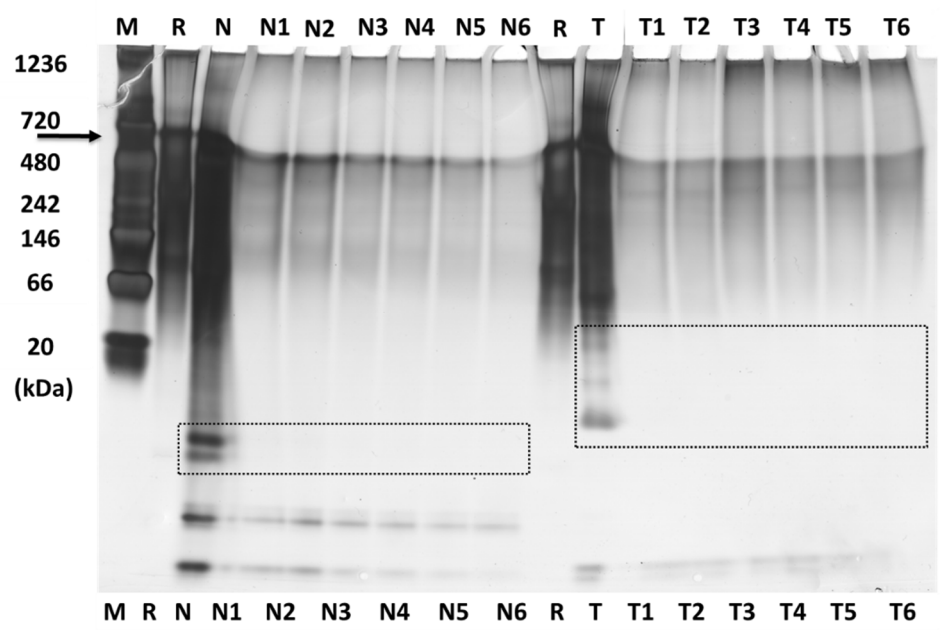

Figure 4. Native gel electrophoresis for crude protein (CP) from *N. oleoabundans* (N) and *T. suecica* (T). M: protein marker. R: Rubisco (arrow at ~540 kDa). Numbers 1-6 refer to tie lines. Wells N and T refer to CP in water. Dotted squares indicate region in which protein bans are lost.

3.3. Protein partitioning estimations

The corresponding estimations of protein partitioning with the NRTL model are given in Fig. 2A for the reference proteins and in Fig. 2B for the microalgae CP. The respective interaction parameters are listed in Table 1. Excellent description of the experimental data is obtained with the system containing four tie lines. This is due to an almost perfect fit to the equilibrium data of four tie lines, for which the optimization procedure provided a more accurate set of interaction parameters to estimate the partition coefficients. The calculated values of k_p for the CP, nonetheless, show the expected trend at different TLL. It can be seen that the largest deviation from the experimental data occurs for TLL 53 %, for which the equilibrium prediction also presented high deviations.

For the implementation of the NRTL model, it was assumed that the IL and salt do not dissociate. Besides, it is also considered that the protein does not possess a net charge. However, for all proteins evaluated, this assumption is not correct, as their pIs are far from the working pH for all tie lines (Perez et al., 2013). The fact that the model's

output provides a good representation of the experimental data means that the adjustable parameters in the NRTL model covers the uncertainty regarding the partitioning mechanism.

We implemented the NRTL model to describe equilibrium and protein partitioning in a biphasic system. Experimental phase equilibrium data is used to estimate the interaction parameters, and thus, the results presented in this research are only valid for the system Iol-Cit. Furthermore, partitioning data is used to calculate the interaction parameters for total protein in the system. The resulting model, is therefore applicable in further studies and design of extraction systems containing Iol-Cit and crude proteins from green microalgae.

Table 2. Binary interactions parameters (IP) [j mol^{-1}] according to the NRTL model for the system Iolilyte (1) - Citrate (2) – water (3) and protein (4), using 6 and 4 tie lines (TL), reference proteins and Crude Protein (CP).

IP	6 TL	4 TL	IP	BSA	Rubisco	CP *N. oleoabundans*	CP *T. suecica*
α	0.3	0.3	α	0.15	0.15	0.15	0.15
Δg_{12}	102156.3	-36699.2	Δg_{14}	-40428.6	-31452.3	414.1	-11067.5
Δg_{13}	-221631.5	-9904.1	Δg_{24}	-43176.1	-23007.2	-680.3	-10935.9
Δg_{21}	-232114.1	-36118.3	Δg_{34}	70799.3	38794.7	71785.3	42233.4
Δg_{23}	-202039.8	-11047.9	Δg_{41}	-23487.7	-26218.9	83437.0	62510.4
Δg_{31}	-110600.3	24359.0	Δg_{42}	-15807.2	-22231.3	13001.1	7529.9
Δg_{32}	160368.3	34645.4	Δg_{43}	-37491.9	-41216.8	1786957.8	265463.7
rmsd [+]	0.21	0.073	***ssq*** [**]	2.06E-4	3.74E-4	3.44	1.99

[+] Root mean square deviation

* Sum of squares

3.4. Outlook

In this investigation we implemented the NRTL model to describe equilibrium and protein partitioning in a biphasic system. Experimental phase equilibrium data is used to estimate the interaction parameters, and thus, the results presented further are only valid for the system Iol-Cit. Furthermore, partitioning data is used to calculate the interaction parameters for total protein in the system. The resulting model, a function of composition and interaction parameters, is therefore applicable in further studies and design of extraction systems containing Il-Cit and crude proteins from green microalgae.

We have demonstrated the partitioning of crude protein from algae in an IL based aqueous two phase system. We have also provided evidence of the simultaneous extraction of proteins from carbohydrates. However, a potential application of IL in algae biorefinery remains challenging. In particular, the following aspects require further development:

- Chemical nature of the CP: A more accurate knowledge on the chemical nature of the proteins in the CP would lead to a better understanding of the partitioning behaviour.
- Binary interaction parameters: In this research we have used an algorithm which depends on equilibrium compositions in order to estimate the corresponding interaction parameters. Although the model output shows a good representation of the experimental data, the calculated *Δg's* may not correspond to experimental interaction parameters. In this regard, phase analysis is recommended. Furthermore, the values presented in Table 1**.** for the partitioning of CP reflect not only the influence of proteins and phase forming components (Iolilyte and salt) but also carbohydrates, lipids and ash present in the crude fraction.
- Recovery of IL: Due to their inherent costs and limited knowledge regarding toxicity and environmental concerns, further research is needed in order to develop effective strategies for recycling the IL after protein extraction.

- Application of the protein extracts: The functionality and potential use of the proteins obtained after the purification process remain unknown.

4. Conclusions

In this research we demonstrated the partitioning of total proteins from crude algae extracts in an aqueous two phase system containing an ionic liquid and an organic salt. It was determined that sugars are preferentially accumulated in the opposite phase as proteins, demonstrating a simultaneous extraction. The extraction efficiencies and K_p of proteins did not vary significantly as function of the tie line length. The same behaviour was observed for the partition coefficient of two reference proteins namely BSA and Rubisco. It was proposed that the partitioning is determined mostly by the net protein charge rather than by the molecular weight of the proteins. Good representation of the experimental equilibrium and partitioning data was achieved with the Non Random Two Liquids model, confirming its flexibility and applicability in algae biorefinery.

Acknowledgements

This project was financed by the Dutch Technology Foundation TTW (former STW) under the project AlgaePro4You, nr. 12635 and within the TKI AlgaeParc Biorefinery program with financial support from the Ministry of Economic Affairs of the Netherlands in the framework of the TKI BioBased Economy under contract nr. TKIBE01009.

Nomenclature

Letter	Definition	Units
a	Activity	*[-]*
CP	Crude Protein	[-]
EE	Extraction Efficiency	%
g	Interaction energy	[J mol^{-1}]
k	Partition coefficient protein	[-]
Q	Penalty term	[-]
R	Universal gas constant	[J mol^{-1} K^{-1}]
T	System temperature	[K]
x	Mole fraction	[mol mol^{-1}]
Greek characters		
α	Non-randomness (NRTL model)	[-]
τ	Adjustable interaction parameter	[-]
γ	Activity coefficient	[-]
Subscripts		
i, *k*, *l*	Component, parameters and tie lines respectively	[-]
ij	Refers to binary interaction between components *i* and *j*	
g	Free glucose	[-]
T, *B*	Top and bottom phase respectively	[-]
exp, calc	Experimental and calculated value respectively	[-]
p	Protein	[-]

Appendix

A: Thermodynamic framework

NRTL model. The general expression for the molar excess Gibbs energy (g^E) according to the NRTL model, for *n* components, is given by:

$$\frac{g^E}{RT} = \sum_{i=1}^{n} x_i \frac{\sum_{j=1}^{n} \tau_{ji} G_{ji} x_j}{\sum_{k=1}^{n} G_{ki} x_k} \quad \text{(A1)}$$

Where:

$$G_{ij} = \exp(-\alpha_{ij} \tau_{ij}) \quad \text{(A1)}$$

$$\tau_{ij} = \frac{g_{ij} - g_{jj}}{RT} = \frac{\Delta g_{ij}}{RT} \quad \text{(A2)}$$

Here, *R* is the universal gas constant (J mol^{-1} K^{-1}) and *T* the system temperature (K). The parameter g_{ij} characterizes the interaction energy of the pair *i-j*, while the parameter α_{ij} accounts for the non-randomness in the mixture; x_i is the corresponding molar fraction of component *i*. For both parameters it holds that $g_{ij}=g_{ji}$ and $\alpha_{ij}= \alpha_{ji}$. Although α_{ij} is adjustable, a fixed value of 0.2-0.3 is frequently used in most studies (Renon and Pruasnitz, 1968). The binary interaction parameters τ_{ij} are usually obtained from experimental and mutual solubility data. The corresponding general expression for activity coefficient *γ* of component *i* is given by:

$$\ln \gamma_i = \frac{\sum_j x_j G_{ji} \tau_{ji}}{\sum_k x_k G_{ki}} + \sum_j \frac{x_j G_{ij}}{\sum_i x_k G_{kj}} \left(\tau_{ij} - \frac{\sum_m x_m G_{mj} \tau_{mj}}{\sum_k x_k G_{kj}} \right) \quad \text{(A3)}$$

Liquid-liquid equilibrium.

The equilibrium condition implies equality in the chemical potentials of both phases and minimal Gibbs free energy (Denes and Lang, 2006). For a two-phase system and *n* components:

$$a_i^T = a_i^B \quad \text{(A4)}$$

$$a_i = \gamma_i x_i \quad \text{(A5)}$$

Here, a_i and γ_i are the activity and activity coefficient of component *i*. *T* and *B* stand for top and bottom phases. Furthermore, the material balances can be written as:

$$\sum_{i=1}^{n} x_i^{T,B} = 1 \quad \text{(A6)}$$

If the molar compositions of both phases are known, Eq. 1-4 are reduced to a system of non-linear algebraic equations in which only the interaction parameters τ_{ij} and α_{ij} are still unknown. The values of the parameters τ_{ij} are therefore calculated by assuming a constant value of α_{ij} and by an iterative procedure described in appendix B and C.

B: Computational algorithms

The solution method presented in this research is adopted from Haghtalab and Paraj, (2012) and involves the estimation of the interaction parameters starting from known experimental compositions (Fig. 1B). Briefly, experimental compositions in both phases are used to initialize the interaction parameters. Next, the activity of all species is calculated using the activity coefficient model (NRTL). In the following step, by minimization of the objective function 1 (OF1). This function conducts a fit based on the equality of activities, and thus, after convergence, a new set of calculated compositions is obtained.

$$OF_1 = \sum_{l}^{6}\sum_{i}^{3}\left[\left(x_{li}\gamma_{li}\right)^{T} - \left(x_{li}\gamma_{li}\right)^{B}\right]^2 + Q\sum_{k}^{6}\tau_k^2 \qquad \text{(B1)}$$

Subscripts *l*, *i* and *k* refer to tie lines (1,2..N), components (Iolilyte 221PG (1), citrate (2), water (3)) and adjustable parameters (1, 2..6), respectively. T and B indicate top and bottom phase. τ_k are the adjustable interaction parameters. *Q* is a penalty term to reduce the risks of multiple solutions associated with parameters of high value (Haghtalab and Paraj, 2012). In this case *Q* was set to 10^{-6}.

Finally, to estimate the binary interaction parameters that lead to the best correlation between the experimental and calculated molar compositions, the objective function 2 (OF2) is implemented.

$$OF_2 = \sqrt{\frac{1}{6N}\sum_{l}^{N}\sum_{i}^{3}\sum_{k}^{2}(x_{lik}^{cal} - x_{lik}^{\exp})^2} \qquad \text{(B2)}$$

As can be seen, OF2 is the root mean square deviation for the compositions. For both objective functions, the criterion for minimization (ε) was set to 10^{-6}.

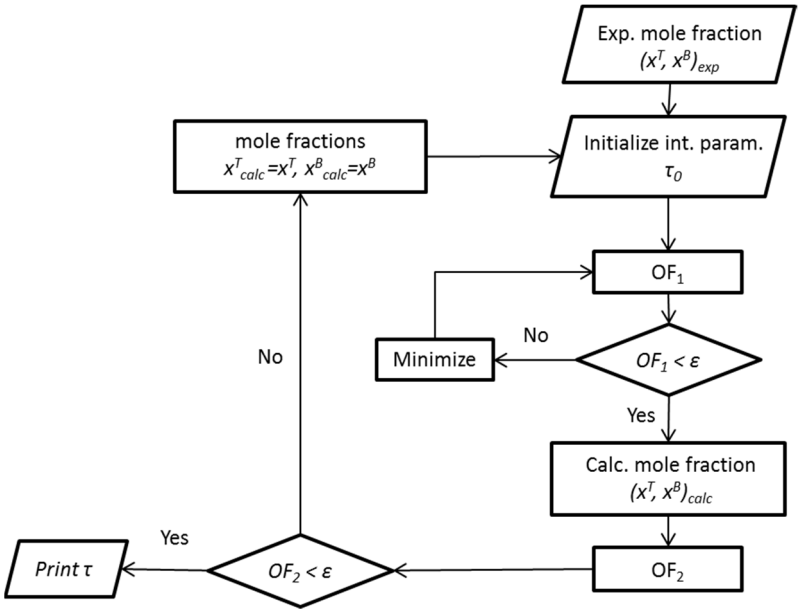

Figure B1. Solution algorithm proposed by Haghtalab and Paraj, (2012) for estimating liquid-liquid interaction parameters.

The set of calculated interaction parameters is used to estimate the binary interaction parameters for the system containing protein. The solution algorithm is presented in Fig. 2B. In short, we assumed that the presence of proteins and other biomolecules do not alter the equilibrium compositions or binary interaction parameters of the phase forming components. Then, we used experimentally obtained compositions to initialize the interaction parameters. This allowed us to have a first estimate of the activity coefficients for protein in each phase. Then, we have used objective function 3 (OF3) to estimate the interaction parameters that lead to a better agreement between the experimental and calculated protein composition, expressed in terms of the partition coefficient k_p.

$$OF3 = \left(\sum_{l=1}^{6} \frac{(k_{p,\exp} - k_{p,calc})^2}{6} \right)^{1/2} \quad \text{(B3)}$$

Where the subscript *p* indicates protein, *l* refers to tie lines and $k_{p,exp}$ - $k_{p,calc}$ is the deviation between experimental and calculated partition coefficients. OF3, which also corresponds to a root mean square deviation, was adapted from the work of Perez et al. (Perez et al., 2013). The criterion for minimization (ε) was set to 10^{-6}.

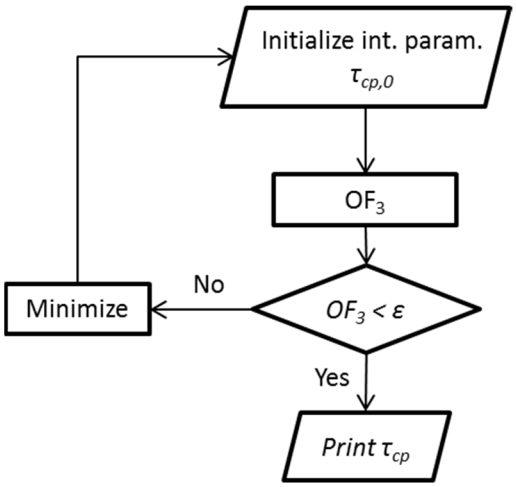

Figure B2. Computational algorithm for estimating interaction parameters of crude proteins (CP).

Chapter 7

Ionic liquid-assisted selective extraction and partitioning of biomolecules from macroalgae

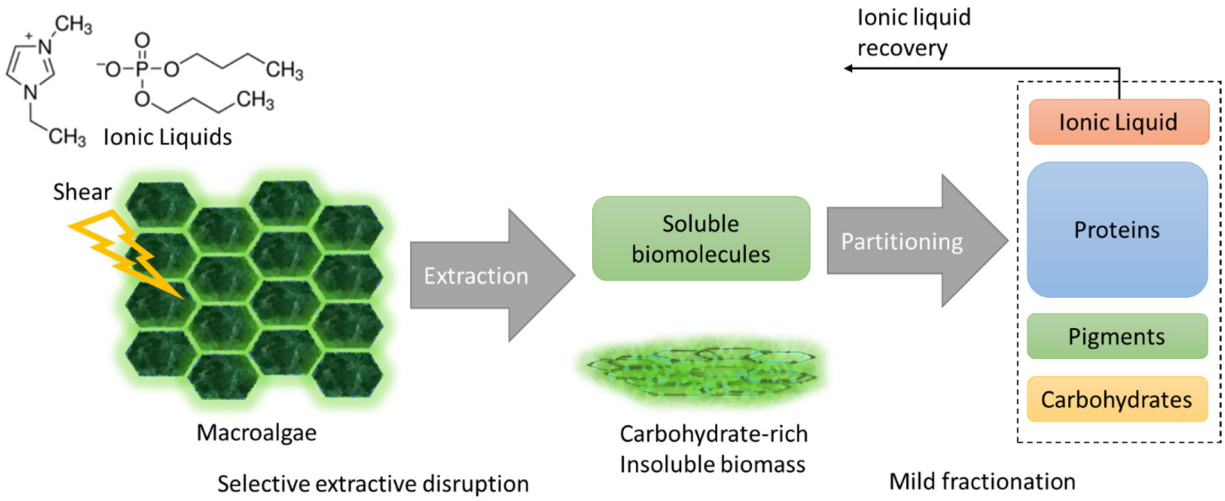

Submitted as:

E. Suarez Garcia, C. Miranda, M.T. Cesário, M.H.M. Eppink, R.H. Wijffels, C. van den Berg. Ionic liquid-assisted selective extraction and partitioning of biomolecules from macroalgae.

Abstract

Macroalgae are a promising feedstock for several industries due to their rich composition and high biomass productivities compared to terrestrial crops. In this investigation we present a novel process for the extraction and fractionation of proteins and carbohydrates from the green alga *Ulva lactuca*. The process involved mechanical disintegration assisted by ionic liquids. Up to 75 % of the proteins and 24 % of the carbohydrates initially present in the biomass were extracted in a single step and under mild conditions with the ionic liquid (IL)- 1-ethyl-3-methyl-imidazolium dibutyl phosphate. Furthermore, biomolecule fractionation was studied by means of two-phase partitioning and ultrafiltration. The complete process, including extraction and ultrafiltration, allowed the recovery of up to 40.2 % of the initial proteins and 10.0 % of the carbohydrates in the retentate phase, while 79.6 % of the IL was recovered in the permeate phase. The proposed extraction-fractionation approach is mild, simple and can be potentially applied for the biorefinery of macroalgae at commercial scale.

1. Introduction

The global demand of biomolecules for industrial and food products is rising (Henchion et al., 2017). With the current overexploitation of land and aquatic resources and the rapid depletion of fossil fuel reserves, novel renewable feedstocks are needed.

Macroalgae are multicellular photosynthetic organisms which are a promising source of biomolecules for several applications (Bharathiraja et al., 2015), including biomaterials (Jung et al., 2013), biofuels (Behera et al., 2015), environmental remediation (Chung et al., 2011), feed (Bleakley and Hayes, 2017; Øverland et al., 2018), food and pharma (Holdt and Kraan, 2011; Wells et al., 2017).

In general, macroalgae are rich in polysaccharides, contain modest amounts of proteins and are poor in lipids (Chan et al., 2006). Because of this, macroalgae have been mainly used as a source of carbohydrates (Jung et al., 2013). However, proteins in macroalgae display an interesting range of functional properties (Samarakoon and Jeon, 2012) and the amino acid profile is comparable to commercial protein isolates (Bleakley and Hayes, 2017), making them particularly interesting for food applications.

The extraction of proteins from macroalgae is not trivial. Proteins are often embedded in a matrix of polysaccharides (Lahaye and Robic, 2007) which is difficult to access under mild conditions. The processes reported in literature include extraction in aqueous and alkaline media (Bleakley and Hayes, 2017; Fleurence et al., 1995), mechanical shear (Barbarino and Lourenço, 2005; Postma et al., 2018) and enzymatic treatments (Amano and Noda, 1992; Fleurence et al., 1995; Postma et al., 2018). Such processes often result in low extraction yields and purities (Tamayo et al., 2018).

Ionic liquids are molten salts which have been successfully applied for the extraction of polysaccharides from wood and cereals (Brandt et al., 2013), and for the fractionation of biomolecules from several feedstocks (Ventura et al., 2017) including microalgae (Suarez Garcia et al., 2018b). The implementation of ILs in macroalgae, however, has been limited to a handful studies where algal biomass is directly treated at high temperatures (90 -160 ^{o}C) and long contact times (3-360 min) to release

carbohydrates (Malihan et al., 2017, 2014; Park and Jeong, 2013; Pezoa-Conte et al., 2015). Mild extraction of proteins using ILs has only been investigated recently to recover phycobiliproteins from the red macroalga *Gracilaria sp*. (Martins et al., 2016).

Despite the promising extraction capabilities of ILs, their high costs (George et al., 2015) and potential toxicity greatly limit their implementation at commercial scale. Although cheap ILs from renewable sources are being synthetized (Brandt-Talbot et al., 2017), there is a clear need to develop alternative and efficient recovery processes (Mai et al., 2014).

In this work, the extraction and fractionation of proteins and carbohydrates from the green macroalga *Ulva lactuca* is investigated. The proposed approach is based on the integration of the disruption and extraction steps by means of bead milling and chemical solubilisation mediated by ILs. Furthermore, biomolecule fractionation is studied using two methods: two-phase partitioning and ultrafiltration. The latter is also proposed in order to recover the IL from the alga extract. All proposed processes are simple and are conducted under mild conditions, which is a unique contribution of the present work.

2. Material and methods

2.1. *Chemicals.*

All chemicals used in this investigation were analytical grade. Chloroform and methanol were obtained from Biosolve®. Phosphate Saline Buffer (PBS) pH 7 was prepared by mixing 0.21 g KH_2PO_4, 0.48 g $Na_2HPO_4.2H_2O$ and 9. 00 g NaCl in 1 L distilled water. KH_2PO_4, $Na_2HPO_4.2H_2O$, NaCl and K_2HPO4 were purchased from Merck Millipore®. Concentrated phenol and concentrated sulfuric acid were obtained from Sigma Aldrich®. The ionic liquid 1-ethyl-3-methyl-imidazolium dibutyl phosphate [Emim][DBP], with a purity of 98 % was obtained from Iolitec®.

2.2. *Macroalga collection and pre-treatment.*

Ulva lactuca was kindly provided by Dr. Willem de Visser from Wageningen Plant Research International (PRI). Samples were collected every month from culture tanks (Nergena, Wageningen university and Research) in the period June-August. After biomass collection, the excess water was removed and the samples were freeze dried in a sublimator 2x3x3 (Zirbus Technology GmbH, Germany) for 72 hours. Dried samples were grinded to a particle size of ~ 0.5 mm using a kitchen coffee grinder, stored in sealed bags and maintained in the dark at room temperature until further use.

2.3. *Ionic liquid assisted extraction.*

Extraction and fractionation experiments were conducted as illustrated in Fig. 1. For IL-assisted extraction (disruptive extraction), solutions containing 10, 20, 30 and 40 wt% [Bmim][DBP] were contacted with a fixed amount of alga biomass (1 wt %) in bead beating tubes (lysis matrix D, MP Biomedicals, USA). Samples were subjected to intense mixing using a Precellys 24 Homogenizer (Bertin Instruments, France) for 3 cycles of 60 s each at 6500 rpm and 120 s pause in between cycles to avoid overheating. The resulting suspensions were centrifuged for 10 minutes at 3500 rpm, and the supernatant (IL-extract) was collected for analysis and for fractionation (routes I and II in Fig. 1). Higher IL concentrations could not be tested due to high viscosity and interferences with the analytical methods.

2.4. *Two-phase partitioning (route I, Fig. 1)*.

IL-extracts were mixed with known amounts of the salt K_2HPO_4 in order to induce two-phase formation. The concentrations of [Emim][DBP] and salt were selected based on prior knowledge of the binodal curve, a phase diagram which marks the working area of a two-phase system. The binodal curve was prepared according to the cloud point titration method as described by Kaul, (2000). In short, a salt-rich solution is added dropwise to a IL-rich solution followed by mixing and settling until a cloud point is observed, which indicates the onset of the two-phase region.

A known amount of K_2HPO_4 was therefore added to the IL-extract, followed by strong mixing for 2 min and settling to allow spontaneous two-phase formation. Samples from the top and bottom phases were collected for analysis.

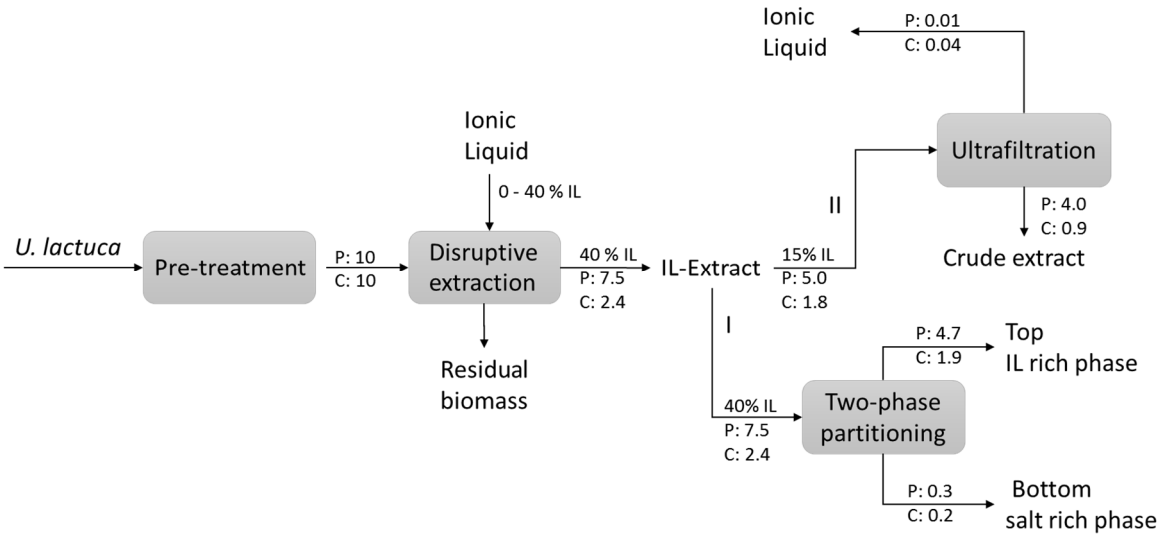

Figure 1. Block diagram for the IL-mediated extraction process, two-phase partitioning (route I) and ultrafiltration (route II). Numbers correspond to mass balances for proteins (P) and carbohydrates (C) as will be described in section 3.

2.5. Biomolecule fractionation and Ionic liquid recovery via ultrafiltration (route II, Fig. 1)

For these experiments, a concentration of IL of 15 % was selected in order to prevent membrane clogging due to high viscosity and biomolecule precipitation. Ultrafiltration experiments were carried out with IL-extracts using two different membrane systems. An ultrafiltration stirred cell (Model 8050) with a 10 kDa poly-ether sulfone membrane (Biomax®) was operated to reach a 5x concentration factor at a constant transmembrane pressure of 2.2 bar and filtrate flow of 0.1 ml min^{-1}. A 3 kDa centrifugal filter (Ultracell®) was run for 40 min at 4000xg to obtain a 4x concentration factor. All filter materials were purchased from Merck Millipore, USA. The retentates and permeates were collected for analysis.

2.6. Biomass characterization and analysis.

Dry weight was estimated gravimetrically after drying a known amount of biomass in a convection oven (Nabertherm, Germany) to constant weight at 100 ^{o}C. Total ash was determined after burning a known amount of algal biomass in a furnace (L 24/11, Nabertherm, Germany) at 575 ^{o}C and regarding the remaining material as total ash. Total lipids were quantified according to the method of Folch (Folch et al., 1957). In short, 5 extraction cycles were conducted on dry biomass using a mixture chloroform:methanol:PBS 2:1:0.8 V V^{-1}. The solvent phase was collected after every step and the excess solvent was evaporated using a vacuum concentrator (RVC 2-25 CDplus, Christ, Germany). The remaining material was weighted and regarded as total lipids.

Proteins were determined with the method of Bradford (Bradford, 1976) using a commercial kit (Pierce® Coomassie protein assay, Thermo Fisher Scientific, USA). Bovine Serum Albumin (Sigma Aldrich®) was used as protein standard and IL solutions as blanks. Bradford is a colorimetric method which correlates protein content to the absorbance shift of the dye coomassie blue, which can be quantified at 595 nm. Total carbohydrates were determined with the method of Dubois (Dubois et al., 1956), which is based on the colorimetric reaction of carbohydrates and phenol in concentrated sulfuric acid, which can be measured at 483 nm. Glucose (Sigma Aldrich®) was used as carbohydrate standard. Absorbances at 595 and 483 nm were measured with a microplate reader (Infinite M200, Tecan, Switzerland).

[Emim][DBP] was quantified by Ultra High Performance Liquid Chromatography (UHPLC Nexera X2, pump LC-30AD, autosampler SIL-30AC, Refractive Index Detector RID-20A, Shimadzu, Japan) using a Rezex® ROA-Organic Acid column coupled with a security guard (300 mm x 7.8 mm, Phenomenex®, USA). Prior to analysis, all samples were centrifuged at 4700 rpm for 20 min to remove suspended particles. Samples were injected (20 µL) and run at 0.6 mL min^{-1} under isocratic mode with 0.005 N H_2SO_4 as

mobile phase. The column was kept at 60°C under a pressure of 55 bar. Solutions of IL in MilliQ water were used as standards.

2.7. Yields and controls

Mass yields (*Y*) per component (i) were estimated according to Eq. 1:

$$Y_i\ \% = \frac{m_{i,e}}{m_{i,b}} \times 100 \qquad (1)$$

Where $m_{i,e}$ is the mass of component *i* (protein, carbohydrates,) in the extract and $m_{i,b}$ is initial mass of component *i* in the initial biomass. All calculations are conducted on dry weigh basis.

Control experiments were conducted with aqueous solutions containing only [Emim][DBP] under the same conditions described in sections 2.3-2.5, in order to take into consideration any interference of the solvent components with the analytical methods or with the membrane materials used during ultrafiltration.

2.8. Statistics

Unless otherwise noticed, all experiments were conducted in duplicate. The data is presented as mean values and the corresponding standard deviation. The variation of the experimental data under different treatments was analysed by one-way analysis of variance (ANOVA) at 95 % confidence level. When significant differences were found (i.e. $p<0.05$), the Tukey's Honest Significant Difference test (HSD) was used to detect significant differences between specific treatments. All analyses were performed in R (V3.4.0).

3. Results and Discussion

3.1. Biomass characterization

The macroalga under investigation contained 3.7 ± 0.3 % proteins, 54.9 ± 1.2 % carbohydrates, 22.8 ± 0.3 % ash and 4.9 ± 0.3 % lipids (DW). These compositions are in good agreement with the reported values for *Ulva lactuca* (De Pádua et al., 2004; Postma et al., 2018). The protein content is, however, significantly lower than the 12-

18 (DW)% reported by Postma et al., (2018) for the same strain. This could be due to variations in culture conditions and season. For example, De Pádua et al., (2004) reported protein contents in the range 3-18 % for several *Ulva* strains collected in different seasons and locations

The method of analysis could also result in significantly different protein contents due to the presence of interfering components which can lead to over and under-estimations (Barbarino and Lourenço, 2005; Berges et al., 1993). During preliminary experiments, [Emim][DBP] showed strong interference with the methods of Dumas, Lowry and BCA. With the method of Bradford, on the contrary, [Emim][DBP] did not display interference and thus, it was used for protein determination and calculations of yields throughout.

3.2. Ionic liquid-assisted extraction: Effect of Ionic liquid concentration

The ionic liquid [Emim][DBP] was selected from several ionic liquids after preliminary experiments due to its ability to extract large amounts of proteins from *U. lactuca* under mild conditions (Appendix A).

In Fig. 2 the extraction yields for proteins and carbohydrates are presented for solutions containing 0 - 40 wt% [Emim][DBP] and fixed biomass concentrations. The corresponding ratios IL-biomass are 0, 10, 20, 30 and 40 g IL $g_{biomass}^{-1}$ (DW). Higher IL concentrations could not be reliably studied due to their high viscosity and complications with the analytical procedures. Samples were carefully analysed against blanks containing only IL in water, in order to rule out false positives. The yields shown in Fig. 2 are referred to the proteins and carbohydrates contained in the initial biomass.

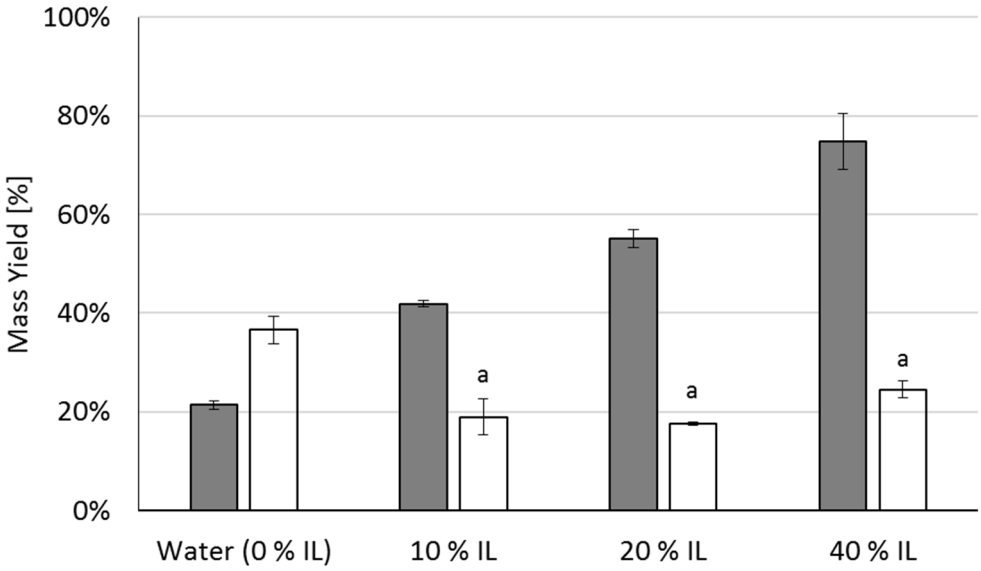

Figure 2. Effect of the concentration of [Emim][DBP] on the extraction of proteins (grey bars) and carbohydrates (white bars) from *U. lactuca* biomass. The data correspond to averages and the errors bars are the standard deviation (n=2). Low case letters indicate statistically equal means at 95 % confidence.

The extraction yields for proteins increase from 21.4 ± 0.8 % under aqueous conditions to 74.9 ± 5.7 % at 40 wt % IL. On the contrary, the yields for carbohydrates are significantly inferior in comparison to aqueous extraction, and remain statistically constant ($p > 0.05$) around 20 % regardless of the concentration of IL. This indicates a highly selective nature of [Emim][DBP] to solubilize proteins over carbohydrates from the alga biomass.

The cell wall of *U. lactuca* is composed of polysaccharide layers of ulvan and cellulose, and embedded proteins interacting by means of hydrogen bonds and ionic forces (Lahaye and Robic, 2007). The poor solubilisation of carbohydrates observed in Fig. 2 can be explained by the mild conditions used during extraction (room temperature, 3 min). In fact, significant cellulose dissolution by ILs appears to take place only at temperatures above 50^{o}C and long contact times (Brandt et al., 2013; Hou et al., 2017). Malihan et al., (2017, 2014) and Pezoa-Conte et al., (2015) investigated the dissolution of carbohydrates from the red alga *G. amansii* and the green alga *U. rigida* respectively. In both studies sugars yields above 65 % were observed, however, the extraction

process took place at temperatures of 100-160^{o}C and IL-biomass ratios in the range 9-33.

The remarkable extraction yields for proteins suggests that [Emim][DBP] is able to partially disentangle the cell-wall structure, allowing the release of proteins, but without solubilizing the carbohydrates. Partial disentanglement could be the result of the destabilization of the polymer chains, since the IL can form strong electron donor-acceptor complexes with the functional groups of the polysaccharides (Pinkert et al., 2009). The significant decrease in carbohydrate yields under the presence of IL in comparison to aqueous extraction, suggests that that [Emim][DBP] provides a more hydrophobic environment which is favourable for proteins extraction, but in which the neutral carbohydrates from *U. lactuca* are less soluble (Fleurence et al., 1995).

3.3. Biomolecule fractionation by two-phase partitioning (route I, Fig. 1)

The partitioning of molecules extracted by [Emim][DBP] from *U. lactuca* was studied in two-phase systems formed with K_2HPO_4. This salt has been broadly studied in several IL systems for biomolecule fractionation since it allows a greater immiscibility region in the phase diagram (Desai et al., 2016b). Moreover, according to the Hofmeister series (Zhang and Cremer, 2006), K_2HPO_4 has a moderate to strong salting-out character and therefore, it is expected to favour the partitioning of proteins in the IL-rich phase and carbohydrates in the salt-rich phase.

The experimental phase diagram for the system [Emim][DBP]-K_2HPO_4 is shown in Fig. 3A. Two operation points were selected for the partitioning study: S1 (40 % IL, 10% Salt) and S2 (15 % IL, 25 % salt). These points fall within the ranges of IL studied in section 3.2.

Nearly 63.0 ± 2.9 % of the proteins and 79.9 ± 9.4 % of the carbohydrates initially present in the IL-extract remained in the top-phase of system S1 after two-phase formation. For the system S2, 41.5 ± 1.8 % of the proteins and 47.0 ± 0.9 % of the carbohydrates were found in the top-phase. Further analysis revealed that 4.2 ± 1.3 % of the proteins and 6.7 ± 2.1 % of the carbohydrates migrated to the bottom-phase of

system S1, while for system S2 only 1.0 ± 0.2 % of the proteins and 12.1 ± 2.3 % of the carbohydrates were transferred to the bottom phase. In Fig. 3B the corresponding alga extract and the two-phase systems are shown. As expected, virtually all the pigments remained in the IL-rich top phase.

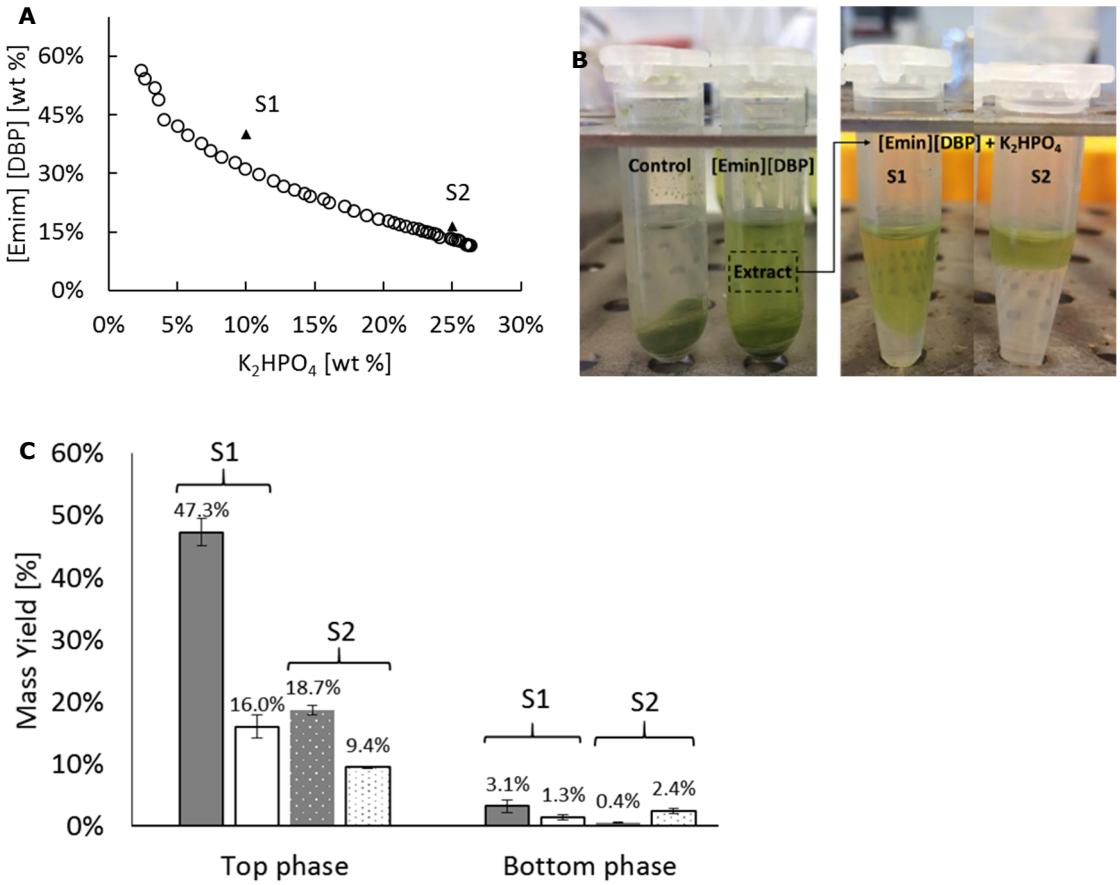

Figure 3. A. Phase diagram for the system [Emim][DBP]-K_2HPO_4 with detail of the operation points S1 and S2. **B.** Algal samples treated with [Emim][DBP] followed by the addition of K_2HPO_4 for two-phase partitioning. **C.** Overall yields (extraction + partitioning) for protein (grey bars) and carbohydrates (white bars). Data presented here are the average values and errors bars as standard deviation (n=2). Dotted bars are assigned for system S2.

Mass balances conducted on the systems S1 and S2 revealed that 30-55 % of the proteins and 14-40 % of the carbohydrates were present in a subtle insoluble layer located between the top and bottom phases. Therefore, the systems under investigation correspond to a three-phase partitioning (TPP) system.

TPP was first reported in 1984 and has been implemented for the fractionation and purification of proteins (Dennison and Lovrien, 1997) and carbohydrates (Sharma and Gupta, 2002) for several applications. In general, TPP makes use of an organic solvent (top) and a salt (bottom) to induce the formation of an insoluble which contains precipitated molecules. The extent of precipitation and the location of the insoluble layer depends on the salting-out character of the phase forming components, their density and on the molecular interactions among neighbouring molecules (Dennison and Lovrien, 1997).

For the system under evaluation, the precipitation of proteins and carbohydrates at the interphase is mainly due to the strong salting-out character of K_2HPO_4. For example, the larger fraction of proteins and carbohydrates in the insoluble layer was found for the system S2, in which the salt content was highest (25 %).

The overall yields, taking into account the steps of extraction and phase partitioning, are shown in Fig. 3C. As can be seen, system S1 leads to the largest overall protein and carbohydrate recoveries (47% and 16 % respectively) but requiring higher concentrations of IL. Although the extraction yields in the bottom phase are substantially low, such molecules are pigment free, which can be interesting for specific market applications. An overview of the mass balances for proteins and carbohydrates under the system S1 is shown in Fig 1.

Contrary to our expectations and to published studies (Ventura et al., 2017), the induction of a two-phase system with K_2HPO_4 did not cause a significant partitioning of proteins and carbohydrates. In other words, the majority of the proteins, carbohydrates and pigments were present in the top IL-rich phase. This can be due to the nature of the extracted proteins, which often form cross-links with polysaccharides via disulphide bonds (Harnedy and FitzGerald, 2013) or non-covalent interactions with other bio-molecules. An example of such glyco-proteins found in *Ulva* strains are Lectins, a structurally diverse group of carbohydrate - binding proteins (Holdt and

Kraan, 2011). The molecular binding of proteins and carbohydrates can explain why no significant partitioning was achieved in the [Emim][DBP]-K_2HPO_4 system.

3.4. Ultrafiltration for biomolecule fractionation and ionic liquid recovery (route II, Fig. 1).

The potential application of [Emim][DBP] in the biorefinery of *U. lactuca* at commercial scale depends not only on its ability to selectively extract biomolecules under mild conditions and high yields, but also on its recovery. In addition, the extracted biomolecules must be separated from the IL in order to allow their use in commercial products. Therefore, ultrafiltration was studied as a promising technology for simultaneous biomolecule fractionation and IL recovery.

In Table 1., the mass yields for proteins, carbohydrates and [Emim][DBP] are presented for two different membrane configurations: 10 kDa poly-ether sulfone (PES) and 3 kDa regenerated cellulose (R.Cell). In the control samples for both configurations no carbohydrates were detected in the retentate or permeate phases (data not shown), indicating that the IL did not lead to a significant solubilisation of the membrane's polysaccharides.

Table 1. shows that over 70 % of the proteins and more than 50 % of the carbohydrates were recovered in the retentate phase, while more than 80 % of [Emim][DBP] migrated to the permeate phase. Visual observations indicated that pigments are retained in the retentate phase (data not shown). The superior recovery of biomolecules in the retentate, and of IL in the permeate, is due to the low *cut offs* and hydrophilic nature of the PES and R.Cell membranes. The low yields of biomolecules in the permeate suggests that the recovered IL could be potentially re-used in the extraction step. The recyclability study is however, out of the scope of the present work.

From the data in Table 1 and mass balances conducted on the filtration system, it can be deduced that ~ 20 % of the proteins and ~ 10-40 % of the carbohydrates are lost, probably as result of the absorptive fouling, which causes biomolecule precipitation on the membranes' layer. Membrane fouling is a common phenomenon in ultrafiltration

which negatively impacts the filtration performance and leads to biomolecule losses and unexpected recovery yields (Safi et al., 2017b; Suarez Garcia et al., 2018c).

Table 1. Mass yields for biomolecules and IL after filtration of alga extracts. Data are the average values and corresponding standard deviations. Letters "A" and "a" indicate statistically equal means at 95 % confidence interval for permeates and retentates respectively.

Membrane		**Proteins**	**Carbohydrates**	**[Emim][DBP]**
PES	Retentate	71.3% ± 8.2%[a]	85.4% ± 8.6%	14.6% ± 0.7%
	Permeate	6.2% ± 2.1%	6.2% ± 2.2%	85.2% ± 6.0%[A]
R.Cell	Retentate	80.4% ± 3.3%[a]	50.0% ± 7.9%	20.4% ± 0.5%
	Permeate	0.3% ± 1.2%	2.4% ± 0.2%	79.6% ± 3.3%[A]

An overview of the mass balances for proteins and carbohydrates after the steps of extraction and filtration with a 3 kDa membrane (R.Cell) is shown in Fig. 1. To the authors' knowledge, this is the first study in which ultrafiltration is investigated for the fractionation of biomolecules from macroalgae and to recover ILs from algal extracts. The only reports about filtration technology in macroalgae are related to the use of diafiltration to remove the excess of salts after protein precipitation with $(NH_4)_2SO_4$ (Kandasamy et al., 2012; Wong and Cheung, 2001).

3.5. Stability of proteins in ionic liquid extracts

ILs are reported to provide a mild environment which favours protein stability and activity. However, at high concentrations, ILs can lead to molecular aggregation and protein denaturation (Desai et al., 2014; Ventura et al., 2017). In the study conducted by Desai and collaborators, the model protein Ribulose-1,5-bisphosphate carboxylase/oxygenase (Rubisco), which is abundadanly found in algae, was subjected to concentrations of the ionic liquid Iolilyte 221 PG in the range 10-60 %. The authors observed that an increasing concentration of IL lead to the formation of protein aggregates and loss of enzyme activity, in particular above 30 % IL. Further research is

therfore needed in order to understand the effect of [Emim][DBP] on their native conformation and to establish if the protein activity is compromised.

3.6. Outlook

We have presented an IL-mediated process for the extraction of biomolecules from the macroalga *U. lactuca* and two approaches for their fractionation: two-phase partitioning and ultrafiltration. The experimental yields obtained with these approaches were compared to several studies in which the biorefinery of green macroalgae was investigated: Aqueous extraction and enzyme hydrolysis (Fleurence et al., 1995; Postma et al., 2018), alkali solubilisation (Fleurence et al., 1995), shear extraction (Postma et al., 2018), aqueous two-phase extraction (Fleurence et al., 1995), ultrasonication (Fleurence et al., 1995), pulsed electric fields (Polikovsky et al., 2016; Postma et al., 2018), IL-mediated extraction (Malihan et al., 2017, 2014; Pezoa-Conte et al., 2015) and combination of technologies (Kandasamy et al., 2012; Wong and Cheung, 2001). The results are plotted in Fig. 4.

The carbohydrate yields measured in the present study are significantly lower in comparison to other investigations, which is due to the selective nature of [Emim][DBP] towards proteins. The maximum carbohydrate yield (67 %,) was obtained by Pezoa-Conte et al., (2015) with an IL-mediated process at high temperatures and extraction times of nearly 6 h. The maximum carbohydrate yield in the present study was 36 % under aqueous mechanical disintegration.

According to Fig 4, in general, extraction under aqueous conditions or using external fields (ultrasonication, pulsed electric fields) lead to low protein yields, which is expected given the complexity and toughness of the macroalgae biomass. With alkaline solubilisation and enzyme hydrolysis further improvements are observed, but the yields remain below 30 %. The highest protein yield (42 %) was reported by Pezoa-Conte et al., (2015), but the proteins are likely to be denatured due to the extreme conditions used for extraction. A unique finding of the present work is that up to75 % of the total initial proteins can be extracted under mild conditions, and that the overall

yields remain relatively high after two-phase partitioning (47 %) and ultrafiltration (40 %).

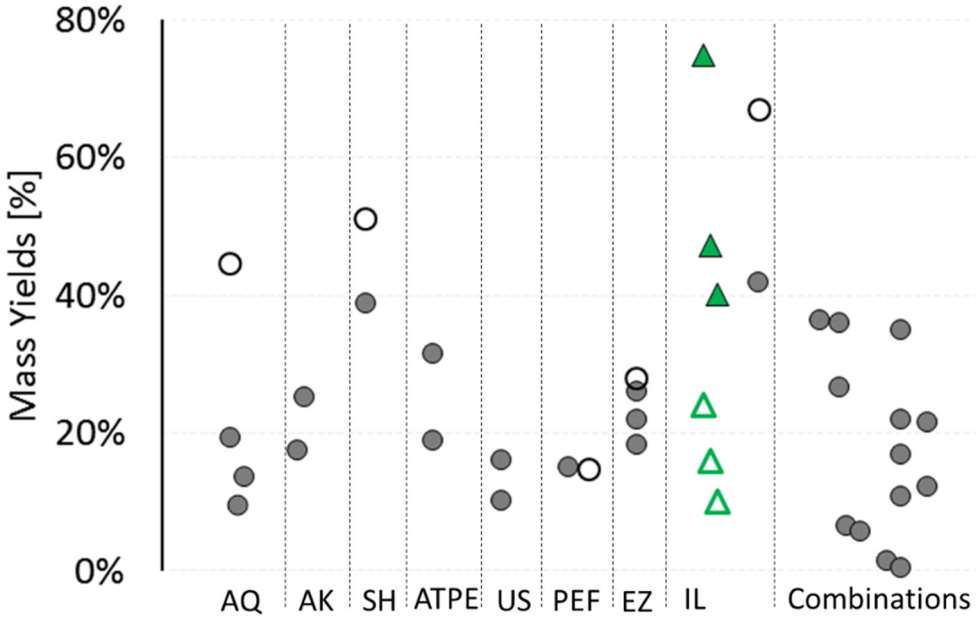

Figure 4. Overview of processes (AQ: Aqueous; AL: Alkali; SH: Shear; ATPE: two-phase extraction; US: Ultrasounds; PEF: Pulsed electric fields; EZ: Enzymes; IL: IL-based processes; Combinations: sequence of several technologies) for the recovery of proteins (filled markers) and carbohydrates (open markers) from green macroalgae. Green (triangle) markers are data from the present study.

Despite the promising results obtained with [Emim][DBP], several aspects still require comprehensive investigation. The mechanism of extraction is far from being elucidated, and the structural effects of the IL on the algal biomass require further understanding. A more complete analysis of the extraction processes is needed in order to quantify the purity of the biomolecules, including the determination of the extraction yields for ash and pigments. Moreover, studies on the reusability of the IL are pending in order to know if [Emim][DBP] retains the extraction capabilities after its recovery via filtration. The crude alga extract (retentate after filtration) contain most of the algal biomolecules, however, it still has significant amounts of IL, making it unsuitable for commercial products. Additional research is needed in order to develop

processes that allow the production of IL-free extracts and to characterize their composition techno-functional properties.

4. Conclusions

In this investigation we report the extraction of biomolecules from the green macroalgae *Ulva lactuva* by means of a mechanical extraction process mediated by the ionic liquid 1-ethyl 3-methyl imidazolium dibutyl phosphate. The extraction process was selective towards proteins over carbohydrates. Under mild conditions (room temperature, 3 min), 75% of the total initial protein and 24 % of the carbohydrates could be extracted in a single step. Fractionation of biomolecules was studied by means of two-phase partitioning and ultrafiltration. It was found that proteins and carbohydrates are preferentially recovered in the retentate phase, while up to 85.2 % of the ionic liquid migrates to the permeate phase. The proposed process is simple, mild and lead to superior protein yields compared to other extraction-fractionation processes reported in literature.

Acknowledgements

This project is financed by the Dutch Technology Foundation STW under the project AlgaePro4You, nr. 12635. From January 2017, STW continued its activities as NWO (Dutch national science foundation) Applied and Engineering Sciences (TTW). Carlota Miranda conducted research activities under the project iBB/2016/2017, iBB/IST-PT: "Biorefining a green seaweed: protein extraction and carbohydrate valorization to bioplastics". The authors are grateful to Pedro Carlos de Barros Fernandes for his valuable feedback during the preliminary phases of the project.

Appendix

A. Screening of ionic liquid for the extraction of biomolecules from *Ulva lactuca*.

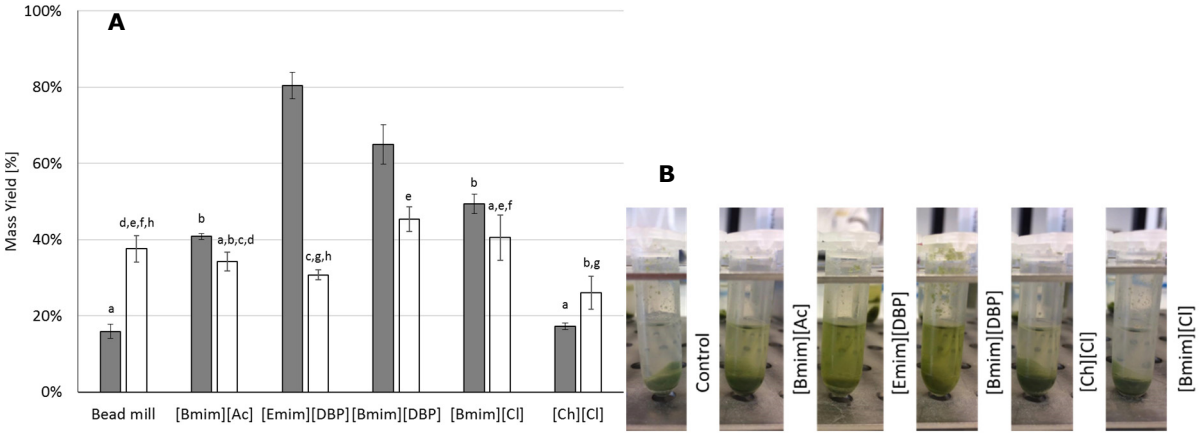

Figure A1. Extraction yields for proteins (grey bars) and carbohydrates (white bars) in samples after treatment with ILs (40 wt%) and bead milling. Data correspond to average values and corresponding standard deviation are shown as error bars (n=3). Low case letter indicates statistically equal means at 95% confidence. **B.** Experimental samples of algal biomass treated with ILs.

Chapter 8

Mild permeabilization of microalgae cells for the selective release of biomolecules using ionic liquids

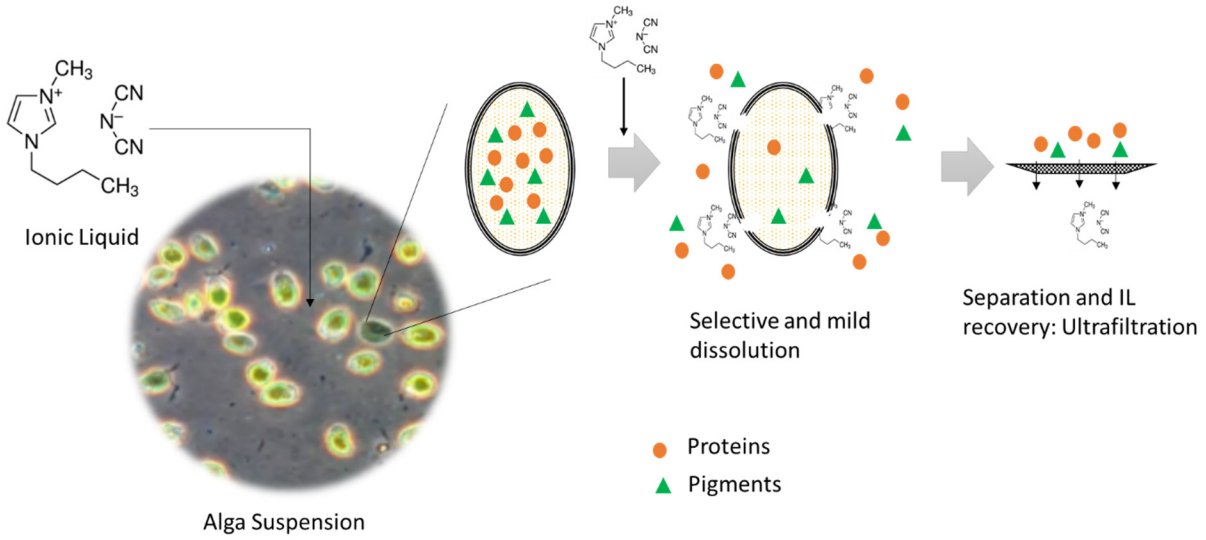

Submitted as:

E. Suarez Garcia, W. van den Brink, M.H.M. Eppink, R.H. Wijffels, C. van den Berg. Mild permeabilization of microalgae cells for the selective release of biomolecules using ionic liquids

Abstract

Microalgae are a sustainable source of biomolecules and chemical building blocks. However, the complex cell architecture hinders the extraction and fractionation process, often leading to low yields and purities and high costs. In this work we demonstrate the use of ionic liquids (ILs) to selectively extract biomolecules under mild conditions. In a single step, without requiring additional mechanical disintegration, up to 77.4 ± 4.6 % of the total initial proteins could be extracted from the green microalga *Tetraselmis suecica* using 1-Butyl-3-methylimidazolium dicyanamide ([Bmim][DCN]). The process was conducted at room temperature, short contact times and low IL-biomass ratios. Experimental data showed that the IL causes modifications of the cell-wall, through which biomolecules leak out. Furthermore, ultrafiltration was used for biomolecule fractionation and IL recovery. After one ultrafiltration step, > 86 % of the extracted proteins were recovered in the retentate and > 65 % of the IL was found in the permeate phase. This process is simple, requires few unit operations and results in high protein yields, however efficient [Bmim][DCN] recovery and re-use still remain as open challenges.

1. Introduction

The rapid expansion of world population along with an accelerated increase in the demand for fuels, materials and food has driven the search for alternative sustainable feedstock's and for biomolecules as building-blocks for various industries (Harun et al., 2010). Microalgae are considered a potential source of such biomolecules due their notable advantages compared to traditional crops: no dependency on fresh water and arable land, high areal productivities and a unique composition in terms of proteins, carbohydrates, pigments, amino acids and fatty acids (Khanra et al., 2018).

The biomolecules of interest in algae are often present intracellularly, surrounded by a rigid cell-wall and making part of the cell assembly and thus not freely accessible for extraction. Hence, the first step to recover algal biomolecules is, in general, cell disintegration. The disintegration of algae cells has been investigated using several methods, including mechanical force (Postma et al., 2017), ultrasound (Parniakov et al., 2015), electric fields ('t Lam et al., 2017), chemical and enzymatic hydrolysis (Sari et al., 2013) and thermal processing (Passos et al., 2015). However, these methods often lead to low yields and purities and often result in the denaturation of labile molecules when extreme conditions of pH and temperature are used (Phong et al., 2018b). Furthermore, biomolecule separation and purification demands, in general, an intricate set of unit operations (Chronakis, 2001; Schwenzfeier et al., 2011; Waghmare et al., 2016) which impact negatively the recovery yields and the process economy. Novel simple methods, which can deliver high extraction yields under selective and mild conditions, are therefore needed.

Ionic liquids (ILs) are salts which are liquid at room temperature. Due to their vast chemical versatility and distinctive physical properties such as negligible flammability and vapour pressure, ILs have been investigated in several fields including chemical synthesis, electrochemistry and polymer science (Brandt et al., 2013; Mai et al., 2014). In addition, their distinctive solvation character has been exploited for the dissolution

of lignin and cellulose from woody biomass (Brandt et al., 2013), and for the extraction of a wide range of biomolecules (Ventura et al., 2017).

The implementation of ILs for the selective extraction of biomolecules from microalgae is limited. Most studies have centred on the extraction of lipids (Kim et al., 2012; Olkiewicz et al., 2015; Orr et al., 2016; Orr and Rehmann, 2016; Teixeira, 2012; To et al., 2018; Wahidin et al., 2016) and pigments (Desai et al., 2016a; Kim et al., 2016). Only few publications have addressed the extraction proteins (Lee et al., 2017b; Wang and Zhang, 2012) and carbohydrates (To et al., 2018). Nearly all investigations conduct extraction at temperatures above 80^{o}C, often requiring long contact times and the use of co-solvents.

Despite the numerous investigations describing excellent performances of ILs in bio-separations, their widespread use is hindered by the high costs (George et al., 2015), poor recovery and potential toxicity (Yoo et al., 2014). Although novel ILs are being synthetized from cheap or even renewable sources (Brandt-Talbot et al., 2017), the development of recovery technologies for ILs is of paramount importance. In general, distillation, adsorption, solvent extraction, membrane processes and induced phase separation have been demonstrated in model systems (Mai et al., 2014). For the case of microalgae, recovery of ILs has been achieved by means of solvent extraction, precipitation of residual extract from the IL, centrifugation and distillation to remove the excess of water/solvents (Desai et al., 2016a; Fujita et al., 2013; Olkiewicz et al., 2015; Orr et al., 2016).

In this work we present a novel approach for the extraction and fractionation of biomolecules from the green microalgae *Tetraselmis suecica*. The approach is based on the single-step preferential and mild extraction of proteins by ionic liquids without the need of a separate disintegration step. Moreover, ultrafiltration is used not only for the fractionation of biomolecules, but as a tool to recover the IL from the extract phase. The investigated process is simple and can be easily scaled up, which offers potential for its implementation in the framework of multiproduct biorefineries.

2. Material and methods

2.1. *Chemicals and Ionic liquid.*

All chemicals used in this investigation were analytical grade. Chloroform and methanol were obtained from Biosolve®. Phosphate Saline Buffer (PBS) pH 7 was prepared by mixing 0.21 g KH_2PO_4, 0.48 g $Na_2HPO_4.2H_2O$ and 9. 00 g NaCl in 1 L distilled water (chemicals procured from Merck®). Phenol solution (Bioreagent), sulfuric acid (95-98 %) and potassium citrate tribasic monohydrate (> 99.0 %) were obtained from Sigma Aldrich®.

The ionic liquid 1-Butyl-3-methylimidazolium dicyanamide ([Bmim][DCN]), with a purity of >98 %, was obtained from Iolitec®. This ionic liquid was selected after preliminary experiments in which several ionic liquids were evaluated for protein recovery from microalgae (Appendix A).

2.2. *Microalga cultivation and harvesting.*

Tetraselmis suecica (UTEX LB2286, University of Texas Culture Collection of Algae, USA) was cultivated in repeated batches in a 25 L flat panel photo-bio reactor (AlgaePARC, The Netherlands) at 20°C. Ten fluorescent lamps (Philips 58 W/840) provided a continuous incident light intensity of 373 µmol $m^{-2}s^{-1}$. A stream of gas containing air and 5 % v/v CO_2 was supplied at a rate of 0.254 vvm to provide carbon source, mixing and pH control (pH 7.5). Walne medium was fed at a ratio of 8.8 mL L^{-1} medium (Michels et al., 2014a). After the end of the exponential phase, cultures were harvested by means of centrifugation (80 Hz, E 10, Evodos®, The Netherlands). The resulting paste was stored in sealed bags at 4°C and was used within 7 days.

2.3. *Ionic liquid-mediated extraction.*

Suspensions containing *T. suecica* biomass and [Bmim][DCN] were prepared at IL-biomass ratios of 0, 1, 2, 5, 10 and 15 $g_{IL}\ g^{-1}_{Biomass}$ (DW). The suspensions were subjected to strong mixing (MultiReaX Vortexer, Heidolph, Germany) for 20 min at room temperature. Next, samples were centrifuged for 10 minutes at 20000 rpm and the

supernatants were recovered for analysis. Furthermore, the supernatant was subjected to ultrafiltration for biomolecule fractionation and IL recovery.

2.4. Biomolecules fractionation and ionic liquid recovery

Filtration experiments were conducted on supernatants after extraction with 5 wt% alga and 25 wt% IL. A volume of 0.5 ml of supernatant was added to centrifugal filters, followed by centrifugation at 4000xg for 30 min in order to reach a concentration factor of 4.2-4.5. Three membrane cut-offs were studied: 3, 10 and 100 kDa (Ultracell, Merk Millipore®, USA). The resulting retentates and filtrates were collected for analysis.

2.5. Reference process and blanks

For all experiments, solutions containing IL in water were used as blanks. Similarly, suspensions of alga in water under stirring (aqueous extraction) and under bead milling (mechanical disintegration) were used as control and reference process respectively. For the filtration experiments, solutions of 25 wt% IL in water were run through the filter in order to determine if the IL can solubilize sugars from the membrane filters. Blanks and controls were subjected to the same conditions as described in section 2.3-2.4.

2.6. *Biomass characterization and analysis*.

Protein content was determined with the method of Bradford (Bradford, 1976). This method was selected due to the negligible interference with [Bmim][DCN]. Measurements were conducted with a commercial kit (Pierce® Coomassie protein assay, Thermo Fisher Scientific, USA), using Bovine Serum Albumin (Sigma Aldrich®) as protein standard and IL solutions as blanks. Bradford is a colorimetric method which correlates protein content to the absorbance shift of the dye Coomassie blue, which can be quantified at 595 nm. Total carbohydrates were determined with the method of Dubois (Dubois et al., 1956). The concentration of carbohydrates is correlated to a colorimetric reaction with phenol in sulfuric acid which can be followed at 483 nm.

Glucose (Sigma Aldrich®) was used as carbohydrate standard. Absorbances at 595 and 483 nm were measured with a microplate reader (Infinite M200, Tecan, Switzerland).

Total lipids were measured with the method of Folch (Folch et al., 1957). Three extraction cycles were conducted, the organic phases collected and the excess solvent removed using a vacuum concentrator (RVC 2-25 CDplus, Christ®, Germany). The remaining material was weighed and regarded as total lipids. Dry weight was estimated gravimetrically after drying a known amount of sample in a convection oven (Nabertherm, Germany) to constant weight at 100°C. Total ash was determined after burning a known amount of algal biomass in a furnace (L 24/11, Nabertherm, Germany) at 575°C and regarding the remaining material as total ash.

Ionic liquid quantification was carried out by Ultra High Performance Liquid Chromatography (UHPLC Nexera X2, pump LC-30AD, auto sampler SIL-30AC, Refractive Index Detector RID-20A, Shimadzu, Japan) using a Rezex® ROA-Organic Acid column coupled with a security guard (300 mm x 7.8 mm, Phenomenex®, USA). Prior to analysis, samples were centrifuged at 4700 rpm for 20 min to remove suspended particles. A 20 µL volume was injected and run at 0.6 mL min^{-1} under isocratic mode with 0.005 N H_2SO_4 as mobile phase. The column was kept at 60 °C under a pressure of 55 bar. Solutions of IL in MilliQ water were used as standards.

2.7. Extraction yields and purities.

Mass yields (*Y*) and purities (*P*) per component (i) were estimated according to Eq. 1 and Eq. 2:

$$Y_i\ \% = \frac{m_{i,e}}{m_{i,b}} \times 100 \qquad (1)$$

$$P_i\ \% = \frac{m_{i,e}}{m_t} \times 100 \qquad (2)$$

Where $m_{i,e}$ is the mass of component *i* (protein, carbohydrates, IL) in each phase, $m_{i,b}$ is initial mass of component i before the extraction or fractionation, and m_t is the total dry weight mass. All calculations are conducted on dry weight basis.

2.8. Protein stability.

The stability of the extracted proteins was studied by native-gel electrophoresis and size-exclusion chromatography (SEC). Extracts were centrifuged prior to each procedure. Samples were diluted with native buffer at a ratio 1:1 V V^{-1}. A volume of 30 µL of the resulting solution was loaded per lane in a 4–20 % Criterion TGX gel. Electrophoresis was run at 125 V for 75 min using Tris-Glycine as running buffer. Gels were stained overnight using Bio-Safe® Coomassie. All materials were procured from Biorad® (USA). Gel images were acquired with an ImageScanner III (GE Healthcare, UK). SEC was performed using a size exclusion column (Bio SEC-3 300Å 7.8 x 300 mm, Agilent, USA). Samples were injected (20 µL) and run under isocratic mode with 0.15 M sodium phosphate buffer pH 7 as mobile phase at 0.5 ml min^{-1} and 23°C. Samples containing Rubisco (D-Ribulose 1,5-Diphosphate Carboxylase, Sigma®) in water were used as reference protein. Proteins were detected at 280 nm with a photodiode array detector (SPD-M20A).

2.9. Flow cytometry

Cell disintegration and cell granularity were analysed from forward scattering (FSC) and side scattering data (SSC) using flow cytometry (BD Accuri C6, USA). A fixed volume of 15 µL was measured at a fluidics rate of 35 µL min^{-1} and a core size of 16 µm.

2.10. Statistics

All experiments were conducted in duplicates. Experimental results are presented as mean values and corresponding standard deviations. The variation of the experimental data under different treatments was analysed by one-way analysis of variance (ANOVA) at 95 % confidence level. When significant differences were found (i.e. $p < 0.05$), the Tukey's Honest Significant Difference test (HSD) was used to identify significant differences between specific treatments. All analyses were performed in R (V3.4.0).

3. Results and Discussion

The ionic liquid [Bmim][DCN] was studied for the extraction of biomolecules from the green microalga *T. suecica.* Extraction was conducted by contacting microalga biomass with different IL concentrations. Light microscopy and flow cytometry were used to better understand the extraction mechanism. Ultrafiltration was implemented for biomolecule fractionation and IL recovery.

3.1. Biomass characterization

The biomass used in this investigation (*T. suecica*) contained a total of 46.1 ± 1.9 % proteins, 28.0 ± 2.1 % carbohydrates, 18.0 ± 0.7 % lipids and 13.6 ± 0.3 % ash. These values are in good agreement with previous reports in which the same strain has been characterized (Suarez Garcia et al., 2018c).

For the extraction experiments in which alga biomass is contacted with ionic liquids, protein determination was conducted with the method of Bradford, as other methods (e.g., Lowry, BCA) showed strong interference with the ionic liquids in solution (data not shown). All analysis and yields presented in the next sections are based on the method of Bradford, using IL-water solutions as blanks in order to avoid false positives.

3.2. Extraction of biomolecules with [Bmim][DCN]

The extraction of biomolecules from *T. suecica* by [Bmim][DCN] was studied at a fixed biomass content and IL concentrations of 5, 10, 25, 50 and 75 wt%. This corresponds to IL-biomass ratios (R) of 1, 2, 5, 10 and 15 ($g_{IL}\ g^{-1}_{Biomass}$ DW). The resulting extraction yields for proteins and carbohydrates are presented in Fig. 1.

Fig. 1 shows two clear trends: An optimal extraction of proteins at R10 and a relatively constant profile for carbohydrate extraction regardless of the concentration of IL. Visual observations also show that the amount of pigments extracted increases with the IL content. This indicates a strong selectivity of [Bmim][DCN] towards proteins and pigments over carbohydrates. Similar observations were made by Lee et al., (2017b) for the extraction of proteins from *C. vulgaris* using several hydrophilic ionic liquids.

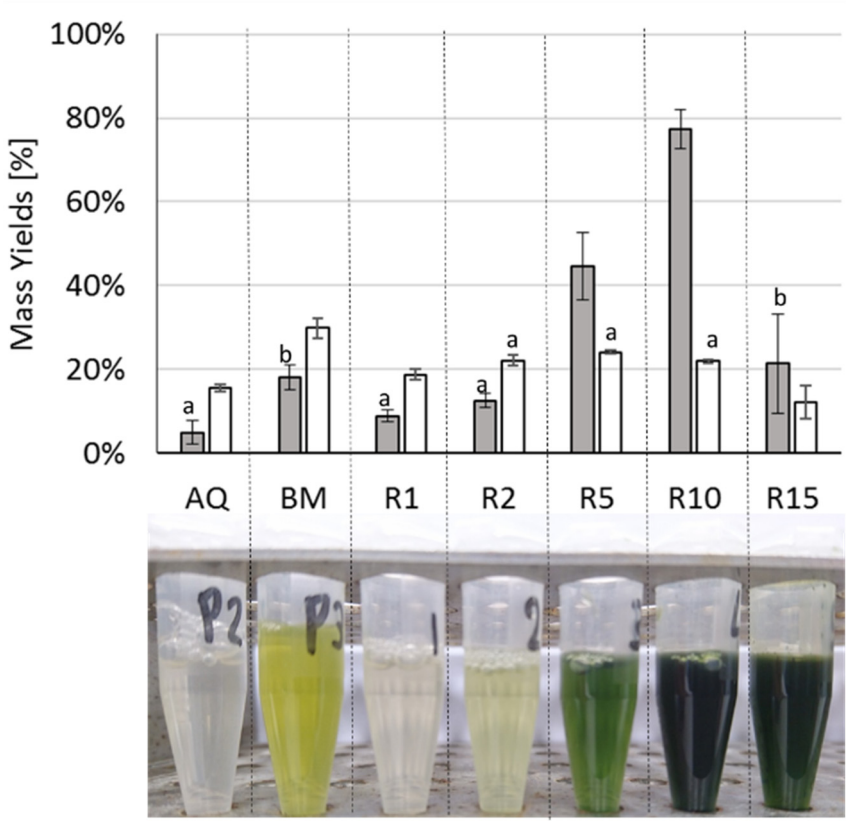

Figure 1. Overview of extracts (bottom) and extraction yields for proteins (grey bars) and carbohydrates (white bars) for biomass treated with [Bmim][DCN] at several IL-biomass ratios (AQ: Aqueous; BM: bead mill; R: Ratio IL-biomass). Data correspond to averages and error bars show standard deviation. Low case letters indicate statistically equal means at 95 % confidence interval.

The extraction yield of carbohydrates remained relatively constant around 20 %, slightly above the yield measured under aqueous extraction (15.6 %). This means that [Bmim][DCN] can only solubilize a minor fraction of the carbohydrates present in *T. suecica*. The carbohydrates of *T. suecica* are present mainly as insoluble polysaccharides in the cell-wall and starch granules (Becker et al., 1998; Kermanshahi-pour et al., 2014). The poor performance of [Bmim][DCN] to solubilize carbohydrates can be due to the mild conditions used during extraction (room temperature, 20 min mixing). Teixeira, (2012) presented an overview of studies on the solubilisation of carbohydrates from microalgae using ILs, showing that significant dissolution only takes place above 80^{o}C and IL-biomass ratios in the range R5 to R20. Similarly, To et al.,

(2018) reported carbohydrate yields of almost 71 % from microalgae using ILs, but requiring incubation temperatures of 70^{o}C for 3 h.

As the IL-biomass ratio increases from R1 to R10, the protein yield increases from 8.8 to 77.4 %, followed by a drastic decrease at R15. At low concentrations, ILs can provide a mild environment for protein extraction (Desai et al., 2016b). However, above a critical concentration, the charge density and salting-out character of the IL become too strong, causing protein unfolding and denaturation (Desai et al., 2016b; Lee et al., 2017b; Naushad et al., 2012).

3.3. Stability of extracted proteins

To further evaluate the effect of [Bmim][DCN] on protein stability, native gel electrophoresis and size exclusion chromatography (SEC) were performed. As can be seen in Fig. 2A, there is a progressive loss of protein bands as the concentration of IL increases, which indicates protein degradation. Low molecular weight proteins appear to be more sensitive, as the protein bands are absent even at low IL concentrations. For the high molecular weight proteins, in particular around 540 kDa which might correspond to Rubisco, a higher stability is observed. At R15 no protein bands are observed, indicating that the native structure of all proteins have been affected.

The SEC chromatograms shown in Fig. 2B confirm our findings. There is a significant shift in the elution peaks for the samples treated at R10 and R15 in comparison to aqueous extracts or to the reference protein Rubisco. The shift of the elution profiles suggests that proteins are being fragmented to smaller peptides and amino acids. The results presented in Fig. 2, in particular for native-gel electrophoresis, can only provide a qualitative evaluation. To understand the effect of the IL on the protein stability and conformation, non-reduced SDS-page electrophoresis and protein activity tests are required.

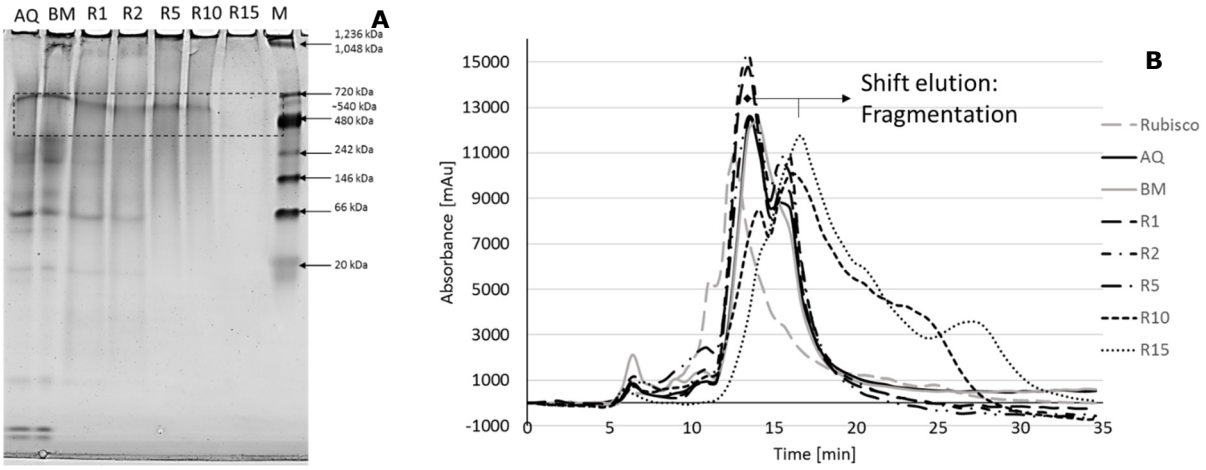

Figure 2. A. Native gel electrophoresis of extracts (M: Marker; Dashed square: region of protein of interest). **B.** SEC-HPLC chromatograms of extracts and Rubisco as reference protein.

3.4. Effect of [Bmim][DCN] on cell disintegration

To further understand the extraction of biomolecules from *T. suecica* by [Bmim][DCN], microscopic observations and flow cytometry measurements were conducted on IL-treated and untreated biomass.

Microscope images revealed that the cells of *T. suecica* are not disintegrated when treated with [Bmim][DCN] at IL-biomass ratios R1 to R15 (Fig. 3A). Moreover, the surface of the cells appeared covered by protuberances. These observations were confirmed by forward scattering (FSC) and side scattering (SSC) data (Fig 3B). FSC clearly shows that there is not a significant variation of the average size of the cells treated with IL, in comparison with the cells subjected to bead milling. In other words, extraction of biomolecules takes place without causing cell disintegration.

SSC, on the contrary, showed that the cell surface undergoes important changes as the IL concentration increases. This surface changes can correspond to the protuberances observed on the surface of the cells. Desai et al., (2016a) conducted surface electron microscopy analysis of microalga cells treated with ILs. The authors noted that the IL

forms a uniform film surrounding the cells, but did not observe any change on the cell surface.

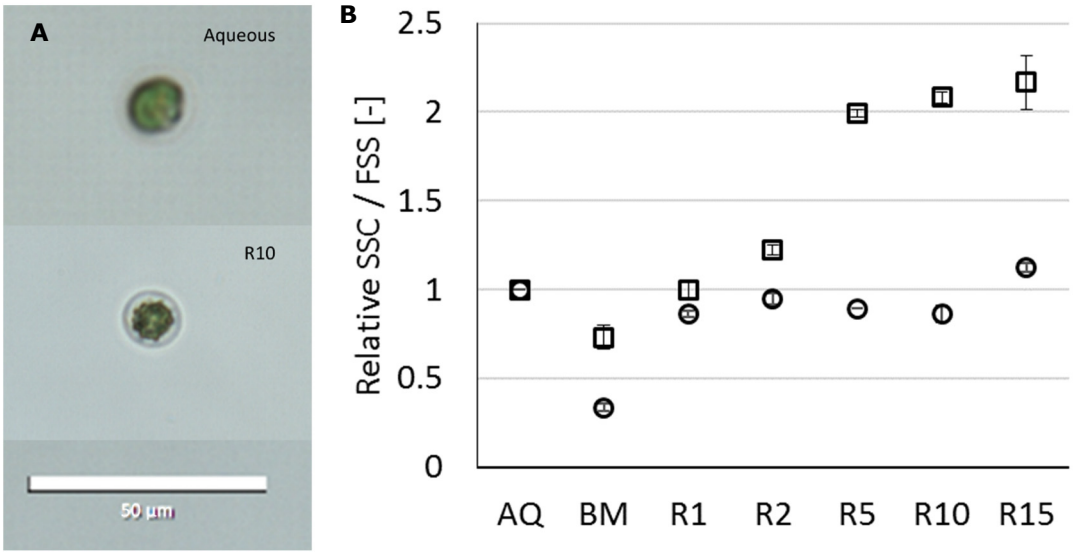

Figure 3. A. Bright field microscope image of an intact *T. suecica* cell and a cell treated with [Bmim][DCN] at R10. **B.** Relative side scattering (SSC, squares) and forward scattering (FSS, circles) for alga samples under aqueous conditions (AQ), bead milling (BM) and treated with [Bmim][DCN] at ratios R1 to R15. Data are averages and error bars correspond to standard deviations.

3.5. Hypothesis on extraction mechanism

[Bmim][DCN] showed selective release of proteins over carbohydrates under mild conditions (Fig. 2) without causing cell disintegration (Fig. 3). We hypothesize that the mechanism of biomolecules extraction involves the partial disruption of the hydrogen bond structure of the cell-wall, leading to the formation of pores through which proteins and pigments can leak-out. Due to the low temperatures and relatively low IL-biomass ratios used in this study, the extent of carbohydrate solubilisation is negligible, which prevented cell disintegration.

ILs are known to solubilize natural polymers such as cellulose and pectin by direct interaction of the IL, in particular the anion, with the hydroxyl groups of the polymer (Brandt et al., 2013; Wang et al., 2016). Hydrophilic ILs displaying low viscosities and high hydrogen bond capacity are reported to be more efficient in the solubilisation process (Brandt et al., 2013; Lee et al., 2017b). The anion [DCN] exhibits a strong

hydrogen bond basicity and can display reactivity with H^+ groups (Nichols et al., 2016). The cell-wall of *T. suecica* is composed of a pectin-like polysaccharide (Becker et al., 1998; Kermanshahi-pour et al., 2014) rich in uronic acids (Schwenzfeier et al., 2011).

Upon contact of the IL with the alga cells, the anion [DCN] can interact with the protons of the carboxylic groups of the ulosonic, heptulosaric and galacturonic acids in the cell-wall (Kermanshahi-pour et al., 2014). Such interactions lead to destabilization of the polymer structure, leading to the formation of pores through which proteins are released. The protuberances observed in Fig. 3A may correspond to the interaction sites of [Bmim][DCN] with the cell-wall polymers.

T. suecica displays a relatively strong cell-wall (Postma et al., 2017; Suarez Garcia et al., 2018a) which needs to be disrupted to allow biomolecule extraction. The disruption step have been commonly achieved by means of mechanical disintegration, a method that demands energy and results in relatively low yields (Fig. 1) as also reported by other authors (Postma et al., 2017; Schwenzfeier et al., 2011; Suarez Garcia et al., 2018a).

3.6. Ultrafiltration for biomolecule fractionation and ionic liquid recovery

Mild IL-assisted biomolecule extraction without requiring cell disintegration is a major step towards process intensification in algae biorefinery. However, the recovery of the IL is essential, not only to realize economically feasible processes but to ensure that the extracted biomolecules are IL-free.

Ultrafiltration experiments were conducted with three membranes cut-offs (3, 10 and 100 kDa) using IL soluble extracts as feed. The measured yields for proteins, carbohydrates and [Bmim][DCN], and the estimated purities are given in Table 1. Due to the lack of a reliable method to estimate alga lipids and ash in every stream, data from E. Suarez Garcia et al., (2018c) were used for the purity estimations.

Table 1. Yields and purities for proteins, carbohydrates and [Bmim][DCN] after ultrafiltration (Re: Retentate; Pe: Permeate). Data are averages and corresponding standard deviations.

		Protein		Carbohydrates		[Bmim][DCN]	
Membrane		**Yield**	**Purities⁺**	**Yield**	**Purities⁺**	**Yield**	**Purities⁺**
3 kDa	**Pe**	0.0 ± 0.7 %	0.1%	22.6 ± 0.5 %	0.7%	69.3 ± 3.6 %	97.0 %
	Re	86.2 ± 10.1 %	22.8%	73.6 ± 5.4 %	3.9%	28.9 ± 0.6 %	67.8 %
10 kDa	**Pe**	0.0 ± 0.6 %	0.1%	22.3 ± 5.1 %	0.8%	65.7 %*	96.9 %
	Re	92.7 ± 0.7 %	26.0%	71.2 ± 5.2 %	4.0%	25.8 %*	64.2 %
100 kDa	**Pe**	2.5 ± 1.4 %	1.1%	22.3 ± 6.7 %	2.3%	65.7 %*	90.8 %
	Re	72.7 ± 9.2 %	22.3%	74.7 ± 12.7 %	4.6%	24.5 %*	66.8 %

* Replicate sample not available

⁺ Estimated assuming yields for lipids and ash reported by E. Suarez Garcia et al., (2018c)

All the membranes tested delivered retention yields above 72 % for proteins and carbohydrates. The permeate phases on the contrary, were practically devoid of proteins, and contained > 22 % of the carbohydrates and 65 - 69 % of [Bmim][DCN]. These results are expected, considering the membrane cut-offs and the molecular sizes of the extracted proteins (Fig. 2A). The yields for proteins are comparable to the values reported by Suarez Garcia et al., (2018c) using similar membrane cut offs under aqueous conditions.

Differences in protein yields in the retentate phase can be due to the formation of a polarization layer on the membrane, which reduces the pores surface and contributes to membrane fouling (Safi et al., 2017b). This can also explain the gaps in the mass balance, since 7-25 % of the proteins were not detected in the retentate or permeate.

The high yields of carbohydrates in the permeate phase (> 22 %) suggests that a substantial amount of carbohydrates exists as small saccharides which can freely cross the membrane. Moreover, the permeate fractions are nearly pigment free (data not shown), which is due to the hydrophilic nature of the membrane material (regenerated cellulose).

Up to 69 % of [Bmim][DCN] was recovered in the permeate phase. This is an important finding since it reflects that [Bmim][DCN] does not form ireversible molecular complex with the alga biomolecules. In addition, it confirms that ultrafiltration can be effectively applied not only to recover ILs, but also to purify the alga extracts. From the several technologies reported for the recovery of ILs (Maia, 2014), this is the first study in which ultrafiltration has been demonstrated for microalgae extracts.

The recovery of ILs from algal extracts often involves washing and precipitation of biomass debris followed by centrifugation and evaporation of the excess water (Desai et al., 2016a; Olkiewicz et al., 2015). The use of anti-solvents and acids have also been successfully implemented (Orr et al., 2016; To et al., 2018). All reported methods, however, require post-treatment steps which are energy intensive. In contrast, the IL recovered in the permeate after UF (> 97 % purity), could be used directly in the extraction step.

3.7. Overview of extraction of algae biomolecules using ionic liquids

[Bmim][DCN] was found to selectively extract large amounts of proteins under mild conditions without requiring cell disintegration. Furthermore, ultrafiltration was proven to be efficient to separate algal biomolecules form the IL. These are promising findings, which demonstrate that high protein yields can be obtained with minimum processing. In spite of this, several aspects require further investigation. Additional research is needed in order to elucidate the underlying mechanism of biomolecule extraction, including the identification of the structural changes on the cell-wall of *T. suecica* and the understanding of the roles of the cation and anion of the IL. The precise determination of lipids and ash is also important to have an accurate measurement of the yields and purities of all component.

We provided an initial proof of IL recovery by means of ultrafiltration. However, the stability and reusability of the IL was not addressed. Similarly, complete purification of the alga extracts is still pending. These are important elements to consider, since they

directly impact the market potential of the extracted biomolecules and the process economics.

Protein analysis was conducted using the method of Bradford. However, this method has been reported to be less accurate than the methods of Dumas, Lowry and BCA (Barbarino and Lourenço, 2005; Berges et al., 1993), which are traditionally used for algae characterisation. Thus, more accurate protein determination methods need to be developed, in order to have certainty on the extraction yields.

Under the [Bmim][DCN]-mediated extraction process followed by ultrafiltration, a total of 54.9 % of the proteins and 4.8 % of the carbohydrates were recovered in the retentate of a 3 kDa membrane. The corresponding purities were 22.8 % for proteins and 3.9% for carbohydrates. This fractionation strategy was compared to other processes reported in literature for microalgae. We considered a broad range of processes analysed by Suarez Garcia et al., (2018a) and included the works of Lee et al., (2017b) and Wang and Zhang, (2012) who investigated protein extraction from microalgae using IL-based extraction, and To et al., (2018), who studied carbohydrate extraction. The overview of processes and corresponding yields is shown in Fig. 4A.

As can be seen, thermal methods (TH), which cause protein coagulation, or technologies based on external fields (pulsed electric fields and ultrasounds), which are ineffective due to the rigid cell-wall in algae, lead in general to poor yields. For the rest of the technologies, the great variation in the reported yields is due to differences in strain morphology and cell-wall composition. The yields obtained in the present study are comparable to the best performing and frequently reported fractionation technologies: Mechanical disintegration (MD), ultrafiltration (UF), chemical and enzymatic hydrolysis (C&E HYD) and pH shift (pHS).

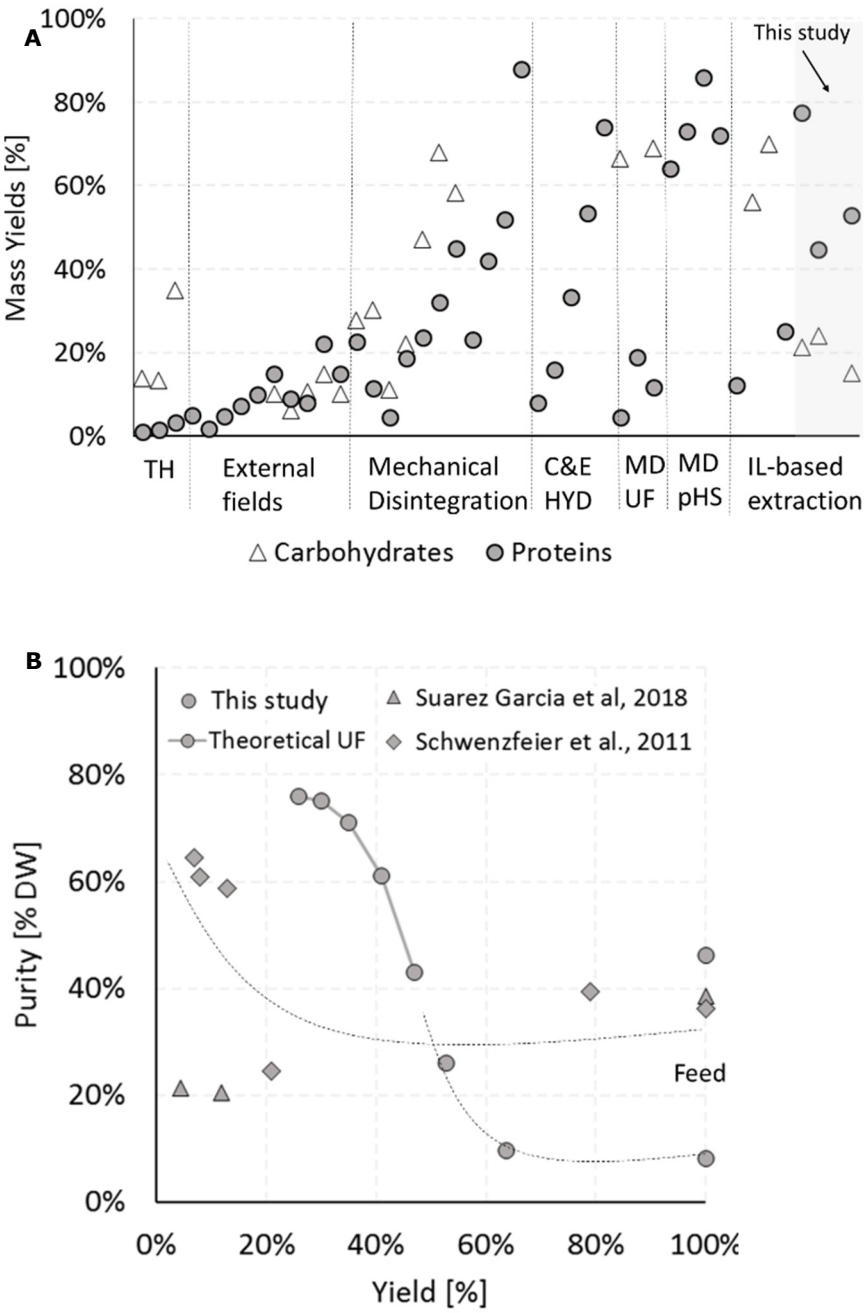

Figure 4. A. Overview of protein (filled circles) and carbohydrate (empty triangles) yields from microalgae using diverse technologies (TH: Thermal; C&E HYD: Chemical and enzymatic hydrolysis; MD UF: Mechanical disintegration and Ultrafiltration; MD pHS: Mechanical disintegration and pH shift). **B.** Protein yield vs purity diagram for extraction- fractionation processes reported for *T. suecica*. Dashed lines are a guide to the eye.

For a more comprehensive comparison, the protein yields and purities of processes reported for the microalga *T. suecica* were compared in Fig. 4B. Schwenzfeier et al., (2011) implemented a process involving disintegration, filtration, chromatography separation, precipitation and dialysis to obtain an algae soluble protein isolate with a purity of 64.4 % and a yield of 7 %. Suarez Garcia et al., (2018c) obtained crude extracts with a protein purity of 21.3 % and yield of 4.4 %, with a process involving bead milling and ultrafiltration. In the present work, we have obtained significant yields after extraction and ultrafiltration, but the resulting yields are low. We have therefore extended the fractionation approach with theoretical filtration steps using the same yields as presented in Table 1. According to this forecast, up to 5 filtration steps are required to remove the IL from the alga extract, with a corresponding protein yield of 26 % and a purity of 76 %. This would be by far the best performing method, considering that no mechanical disintegration is needed and that UF is easy to implement and scale up.

4. Conclusions

The present study investigates the use of ionic liquids for mild and selective extraction of biomolecules from the green microalgae *Tetraselmis suecica*. The experimental data clearly showed that the ionic liquid 1-Butyl-3-methylimidazolium dicyanamide is able to extract up to 77.4 % of the total initial proteins without causing cell disintegration. This is a unique finding as it proves selective extraction under mild conditions in a single unit operation. The mechanism of extraction can be related to the ability of the dicyanamide anion to interact with the polymers of the cell-wall of *T. suecica*, leading to the formation of pores through which proteins and pigments migrate to the soluble phase. Ultrafiltration was used for biomolecule fractionation and IL recovery. Up to 86.2 % of the proteins and 73.6 % of the carbohydrates were recovered in the retentate phase, and 69.4 % of the IL was found in the permeate phase of a 3 kDa membrane. This is the first demonstration of ultrafiltration for simultaneous biomolecule fractionation and IL recovery from microalgae extracts. In overall, the proposed

process IL-extraction + ultrafiltration outperforms the reported extraction-separation methods for *T. suecica*, and can be potentially be implemented at commercial scale.

Acknowledgements

This project is financed by the Dutch Technology Foundation STW under the project AlgaePro4You, nr. 12635. From January 2017, STW continued its activities as NWO (Dutch national science foundation) Applied and Engineering Sciences (TTW).

Appendix

A. Screening of ionic liquids for the extraction of biomolecules from *Tetraselmis suecica*.

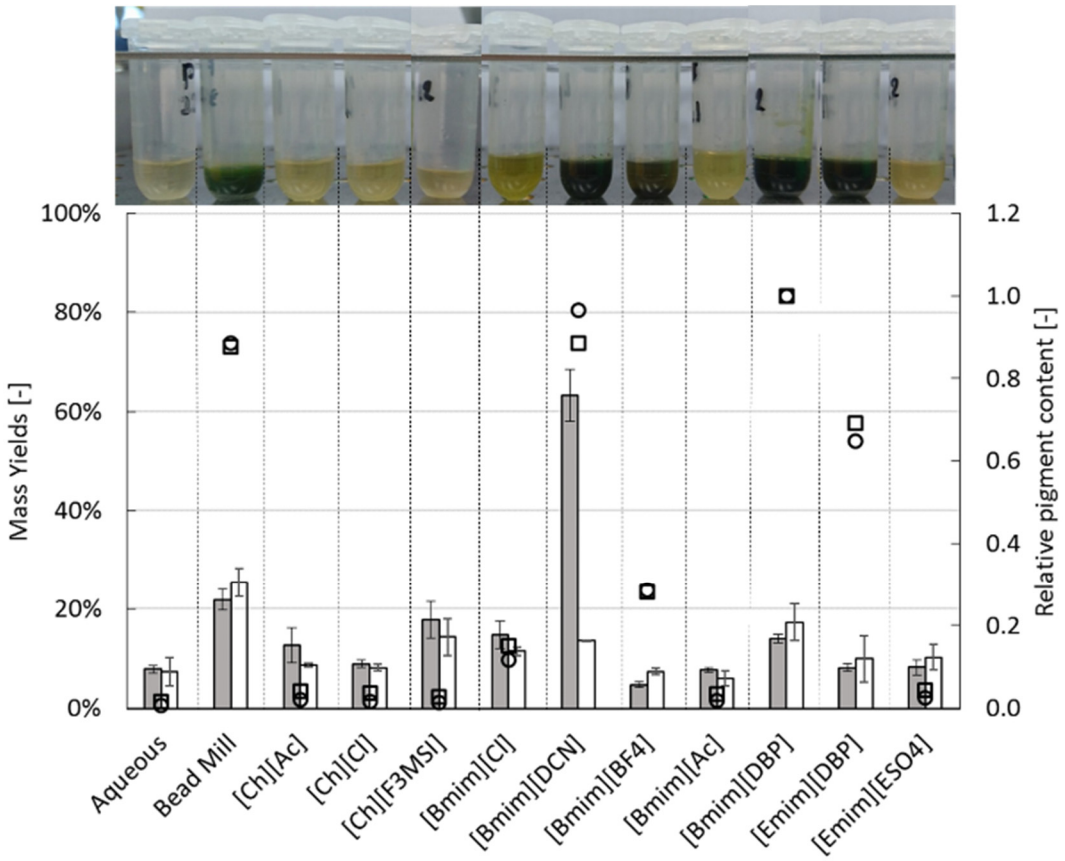

Figure A1. Overview of soluble extracts (top) and extraction yields of proteins (grey bars) and carbohydrates (white bars) of alga biomass treated with different ionic liquids. Data correspond to averages with standard deviations as error bars (for a complete statistical significance overview, the reader is referred to the supplementary information). Open markers show relative pigment release at 420 nm (squares) and 680 nm (circles).

Chapter 9

General Discussion:

Integrated biorefineries for algal biomolecules

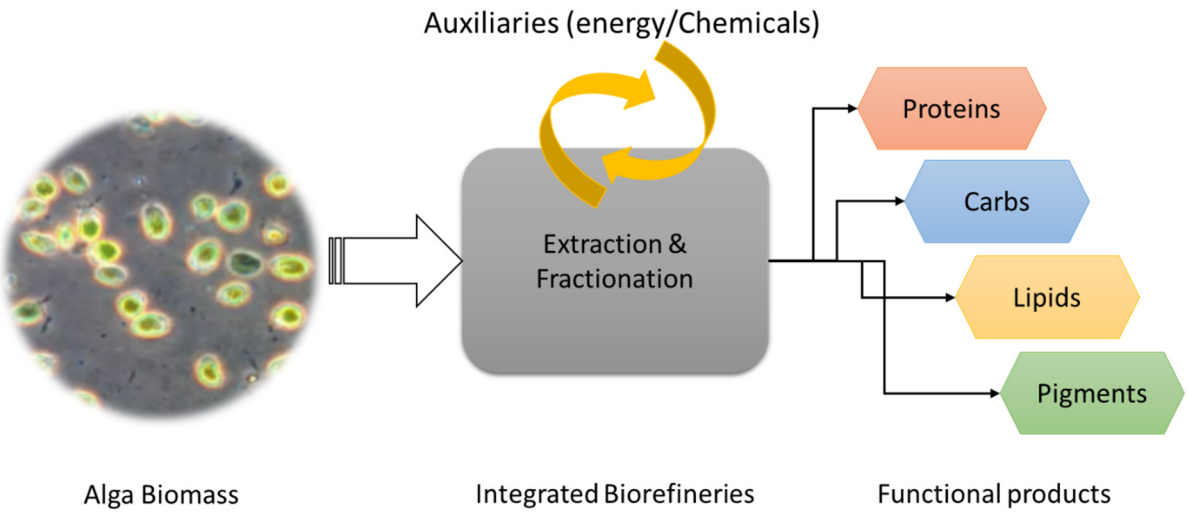

Submitted as:

E. Suarez Garcia, M.H.M. Eppink, R.H. Wijffels, C. van den Berg. Integrated biorefineries for algal biomolecules

Abstract

Algae are a renewable source of biomolecules for multiple applications ranging from fuels to specialties. However, their implementation as feedstock in industrial processes has only been achieved for few high value products. This is due to the elevated costs in cultivation and downstream processing. In order to decrease the biorefinery costs, and to enhance the overall process profitability, new separation processes need to be developed. Such processes must start from the understanding of the cell architecture, as a basis to develop an optimal fractionation strategy, and must include selective and mild disentanglement processes, in order to preserve the functionality of the target molecules. In this regard, we propose novel integration concepts such as self-disintegration, simultaneous disintegration and disentanglement and self-separating systems within the framework of process intensification, in such a way that auxiliary chemicals, solvents and numerous unit operations become redundant.

1. Introduction

Algae are photosynthetic organisms which can produce large amounts of proteins, carbohydrates, lipids and pigments (Bharathiraja et al., 2015). Because of their primary source of energy and carbon (sun light and CO_2) and the independency on arable land and fresh water, algae are considered as a renewable feedstock for several industry sectors (Behera et al., 2015; Cuellar-Bermudez et al., 2015; Vigani et al., 2015).

In fact, the range of algal products covers bulk commodities, chemical building blocks, fuels, feed, pigments, food, cosmetics and specialties (Behera et al., 2015; Cuellar-Bermudez et al., 2015; Draaisma et al., 2013; Jung et al., 2013; Ruiz Gonzalez et al., 2016). However, algae are not yet a prevalent raw material in industry. The costs of cultivation and biorefinery are still prohibitive (Ruiz Gonzalez et al., 2016) in comparison to traditional oil and crop derived biomasses. In particular, the biorefinery costs, at current 50 - 60 % of the total costs, must be reduced to a typical 30 % for a biotechnological process (’t Lam et al., 2018). To achieve this, several authors have proposed the development of novel cell disintegration and extraction techniques (’t Lam et al., 2018), multiproduct valorisation (Gifuni et al., 2018), cascade of extractions (Soto-Sierra et al., 2018) and mild processing (Dixon and Wilken, 2018).

In addition to these novel trends, we propose to design a biorefinery chain based on the knowledge of the cell structure as a first step to develop the right disintegration-extraction-fractionation methods. Furthermore, other concepts such as simultaneous disintegration-disentanglement and self-separating systems are proposed as future directions in algae biorefinery in a framework of process intensification.

2. The challenge of biomolecule extraction from algae

The extraction of biomolecules from algal biomass can be evaluated from two main dimensions (Fig. 1): unit operations and cell-structure. The unit operations dimension (Fig. 1A) includes technologies for cell disintegration, extraction, fractionation and purification. Typically, they are applied in a sequential way, leading to multiple side

streams. This corresponds to the traditional “empirical approach” (Fig. 1C), where the available unit operations are implemented based on common process engineering knowledge and where the cell is seen as a black box.

The cell-structure dimension (Fig.1B) comprises morphology and cell physiology, aspects which are often overlooked (Dixon and Wilken, 2018; Gifuni et al., 2018). Knowledge on the cell composition, cell-wall strength, localization of cellular compartments and organelles, hydrophobicity and charge, can be used to devise an optimal biorefinery. New biorefineries should be designed following a “mechanistic approach” (Fig. 1D), where the cell-structure provides the foundations to define the unit operations and the operational settings such as the energy input and process times.

2.1. Unit operations dimension

A broad range of unit operations has been reported for biorefinery of algae (Fig. 1A). For cell disintegration, the most common methods include bead milling (chapter 2-5), homogenization (Safi et al., 2014a), high-voltage electric discharges (Zhang et al., 2018), pulsed electric fields and ultrasounds (Grimi et al., 2014; Parniakov et al., 2015), thermal processing and microwaves (Jazrawi et al., 2015; Passos et al., 2015), chemical and enzymatic hydrolysis (Safi et al., 2017a; Sari et al., 2015) and dissolution using ionic liquids (Desai et al., 2016a; Fujita et al., 2013; Teixeira, 2012). Other innovative technologies have been proposed, among which hydrodynamic cavitation (Lee et al., 2015), microfluidization (Cha et al., 2012) and explosive decompression (Lorente et al., 2018; Phong et al., 2018b; Gunerken et al., 2019).

In general, mechanical methods lead to nearly complete cell disintegration and moderate to high extraction yields (chapter 2, 4-5, (Safi et al., 2014a)) at a high energy input. We showed that by optimizing the operation parameters (chapter 2-3), and by controlling the disintegration time (chapter 5), the energy consumption can be reduced from ~ 10 to 0.45 kWh kg_{DW}^{-1}. However, these are still orders of magnitudes higher

than the energy required to break the cells ($1.9x10^{-4}$ - $2.5x10^{-3}$ kWh kg_{DW}^{-1})(Günther et al., 2016; Lee et al., 2013).

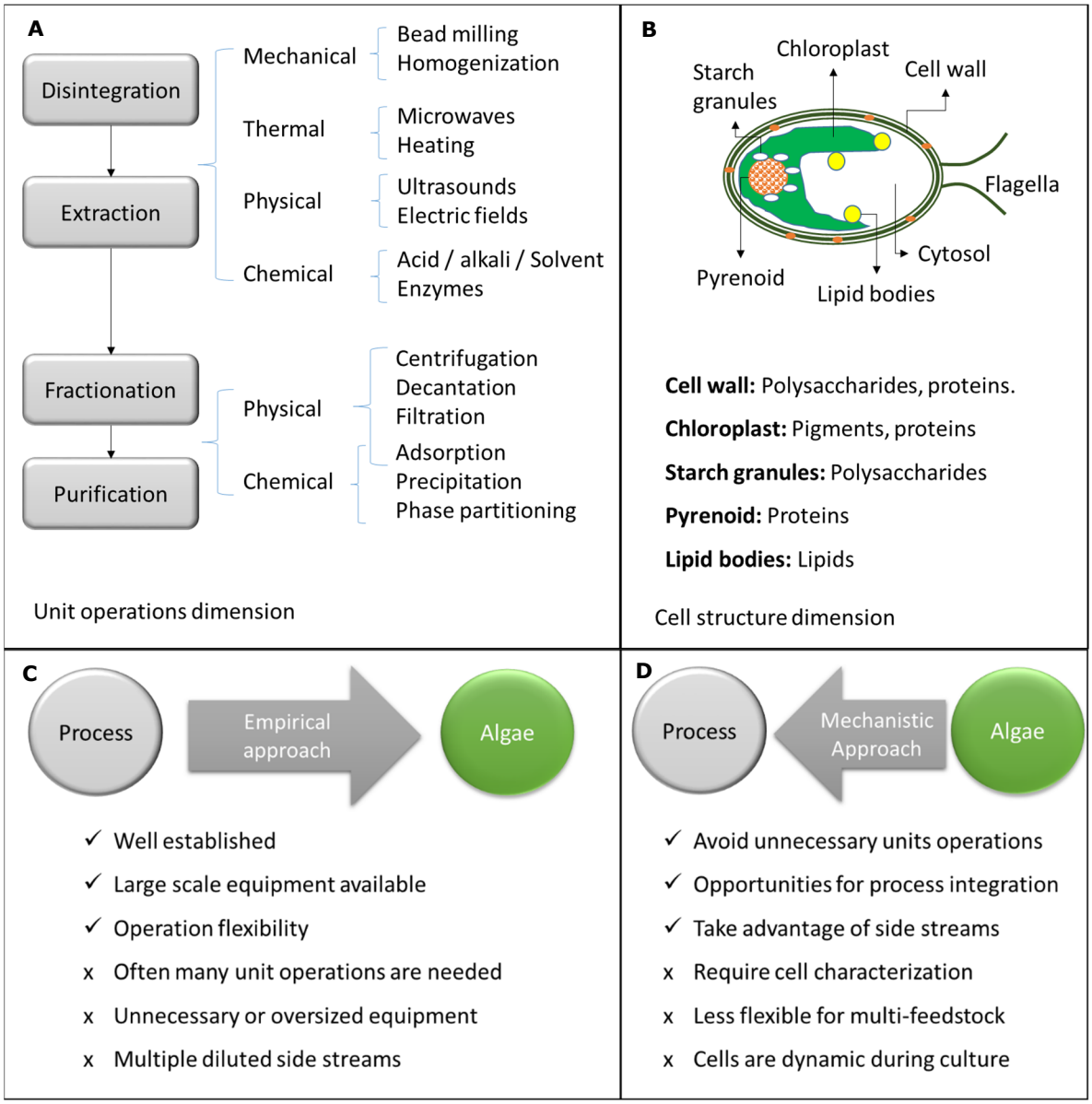

Figure 1. A. Unit operations dimension, showing an overview of typical process units used in algae biorefinery. **B.** Cell-structure dimension, with schematic representation of an algal cell and its composition. **C.** Empirical biorefinery approach: application of technologies. **D.** Proposed mechanistic approach based on the cell structure. Checkmarks and crosses refer to advantages and disadvantages of each approach.

Ultrasound and electric fields are external fields which generally result in low disintegration efficiencies and low extraction yields (’t Lam et al., 2017), which is due to the presence of a rigid polysaccharide-rich cell-wall in algae. Chemical and enzymatic

methods usually lead to high disintegration and extraction yields and lower energy consumptions (0.3 kWh kg_{DW}^{-1}, (Safi et al., 2017a; Sari et al., 2013)). However, the costs associated with the enzymes and chemicals are still prohibitive (Sari et al., 2015). Similarly, the use of ionic liquids as green solvents have shown promising results (chapters 7-8), but their high costs and toxicity (Brandt et al., 2013) prevent large scale applications.

In general, the high energy consumption observed with existing unit operations is due to the high water content of the algal suspensions, and the long processing times that are used. Most of the energy input is dissipated in the water medium. Moreover, most of the disintegration methods investigated so far are unspecific, don't take into consideration the cell-wall properties (chapter 3), and are based on the introduction of energy from an external source into the diluted cell suspension (empirical approach).

A second problem commonly observed with traditional mechanical disintegration unit operations is the excessive comminution (high shear-long times) which lead to stable oil-in-water emulsions (Huimin et al., 2014; Law et al., 2018) or Pickering emulsions (chapter 3, Tenorio et al., (2017)). As a consequence, the biomolecules are more difficult to separate and purify (Van Hee et al., 2004; Zinkoné et al., 2018).

Besides aqueous (Safi et al., 2014c) alkaline (Sari et al., 2015) and enzymatic extraction (Sari et al., 2013), ionic liquids (ILs) have been investigated for the direct dissolution of algal biomass (Fujita et al., 2013) and for the extraction of carbohydrates (Pezoa-Conte et al., 2015; Teixeira, 2012), lipids (Kim et al., 2012; Orr et al., 2016; Orr and Rehmann, 2016), pigments (Desai et al., 2016a)and proteins (Lee et al., 2017b). The main advantage of ILs is their vast chemical diversity, for which they are considered designer solvents, and the high extraction yields that can be achieved.

There are several drawbacks associated with ILs, including high costs (Brandt et al., 2013), potential toxicity (Ventura et al., 2017), high temperatures required for effective extraction (Teixeira, 2012), and difficult back-extraction (Mai et al., 2014). In this

regard, ILs from algal extracts are typically recovered using extraction followed by cenrifugation to remove the insoluble biomass and distillation to remove the excess solvent (Desai et al., 2016a; Orr et al., 2016), unit operations which are expensive and energy intensive. In chapter 7 and 8, it was demonstrated that ILs can be used for selective extraction under mild condition, and that ultrafiltration is a promising method for their recovery. This approach, however, is still undesirabe, as multiple filtration steps will be needed to guarantee that the ILs are completely recovered fom the extract.

The unit operations commonly applied for the separation and purification of algae biomolecules are isoelectric precipitation (Ba et al., 2016; Benelhadj et al., 2016; Cavonius et al., 2015; Chronakis, 2001; Gerde et al., 2013; Ursu et al., 2014), (ultra)filtration (chapter 4, 7-8, Lorente et al., 2018; Safi et al., 2014b; Ursu et al., 2014), aqueous two-phase partitioning (chapter 6,7, Suarez Ruiz et al., 2018) and sequences of unit operations (Chronakis, 2001; Schwenzfeier et al., 2011; Waghmare et al., 2016). Often, these methods are not specific for the cell structure of algae (Knoetzel et al., 1988; Schwenzfeier et al., 2014; Tamayo et al., 2018), target a single product (’t Lam et al., 2018) and follow the traditional sequence of unit operations (Fig. 1A), resulting in low yields/purities, undervalued side streams and high costs (’t Lam et al., 2018)

2.2. Cell-structure dimension

In Fig. 2A, a representation of the main structures of two model organisms is shown, the microalga *Tetraselmis suecica* (chapters 2-6,8) and the macroalga *Ulva lactuca* (chapter 7).

For microalgae three main structures are highlighted: cell-wall, chloroplast and pyrenoid. The cell-wall is mainly composed of polysaccharides, but also contains a small percentage of proteins and ash (Becker et al., 1998; Kermanshahi-pour et al., 2014). In the chloroplast the main metabolic functions take place. It is a complex cellular compartment rich in pigments, glyco- and phospholipids and proteins (Gibbs, 1962; Yang et al., 2017). Neutral lipids are usually accumulated in lipid bodies, which

also contain specific proteins (Goold et al., 2015). The pyrenoid is embedded in the chloroplast and surrounded, in green algae, by a starch sheath. The pyrenoid is densely packed with the enzyme rubisco (Meyer et al., 2017), which is important for carbon fixation.

Green macroalgae (chapter 7) are in general poor in lipids, contain low amounts of proteins and are rich in carbohydrates. The cell-wall contains an intricate arrangement of polysaccharides (cellullose, ulvan and β-glucans) in which proteins are embedded (Lahaye and Robic, 2007). The morphological differences among algal strains and their connection to fractionation methods has not been thoroughly considered as a basis for the biorefinery.

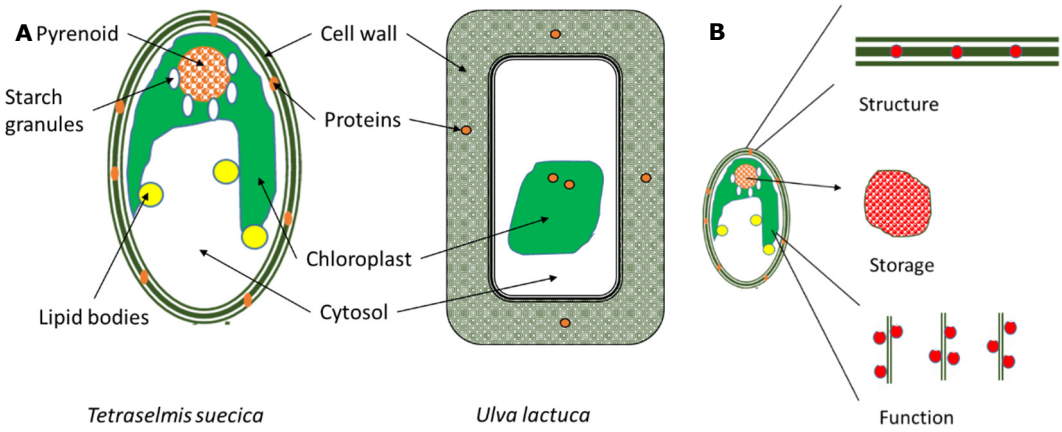

Figure 2. A. Representation of the main structures in micro and macroalgae. Two model strains are represented: *Tetraselmis suecica* (chapters 2-6,8) and *Ulva lactuca* (chapter 7). **B.** schematic view of three categories of algal biomolecules according to cell morphology and function.

Several studies have addressed the influence of cell-wall composition on the disintegration and extraction performance (Alhattab et al., 2018; Baudelet et al., 2017; Safi et al., 2014c; Wang and Lan, 2018). However, the fractionation and purification steps are rarely covered. Moreover, most investigations do not take into consideration the purity of the extracted molecules and mostly focus on yields and efficiencies. Purity is a key indicator as it provides a precise mass balance of the extracted biomolecules

and allows a more comprehensive evaluation of a biorefinery process (chapters 4-5, 8, Soto-Sierra et al., 2018).

In chapter 5 it was proposed that the low yields and purities of proteins extracted during aqueous bead milling can be explained by their function within the cells (Fig. 2B). Proteins present in the cytoplasm ("storage") are easily extracted upon cell disintegration, as they are water soluble and readily available. Other proteins, associated with membranes and organelles, have a more metabolic "function" and are often bound to lipids and pigments. A third group of proteins conduct a more "structural" role, for example, as part of the outer cell-wall and membranes. Proteins associated with membranes and pigments display a more hydrophilic nature, or are embedded in the cell-wall polysaccharides, and therefore they cannot be extracted in an aqueous medium by simple mechanical shear.

The categories storage, function and structure (Fig. 2B) also apply to other biomolecules. Lipids, for example, are mainly found in lipid bodies (storage) or membrane lipids (structure), depending on the algal strain and cultivation conditions. Similarly, carbohydrates usually play a structural (cell-wall) or storage role (starch granules). This categorization is important for the design of an optimal extraction-fractionation processes.

Because the biomolecules in algae are usually located in several structures within the cell, and are often interconnected or forming macromolecular complexes, the application of traditional unit operations lead to low yield and low purities. Tamayo et al., (2018) presented a complete overview of the yield-purity (Y-P) diagram for proteins extracted using a wide range of technologies. In their work aquatic biomass (including micro and macroalgae) and leaves were compared to crops and cereals (Fig. 3). The authors found that the Y-P curve for algae falls in the bottom left corner while that for crops is located in the upper-right corner.

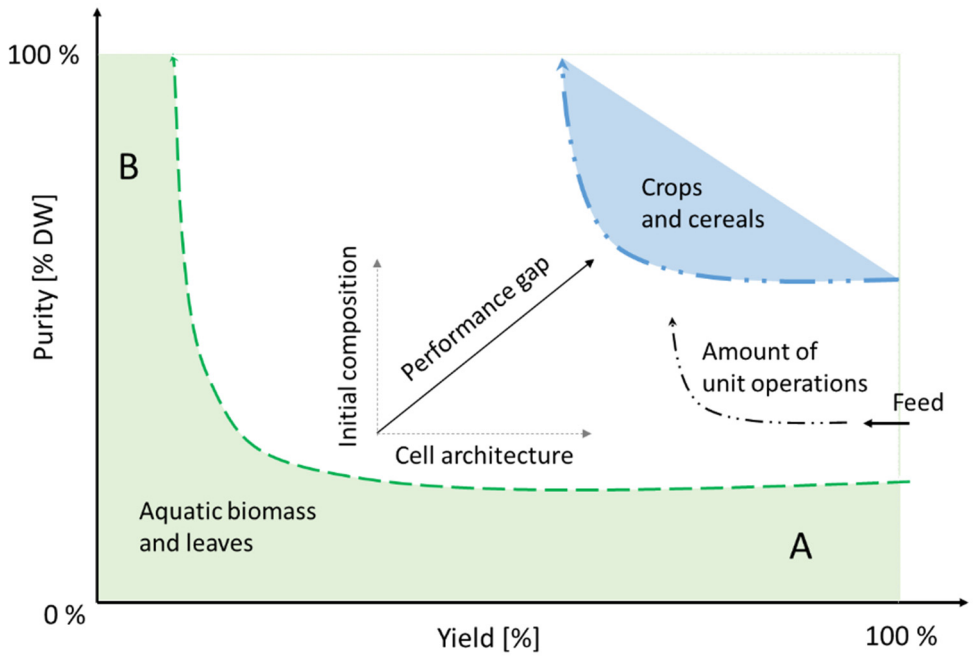

Figure 3. Yield-Purity diagram for protein extraction from aquatic biomass and crops. Area in green (bottom-left) and blue (top-right) correspond to data reported by Tamayo et al., (2018). A and B are opposing regions common in algae processing. The shape of the curve is dictated by the number of unit operations. The performance gap (difference in efficiency between the biorefinery of crops and that of aquatic biomass) is determined by two main factors: the initial protein concentration and cell architecture.

The performance gap (distance between Y-P curve for crops and algae, Fig. 3), can be explained by three main factors: initial composition, cell structure and unit operations. The initial composition is crucial, as it sets the start of the Y-P curve (feed in Fig 3). The amount of unit operations is defined by the target product application, which also sets the window of operation, and by the cell structure, which dictates how the biomolecules can be extracted (chapter 4-5).

Crops are usually located in the top-right region of the Y-P curve because of the high initial composition and simple structure: starch granules, lipid and/or protein bodies enclosed by a rigid shell. The fractionation can therefore be conducted in a few steps only by dry or wet processing (Berghout et al., 2014; Wang et al., 2004) and results in high yields and purities.

Methods reporting high yields of algal molecules (Ba et al., 2016; Cavonius et al., 2015; Safi et al., 2014c) are often unspecific and lead to the co-extraction of other biomolecules (high yield, low purity, few unit operations: Region A in Fig 3). On the opposite, high purities and low yields (Region B, Fig. 3) can be obtained after multiple unit operations and intensive processing (Chronakis, 2001; Schwenzfeier et al., 2011; Waghmare et al., 2016).

3. Towards a mechanistic approach in algae borefinery

Several examples from literature are presented in this next section, which illustrate the transition from empirical to a mechanistic biorefinery approach.

3.1. Design the right cell architecture

Cells can be genetically engineered to simplify the biorefinery process, reduce energy consumption or to enhance the fractionation performance (Spolaore et al., 2006). For example, mutant strains which overproduce and accumulate lipids have long been used to improve the economic feasibility of biofuel production (Breuer et al., 2014). Similarly, cyanobacteria strains have been transformed to overproduce proteins (Trautmann et al., 2016), leading to superior protein extraction yields and purities (Fig. 4A). Recently, 't Lam et al., (2017) reported that the extraction yield of proteins using pulsed electric fields (PEF) increased 4-fold at 0.05 kWh kg_{DW}^{-1} for a cell-wall deficient mutant of *C. reinhardtii* in comparison to the wild type (Fig 4A). Disadvantages of this approach include time and effort required to produce the mutants and the poor performance that the transformed strains could display during culture

3.2. Cell disintegration by lytic organisms, enzymes and selective chemicals

Traditional disintegration methods depend on the supply of energy from an external source, on expensive enzyme cocktails, or on chemicals which need to be back-extracted. Alternatively, several microorganisms (bacteria, algae, cyanobacteria and viruses), when co-cultured with algal cells, can secrete lytic enzymes which disrupt the cell-walls (Lenneman et al., 2014). This method is highly selective, mild and can be

performed in a single step. The main limitations are the effort required to select the right lytic organism, difficulties with the accurate control of the co-culture, and the time needed for complete cell disintegration

The use of lytic enzymes (Sari et al., 2013; Soto Sierra et al., 2017), chemical hydrolysis (Safi et al., 2017a), and cell-wall permeabilization with ILs (Fig. 4A-iii) (chapter 8, (Desai et al., 2016a)) are highly specific and energy efficient. However, chemical hydrolysis could lead to denaturation of sensitive molecules, enzymes and ILs can be costly (George et al., 2015), and additional separation steps are required to recover the ILs (chapter 7-8).

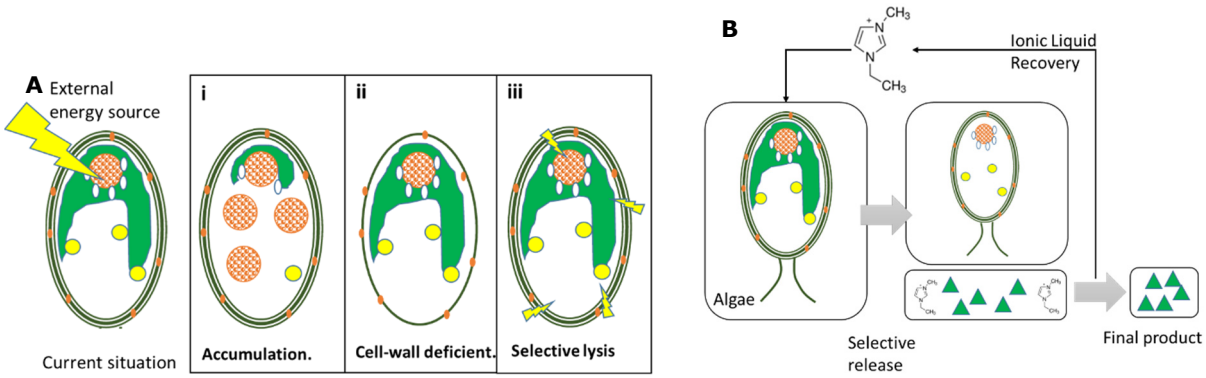

Figure 4. Novel approaches based on genetic transformation (i and ii) and selective lysis with microorganisms, enzymes and chemicals (iii). **B.** Conceptual representation of in situ extraction using ILs (chapter 8).

3.3. Demulsification

Excessive comminution during mechanical disintegration causes the formation of small cell debris which are highly stable in suspension and therefore difficult to fractionate (chapter 2-5, Zinkoné et al., 2018). Such stability can be broken (demulsification) by thermal processing and pH adjustment, and by the addition of medium-chain alcohols, electrolytes, free oils, enzymes, organic coagulants and air bubbles (Chabrand and Glatz, 2009; Luthy et al., 1978). The addition of external agents is disadvantageous as it implies additional operational costs.

Demulsification by means of external fields is another promising approach, as it avoids the use of auxiliary chemicals. Besides centrifugation (Law et al., 2018), ’t Lam et al., (2018) summarized several technologies including electric fields, ultrasounds and lasers. These unit operations have been demonstrated for the separation of oil fractions from algae, but could be potentially implemented in order to prevent emulsion formation during mechanical disintegration The main drawback of external fields is the additional capital expenditures required to generate the field through the extraction unit. Furthermore, because algae suspensions are normally diluted systems, high energy inputs could be necessary.

3.4. Membraneless osmosis

The main disadvantage of traditional aqueous two-phase systems (ATPS) is the utilization of external chemicals (organic solvents, polymers, salts, ionic liquids) which need to be back-extracted (chapter 7-8, Ventura et al., 2017). Alternatively, phase separation can be achieved without the need of external chemicals, a fractionation concept called membraneless osmosis (Antonov, 2000).

The phenomena behind phase separation in membraneless osmosis is based on the differences in the chemical potential of molecules present in the mixture (Antonov et al., 1982). Proteins are separated from sugars in a similar way as the salting-out phenomena in salt-rich solutions, therefore the term sugaring-out has been used (Sankaran et al., 2018a). Once in solution, proteins and polysaccharides are separated into two distinct phases and the water molecules migrate, across the interphase, towards the more hydrophilic solution. In overall, the more hydrophobic phase (protein-rich) is concentrated while the polysaccharide-rich phase is diluted (Antonov et al., 1982).

This principle has been proven for colloidal-dispersed systems such as skimmed milk, blood plasma, microbial broths, plant-based extracts and chloroplasts (Antonov, 2000). Membraneless osmosis can be conducted at room temperature and phase formation takes place rapidly (within seconds) regardless of the system volume. Besides, the

separation-concentration performance and the energy consumption are greatly improved compared to other methods, without adding chemically based polymers or salts (Antonov, 2000).

3.5. Ionic liquid recovery

IL recovery can be accomplished by making use of their physicochemical and thermophysical properties. Du et al., (2017) reported a process to extract lipids from microalgae using switchable ILs. The IL was recovered by switching the solvent hydrophilicity using CO_2. A second interesting approach is to induce phase changes by means of temperature variations. Several thermo-morphic ILs have been reported with critical temperatures ranging from - 40 to 157^{o}C (Qiao et al., 2017). For example, distillable ILs can be removed by evaporation at 45^{o}C (Song et al., 2018), a temperature which could still be considered mild. In recent years, a new type of ILs was proposed as novel platform in green chemistry: sponge-like ILs (Lozano et al., 2015). The solid-liquid phase of these ILs can be manipulated by centrifugation and cooling from room temperature to 4^{o}C.

3.6. Multi-product biorefinery and functionality

The market potential of algal products can become an important driver in algae biorefinery. The works by ’t Lam et al., (2018), Gifuni et al., (2018), Khanra et al., (2018), Koller et al., (2014) and Soto-Sierra et al., (2018) already show a general trend towards multiproducts, functionality and economic revenues. In chapters 4-5 it was also proposed that new biorefineries should be developed from the functional properties and applications of the extracted fractions, rather than on their purity.

3.7. Process integration

Many authors have investigated sequences of unit operations to purify biomolecules from algae (Chronakis, 2001; Kadam et al., 2016; Schwenzfeier et al., 2011; Waghmare et al., 2016; Wong and Cheung, 2001), often resulting in low yields and purities (regions A and B of Fig. 3). Recent reviews have also proposed sequences of unit operations, but with a more clear mechanistic approach. Dixon and Wilken, (2018), Gifuni et al.,

(2018), Soto-Sierra et al., (2018) and Khanra et al., (2018) proposed cascades of extractions based on the composition of the biomass and on the value of the target molecules and their potential market application.

Mild and highly specific methods are preferred, so the extraction steps do not compromise the functionality of the molecules in later stages of the refining process (Dixon and Wilken, 2018; Gifuni et al., 2018). The overall extraction yields can be optimized by selecting the order of biomolecule extraction (Ansari et al., 2017) and by fully utilizing the side products (Gifuni et al., 2018; Tamayo et al., 2018).

Besides the traditional cascade of extractions, process integration has not been explored sufficiently. Only few reports have presented integration alternatives for cultivation-harvesting and harvesting-disintegration (’t Lam et al., 2018). In Table 1, an overview of reported integration concepts for the steps of extraction and fractionations are presented.

Table 1. Overview of reported process integration for extraction-fractionation of algal biomolecules.

Technology	Target	Reference
IL-assisted bead milling and two-phase partitioning	Proteins	Chapter 7
In situ selective extraction with ILs	Proteins	Chapter 8
Sugaring-out biphasic flotation + ultrasounds	Proteins	(Sankaran et al., 2018b)
Alkali-assisted ultrasound	Proteins	(Phong et al., 2018a)
IL-assisted ultrasound	Proteins	(Lee et al., 2017b)
Ultrasound and two-phase partitioning	Proteins	(Phong et al., 2017)
Extraction and transesterification	Lipids	(Salam et al., 2016)
IL-assisted microwave transesterification	Lipids	(Wahidin et al., 2016)
Enzyme assisted alkaline solubilisation	Proteins	(Sari et al., 2013)
Bead milling and two-phase partitioning	Proteins	(Cisneros and Rito-Palomares, 2004)

As can be seen, most of the reports combine a cell disintegration method under the presence of an agent (enzymes, ILs, salts, polymers) which favours extraction and/or allows two-phase fractionation. This is the same approach investigated in chapter 7 (IL-assisted bead milling) and chapter 8 (Fig. 4B, in situ extraction).

Although these processes result in high performances and low energy consumption, they still rely on external chemicals or additional unit operations, ultimately resembling the typical biorefinery chain. Future research must be directed towards auxiliary-free simplified systems, which make use of the cells' biochemical properties to self-separate.

4. Future directions: biorefinery intensification

We have highlighted several challenges in algae biorefinery (section 2) and various potential solutions through innovative concepts reported in literature (section 3). In this section we expand these ideas and present three approaches which may contribute towards intensification of algae biorefineries: self-disintegration, simultaneous disintegration and disentanglement, and self-separation.

4.1. Self-disintegration

Genetic manipulations can be conducted to engineer strains which self-disintegrate at the end of the cultivation period. This would allow cultivation, disintegration and potentially harvesting to be conducted in singe step. In addition, it will guarantee minimum energy consumption and high specificity, without the need of auxiliary chemical or unit operations.

4.2. Simultaneous disruption and disentanglement

At the end of the cultivation period, algae can be cultured with microorganisms which can produce the specific enzymes required for disintegration and disentanglement, in such a way that several products can be solubilized sequentially from the biomass in a single unit operation (Fig. 5). Such process would be mild, highly selective and energy efficient, requiring simple intermediate washing steps to the recover the soluble products. This approach, however, requires extensive screening of microorganisms

which can disentangle different cell structures (e.g., cell-walls, chloroplast, pyrenoid, membranes), and can be disadvantageous in terms of process flexibility, as the hydrolytic enzymes will be selective only towards certain algal strains.

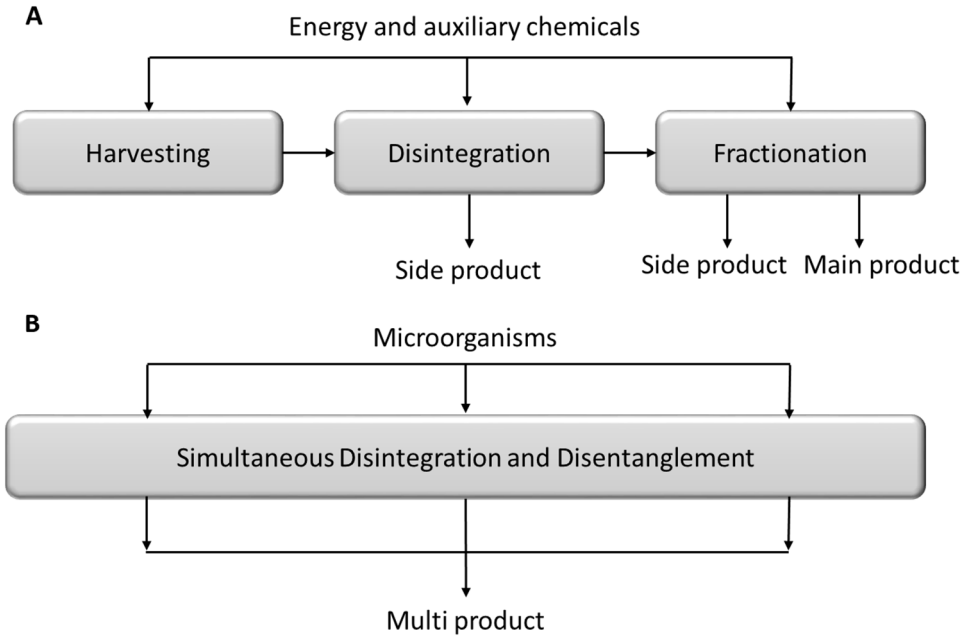

Figure 5. Typical biorefinery chain (A) in comparison to simultaneous disintegration and disentanglement (B).

4.3. *Self-separating systems*

In this approach, the polysaccharides and proteins present in algae could be used to induce their thermodynamic incompatibility, leading to the formation of two phase in which proteins and carbohydrates are fractionated. In order to achieve this, after harvesting and cell disruption, the mixture of suspended molecules is mixed with "seed" molecules in order to trigger phase splitting. After phase-separation, a portion of the separated molecules are recycled to the extraction in order to keep system under continuous operation (Fig 6A).

In order to achieve self-separation, the algae suspension after cell disintegration must contain the right type of molecules, above a critical concentration necessary for two-phase formation. Antonov, (2000) presented an overview of phase diagrams for protein-polysaccharide pairs, among which pectin and rubisco (ribulose-1,5-

bisphosphate carboxylase/oxygenase). Certain algal strains are rich in pectin-like polysaccharides (Domozych et al., 2012; Kermanshahi-pour et al., 2014), while rubisco is one of the most abundant proteins in algae. Pectin-like polysaccharides from the cell wall of *T. suecica* can reach approximately 2-5 wt% (DW) of the total biomass (Kermanshahi-pour et al., 2014; Scholz et al., 2014). Regarding rubisco, the content for green algae is ~ 3 mg $mg_{Chlorophyl}^{-1}$ (Yokota and Canvin, 1985). Since green algae contain around 2 wt% chlorophyll, the expected total content of rubisco is ~ 5 wt % (DW).

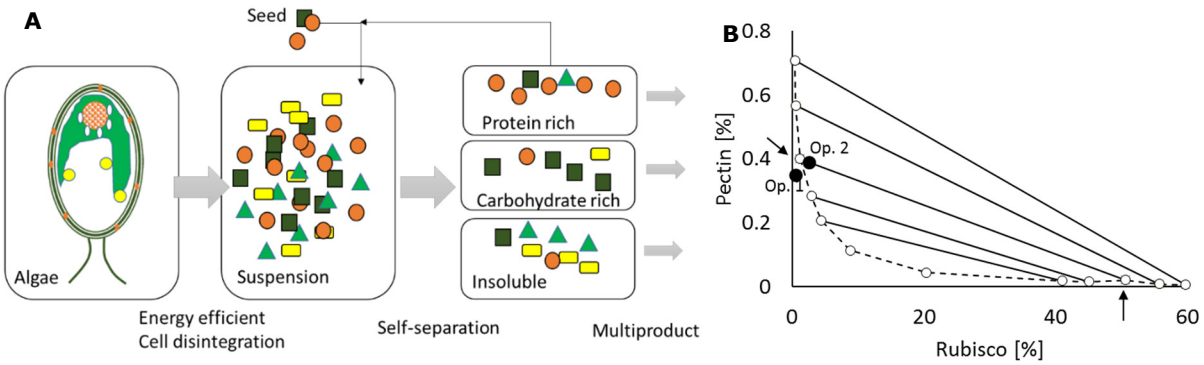

Figure 6. A. Schematic representation of self-separating systems using membraneless osmosis. **B.** Binodal curve (empty markers) and tie lines (solid lines) for the system Rubisco-Pectin (Antonov, 2000). Filled markers are hypothetical operation points (Op1: After cell disintegration; Op2: after addition of "seed" biomolecules). Arrows point out the composition of top and bottom phases after phase splitting.

For an algal suspension containing 10 wt% biomass (chapter 2, 4-5), the concentration of pectin polysaccharides and rubisco in suspension after bead milling will be 0.35 % and 0.5 %, respectively. Under these conditions, the system theoretically will remain in the single-phase region (Op1, Fig. 6B). It is necessary to add an extra amount of biomolecules ("seed", Fig. 6A) to reach a concentration of 0.4 % polysaccharides and 2-2.5 % proteins (Op2, Fig. 6B), where the system will form two-phases. In this point, the bottom phase will contain nearly 50 % of proteins and the upper phase will contain close to 0.4 % polysaccharides (Fig. 6B). A fraction of the protein-rich phase can then be recycled back in the system for the next fractionation cycle (Fig. 6), which can be conducted by common operation such as acidification and ultrafiltration.

Despite the evident advantages of this method, significant research is needed in order to understand the complex interaction of biomolecules in suspension and their thermodynamic incompatibility, and the effect of other proteins and sugars present in the system. In addition, since the phase diagram is a fingerprint for every polysaccharide-protein pair, a new binodal curve will be required for every algal strain under consideration

5. Concluding remarks

Recent publications have addressed key elements in the field of algae biorefinery which need to be taken into consideration in future research and commercial developments. However, other crucial aspects are often overlooked. Algae biorefinery must start from the understanding of the cell structure and composition, and must include the complete spectrum of potential market applications, as a basis for process design. The cascade of separation steps must prioritize high value products and mild processing. Beyond a mere sequence of unit operations, process intensification should receive more attention. Emphasis should be given to self-disintegration and self-separating systems, mild and in situ selective disentanglement, and process intensification, as they guarantee minimum energy consumption, chemicals-free separations and minimum processing.

Acknowledgements

This project is financed by the Dutch Technology Foundation STW under the project AlgaePro4You, nr. 12635. From January 2017, STW continued its activities as NWO (Dutch national science foundation) Applied and Engineering Sciences (TTW).

References

‘t Lam, G.P., van der Kolk, J.A., Chordia, A., Vermuë, M.H., Olivieri, G., Eppink, M.H.M., Wijffels, R.H., 2017. Mild and Selective Protein Release of Cell Wall Deficient Microalgae with Pulsed Electric Field. ACS Sustain. Chem. Eng. 5, 6046–6053.

’t Lam, G.P., Postma, P.R., Fernandes, D.A., Timmermans, R.A.H., Vermuë, M.H., Barbosa, M.J., Eppink, M.H.M., Wijffels, R.H., Olivieri, G., 2017. Pulsed Electric Field for protein release of the microalgae Chlorella vulgaris and Neochloris oleoabundans. Algal Res. 24, 181–187.

’t Lam, G.P., Vermuë, M.H., Eppink, M.H.M., Wijffels, R.H., van den Berg, C., 2018. Multi-Product Microalgae Biorefineries: From Concept Towards Reality. Trends Biotechnol. 36, 216–227.

(FAO), F. and A.O. of the U.N., 2001. Food balance sheets, WHO regional publications. European series.

Abiusi, F., Sampietro, G., Marturano, G., Biondi, N., Rodolfi, L., Ottavio, M.D., Tredici, M.R., 2014. Growth , Photosynthetic Efficiency , and Biochemical Composition of Tetraselmis suecica F & M-M33 Grown With LEDs of Different Colors 111, 956–964.

Abo-Shady, A.M., Mohamed, Y.A., Lasheen, T., 1993. Chemical composition of the cell wall in some green algae species. Biol. Plant. 35, 629–632.

Abu Hajar, H.A., Riefler, R.G., Stuart, B.J., 2017. Cultivation of the microalga Neochloris oleoabundans for biofuels production and other industrial applications (a review). Appl. Biochem. Microbiol. 53, 640–653.

Acién, F.G., Fernández, J.M., Magán, J.J., Molina, E., 2012. Production cost of a real microalgae production plant and strategies to reduce it. Biotechnol. Adv. 30, 1344–1353.

Adarme-vega, T.C., Lim, D.K.Y., Timmins, M., Vernen, F., Li, Y., Schenk, P.M., 2012. Microalgal biofactories : a promising approach towards sustainable omega-3 fatty acid production. Microb. Cell Fact. 11, 1.

Alexandratos, N., Bruinsma, J., 2012. WORLD AGRICULTURE TOWARDS 2030 / 2050 The 2012 Revision.

Alhattab, M., Kermanshahi-Pour, A., Brooks, M.S.L., 2018. Microalgae disruption techniques for product recovery: influence of cell wall composition. J. Appl. Phycol. 1, 1–28.

Amano, H., Noda, H., 1992. Proteins of Protoplasts from Several Seaweeds. Nippon Suisan Gakkaishi 58, 291–299.

Ansari, F.A., Shriwastav, A., Gupta, S.K., Rawat, I., Bux, F., 2017. Exploration of Microalgae Biorefinery by Optimizing Sequential Extraction of Major Metabolites from Scenedesmus obliquus. Ind. Eng. Chem. Res. 56, 3407–3412.

Antonov, Y., Grinberg, Y.., Zhuravskaya, N.., Tolstoguzov, V.., 1982. The concentration of the proteins from skimmed milk by membraneless isobaric osmosis. Carbohydrates Polym. 2, 81–90.

Antonov, Y.A., 2000. Use of Membraneless Osmosis for Concentration of Proteins from Molecular-Dispersed and Colloidal-Dispersed Solutions (Review). Appl. Biochem. Microbiol. 36, 325–337.

Asghari, A.K., Norton, I., Mills, T., Sadd, P., Spyropoulos, F., 2015. Interfacial and foaming characterisation of mixed protein-starch particle systems for food-foam applications. Food Hydrocoll. 53, 311–319.

Atkins, P., Paula, J., 2006. Physical Chemistry, 8th ed. Oxford University Press.

Austin, L., 1973. Understanding ball mill sizing. Ind. Eng. Chem. Process Des. … 12, 121–129.

Ba, F., Violeta, A., Laroche, C., Djelveh, G., 2016. Haematococcus pluvialis soluble proteins : Extraction , characterization , concentration / fractionation and emulsifying properties. Bioresour. Technol. 200, 147–152.

Balasundaram, B., Skill, S.C., Llewellyn, C.A., 2012. A low energy process for the recovery of bioproducts from cyanobacteria using a ball mill 69, 48–56.

Banerjee, S., Bhattacharya, S., 2012. Critical Reviews in Food Science and Nutrition Food Gels: Gelling Process and New Applications Food Gels: Gelling Process and New Applications. Crit. Rev. Food Sci. Nutr. 52, 334–346.

Barbarino, E., Lourenço, S.O., 2005. An evaluation of methods for extraction and quantification of protein from marine macro- and microalgae. J. Appl. Phycol. 17, 447–460.

Barron, J.M., Twibell, R.G., Hill, H.A., Hanson, K.C., Gannam, A.L., 2016. Development of diets for the intensive culture of Pacific lamprey. Aquac. Res. 47, 3899–3906.

Batista, A.P., Nunes, M.C., Fradinho, P., Gouveia, L., Sousa, I., Raymundo, A., Franco, J.M., 2012. Novel foods with microalgal ingredients - Effect of gel setting conditions on the linear viscoelasticity of Spirulina and Haematococcus gels. J. Food Eng. 110, 182–189.

Baudelet, P.H., Ricochon, G., Linder, M., Muniglia, L., 2017. A new insight into cell walls of Chlorophyta. Algal Res. 25, 333–371.

Becker, B., Melkonian, M., Kamerling, J.P., 1998. The cell wall (theca) of Tetraselmis striata (Chlorophyta): Macromolecular composition and structural elements of the complex polysaccharides. J. Phycol. 34, 779–787.

Becker, E.W., 2007. Micro-algae as a source of protein. Biotechnol. Adv. 25, 207–210.

Becker, M., Kwade, A., Schwedes, J., 2001. Stress intensity in stirred media mills and its effect on specific energy requirement. Int. J. Miner. Process. 61, 189–208.

Behera, S., Singh, R., Arora, R., Sharma, N.K., Shukla, M., Kumar, S., 2015. Scope of Algae as Third Generation Biofuels. Front. Bioeng. Biotechnol. 2, 1–13.

Beinert, S., Fragnière, G., Schilde, C., Kwade, A., 2015. Analysis and modelling of bead contacts in wet-operating stirred media and planetary ball mills with CFD-DEM simulations. Chem. Eng. Sci. 134, 648–662.

Benavides, J., Rito-Palomares, M., 2006. Simplified two-stage method to B-phycoerythrin recovery from Porphyridium cruentum. J. Chromatogr. B Anal. Technol. Biomed. Life Sci. 844, 39–44.

Benelhadj, S., Gharsallaoui, A., Degraeve, P., Attia, H., Ghorbel, D., 2016. Effect of pH on the functional properties of Arthrospira (Spirulina) platensis protein isolate. Food Chem. 194, 1056–1063.

Berges, J.A., Fisher, A.E., Harrison, P.J., 1993. A comparison of Lowry, Bradford and Smith protein using different protein standards and protein isolated from the marine diatom Thalassiosira pseudonana. Mar. Biol. 115, 187–193.

Berghout, J.A.M., Boom, R.M., Van Der Goot, A.J., 2014. The potential of aqueous fractionation of lupin seeds for high-protein foods. Food Chem. 159, 64–70.

Berry, J.D., Neeson, M.J., Dagastine, R.R., Chan, D.Y.C., Tabor, R.F., 2015. Measurement of surface and interfacial tension using pendant drop tensiometry. J. Colloid Interface Sci. 454, 226–237.

Berry, T.K., Yang, X., Foegeding, E.A., 2009. Foams prepared from whey protein isolate and egg white protein: 2. Changes associated with angel food cake functionality. J. Food Sci. 74, E269–E277.

Bharathiraja, B., Chakravarthy, M., Ranjith Kumar, R., Yogendran, D., Yuvaraj, D., Jayamuthunagai, J., Praveen Kumar, R., Palani, S., 2015. Aquatic biomass (algae) as a future feed stock for bio-refineries: A review on cultivation, processing and products. Renew. Sustain. Energy Rev. 47, 635–653.

Bikker, P., van Krimpen, M.M., van Wikselaar, P., Houweling-Tan, B., Scaccia, N., van Hal, J.W., Huijgen, W.J.J., Cone, J.W., López-Contreras, A.M., 2016. Biorefinery of the green seaweed Ulva lactuca to produce animal feed, chemicals and biofuels. J. Appl. Phycol. 28, 3511–3525.

Bird, R.B., Stewart, W.E., Lightfoot, E.N., 2002. Transport Phenomena, 2nd ed. John Wiley & Sons.

Bleakley, S., Hayes, M., 2017. Algal Proteins: Extraction, Application, and Challenges Concerning Production. Foods 6, 33.

Blecher, L., Kwade, A., Schwedes, J., 1996. Motion and stress intensity of grinding beads in a stirred media mill. Part 1 : Energy density distribution and motion of single grinding beads. Powder Technol. 86, 59–68.

Boaglio, A., Bassani, G., Picó, G., Nerli, B., 2006. Features of the milk whey protein partitioning in polyethyleneglycol-sodium citrate aqueous two-phase systems with the goal of isolating human alpha-1 antitrypsin expressed in bovine milk. J. Chromatogr. B Anal. Technol. Biomed. Life Sci. 837, 18–23.

Bradford, M.M., 1976. A rapid and sensitive method for the quantitation of microgram quantities of protein utilizing the principle of protein-dye binding. Anal. Biochem. 72, 248–254.

Brandt-Talbot, A., Gschwend, F.J.V., Fennell, P.S., Lammens, T.M., Tan, B., Weale, J., Hallett, J.P., 2017. An economically viable ionic liquid for the fractionation of lignocellulosic biomass. Green Chem. 19, 3078–3102.

Brandt, A., Gräsvik, J., Hallett, J.P., Welton, T., 2013. Deconstruction of lignocellulosic biomass with ionic liquids. Green Chem. 15, 550–583.

Breuer, G., Jaeger, L. De, Artus, V.P.G., Martens, D.E., Springer, J., Draaisma, R.B., Eggink, G., Wijffels, R.H., Lamers, P.P., 2014. Superior triacylglycerol (TAG) accumulation in starchless mutants of Scenedesmus obliquus : (II) evaluation of TAG yield and productivity in controlled photobioreactors. Biotechnol. Biofuels 7, 1–11.

Brookman, J., 1974. Mechanism of cell disintegration in a high pressure homogenizer. Biotechnol. Bioeng. 16, 371–383.

Brown, M.R., 1991. The amino-acid and sugar composition of 16 species of microalgae used in mariculture 145, 79–99.

Bunge, F., Pietzsch, M., Müller, R., Syldatk, C., 1992. Mechanical disruption of Arthrobacter sp. DSM 3747 in stirred ball mills for the release of hydantoin-cleaving enzymes. Chem. Eng. Sci. 47, 225–232.

Cabanelas, I.T.D., Van Der Zwart, M., Kleinegris, D.M.M., Wijffels, R.H., Barbosa, M.J., 2016. Sorting cells of the microalga Chlorococcum littorale with increased triacylglycerol productivity. Biotechnol. Biofuels 9, 1–12.

Cavonius, L.R., Albers, E., Undeland, I., 2015. pH-shift processing of Nannochloropsis oculata microalgal biomass to obtain a protein-enriched food or feed ingredient. Algal Res. 11, 95–102.

CCAP, (Culture Collection of Algae and Protozoa), 2015. Bold's Basal Medium (BB).

Cha, K.H., Koo, S.Y., Song, D.G., Pan, C.H., 2012. Effect of microfluidization on bioaccessibility of carotenoids from chlorella ellipsoidea during simulated digestion. J. Agric. Food Chem. 60, 9437–9442.

Chabrand, R.M., Glatz, C.E., 2009. Destabilization of the emulsion formed during the enzyme-assisted aqueous extraction of oil from soybean flour. Enzyme Microb. Technol. 45, 28–35.

Chan, C.X., Ho, C.L., Phang, S.M., 2006. Trends in seaweed research. Trends Plant Sci. 11, 165–166.

Chronakis, I.S., 2001. Gelation of edible blue-green algae protein isolate (Spirulina platensis strain Pacifica): Thermal transitions, rheological properties, and molecular forces involved. J. Agric. Food Chem. 49, 888–898.

Chronakis, I.S., Galatanu, A.N., Nylander, T., Lindman, B., 2000. The behaviour of protein preparations from blue-green algae (Spirulina platensis strain Pacifica) at the air/water interface. Colloids Surfaces A Physicochem. Eng. Asp. 173, 181–192.

Chung, I.K., Beardall, J., Mehta, S., Sahoo, D., Stojkovic, S., 2011. Using marine macroalgae for carbon sequestration: A critical appraisal. J. Appl. Phycol. 23, 877–886.

Cisneros, M., Rito-Palomares, M., 2004. A simplified strategy for the release and primary recovery of c-phycocyanin produced by Spirulina maxima. Chem. Biochem. Eng. Q. 18, 385–390.

Coons, J.E., Kalb, D.M., Dale, T., Marrone, B.L., 2014. Getting to low-cost algal biofuels: A monograph on conventional and cutting-edge harvesting and extraction technologies. Algal Res. 6, 250–270.

Cuellar-Bermudez, S.P., Aguilar-Hernandez, I., Cardenas-Chavez, D.L., Ornelas-Soto, N., Romero-Ogawa, M.A., Parra-Saldivar, R., 2015. Extraction and purification of high-value metabolites from microalgae: Essential lipids, astaxanthin and phycobiliproteins. Microb. Biotechnol. 8, 190–209.

De Pádua, M., Growoski Fontoura, P.S., Mathias, A.L., 2004. Chemical composition of Ulvaria oxysperma (Kützing) bliding, Ulva lactuca (Linnaeus) and Ulva fascita (Delile). Brazilian Arch. Biol. Technol. 47, 49–55.

de Winter, L., Klok, A.J., Cuaresma Franco, M., Barbosa, M.J., Wijffels, R.H., 2013. The synchronized cell cycle of Neochloris oleoabundans and its influence on biomass composition under constant light conditions. Algal Res. 2, 313–320.

Denes, F., Lang, P., 2006. Liquid – Liquid – Liquid Equilibrium. Symp. A Q. J. Mod. Foreign Lit. 877–890.

Dennison, C., Lovrien, R., 1997. Three phase partitioning: Concentration and purification of proteins. Protein Expr. Purif. 11, 149–161.

Desai, R.K., Streefland, M., Wijffels, R.H., Eppink, M.H.M., 2016a. Novel astaxanthin extraction from Haematococcus pluvialis using cell permeabilising ionic liquids. Green Chem. 18, 1261–1267.

Desai, R.K., Streefland, M., Wijffels, R.H., H. M. Eppink, M., 2016b. Extraction of Proteins with ABS, in: Ionic-Liquid- Based Aqueous Biphasic Systems. pp. 123–134.

Desai, R.K., Streefland, M., Wijffels, R.H., H. M. Eppink, M., 2014. Extraction and stability of selected proteins in ionic liquid based aqueous two phase systems. Green Chem. 16, 2670.

Diamond, A.D., Hsu, J.T., 1990. Protein partitioning in PEG/dextran aqueous two-phase systems. AIChE J. 36, 1017–1024.

Dickinson, E., 2010. Food emulsions and foams: Stabilization by particles. Curr. Opin. Colloid Interface Sci. 15, 40–49.

Dimitrova, T.D., Leal-Calderon, F., 2001. Bulk elasticity of concentrated protein-stabilized emulsions. Langmuir 17, 3235–3244.

Dissanayake, M., Kelly, A.L., Vasiljevic, T., 2010. Gelling properties of microparticulated whey proteins. J. Agric. Food Chem. 58, 6825–6832.

Dixon, C., Wilken, L.R., 2018. Green microalgae biomolecule separations and recovery. Bioresour. Bioprocess. 5.

Dogonchi, A.S., Hatami, M., Domairry, G., 2015. Motion analysis of a spherical solid particle in plane Couette Newtonian fluid flow. Powder Technol. 274, 186–192.

Domozych, D.S., Ciancia, M., Fangel, J.U., Mikkelsen, M.D., Ulvskov, P., Willats, W.G.T., 2012. The Cell Walls of Green Algae: A Journey through Evolution and Diversity. Front. Plant Sci. 3, 1–7.

Doucha, J., Lívanský, K., 2008. Influence of processing parameters on disintegration of Chlorella cells in various types of homogenizers. Appl. Microbiol. Biotechnol. 81, 431–440.

Draaisma, R.B., Wijffels, R.H., Slegers, P.M., Brentner, L.B., Roy, A., Barbosa, M.J., 2013. Food commodities from microalgae. Curr. Opin. Biotechnol. 24, 169–177.

Dreyer, S., Salim, P., Kragl, U., 2009. Driving forces of protein partitioning in an ionic liquid-based aqueous two-phase system. Biochem. Eng. J. 46, 176–185.

Du, Y., Schuur, B., Brilman, D.W.F., 2017. Maximizing Lipid Yield in Neochloris oleoabundans Algae Extraction by Stressing and Using Multiple Extraction Stages with N ‐ Ethylbutylamine as Switchable Solvent. Ind. Eng. Chem. Res. 56, 8073–8080.

Du, Z., Yu, Y.L., Wang, J.H., 2007. Extraction of proteins from biological fluids by use of an ionic liquid/aqueous two-phase system. Chem. - A Eur. J. 13, 2130–2137.

Dubois, M., Gilles, K.A., Hamilton, J.K., Rebers, P.A., Smith, F., 1956. Colorimetric Method for Determination of Sugars and Related Substances. Anal. Chem. 28, 350–356.

EC, 2018. Report from the commission on the council and the european parliament.

Emre, G., Els, D.H., Michel, E., Kathy, E., Rene, W., 2016. Influence of nitrogen depletion in the growth of N. oleoabundans on the release of cellular components after beadmilling. Bioresour. Technol.

Enzing, C., Ploeg, M., Barbosa, M., Sijtsma, L., 2014. Microalgae-based products for the food and feed sector: an outlook for Europe, JRC Scientific and Policy Reports. European Comission.

Eppink, M.H.M., Olivieri, G., Reith, H., Berg, C. Van Den, Barbosa, M.J., Wijffels, R.H., 2017. From Current Algae Products to Future Biorefinery Practices : A Review, in: Adv Biochem Eng Biotechnolhnol.

FAO, 2013. Food Supply - Livestock and Fish Primary Equivalent [WWW Document]. FAOSTAT.

Fleurence, J., 1999. Seaweed proteins: Biochemical, nutritional aspects and potential uses. Trends Food Sci. Technol. 10, 25–28.

Fleurence, J., Le Coeur, C., Mabeau, S., Maurice, M., Landrein, A., 1995. Comparison of different extractive procedures for proteins from the edible seaweeds Ulva rigida and Ulva rotundata. J. Appl. Phycol. 7, 577–582.

Folch, J., Lees, M., Sloane, G.H., Al., E., 1957. A simple method for the isolation and purification of total lipides from animal tissues. J. Biol. Chem 226, 497–509.

Fujita, K., Kobayashi, D., Nakamura, N., Ohno, H., 2013. Direct dissolution of wet and saliferous marine microalgae by polar ionic liquids without heating. Enzyme Microb. Technol. 52, 199–202.

Galland-Irmouli, A.V., Fleurence, J., Lamghari, R., Luçon, M., Rouxel, C., Barbaroux, O., Bronowicki, J.P., Villaume, C., Guéant, J.L., 1999. Nutritional value of proteins from edible seaweed Palmaria palmata (Dulse). J. Nutr. Biochem. 10, 353–359.

Garcia, S., Van Leeuwen, J.J.A., Safi, C., Sijtsma, L., Van Den Broek, L.A.M., Eppink, M.H.M., Wijffels, R.H., Van Den Berg, C., 2018. Techno-Functional Properties of Crude Extracts from the Green Microalga Tetraselmis suecica. J. Agric. Food Chem. 66, 7831–7838.

Geankoplis, C.J., 1993. Transport Processes and Unit Operation, 3rd ed. Prentice Hall.

George, A., Brandt, A., Tran, K., Zahari, S.M.S.N.S., Klein-Marcuschamer, D., Sun, N., Sathitsuksanoh, N., Shi, J., Stavila, V., Parthasarathi, R., Singh, S., Holmes, B.M., Welton, T., Simmons, B.A., Hallett, J.P., 2015. Design of low-cost ionic liquids for lignocellulosic biomass pretreatment. Green Chem. 17, 1728–1734.

Gerde, J.A., Wang, T., Yao, L., Jung, S., Johnson, L.A., Lamsal, B., 2013. Optimizing protein isolation from defatted and non-defatted Nannochloropsis microalgae biomass. ALGAL 2, 145–153.

Geresh, S., Mamontov, A., Weinstein, J., 2002. Sulfation of extracellular polysaccharides of red microalgae: Preparation, characterization and properties. J. Biochem. Biophys. Methods 50, 179–187.

Gers, R., Climent, E., Legendre, D., Anne-Archard, D., Frances, C., 2010. Numerical modelling of grinding in a stirred media mill: Hydrodynamics and collision characteristics. Chem. Eng. Sci. 65, 2052–2064.

Ghadiryanfar, M., Rosentrater, K.A., Keyhani, A., Omid, M., 2016. A review of macroalgae production , with potential applications in biofuels and bioenergy. Renew. Sustain. Energy Rev. 54,

473–481.

Gibbs, S.P., 1962. The ultrastructure of the chloroplasts of algae. J. Ultrasructure Res. 7, 418–435.

Gifuni, I., Pollio, A., Safi, C., Marzocchella, A., Olivieri, G., 2018. Current Bottlenecks and Challenges of the Microalgal Biorefinery. Trends Biotechnol. xx, 1–11.

Ginneken, V. Van, Vries, E. De, 2018. Seaweeds as Biomonitoring System for Heavy Metal (HM) Accumulation and Contamination of Our Oceans. Am. J. Plant Sci. 9, 1514–1530.

Gladue, R.M., Maxey, J.E., 1994. Microalgal feeds for aquaculture. J. Appl. Phycol. 6, 131–141.

Glyk, A., Scheper, T., Beutel, S., 2015. PEG – salt aqueous two-phase systems : an attractive and versatile liquid – liquid extraction technology for the downstream processing of proteins and enzymes 6599–6616.

Gödel, S., Becker, B., Melkonian, M., 2000. Flagellar membrane proteins of Tetraselmis striata butcher (Chlorophyta). Protist 151, 147–159.

Goettel, M., Eing, C., Gusbeth, C., Straessner, R., Frey, W., 2013. Pulsed electric fi eld assisted extraction of intracellular valuables from microalgae. Algal Res. 2, 401–408.

González, M.A., Paula A. Aguayo, Inostroza, I. de L., Castro, P.A., Fuentes, G.A., Gómez, & P.I., 2015. Ultrastructural and molecular characterization of Tetraselmis strains (Chlorodendrophyceae , Chlorophyta) isolated from Chile. Gayana Bota 72, 47–57.

Goold, H., Beisson, F., Peltier, G., Li-Beisson, Y., 2015. Microalgal lipid droplets: composition, diversity, biogenesis and functions. Plant Cell Rep. 34, 545–555.

Green, A.J., Littlejohn, K.A., Hooley, P., Cox, P.W., 2013. Formation and stability of food foams and aerated emulsions: Hydrophobins as novel functional ingredients. Curr. Opin. Colloid Interface Sci. 18, 292–301.

Greenwell, H.C., Laurens, L.M.L., Shields, R.J., 2010. Placing microalgae on the biofuels priority list : a review of the technological challenges. J. fof R. Soc. interface 7, 703–726.

Grimi, N., Dubois, A., Marchal, L., Jubeau, S., Lebovka, N.I., Vorobiev, E., 2014. Selective extraction from microalgae Nannochloropsis sp. using different methods of cell disruption. Bioresour. Technol. 153, 254–259.

Guil-Guerrero, J.., R, N.-J., Lopez MArtinez, J.., Campra Madrid, P., Rebolloso-Fuentes, M., M., 2004. Functional properties of the biomass of three microalgal species. J. Food Eng. 65, 511–517.

Günerken, E., D'Hondt, E., Eppink, M.H.M., Garcia-Gonzalez, L., Elst, K., Wijffels, R.H., 2015. Cell disruption for microalgae biorefineries. Biotechnol. Adv. 33, 243–260.

Günther, S., Gernat, D., Overbeck, A., Kampen, I., Kwade, A., 2016. Micromechanical properties and energy requirements of microalgae Chlorella vulgaris for cell disruption. Chem. Eng. Technol. 39, 1693–1699.

Hagen, C., Siegmund, S., Braune, W., 2016. Ultrastructural and chemical changes in the cell wall of Haematococcus pluvialis (Volvocales , Chlorophyta) during aplanospore formation Ultrastructural and chemical changes in the cell wall of Haematococcus pluvialis (Volvocales , Chlorophyta) during 0262.

Haghtalab, A., Paraj, A., 2012. Computation of liquid-liquid equilibrium of organic-ionic liquid systems using NRTL, UNIQUAC and NRTL-NRF models. J. Mol. Liq. 171, 43–49.

Halim, R., Rupasinghe, T.W.T., Tull, D.L., Webley, P.A., 2013. Mechanical cell disruption for lipid extraction from microalgal biomass. Bioresour. Technol. 140, 53–63.

Harnedy, P.A., FitzGerald, R.J., 2013. Extraction of protein from the macroalga Palmaria palmata. LWT - Food Sci. Technol. 51, 375–382.

Hartman, A., Johansson, G., Albertsson, P., 1974. Partition of Proteins in a Three-Phase System 81, 75–81.

Hartounian, H., Kaler, E.W., Sandler, S.I., 1994. Aqueous Two-Phase Systems. 2. Protein Partitioning. Ind. Eng. Chem. Res. 33, 2294–2300.

Harun, R., Singh, M., Forde, G.M., Danquah, M.K., 2010. Bioprocess engineering of microalgae to produce a variety of consumer products. Renew. Sustain. Energy Rev. 14, 1037–1047.

Havea, P., Carr, A.J., Creamer, L.K., 2004. The roles of disulphide and non-covalent bonding in the functional properties of heat-induced whey protein gels. J. Dairy Res. 71, 330–339.

Havea, P., Singh, H., Creamer, L.K., 2002. Heat-induced aggregation of whey proteins: Comparison of cheese WPC with acid WPC and relevance of mineral composition. J. Agric. Food Chem. 50, 4674–4681.

Heaney-Kieras, J., Rodén, L., Chapman, D.J., 1977. The covalent linkage of protein to carbohydrate in the extracellular protein-polysaccharide from the red alga Porphyridium cruentum. Biochem. J. 165, 1–9.

Hedenskog, G., Enebo, L., Vendlová, J., Prokeš, B., 1969. Investigation of some methods for increasing the digestibility *in vitro* of microalgae. Biotechnol. Bioeng. 11, 37–51.

Henchion, M., Hayes, M., Mullen, A., Fenelon, M., Tiwari, B., 2017. Future Protein Supply and Demand: Strategies and Factors Influencing a Sustainable Equilibrium. Foods 6, 53.

Holdt, S.L., Kraan, S., 2011. Bioactive compounds in seaweed: Functional food applications and legislation. J. Appl. Phycol. 23, 543–597.

Hou, Q., Ju, M., Li, W., Liu, L., Chen, Y., Yang, Q., Zhao, H., 2017. Pretreatment of lignocellulosic biomass with ionic liquids and ionic liquid-based solvent systems. Molecules 22, 1–24.

Huimin, X., Lin, L., Shilin, G., Elfalleh, W., Shenghua, H., Qinghai, S., Ying, M., 2014. Formation, Stability, and Properties of an Algae Oil Emulsion for Application in UHT Milk. Food Bioprocess Technol. 7, 567–574.

Illman, A.M., Scragg, A.H., Shales, S.W., 2000. Increase in Chlorella strains calorific values when grown in low nitrogen medium. Enzyme Microb. Technol. 27, 631–635.

Jazrawi, C., Biller, P., He, Y., Montoya, A., Ross, A.B., Maschmeyer, T., Haynes, B.S., 2015. Two-stage hydrothermal liquefaction of a high-protein microalga. Algal Res. 8, 15–22.

Jordan, P., Vilter, H., 1991. Extraction of proteins from material rich in anionic mucilages: Partition and fractionation of vanadate-dependent bromoperoxidases from the brown algae Laminaria digitata and L. saccharina in aqueous polymer two-phase systems. BBA - Gen. Subj. 1073, 98–106.

Jung, K.A., Lim, S.R., Kim, Y., Park, J.M., 2013. Potentials of macroalgae as feedstocks for biorefinery. Bioresour. Technol. 135, 182–190.

Kadam, S.U., ??lvarez, C., Tiwari, B.K., O'Donnell, C.P., 2016. Extraction and characterization of protein from Irish brown seaweed Ascophyllum nodosum. Food Res. Int.

Kandasamy, G., Karuppiah, S.K., Rao, P.V.S., 2012. Salt- and pH-induced functional changes in protein concentrate of edible green seaweed Enteromorpha species. Fish. Sci. 78, 169–176.

Kapaun, E., Reisser, W., 1995. A chitin-like glycan in the cell wall of a Chlorella sp. (Chlorococcales, Chlorophyceae). Planta 197, 577–582.

Kaul, A., 2000. The Phase Diagram, in: Aqueous Two-Phase Systems: Methods and Protocols. pp. 11–21.

Kermanshahi-pour, A., Sommer, T.J., Anastas, P.T., Zimmerman, J.B., 2014. Enzymatic and acid hydrolysis of Tetraselmis suecica for polysaccharide characterization. Bioresour. Technol. 173, 415–421.

Khanra, S., Mondal, M., Halder, G., Tiwari, O.N., Gayen, K., Bhowmick, T.K., 2018. Downstream processing of microalgae for pigments, protein and carbohydrate in industrial application: A review. Food Bioprod. Process. 110, 60–84.

Kim, D.Y., Vijayan, D., Praveenkumar, R., Han, J.I., Lee, K., Park, J.Y., Chang, W.S., Lee, J.S., Oh, Y.K., 2016. Cell-wall disruption and lipid/astaxanthin extraction from microalgae: Chlorella and Haematococcus. Bioresour. Technol. 199, 300–310.

Kim, Y.H., Choi, Y.K., Park, J., Lee, S., Yang, Y.H., Kim, H.J., Park, T.J., Hwan Kim, Y., Lee, S.H., 2012. Ionic liquid-mediated extraction of lipids from algal biomass. Bioresour. Technol. 109, 312–315.

Kiskini, A., Zondervan, E., Wierenga, P.A., Poiesz, E., Gruppen, H., 2015. Using product driven process synthesis in the biorefinery. Comput. Chem. Eng. 91, 257–268.

Knoetzel, J., Braumann, T., Grimme, L.H., 1988. Pigment-protein complexes of green algae: Improved methodological steps for the quantification of pigments in pigment-protein complexes derived from the green algae Chlorella and Chlamydomonas. J. Photochem. Photobiol. B Biol. 1, 475–491.

Koller, M., Muhr, A., Braunegg, G., 2014. Microalgae as versatile cellular factories for valued products. Algal Res. 6, 52–63.

Kula, M. -R, Schütte, H., 1987. Purification of Proteins and the Disruption of Microbial Cells. Biotechnol. Prog. 3, 31–42.

Kwade, A., Blecher, L., Schwedes, J., 1996. Motion and stress intensity of grinding beads in a stirred media mill. Part 2: Stress intensity and its effect on comminution. Powder Technol. 86, 69–76.

Kwade, A., Schwedes, J., 2002. Breaking characteristics of different materials and their effect on stress intensity and stress number in stirred media mills. Powder Technol. 122, 109–121.

Lahaye, M., Robic, A., 2007. Structure and function properties of Ulvan, a polysaccharide from green seaweeds. Biomacromolecules 8, 1765–1774.

Lamers, P.P., van de Laak, C.C.W., Kaasenbrood, P.S., Lorier, J., Janssen, M., De Vos, R.C.H., Bino,

R.J., Wijffels, R.H., 2010. Carotenoid and fatty acid metabolism in light-stressed Dunaliella salina. Biotechnol. Bioeng. 106, 638–648.

Law, S.Q.K., Mettu, S., Ashokkumar, M., Scales, P.J., Martin, G.J.O., 2018. Emulsifying properties of ruptured microalgae cells: Barriers to lipid extraction or promising biosurfactants? Colloids Surfaces B Biointerfaces 170, 438–446.

Lee, A.K., Lewis, D.M., Ashman, P.J., 2015. Microalgal cell disruption by hydrodynamic cavitation for the production of biofuels. J. Appl. Phycol. 27, 1881–1889.

Lee, A.K., Lewis, D.M., Ashman, P.J., 2013. Force and energy requirement for microalgal cell disruption: An atomic force microscope evaluation. Bioresour. Technol. 128, 199–206.

Lee, S.Y., Khoiroh, I., Ooi, C.W., Ling, T.C., Show, P.L., 2017a. Recent Advances in Protein Extraction Using Ionic Liquid-based Aqueous Two-phase Systems. Sep. Purif. Rev. 00, 1–14.

Lee, S.Y., Show, P.L., Ling, T.C., Chang, J.S., 2017b. Single-step disruption and protein recovery from Chlorella vulgaris using ultrasonication and ionic liquid buffer aqueous solutions as extractive solvents. Biochem. Eng. J. 124, 26–35.

Lenneman, E.M., Wang, P., Barney, B.M., 2014. Potential application of algicidal bacteria for improved lipid recovery with specific algae. FEMS Microbiol. Lett. 354, 102–110.

Libouga, D.G., Aguié-Béghin, V., Douillard, R., 1996. Thermal denaturation and gelation of rubisco: Effects of pH and ions. Int. J. Biol. Macromol. 19, 271–277.

Lin, D.Q., Wu, Y.T., Mei, L.H., Zhu, Z.Q., Yao, S.J., 2003. Modeling the protein partitioning in aqueous polymer two-phase systems: Influence of polymer concentration and molecular weight. Chem. Eng. Sci. 58, 2963–2972.

Lorente, E., Hapońska, M., Clavero, E., Torras, C., Salvadó, J., 2018. Steam Explosion and Vibrating Membrane Filtration to Improve the Processing Cost of Microalgae Cell Disruption and Fractionation. Processes 6, 28.

Lowry, O., Rosebrough, N., Farr, L., Randall, R., Al., E., 1951. Protein measurement with the folin phenol reagent. J. Biol. Chem 193, 265–275.

Lozano, P., Bernal, J.M., Garcia-verdugo, E., Sanchez-gomez, G., Vaultier, M., Isabel, M., Luis, S. V, 2015. Sponge-like ionic liquids : a new platform for green biocatalytic chemical processes. Green Chem. 17, 3706–3717.

Luo, X., Smith, P., Raston, C.L., Zhang, W., 2016. Vortex fluidic device-intensified aqueous two phase extraction of C-phycocyanin from spirulina maxima. ACS Sustain. Chem. Eng. 4, 3905–3911.

Lupatini, A.L., Colla, L.M., Canan, C., Colla, E., 2017. Potential application of microalga Spirulina platensis as a protein source. J. Sci. Food Agric. 97.

Lupatini, A.L., Souza, L.E.S., Bispo, L.O., Nogues, D., Canan, C., Colla, E., 2016. GELATION CAPACITY OF Spirulina platensis PROTEIN CONCENTRATE OBTAINED BY ULTRASOUND AND AGITATION EXTRACTION, in: XXV Congresso Brasileiro de Ciencia e Technologia de Alimentos.

Luthy, R.G., Selleck, R.E., Galloway, T.R., Selleck, R.E., Galloway, T.R., 1978. Removal of emulsified oil with dissolved air flotation organic coagulants and. J. water Pollut. Control Fed. 50, 331–346.

Ma, Y., Wang, Z., Yu, C., Yin, Y., Zhou, G., 2014. Evaluation of the potential of 9 Nannochloropsis strains for biodiesel production. Bioresour. Technol. 167, 503–509.

Madeira, P.P., Xu, X., 2005. Prediction of protein partition in polymer / salt aqueous two-phase systems using the modified Wilson model. Biochem. Eng. J. 24, 147–155.

Mai, N.L., Ahn, K., Koo, Y.M., 2014. Methods for recovery of ionic liquids - A review. Process Biochem. 49, 872–881.

Malihan, L.B., Mittal, N., Nisola, G.M., Weldemhret, T.G., Kim, H., Chung, W.J., 2017. Macroalgal biomass hydrolysis using dicationic acidic ionic liquids. J. Chem. Technol. Biotechnol. 92, 1290–1297.

Malihan, L.B., Nisola, G.M., Mittal, N., Seo, J.G., Chung, W.J., 2014. Blended ionic liquid systems for macroalgae pretreatment. Renew. Energy 66, 596–604.

Martin, A.H., Nieuwland, M., Jong, G.A.H. De, 2014. Characterization of Heat-Set Gels from RuBisCO in Comparison to Those from Other Proteins. J. Agric. Food Chem. 62, 10783–10791.

Martins, M., Vieira, F.A., Correia, I., Ferreira, R.A.S., Abreu, H., Coutinho, J.A.P., Ventura, S.P.M., 2016. Recovery of phycobiliproteins from the red macroalga: Gracilaria sp. using ionic liquid aqueous solutions. Green Chem. 18, 4287–4296.

Mashmoushy, H., Zhang, Z., Thomas, C.R., 1998. Micromanipulation measurement of the mechanical properties of baker's yeast cells. Biotechnol. Tech. 12, 925–929.

Melendres, A. V., Honda, H., Shiragami, N., Unno, H., 1991. A kinetic analysis of cell disruption by bead mill. Bioseparation 2, 231–236.

Meyer, M.T., Genkov, T., Skepper, J.N., Jouhet, J., Mitchell, M.C., Spreitzer, R.J., Griffiths, H., 2012. Rubisco small-subunit -helices control pyrenoid formation in Chlamydomonas. Proc. Natl. Acad. Sci. 109, 19474–19479.

Meyer, M.T., Whittaker, C., Griffiths, H., 2017. The algal pyrenoid: key unanswered questions. J. Exp. Bot. 68, 3739–3749.

Michels, M.H.A., Camacho-rodríguez, J., Vermuë, M.H., Wijffels, R.H., 2014a. Effect of cooling in the night on the productivity and biochemical composition of Tetraselmis suecica. ALGAL 6, 145–151.

Michels, M.H.A., Slegers, P.M., Vermuë, M.H., Wijffels, R.H., 2014b. Effect of biomass concentration on the productivity of Tetraselmis suecica in a pilot-scale tubular photobioreactor using natural sunlight. Algal Res. 4, 12–18.

Michels, M.H.A., Van Der Goot, A.J., Norsker, N.H., Wijffels, R.H., 2010. Effects of shear stress on the microalgae Chaetoceros muelleri. Bioprocess Biosyst. Eng. 33, 921–927.

Michels, M.H.A., van der Goot, A.J., Vermuë, M.H., Wijffels, R.H., 2016. Cultivation of shear stress sensitive and tolerant microalgal species in a tubular photobioreactor equipped with a centrifugal pump. J. Appl. Phycol. 28, 53–62.

Middelberg, A.P.J., 1995. Process-scale disruption of microorganisms. Biotechnol. Adv. 13, 491–551.

Montalescot, V., Rinaldi, T., Touchard, R., Jubeau, S., Frappart, M., Jaouen, P., Bourseau, P., 2015. Optimization of bead milling parameters for the cell disruption of microalgae : Process modeling and application to Porphyridium cruentum and Nannochloropsis oculata. Bioresour. Technol. 196, 339–346.

Naushad, M., ALOthman, Z.A., Khan, A.B., Ali, M., 2012. Effect of ionic liquid on activity, stability, and structure of enzymes: A review. Int. J. Biol. Macromol. 51, 555–560.

Nichols, C.M., Wang, Z.C., Yang, Z., Lineberger, W.C., Bierbaum, V.M., 2016. Experimental and Theoretical Studies of the Reactivity and Thermochemistry of Dicyanamide: N(CN)2-. J. Phys. Chem. A 120, 992–999.

Olguín, E.J., Hernández, B., Araus, A., Camacho, R., González, R., Ramírez, M.E., Galicia, S., Mercado, G., 1994. Simultaneous high-biomass protein production and nutrient removal using Spirulina maxima in sea water supplemented with anaerobic effluents. World J. Microbiol. Biotechnol. 10, 576–578.

Olkiewicz, M., Caporgno, M.P., Font, J., Legrand, J., Lepine, O., Plechkova, N. V., Pruvost, J., Seddon, K.R., Bengoa, C., 2015. A novel recovery process for lipids from microalgæ for biodiesel production using a hydrated phosphonium ionic liquid. Green Chem. 17, 2813–2824.

Orr, V.C.A., Plechkova, N. V., Seddon, K.R., Rehmann, L., 2016. Disruption and Wet Extraction of the Microalgae Chlorella vulgaris Using Room-Temperature Ionic Liquids. ACS Sustain. Chem. Eng. 4, 591–600.

Orr, V.C.A., Rehmann, L., 2016. Ionic liquids for the fractionation of microalgae biomass. Curr. Opin. Green Sustain. Chem. 2, 22–27.

Øverland, M., Mydland, L.T., Skrede, A., 2018. Marine macroalgae as sources of protein and bioactive compounds in feed for monogastric animals. J. Sci. Food Agric.

Palsdottir, H., Hunte, C., 2004. Lipids in membrane protein structures. Biochim. Biophys. Acta - Biomembr. 1666, 2–18.

Pan, Z., Huang, Y., Wang, Y., Wu, Z., 2017. Disintegration of Nannochloropsis sp. cells in an improved turbine bead mill. Bioresour. Technol. 245, 641–648.

Park, D.-H., Jeong, G.-T., 2013. Production of Reducing Sugar from Macroalgae Saccharina japonica Using Ionic Liquid Catalyst. Korean Chem. Eng. Res. 51, 106–110.

Parniakov, O., Barba, F.J., Grimi, N., Marchal, L., Jubeau, S., Lebovka, N., Vorobiev, E., 2015. Pulsed electric field and pH assisted selective extraction of intracellular components from microalgae nannochloropsis. Algal Res. 8, 128–134.

Passos, F., Carretero, J., Ferrer, I., 2015. Comparing pretreatment methods for improving microalgae anaerobic digestion: Thermal, hydrothermal, microwave and ultrasound. Chem. Eng. J. 279, 667–672.

Patil, G., Raghavarao, K.S.M.S., 2007. Aqueous two phase extraction for purification of C-phycocyanin. Biochem. Eng. J. 34, 156–164.

Perez, B., Malpiedi, L.P., Tubío, G., Nerli, B., de Alcântara Pessôa Filho, P., 2013. Experimental determination and thermodynamic modeling of phase equilibrium and protein partitioning in

aqueous two-phase systems containing biodegradable salts. J. Chem. Thermodyn. 56, 136–143.

Pezoa-Conte, R., Leyton, A., Anugwom, I., von Schoultz, S., Paranko, J., Mäki-Arvela, P., Willför, S., Muszyński, M., Nowicki, J., Lienqueo, M.E., Mikkola, J.P., 2015. Deconstruction of the green alga Ulva rigida in ionic liquids: Closing the mass balance. Algal Res. 12, 262–273.

Phong, W.N., Le, C.F., Show, P.L., Chang, J.-S., Ling, T.C., 2017. Extractive disruption process integration using ultrasonication and an aqueous two-phase system for protein recovery from Chlorella sorokiniana. Eng. Life Sci. 17, 357–369.

Phong, W.N., Show, P.L., Le, C.F., Tao, Y., Chang, J.S., Ling, T.C., 2018a. Improving cell disruption efficiency to facilitate protein release from microalgae using chemical and mechanical integrated method. Biochem. Eng. J. 135, 83–90.

Phong, W.N., Show, P.L., Ling, T.C., Juan, J.C., Ng, E.P., Chang, J.S., 2018b. Mild cell disruption methods for bio-functional proteins recovery from microalgae—Recent developments and future perspectives. Algal Res. 31, 506–516.

Pinkert, A., Marsh, K.N., Pang, S., Staiger, M.P., 2009. Ionic lquids and their interaction with cellulose. Chem. Rev. 109, 6712–6728.

Polikovsky, M., Fernand, F., Sack, M., Frey, W., Müller, G., Golberg, A., 2016. Towards marine biorefineries: Selective proteins extractions from marine macroalgae Ulva with pulsed electric fields. Innov. Food Sci. Emerg. Technol. 37, 194–200.

Postma, P.R., Cerezo-Chinarro, O., Akkerman, R.J., Olivieri, G., Wijffels, R.H., Brandenburg, W.A., Eppink, M.H.M., 2018. Biorefinery of the macroalgae Ulva lactuca: extraction of proteins and carbohydrates by mild disintegration. J. Appl. Phycol. 30, 1281–1293.

Postma, P.R., Miron, T.L., Olivieri, G., Barbosa, M.J., Wijffels, R.H., Eppink, M.H.M., 2015. Mild disintegration of the green microalgae Chlorella vulgaris using bead milling. Bioresour. Technol. 184, 297–304.

Postma, P.R., Pataro, G., Capitoli, M., Barbosa, M.J., Wijffels, R.H., Eppink, M.H.M., Olivieri, G., Ferrari, G., 2016. Selective extraction of intracellular components from the microalga Chlorella vulgaris by combined pulsed electric field-temperature treatment. Bioresour. Technol. 203, 80–88.

Postma, P.R., Suarez Garcia, E., Safi, C., Yonathan, K., Olivieri, G., Barbosa, M.J., Wijffels, R.H., Eppink, M.H.M., 2017. Energy efficient bead milling of microalgae: Effect of bead size on disintegration and release of proteins and carbohydrates. Bioresour. Technol. 224, 670–679.

Qiao, Y., Ma, W., Theyssen, N., Chen, C., Hou, Z., 2017. Temperature-Responsive Ionic Liquids : Fundamental Behaviors and Catalytic Applications. Chem. Rev. 117, 6881–6928.

Renon, H., Pruasnitz, J.M., 1968. Local compositions in thermodynamics excess functions for liquids mixtures. AIChE J. 14, 116–128.

Rosa, P.A.J., Azevedo, A.M., Sommerfeld, S., Bäcker, W., Aires-Barros, M.R., 2011. Aqueous two-phase extraction as a platform in the biomanufacturing industry: Economical and environmental sustainability. Biotechnol. Adv. 29, 559–567.

Ruiz Gonzalez, J., Olivieri, G., de Vree, J., Bosma, R., Willems, P., Reith, H., Eppink, M., Kleinegris,

D.M.M., Wijffels, R.H., Barbosa, M., 2016. Towards industrial products from microalgae. Energy Environ. Sci.

Safi, C., Cabas Rodriguez, L., Mulder, W.J., Engelen-Smit, N., Spekking, W., van den Broek, L.A.M., Olivieri, G., Sijtsma, L., 2017a. Energy consumption and water-soluble protein release by cell wall disruption of Nannochloropsis gaditana. Bioresour. Technol. 239, 204–210.

Safi, C., Charton, M., Ursu, A.V., Laroche, C., Zebib, B., Pontalier, P.Y., Vaca-Garcia, C., 2014a. Release of hydro-soluble microalgal proteins using mechanical and chemical treatments. Algal Res. 3, 55–60.

Safi, C., Liu, D.Z., Yap, B.H.J., Martin, G.J.O., Vaca-Garcia, C., Pontalier, P.Y., 2014b. A two-stage ultrafiltration process for separating multiple components of Tetraselmis suecica after cell disruption. J. Appl. Phycol. 26, 2379–2387.

Safi, C., Olivieri, G., Campos, R.P., Engelen-Smit, N., Mulder, W.J., van den Broek, L.A.M., Sijtsma, L., 2017b. Biorefinery of microalgal soluble proteins by sequential processing and membrane filtration. Bioresour. Technol. 225, 151–158.

Safi, C., Ursu, A.V., Laroche, C., Zebib, B., Merah, O., Pontalier, P.Y., Vaca-Garcia, C., 2014c. Aqueous extraction of proteins from microalgae: Effect of different cell disruption methods. Algal Res. 3, 61–65.

Salam, K.A., Velasquez-Orta, S.B., Harvey, A.P., 2016. A sustainable integrated in situ transesterification of microalgae for biodiesel production and associated co-products - A review. Renew. Sustain. Energy Rev. 65, 1179–1198.

Samarakoon, K., Jeon, Y.J., 2012. Bio-functionalities of proteins derived from marine algae - A review. Food Res. Int. 48, 948–960.

Sankaran, R., Manickam, S., Jiun, Y., Chuan, T., Chang, J., 2018a. Extraction of proteins from microalgae using integrated method of sugaring- out assisted liquid biphasic flotation (LBF) and ultrasound. Ultrason. - Sonochemistry 48, 231–239.

Sankaran, R., Manickam, S., Yap, Y.J., Ling, T.C., Chang, J.S., Show, P.L., 2018b. Extraction of proteins from microalgae using integrated method of sugaring-out assisted liquid biphasic flotation (LBF) and ultrasound. Ultrason. Sonochem. 48, 231–239.

Sari, Y.W., Bruins, M.E., Sanders, J.P.M., 2013. Enzyme assisted protein extraction from rapeseed, soybean, and microalgae meals. Ind. Crops Prod. 43, 78–83.

Sari, Y.W., Mulder, W.J., Sanders, J.P.M., Bruins, M.E., 2015. Towards plant protein refinery: Review on protein extraction using alkali and potential enzymatic assistance. Biotechnol. J. 10, 1138–1157.

Sarifudin, A., Assiry, A.M., 2014. Some physicochemical properties of dextrin produced by extrusion process. J. Saudi Soc. Agric. Sci. 13, 100–106.

Schneider, N., Fortin, T.J., Span, R., Gerber, M., 2016. Thermophysical properties of the marine microalgae Nannochloropsis salina ☆Fuel Process. Technol. 152, 390–398.

Scholz, M.J., Weiss, T.L., Jinkerson, R.E., Jing, J., Roth, R., Goodenough, U., Posewitz, M.C., Gerken, H.G., 2014. Ultrastructure and composition of the Nannochloropsis gaditana cell wall. Eukaryot.

Cell 13, 1450–1464.

Schütte, H., Kroner, K.H., Hustedt, H., Kula, M.-R., 1983. Experiences with a 20 litre industrial bead mill for the disruption of microorganisms. Enzyme Microb. Technol. 5, 143–148.

Schwenzfeier, A., Helbig, A., Wierenga, P.A., Gruppen, H., 2013a. Emulsion properties of algae soluble protein isolate from Tetraselmis sp . Food Hydrocoll. 30, 258–263.

Schwenzfeier, A., Lech, F., Wierenga, P.A., Eppink, M.H.M., Gruppen, H., 2013b. Foam properties of algae soluble protein isolate: Effect of pH and ionic strength. Food Hydrocoll. 33, 111–117.

Schwenzfeier, A., Wierenga, P.A., Eppink, M.H.M., Gruppen, H., 2014. Effect of charged polysaccharides on the techno-functional properties of fractions obtained from algae soluble protein isolate. Food Hydrocoll. 35, 9–18.

Schwenzfeier, A., Wierenga, P.A., Gruppen, H., 2011. Isolation and characterization of soluble protein from the green microalgae Tetraselmis sp. Bioresour. Technol. 102, 9121–9127.

Serrien, G., Geeraerts, G., Ghosh, L., Joos, P., 1992. Dynamic surface properties of adsorbed protein solutions: BSA, casein and buttermilk. Colloids and Surfaces 68, 219–233.

Sharma, A., Gupta, M.N., 2002. Three phase partitioning of carbohydrate polymers: Separation and purification of alginates. Carbohydr. Polym. 48, 391–395.

Shields, R.J., Lupatsch, I., 2012. Algae for Aquaculture and Animal Feeds. Tech. – Theor. und Prax. 21. 21, 23–37.

Shiu, C., Zhang, Z., Thomas, C.R., 2002. Bacterial Species, in: Durieux, Alain; Simon, jean P. (Ed.), Applied Microbiology. Kluver Academic Pu, pp. 155–162.

Silvério, S.C., Rodríguez, O., Teixeira, J.A., Macedo, E.A., 2013. The Effect of Salts on the Liquid–Liquid Phase Equilibria of PEG600 + Salt Aqueous Two-Phase Systems. J. Chem. Eng. Data 58, 3528–3535.

Simoni, L.D., Lin, Y., Brennecke, J.F., Stadtherr, M.A., 2008. Modeling liquid-liquid equilibrium of ionic liquid systems with NRTL, electrolyte-NRTL, and UNIQUAC. Ind. Eng. Chem. Res. 47, 256–272.

Sinha, A., Singh, A., Kumar, S., Khare, S.K., 2014. Microbial mineralization of struvite : A promising process to overcome phosphate sequestering crisis. Water Res. 54, 33–43.

Song, C.P., Yap, Q.Y., Yin, M., Nagasundara, R.R., 2018. Environmentally Benign and Recyclable Aqueous Two-Phase System Composed of Distillable CO2-Based Alkyl Carbamate Ionic Liquids. ACS Sustain. Chem. Eng. 6, 10344–10354.

Sorensen, M., Berge, G.M., Reitan, K.I., Ruyter, B., 2016. Microalga Phaeodactylum tricornutum in feed for Atlantic salmon (Salmo salar) -Effect on nutrient digestibility, growth and utilization of feed. Aquaculture 460, 116–123.

Soto-Sierra, L., Stoykova, P., Nikolov, Z.L., 2018. Extraction and fractionation of microalgae-based protein products. Algal Res. 36, 175–192.

Soto Sierra, L., Dixon, C.K., Wilken, L.R., 2017. Enzymatic cell disruption of the microalgae Chlamydomonas reinhardtii for lipid and protein extraction. Algal Res. 25, 149–159.

Spolaore, P., Joannis-Cassan, C., Duran, E., Isambert, A., 2006. Commercial Applications of Microalgae Pauline. J. Biosci. Bioeng. 101, 87–96.

Suarez Garcia, E., Leeuwen, J. v., Safi, C., Sijtsma, L., Eppink, M.H.M., Wijffels, R.H., van den Berg, C., 2018a. Selective and energy efficient extraction of functional proteins from microalgae for food applications. Bioresour. Technol. 268, 197–203.

Suarez Garcia, E., Suarez Ruiz, C.A., Tilaye, T., Eppink, M.H.M., Wijffels, R.H., van den Berg, C., 2018b. Fractionation of proteins and carbohydrates from crude microalgae extracts using an ionic liquid based-aqueous two phase system. Sep. Purif. Technol. 204, 56–65.

Suarez Garcia, E., Van Leeuwen, J.J.A., Safi, C., Sijtsma, L., Van Den Broek, L.A.M., Eppink, M.H.M., Wijffels, R.H., Van Den Berg, C., 2018c. Techno-Functional Properties of Crude Extracts from the Green Microalga Tetraselmis suecica. J. Agric. Food Chem. 66, 7831–7838.

Suarez Ruiz, C.A., Emmery, D.P., Wijffels, R.H., Eppink, M.H.M., van den Berg, C., 2018. Selective and mild fractionation of microalgal proteins and pigments using aqueous two-phase systems. J. Chem. Technol. Biotechnol. 93, 2774–2783.

Suarez Ruiz, C.A., van den Berg, C., Wijffels, R.H., Eppink, M.H.M., 2017. Rubisco separation using biocompatible aqueous two-phase systems. Sep. Purif. Technol. 1–8.

Tamayo, A., Kyriakopoulou, K.E., Suarez-garcia, E., Berg, C. Van Den, Jan, A., Goot, V. Der, 2018. Understanding differences in protein fractionation from conventional crops , and herbaceous and aquatic biomass. Trends Food Sci. Technol. 71, 235–245.

Taylor, P., Schmitt, C., Sanchez, C., Desobry-banon, S., Hardy, J., Schmitt, C., Sanchez, C., Desobry-banon, S., Hardy, J., 2010. Critical Reviews in Food Science and Nutrition Structure and Technofunctional Properties of Protein- Polysaccharide Complexes : A Review. Crit. Rev. Food Sci. Nutr. 37–41.

Teixeira, R.E., 2012. Energy-efficient extraction of fuel and chemical feedstocks from algae. Green Chem. 14, 419–427.

Tenorio, A.T., de Jong, E.W.M., Nikiforidis, C. V., Boom, R.M., van der Goot, A.J., 2017. Interfacial properties and emulsification performance of thylakoid membrane fragments. Soft Matter 1, 15161.

Teuling, E., Schrama, J.W., Gruppen, H., Wierenga, P.A., 2017. Effect of cell wall characteristics on algae nutrient digestibility in Nile tilapia (Oreochromis niloticus) and African catfish (Clarus gariepinus). Aquaculture 479, 490–500.

To, T.Q., Procter, K., Simmons, B.A., Subashchandrabose, S., Atkin, R., 2018. Low cost ionic liquid-water mixtures for effective extraction of carbohydrate and lipid from algae. Faraday Discuss. 206, 93–112.

Tornberg, E., 1978. The interfacial behaviour of three food proteins studied by the drop volume technique. J. Sci. Food Agric. 29, 762–776.

Trautmann, A., Watzer, B., Wilde, A., Forchhammer, K., Posten, C., 2016. Effect of phosphate availability on cyanophycin accumulation in Synechocystis sp. PCC 6803 and the production strain BW86. Algal Res. 20, 189–196.

Trivedi, J., Aila, M., Bangwal, D.P., Kaul, S., Garg, M.O., 2015. Algae based biore fi nery — How to make sense ? Renew. Sustain. Energy Rev. 47, 295–307.

Ursu, A., Marcati, A., Sayd, T., Sante-lhoutellier, V., Djelveh, G., Michaud, P., 2014. Bioresource Technology Extraction , fractionation and functional properties of proteins from the microalgae Chlorella vulgaris. Bioresour. Technol. 157, 134–139.

US DOE, 2010. National Algal Biofuels Technology Roadmap. U.S. Department of Energy, Office of Energy Efficiency and Renewable Energy, Biomass Program.

van den Hoek, C., Mann, D., Jahns, H.M., 1995. Algae: An Introduction to Phycology. Cambridge University Press.

Van Hee, P., Middelberg, A.P.J., Van Der Lans, R.G.J.M., Van Der Wielen, L.A.M., 2004. Relation between cell disruption conditions, cell debris particle size, and inclusion body release. Biotechnol. Bioeng. 88, 100–110.

Vanthoor-koopmans, M., Wijffels, R.H., Barbosa, M.J., Eppink, M.H.M., 2012. Biorefinery of microalgae for food and fuel. Bioresour. Technol. 135, 142–149.

Vanthoor-Koopmans, M., Wijffels, R.H., Barbosa, M.J., Eppink, M.H.M., 2013. Biorefinery of microalgae for food and fuel. Bioresour. Technol.

Ventura, S.P.M., e Silva, F.A., Quental, M. V., Mondal, D., Freire, M.G., Coutinho, J.A.P., 2017. Ionic-Liquid-Mediated Extraction and Separation Processes for Bioactive Compounds: Past, Present, and Future Trends. Chem. Rev. acs.chemrev.6b00550.

Vigani, M., Parisi, C., Rodr, E., Barbosa, M.J., Sijtsma, L., Ploeg, M., 2015. Food and feed products from micro- algae : Market opportunities and challenges for the EU. Food Sci. Technol. 42, 81–92.

Waghmare, A.G., Salve, M.K., LeBlanc, J.G., Arya, S.S., 2016. Concentration and characterization of microalgae proteins from Chlorella pyrenoidosa. Bioresour. Bioprocess. 3, 16.

Wahidin, S., Idris, A., Shaleh, S.R.M., 2016. Ionic liquid as a promising biobased green solvent in combination with microwave irradiation for direct biodiesel production. Bioresour. Technol. 206, 150–154.

Wang, C., Lan, C.Q., 2018. Effects of shear stress on microalgae – A review. Biotechnol. Adv. 36, 986–1002.

Wang, H., Johnson, L.A., Wang, T., 2004. Preparation of soy protein concentrate and isolate from extruded-expelled soybean meals. JAOCS, J. Am. Oil Chem. Soc. 81, 713–717.

Wang, R., Chang, Y., Tan, Z., Li, F., 2016. Applications of choline amino acid ionic liquid in extraction and separation of flavonoids and pectin from ponkan peels. Sep. Sci. Technol. 51, 1093–1102.

Wang, X., Zhang, X., 2012. Optimal extraction and hydrolysis of Chlorella pyrenoidosa proteins. Bioresour. Technol. 126, 307–313.

Wells, M.L., Potin, P., Craigie, J.S., Raven, J.A., Merchant, S.S., Helliwell, K.E., Smith, A.G., Camire, M.E., Brawley, S.H., 2017. Algae as nutritional and functional food sources: revisiting our understanding. J. Appl. Phycol. 29, 949–982.

Wenjuan, Q., Haile, M., Ting, W., 2013. Alternating two frequency countercurrent ultrasonic

assisted extraction of protein and polysaccharide from porphyra yezoensis . Trans. chinese Soc. Agric. Eng. 29, 285–292.

Wijffels, R.H., Barbosa, M.J., Eppink, M.H.M., 2010. Microalgae for the production of bulk chemicals and biofuels. Biofuels Bioprodutcs & Biorefining 4, 287–295.

Wong, K.., Cheung, P.C.., 2001. Nutritional evaluation of some subtropical red and green seaweeds Part II. In vitro protein digestibility and amino acid profiles of protein concentrates. Food Chem. 72, 11–17.

Wu, D., Hornof, V., 1999. Dynamic Interfacial Tension in Hexadecaneiwater Systems Containing Ready-Made and in-Situ- Formed Surfactants. Chem. Eng. Comm 172, 85–106.

Wu, Y.-T., Lin, D.-Q., Zhu, Z.-Q., 1998. Thermodynamics of aqueous two-phase systems—the effect of polymer molecular weight on liquid–liquid equilibrium phase diagrams by the modified NRTL model. Fluid Phase Equilib. 147, 25–43.

Yamamoto, Y., Soda, R., Kano, J., Saito, F., 2012. DEM simulation of bead motion during wet bead milling using an enlarged particle model. Int. J. Miner. Process. 114–117, 93–99.

Yang, M., Jiang, J.-P., Xie, X., Chu, Y.-D., Fan, Y., Cao, X.-P., Xue, S., Chi, Z.-Y., 2017. Chloroplasts Isolation from Chlamydomonas reinhardtii under Nitrogen Stress. Front. Plant Sci. 8, 1–12.

Yokota, A., Canvin, D.T., 1985. Ribulose Bisphosphate Carboxylase/Oxygenase Content Determined with [14C]Carboxypentitol Bisphosphate in Plants and Algae. Plant Physiol. 77, 735–739.

Yoo, B., Shah, J.K., Zhu, Y., Maginn, E.J., 2014. Amphiphilic interactions of ionic liquids with lipid biomembranes: A molecular simulation study. Soft Matter 10, 8641–8651.

Zhang, R., Grimi, N., Marchal, L., Vorobiev, E., 2018. Application of high-voltage electrical discharges and high-pressure homogenization for recovery of intracellular compounds from microalgae Parachlorella kessleri. Bioprocess Biosyst. Eng. 0, 0.

Zhang, Y., Cremer, P.S., 2006. Interactions between macromolecules and ions: the Hofmeister series. Curr. Opin. Chem. Biol. 10, 658–663.

Zhang, Y.H.P., 2013. Next generation biorefineries will solve the food, biofuels, and environmental trilemma in the energy-food-water nexus. Energy Sci. Eng. 1, 27–41.

Zhao, L., Peng, Y. liang, Gao, J. mei, Cai, W. min, 2014. Bioprocess intensification: An aqueous two-phase process for the purification of C-phycocyanin from dry Spirulina platensis. Eur. Food Res. Technol. 238, 451–457.

Zinkoné, T.R., Gifuni, I., Lavenant, L., Pruvost, J., Marchal, L., 2018. Bead milling disruption kinetics of microalgae: Process modeling, optimization and application to biomolecules recovery from Chlorella sorokiniana. Bioresour. Technol. 267, 458–465.

Summary

In the next 30 years it is expected that world population will reach 9.5 billion, for which the supply of food, and in particular of proteins, must increase significantly. This expansion could threaten terrestrial and aquatic ecosystems critically, since the current food production system relies almost entirely on agriculture and fishing. Algae, including micro and macroalgae, could be the solution to the challenge of food and protein supply, as they do not require fresh water or arable land, and because they can produce substantial amounts of proteins at superior biomass productivities compared to crops. However, the proteins in algae are usually present intracellularly, in the cytoplasm or embedded in molecular assemblies and organelles. To obtain these biomolecules, several unit operations are typically applied in a sequential way: cell disintegration, extraction, fractionation and purification. Often, these unit operations require significant amounts of energy and auxiliary chemicals leading to product degradation or generation of several by-products, which are undervalued. Therefore, new biorefinery concepts are needed, which are more compact (integration) and in which mild processing is favoured (product functionality) (**Chapter 1**).

The research conducted in this thesis is divided in two sections. In the first section (chapters 2-5), the biorefinery strategy is based on mechanical disintegration by bead milling. In addition, we present evidence on the functional properties of the extracted biomolecules. The second section (chapters 6-8) investigates the biorefinery of algal molecules by means of ionic liquids as novel extractants.

In **Chapter 2**, the effect of bead size (0.3-1 mm) on the kinetics of cell disintegration and release of biomolecules, was investigated for three industry relevant microalgae strains: *Tetraselmis suecica*, *Neochloris oleoabundans* and *Chlorella vulgaris*. Furthermore, the stress model, in which the comminution process is quantified in terms of frequency and intensity of collisions in the mill, was applied. For all algal strains it was observed that the disintegration and release of biomolecules follows a first order kinetics. Disintegration and protein release occur first almost simultaneously, while the release of carbohydrates takes place at slower rates,

indicating selective release of proteins. It was hypothesized that aqueous proteins present in the cytoplasm are released rapidly upon cell disruption, while carbohydrates from the cell-wall or starch granules require additional shear to be released. Moreover, it was observed that the disintegration rates, biomolecule release and extraction yields were independent of the bead size for *Tetraselmis suecica*. This was due to the relatively weak cell-wall of this strain, and by the fact that the bead mill was operated in a region in which excessive energy was transferred to the cells to allow complete disintegration. The measured energy consumptions and protein yields (from the initial biomass) were strain dependent, and varied from 0.45-7 kWh kg_{DW}^{-1} and from 15 to 38 % Dry Weight (DW) respectively.

Several questions remained open regarding the cell disintegration mechanism in bead mills. Therefore, in **Chapter 3** a mathematical model was proposed, in order to predict the disintegration rates of microalgae cells, having as input process variables (flow rate, biomass concentration), operational parameters (agitation speed, bead size, bead filling) and cell-related parameters (cell size and cell strength). The model was based on the calculation of velocity profiles of the beads in the mill chamber, from which the theoretical frequency and energy of collision were estimated. Furthermore, cell-wall strength and cell size were incorporated in order to estimate the proportion of cells that are disintegrated under batch operation. The concept of effective disruption energy was used to account for the fraction of energy that effectively reaches the cells and causes disintegration. The model was validated for two microalgal strains (*Chlorella vulgaris* and *Tetraselmis suecica*) at various values of bead size (0.3-1 mm) and bead fillings (2.5-75 %), and at two different scales (80 and 500 mL).

A disintegration- fractionation strategy based on bead milling and ultrafiltration was implemented in **Chapter 4** in order to evaluate the functional activity of biomolecules extracted from *Tetraselmis suecica* under mild conditions. After cell disintegration, the soluble fraction was filtered using membranes of three different cut offs: 0.2 µm, 300 kDa and 10 kDa. It was found that the microalgae fractions displayed superior or

comparable functional activity in comparison to whey protein isolate. Additionally, it was observed that the fractions obtained in the retentate phase after filtration, showed the highest performance in terms of surface activity and gelation. This superior performance was attributed to the presence of larger molecular weight proteins and to their interaction with pigments and polysaccharides, in a similar way as Pickering emulsions. Despite the promising results regarding functional properties, in this process the protein yields were 12 % after disintegration and up to 6 % after filtration (referred to the initial biomass), with protein purities ranging from 10 to 22 (DW) %.

The knowledge gathered in chapters 2-4 motivated the research conducted in **Chapter 5.** Here a simple fractionation strategy was implemented: A single extraction step by short (8 min) bead milling after which the soluble phase was recovered as main product. Upon cell disintegration, proteins are released rapidly, reaching maximum extraction within 10 min. Carbohydrates, on the contrary, are released slowly, even after 3 h operation. The release of carbohydrates was linked to the starch loss from the biomass. Analysis of the functional activity (surface activity and gelation) of the soluble extract revealed a superior or similar performance in comparison to whey protein isolate. Furthermore, the protein purity in the soluble extract reached 50 % (DW), which was due to a superior protein content in the initial biomass and to the short bead milling times, which favours the release of proteins over carbohydrates. The overall energy consumption was 0.6 kWh kg_{DW}^{-1}, and the protein yield reached 23 % (DW, referred to the initial biomass), indicating that potentially high value molecules can be obtained with simple and mild processing.

In the second section of this thesis, ionic liquids are investigated as novel solvents for the extraction and fractionation of biomolecules. Ionic liquids (ILs) are salts which are liquid at room temperature. They have been proposed in several studies as promising solvents for the extraction of biomolecules from biomass (e.g., wood) and for the fractionation of a broad range of biomolecules, in particular proteins.

Chapter 6 presents a study in which crude proteins (proteins extracted after a process involving bead milling, solid-liquid separation and membrane filtration) where subjected to an aqueous two-phase system (ATPS) in order to evaluate the fractionation performance. The study was conducted for two microalgae strains: *Neochloris oleoabundans* and *Tetraselmis suecica*. The ATPS system used here was composed of the ionic liquid Iolilyte 221PG and the salt potassium citrate. Furthermore, an activity coefficient model (Non Random Two Liquids) was implemented in order to describe the experimental data. The extraction efficiencies of proteins for both strains were superior to 75 % (DW). Proteins concentrated preferentially in the top layer (IL-rich) while carbohydrates migrated to the bottom phase (salt-rich). The partition coefficient for proteins varied in the range 50-100 [-]. Overall, the extraction efficiencies and partitioning performance was independent of the IL concentration, in terms of tie line length.

The research conducted in chapter 6 confirmed that ILs-based ATPS can effectively fractionate algal biomolecules. Besides, their ability to extract biomolecules directly from the biomass, at mild conditions, without requiring multiple unit operations, was addressed in chapters 7 and 8.

In **Chapter 7** a new model organism was investigated: the macroalgae *Ulva lactuca*. After a preliminary screening, the ionic liquid 1-ethyl-3-methyl-imidazolium dibutyl phosphate was selected as it resulted in selective extraction of proteins at high yields. Biomolecule extraction was investigated in a single step involving bead milling assisted by the IL at room temperature. The soluble phase (extract) was collected and subjected to two-phase partitioning and ultrafiltration. Protein extraction yields up to 75 % were obtained during extraction, significantly superior to the methods reported so far for the same strain. Fractionation by means of ultrafiltration allowed the recovery of nearly 40 % of the proteins in the retentate phase while 85 % of the ionic liquid was present in the permeate phase.

Similarly, the extraction of biomolecules from the microalgae *Tetraselmis suecica* using ILs was investigated in **Chapter 8.** The ionic liquid 1-Butyl-3-methylimidazolium dicyanamide was found to extract significant amounts of proteins from the biomass, under mild conditions. Furthermore, extraction was selective towards proteins over carbohydrates. Additional investigations confirmed that this IL is able to extract proteins without requiring mechanical disintegration, at yields of nearly 77 %. It was hypothesized that the IL permeabilizes the cell-wall, through which proteins are extracted. The permeabilization could take place due to the ILs' ability to party destabilize the hydrogen bond structure of the polymers in the cell-wall. Thus, significant extraction of protein was observed, but the amount of solubilized carbohydrates was negligible. After extraction, ultrafiltration was implemented, allowing the overall recovery of 64 % of the total proteins and more than 69 % of the ionic liquid in the permeate phase. Theoretical estimations were conducted to determine the number of filtration steps needed to remove completely the IL from the extract. It was found that 5 steps are needed, if the same fractionation yields are maintained. This could result in an overall yield of 26 % and a purity of 76 %

Several key aspects of the fractionation strategies investigated in this thesis are discussed in **Chapter 9**. First, it is proposed that the design of biorefineries must start from the understanding of the cell structure rather than from the typical empirical application of unit operations. Several examples are presented to illustrate the transition from an empirical to a more mechanistic approach, in particular regarding cell disintegration, fractionation, back-extraction, process integration and multi-product functionality. Moreover, novel biorefinery concepts are proposed in the framework of process intensification: Self disintegration, simultaneous disintegration and disentanglement, and self-separating systems. These concepts could ensure minimum processing and energy consumption, without the need for auxiliary solvents/chemicals while preserving the functional activity of the extracted biomolecules.

Resumen

En los próximos 30 años se espera que la población mundial alcance los 9.5 mil millones de habitantes, por lo que el suministro de alimentos, y en particular de proteínas, debe aumentar significativamente. Esta expansión podría amenazar críticamente los ecosistemas terrestres y acuáticos, ya que el sistema actual de producción de alimentos depende casi exclusivamente de la agricultura y la pesca. Las algas, incluyendo microalgas y macroalgas, podrían ser la solución al desafío del producir sufficiente cantidad de alimentos y proteínas, ya que no requieren agua dulce ni tierra cultivable, y porque pueden producir cantidades significativas de proteínas con una productividad superior en comparación con los cultivos terrestres tradicionales. Sin embargo, las proteínas en las algas suelen estar ubicadas intracelularmente en el citoplasma o incrustadas en ensamblajes moleculares y orgánulos. Para obtener estas biomoléculas, varias operaciones unitarias se aplican típicamente de manera secuencial: desintegración, extracción, fraccionamiento y purificación. A menudo, estas operaciones unitarias requieren cantidades importantes de energía y productos químicos auxiliares que conducen a la degradación del producto o la generación de varios subproductos de bajo valor. Por lo tanto, se necesitan nuevos conceptos de biorrefinería, que son más compactos (integración) y en los que se favorece un procesamiento moderado (funcionalidad del producto) (**Capítulo 1**).

La investigación realizada en esta tesis se divide en dos secciones. En la primera sección (capítulos 2-5), la estrategia de biorrefinería se basa en la desintegración mecánica por medio de molino de bolas. Además, se presenta evidencia acerca de las propiedades funcionales de las biomoléculas extraídas. En la segunda sección (capítulos 6-8), se investigan conceptos de biorefinería de moléculas de algas usando líquidos iónicos como nuevos extractantes.

En el **Capítulo 2** se investigó el efecto del tamaño de bolas (0.3-1 mm) sobre la cinética de desintegración celular y la liberación de biomoléculas. Tres algas de interés industrial fueron estudiadas: *Tetraselmis suecica*, *Neochloris oleoabundans* y *Chlorella*

vulgaris. Además, se aplicó el denominado "modelo de estrés", en el cual el proceso de trituración se cuantifica en términos de frecuencia e intensidad de colisiones en el molino de bolas. Para todas las microalgas usadas, se observó que la desintegración y liberación de biomoléculas siguen una cinética de primer orden. La desintegración y la liberación de proteínas ocurren primero -casi simultáneamente- mientras que la liberación de azucares tiene lugar a velocidades más bajas, lo que indica una liberación selectiva de proteínas. Se planteó la hipótesis de que las proteínas hidro-solubles presentes en el citoplasma se liberan rápidamente al romperse las células, mientras que los azucares de la pared celular o de los gránulos de almidón requieren un molido mas prolongado. Además, se observó –para *Tetraselmis suecica*- que las tasas de desintegración, la liberación de biomoléculas y los tasas de extracción son independientes del tamaño de las bolas. Esto se debie a la pared celular relativamente débil de esta microalga y al hecho de que el molino de bolas se opero en una región en la que se transfirió energía excesiva asugurando una desintegración completa. Los consumos de energía medidos y las tasas de extracción de proteínas (comparado con la biomasa inicial) dependieron de la alga en consideración y variaron de 0,45 a 7 kWh kg_{DW}^{-1} y de 15 a 38 % (peso seco) respectivamente.

Varios interrogantes quedaron con respecto al mecanismo de desintegración celular en los molinos de bolas. Por lo tanto, en el **Capítulo 3**, se propuso un modelo matemático para predecir las tasas de desintegración de microalgas, considerando variables de proceso (caudal, concentración de biomasa), parámetros operativos (velocidad de agitación, tamaño de perla, relleno de perlas) y parámetros relacionados con las microalgas (tamaño resistencia de la pared celular). El modelo se basó en el cálculo de los perfiles de velocidad de las bolas en el molino, a partir de los cuales se estimaron la frecuencia teórica y la energía de las colisiones. Además, se incorporaron la resistencia de la pared celular y el tamaño de las células para estimar la proporción de células que se desintegran durante el molido en modo batch. El concepto de energía efectiva de desintegracion se utilizó para explicar la fracción de energía que llega efectivamente a las células y provoca su rupura. El modelo se validó con dos typos de

microalgas (*Chlorella vulgaris y Tetraselmis suecica*), varios valores de tamaño de bolas (0.3-1 mm), diferentes rellenos de bolas (2,5-75%) y en dos escalas distintas (80 y 500 ml).

En el **Capítulo 4** se implementó una estrategia de desintegración-fraccionamiento usando molino de bolas y ultrafiltración. También se evaluó la actividad funcional de las biomoléculas extraídas de *Tetraselmis suecica*. Después de la desintegración celular, la fracción soluble se filtró utilizando membranas de tres tamaños diferentes: 0.2 µm, 300 kDa y 10 kDa. Se encontró que las fracciones de microalgas exhiben una actividad funcional superior o comparable con proteínas de suero the leche. Adicionalmente, se observó que las fracciones obtenidas en el retentado después de la filtración, mostraron el mayor rendimiento en términos de actividad superficial y gelificación. Este rendimiento superior se atribuyó a la presencia de proteínas de mayor peso molecular y a su interacción con pigmentos y polisacáridos, de manera similar a las emulsiones Pickering. A pesar de los resultados prometedores con respecto a las propiedades funcionales, en este proceso los porcentajes de extracción de proteínas fueron del 12 % después de la desintegración y hasta del 6 % después de la filtración (referida a la biomasa inicial), con una pureza de proteínas del 10 al 22 % (peso seco).

Los conocimientos reunidos en los capítulos 2-4 motivaron la investigación realizada en el **Capítulo 5**. Aquí se implementó una estrategia de fraccionamiento simple: un solo paso de extracción rápida mediante molino de bolas (8 min), después de lo cual la fase soluble se recuperó como producto principal. Tras la desintegración celular, las proteínas se liberan rápidamente, alcanzando una extracción máxima en 10 minutos. Los carbohidratos, por el contrario, se liberan lentamente, incluso después de 3 horas de molido. La liberación de carbohidratos se relacionó con la pérdida de almidón presente en la biomasa. El análisis de la actividad funcional (actividad superficial y gelificación) del extracto soluble reveló un rendimiento superior o similar en comparación con proteínas de suero de leche. Además, la pureza de la proteína en el

extracto soluble alcanzó el 50% (peso seco), lo que se debió a un contenido de proteína superior en la biomasa inicial y al corto tiempo dedesintegración, lo que favorece la liberación de proteínas sobre los carbohidratos. El consumo total de energía fue de 06 kWh kg_{DW}^{-1}, y el el porcentaje de extracción de proteínas alcanzó el 23% (peso seco, referido a la biomasa inicial), lo que indica que se pueden obtener moléculas funcionales con un proceso sencillo de fraccionamiento.

En la segunda sección de esta tesis, varios líquidos iónicos se investigaron como nuevos agentes para la extracción y el fraccionamiento de biomoléculas. Los líquidos iónicos (IL) son sales que son líquidas a temperatura ambiente. Se han propuesto en varios estudios como disolventes prometedores para la extracción de biomoléculas de biomasas (por ejemplo, madera) y para el fraccionamiento de una amplia gama de biomoléculas, en particular proteínas.

El **Capítulo 6** presenta un estudio en el que proteínas crudas (proteínas extraídas después de un proceso que involucra el molido de bolas, separación sólido-líquido y filtración por membrana) se sometieron a un sistema acuoso de dos fases (ATPS) para evaluar el rendimiento del fraccionamiento. El estudio se realizó con microalgas: *Neochloris oleoabundans* y *Tetraselmis suecica*. El sistema ATPS utilizado aquí estaba compuesto por el líquido iónico Iolilyte 221PG y la sal citrato de potasio. Además, se implementó un modelo de coeficiente de actividad (NRTL) para describir los datos experimentales. Las eficiencias de extracción de proteínas para ambas microalgas fueron superiores al 75 %. Luego de la separación, las proteínas se concentraron preferentemente en la fase superior (rica en IL) mientras que los carbohidratos migraron a la fase inferior (rica en sal). El coeficiente de partición para proteínas varió en el rango 50-100 [-]. En general, las eficiencias de extracción y el rendimiento de la partición fueron independientes de la concentración de IL en el rango evaluado.

La investigación realizada en el capítulo 6 confirmó que los ATPS basados en IL pueden fraccionar eficazmente las biomoléculas de algas. Además, su capacidad para extraer

biomoléculas directamente de biomasa de algas, en condiciones moderadas, sin requerir múltiples operaciones unitarias, se abordó en los capítulos 7 y 8.

En el **Capítulo 7** se investigó un nuevo organismo modelo: la macroalga *Ulva lactuca*. Después de una selección preliminar, se seleccionó el líquido iónico dibutil-fosfato 1-etil-3-metil-imidazolio, ya que dio como resultado la extracción selectiva de proteínas con rendimietos altos en comparacion on otros IL. La extracción de biomoléculas se investigó en un solo paso, que inlcluye molino de bolas asistidao por el IL a temperatura ambiente. La fase soluble (extracto) se recogió y se sometió a partición bifásica y ultrafiltración. Se obtuvieron porcentajes de extracción de proteínas de hasta el 75% durante la extracción, significativamente superiores a los métodos informados hasta ahora para la misma macroalga. El fraccionamiento mediante ultrafiltración permitió la recuperación de casi el 40 % de las proteínas en el retentado, mientras que el 85 % del líquido iónico estaba presente en el permeado.

De manera similar, en el **Capítulo 8** se investigó la extracción de biomoléculas de la microalga *Tetraselmis suecica* utilizando líquidos iónicos. El IL 1-Butil-3-metilimidazolio dicianamida extrajo cantidades significativas de proteínas de alga en condiciones moderadas. Además, la extracción fue selectiva hacia proteínas sobre carbohidratos. Investigaciones adicionales confirmaron que este IL es capaz de extraer proteínas sin requerir desintegración mecánica, con rendimientos de casi el 77 %. Se planteó la hipótesis de que el IL permeabiliza la pared celular, a través de la cual se extraen las proteínas. La permeabilización podría tener lugar debido a la capacidad del IL para desestabilizar la estructura de puentes de hidrógeno de los polímeros en la pared celular. Por lo tanto, se observó una extracción significativa de proteínas, pero la cantidad de carbohidratos solubilizados fue significativamente inferior. Después de la extracción, se implementó ultrafiltración, lo que permitió la recuperación de hasta el 64 % de las proteínas totales y más del 69 % del líquido iónico en la fase de permeado. Se realizaron estimaciones teóricas para determinar el número de pasos de filtración necesarios para eliminar completamente la IL del extracto. Se encontró que se

necesitan 5 pasos, si se mantienen los mismos rendimientos en cada fraccionamiento. Esto podría resultar en una extracción global de proteínas del 26 % y una pureza de 76 %.

Varios aspectos cruciales de las estrategias de fraccionamiento investigadas en esta tesis se discuten en el **Capítulo 9**. Primero, se propone que el diseño de las biorrefinerías debe partir de la comprensión de la estructura celular en lugar de la aplicación empírica típica de operaciones unitarias. Se presentan varios ejemplos para ilustrar la transición desde un enfoque empírico a uno más mecanicistico, en particular con respecto a la desintegración celular, el fraccionamiento, la extracción, la integración de procesos, multiproductos y funcionalidad de las biomoléculas extraídas. Además, se proponen nuevos conceptos de biorrefinería en el marco de la intensificación del proceso: auto-desintegración, desintegración y desagregación simultáneos, y sistemas de auto-separación. Estos conceptos podrían garantizar un procesamiento y un consumo de energía mínimos, sin la necesidad de disolventes / productos químicos auxiliares a la vez que se preserva la actividad funcional de las biomoléculas extraídas.

Acknowledgments

As this journey comes to an end, I certainly look forward to new learnings as entrepreneur but also reflect on the last four years and the people who made possible this exceptional experience. With a bit of anguish since I won't be able to thank everyone sufficiently:

Rene, **Guiseppe**, **Michel** and **Corjan**. You were my supervisors through my PhD. Your expertise is out debate. I'm grateful to you for your guidance, patience, effort and time, especially during meetings and revising manuscripts. Discussions with you were always stimulating and gave me the confidence to continue forward with my research. **Corjan**, in the last weeks you also became a mentor of my entrepreneurial ideas, what a thrilling experience!. Thank you for your devoted support.

Lolke, **Jelle**, **Carl**. You were also part of my research project and were always willing to help me. You enriched substantially this research experience.

To the staff members of BPE: **Sarah**, **Maria**, **Marcel**, **Ruud**, **Dirk**, **Arjen**, **Hans**, **Marian**, **Miranda**, **Marina**. In several occasions I had the pleasure to spend quality time with you and also to learn from you. **Snezana**, **Wendy**, **Rick**, **Ruud, Fred** and **Sebastiaan**: you were always ready to help, responding promptly to all -perhaps often annoying- requests and problems from me and my students. **Arjen** and **Sebastiaan**, thanks for the many informal chats we had about various matters.

A significant portion of the work reflected in this thesis was possible thanks to the committed effort of a remarkable group of students: **Pascal**, **Tewodros**, **Calvin, Carlota**, **Ana**, **Fiona**, **Wijnand**, **Prissylia** and **Diana**. Guys, don't forget to unleash all the potential that is in you.

I had lots of fun and good times with all the fellow colleagues at BPE. To the incredible group of PhDs and postdocs: **Mitsue**, **Ilse**, **Alex**, **Sebastian**, **Christian**, **Renske**, **Camilo**, **Iris**, **Pauline, Kiira, Rocca**, **Robin**, **Barbara**, **Enrico**, **Fengzheng**, **Chunzhe**, **Anna**, **Fabian**, **Yourito**, **Ward**, **Tim**, **Guido**, **Luci**, **Pieter**, **Kira**, **Narcis**, **Catalina**, **Jeroen**, **Josue**, **Rafael, Joao**, **Mihris**, **Lukas**, **Dorinde**, **Douwe**, **Mark**, **Packo**, **Jorijn**, **Agi**, **Elisa**, **Rupali**, **Richard**,

Gerard, **Xiao**, **Abdulaziz, Kylie**, **Stephanie**, **Calvin**, **Jin**, **Malgorzata**, **Sofia**, **Iago**, **Marta**. This PhD has real value because of you and the many fun memories that will stay with me. Everyone of you are incredibly capable and unique. Thanks for being there in so many -Dinners&Beers, coffee breaks, house parties, BBQs, Spot and Japanese place-times, and of course, in several awesome borrels and the PhD trip. **Sofia** and **Calvin**: I'm also honoured to have you as paranymphs in my PhD defence.

A los miembros de **Macondo**, una verdadera familia Colombiana en Holanda. Creo que va a ser impossible repetir tan memorables fiestas y buenos momentos.

Empecé esta tesis usando una cita de un famoso científico que refleja muy bien por que fue posible para mi llegar a este punto. Todo en mi vida ha occurrido gracias a la grandeza y sacrificio de mi familia. **Ma**, **Pa**, **Gilber** - **Yuri**- **Ana I**, **Wil** - **Astrid** - **Luciana**, **llilli** - **Yis** - **Sofia** - **Mapi**, **Luna** - **Carlos**, **Nanys**. Ustedes siempre me han puesto primero que a ustedes mismos. Esa es la definición real de amor. Son una fuente constante de inspiración y motivación. Es imposible expresar en palabras cuanto los admiro y quiero, y cuan agredecido estoy.

Laura, non potevo essere più fortunato ad averti incontrato all'inizio del dottorato - in un modo particolarmente divertente -. Negli ultimi anni abbiamo attraversato una sorta di montagne russe, ma poi eravamo lì, superando ostacoli, insieme. Hai anche deciso di restare in giro dopo aver scoperto che mi piaceva la pizza all'ananas. Sei una donna meravigliosa, con così tanti talenti che devi ancora abbracciare completamente. Eri -e sei- sempre pronta al mio fianco, per sostenermi, per aiutarmi e capirmi. Grazie amore mio.

Thesis Cover: Thesis cover designed by **Daniela Suarez Garcia, Ar**.

Complexity is transformed: It is purified, it comes to the basic, to the simple, to the origin. But it reaches new forms, it attains other uses and functions. It becomes diverse again.

About the author

Curriculum Vitae

Edgar Suárez Garcia was born on April 25-1985 in Pueblorrico, Colombia. He followed secondary education at Liceo Enrique Velez Escobar in Itagui-Colombia and completed a BSc. in Biological Engineering at National University of Colombia.

Then, Edgar moved to the Netherlands to follow a MSc. in Chemical Engineering at Eindhoven University of Technology. He investigated adsorption processes for the recovery of valuable compounds from industrials streams as part of his MSc. thesis and continued with an internship at Corbion (former Purac, Gorinchem, The Netherlands) in the process technology department.

After obtaining his MSc. degree, Edgar worked as Process Engineer at Bodec Process Technology (Helmond, The Netherlands), where he contributed in several engineering projects in various companies and on topics related to the valorisation of agricultural streams. In 2015 Edgar started a doctoral program at the department of Bioprocess Engineering, Wageningen University and Research. The results of his PhD. research are presented in this thesis.

Edgar is now setting up his own company about innovative biorefinery processes for the production of functional products.

List of Publications

Published

P.R.Postma, **E. Suarez Garcia**, C.Safi, K.Yonathan, G.Olivieri, M.J.Barbosa., R.H.Wijffels, M.H.M.Eppink (2017). Energy efficient bead milling of microalgae: Effect of bead size on disintegration and release of proteins and carbohydrates. Bioresource Technology 224, 670-679.

E. Suarez Garcia, J.J.A. van Leeuwen, C. Safi, L. Sijtsma, L..A.M. van den Broek, M.H.M. Eppink, R.H. Wijffels, C. van den Berg (2018). Techno-Functional Properties of Crude Extracts from the Green Microalga *Tetraselmis suecica*. Journal of Agricultural and Food Chemistry 66 (29), 7831-7838.

E. Suarez Garcia, J.J.A. van Leeuwen, C. Safi, L. Sijtsma, M.H.M. Eppink, R.H. Wijffels, C. van den Berg (2018). Selective and energy efficient extraction of functional proteins from microalgae for food applications. Bioresource Technology 268, 197-203.

E. Suarez Garcia, C. Suarez Ruiz, M.H.M. Eppink, R.H. Wijffels, C. van den Berg (2018). Fractionation of proteins and carbohydrates from crude microalgae extracts using an Ionic liquid based-Aqueous Two Phase System. Separation and Purification Technology 204, 56-65.

Tamayo Tenorio, A., Kyriakopoulou, K., **Suarez Garcia, E.**, van den Berg, C., van der Goot, A.J (2018). Understanding differences in protein fractionation from conventional crops and herbaceous and aquatic biomass - Consequences for industrial use. Trends in Food Science & Technology 71 235-245.

Submitted

E. Suarez Garcia, C. Lo, M.H.M. Eppink, R.H. Wijffels, C. van den Berg. Understanding mild cell disintegration of microalgae in bead mills for the release of biomolecules. Chemical Engineering science.

E. Suarez Garcia, C. Miranda, M.T. Cesário, M.H.M. Eppink, R.H. Wijffels, C. van den Berg. Ionic liquid-assisted selective extraction and partitioning of biomolecules from macroalgae.

E. Suarez Garcia, W. van den Brink, M.H.M. Eppink, R.H. Wijffels, C. van den Berg. Mild permeabilization of microalgae cells for the selective release of biomolecules using ionic liquids

E. Suarez Garcia, M.H.M. Eppink, R.H. Wijffels, C. van den Berg. Integrated biorefineries for algal biomolecules.

Overview of completed training activities

Discipline Specific Activities

Conferences

- Algae & Seaweeds Workshop (2016, Wageningen, Netherlands)[1]
- 13th International Conference on Renewable Resources & Biorefineries (2017, Wroclaw-Poland)[1]
- 10th World Congress Chemical Engineering (2017, Barcelona-Spain)[2]
- Algal Biorefineries for Europe (2017, Brussels-Belgium)[1]
- NBC-18 Biotechnology in Harmony (2018, Ede-Netherlands)[2]
- Global food science student competition (2018, Wuxi-China)[2]
- AlgaEurope 2018 (2018, Amterdam-Netherlands)[1]

Courses

- Advanced Thermodynamics (OSPT, 2015)
- Biorefineries for Biomolecules (VLAG, 2015)
- Microalgal Biorefineries (VLAG, 2016)
- Process economics and cost engineering (OSPT, 2017)
- Zero wastes biorefineries (VLAG, 2018)1
- Innovation toward plantbased consumption (University of Copenhagen, 2018)
- Philosophy and Ethics of Food Science & Technology (VLAG, 2019)

General Courses

- Brain training (WGS, 2016)
- Project and time management (WGS, 2017)
- Entrepreneurship in and outside science (WGS, 2017)
- Essentials of scientific writing and presenting (Wageningen In'to Languages, 2017)
- Carreer perpectives (WGS, 2018)

Optional

- Life sciences with Industry (Lorentz Center, 2015)
- Preparation of research proposal (2015)
- PhD Days and group meetings (2015-2018)
- Young ASFG (2015-2017)
- PhD study trip to San Diego (preparation and participation)[1,2]

Teaching

- Transfer Processes
- Advanced Biorefineries
- Microalgae Biorefineries
- Supervision of 8 MSc. students and 1 internship student

1. Poster presentation. 2. Oral presentation

The research described in this thesis was financially supported by the Dutch national science foundation (NWO), Applied and Engineering Sciences (TTW), under project AlgaePro4You (nr. 12635).